TOWARDS LAND CHANGE MANAGEMENT USING ECOSYSTEM DYNAMICS AND LAND COVER CHANGE IN RURAL EASTERN CAPE

ZAHN MÜNCH (MSc)

Dissertation presented for the degree
Doctor of Philosophy in Geoinformatics
in the Faculty of Science
at Stellenbosch University

Supervisor: Prof Adriaan van Niekerk
Department of Geography and Environmental Studies
December 2019

DECLARATION

By submitting this dissertation electronically, I declare that the entirety of the work contained therein is my own original work, that I am the sole author thereof (save to the extent explicitly stated otherwise), that reproduction and publication thereof by Stellenbosch University will not infringe any third party rights and that I have not previously in its entirety or in part submitted it for obtaining any qualification.

This dissertation includes three original articles published in or submitted to peer-reviewed journals. The development and writing of the papers (published and unpublished) were my principal responsibility. For each of the instances where this is not the case, a declaration is provided in the dissertation indicating the nature and extent of the contributions of co-authors.

With regard to Chapters 3, 4 and 6, the nature and scope of my contribution were as follows:

Chapter	Nature of contribution	Extent of contribution (%)
Chapter 3	This chapter was published as a journal article in *Geosciences*: Volume 7, 7 (Münch Z, Okoye PI, Gibson LA, Mantel S & Palmer AR 2017) and was co-authored by members of WRC project K5/2400/4 who helped in the conceptualisation and writing of the manuscript. Author contributions: S Mantel and AR Palmer conceived of the project. I designed the experiments, completed the literature review, analysed the components and wrote the manuscript. PI Okoye performed data collection and land cover classification. LA Gibson provided editorial support.	S Mantel (0.5%) AR Palmer (0.5%) PI Okoye (9%) LA Gibson (10%) Z Münch (80%)
Chapter 4	This chapter was submitted for publication as a journal article in the *ISPRS Journal of Photogrammetry and Remote Sensing* and is currently under review. The chapter was authored by me with editorial support from my editor, E Katzenellenbogen. I conceptualised the research and authored the manuscript, carried out the literature review, the data collection, and analysis.	E Katzenellenbogen (5%) Z Münch (95%)
Chapter 5	Sections of this chapter have been published as a journal article in *Helyon*: Volume 4, e00693 (Gibson LA, Münch Z, Palmer AR & Mantel 2018). I have revised the chapter for inclusion in this dissertation. LA Gibson and I conceptualised, collected and analysed the data and authored the original manuscript. I completed the literature review and produced the final text.	S Mantel (0.5%) AR Palmer (0.5%) LA Gibson (40%) Z Münch (59%)
Chapter 6	This chapter was published as a journal article in *Land*: Volume 8, 33 (Münch Z, Gibson LA & Palmer AR 2019) and was co-authored by LA Gibson who helped in the conceptualisation and writing of the manuscript with editorial support from AR Palmer. I completed the literature review, the data collection, the analysis of the components and produced the first draft of the manuscript.	AR Palmer (1%) LA Gibson (14%) Z Münch (85%)

Date: December 2019

SUMMARY

Land cover change, triggered by natural and anthropogenic land use change, affects ecosystem services provided by grasslands. Woody encroachment into the grasslands is a threat to function and productivity of rangelands, and threaten rural livelihoods, intensified by rising CO_2 levels associated with climate change. Processes of change can only effectively be identified after spatial land transition has been revealed and patterns of change quantified. Accurately quantifying the rates and extent of land cover change is the first step in relating underlying land use processes and the environmental effects thereof to land cover change trajectories involving grassland transformation.

The study aims to demonstrate how land cover change, in particular woody encroachment influences landscape functions provided by grasslands in the Eastern Cape. The study seeks to determine how accurately land cover transformation can be quantified and modelled using existing datasets that may contain map error and raises the question how the error pattern can affect modelling of future evapotranspiration and carbon storage. A further question is how the drivers of change vary between regions under different land tenure, i.e. dualistic or commercial systems.

Systematic land cover change analysis and future land change modelling were used to characterise land cover change trajectories and flows in the landscape. Flows were described using (1) an indicator-based approach, and (2) intensity analysis and change budget. Hypothetical map error was determined for observed and modelled land cover maps. Overall change was partitioned into quantity, exchange and shift disagreement and intensity. The change budget was computed both at catchment and local level. Map error was further investigated using a local geographically weighted method. Local geographically weighted correspondence matrices were constructed to determine spatially explicit probabilities of change and error at catchment level and per land cover class. By consulting the overall allocation difference maps, hotspots of change and probable error were identified for further investigation. Trends in remote sensing-derived biophysical variables were analysed to determine how land cover change would affect the surface energy budget and the carbon cycle, as proxies for water use and rangeland productivity.

Primary drivers of landscape modification comprised rangeland degradation, woody encroachment, urbanisation, increased dryland cultivation and commercial afforestation, with the latter concentrated in the commercial catchment. Though grassland persistence still dominated land cover in the landscape, catchments under dualistic land tenure experienced

steeper declines in the grassland area. Woody encroachment was also found predominantly in these catchments.

Overall accuracy for the input land cover maps were reported as >80%, equating to theoretical land cover change accuracy of 67–72%. Landscape change varied between 18% and 42%, with 19% estimated from direct overlay of land cover maps with 30 m resolution pixels. By applying a multi-resolution aggregation technique, the study showed that lower resolution input data would identify less change in the landscape, mainly because the allocation error diminishes at lower resolutions. For higher change accuracies and reliability, the accuracy of input land cover maps would have to be increased.

Hypothetical map error in observed land cover change maps were found to be higher in catchments under dualistic tenure for gaining transitions, whereas losing transitions showed higher error in catchments practicing commercial farming. The hypothetical error accounted for almost 50% of the reported change. The modelled land cover change showed higher allocation disagreement, suggesting that the land change model was not very reliable, particularly for the commercial catchment**.**

Analysis of remotely sensed data products such as albedo, net primary production and evapotranspiration, in combination with land cover change data has led to better understanding of the landscape of the catchments. Though grasslands are predicted to decrease in favour of woody invasive plant species and cultivated land, this study predicted a decrease of 12% and 6% respectively in net carbon storage and water use by vegetation. Information from multiple sources, in both quality and type, were integrated to better understand rangeland productivity degradation and to compare the impact of climate versus land management in the different catchments. Quantifying changes in biophysical parameters can assist scientists and managers in addressing global challenges.

KEY WORDS:

Land cover, land cover change, land change modelling, hypothetical error, intensity analysis, geographically weighted, evapotranspiration, net primary production

OPSOMMING

Verandering in grondbedekking wat deur natuurlike en antropogeniese verandering in grondgebruik veroorsaak word, beïnvloed die ekostelseldienste wat deur grasvelde gelewer word. Houtagtige indringing van die grasvelde is ’n bedreiging vir die funksionering en produktiwiteit van weivelde en bedreig landelike lewensbestaan. Hierdie proses word aangehelp deur die toenemende CO_2-vlakke wat met klimaatsverandering verband hou.

Prosesse van verandering kan eers effektief geïdentifiseer word nadat ruimtelike landoorgang geopenbaar is en patrone van verandering gekwantifiseer is. Die akkurate kwantifisering van die trajek en omvang van grondbedekkingsverandering is die eerste stap om die onderliggende prosesse vir grondgebruik en die omgewingseffekte daarvan aan grondbedekkingstrajeksies te koppel. Laasgenoemde hou direkte verband met die transformasie van grasveld.

Hierdie studie het ten doel om te demonstreer hoe grondbedekkingsverandering, veral deur houtagtige indringerplante, die landskapfunksies wat grasvelde in die Oos-Kaap verrig beïnvloed. Die studie poog om te bepaal hoe akkuraat die transformasie van grondbedekking met bestaande datastelle, wat kaartfoute bevat, gekwantifiseer en gemodeller kan word. Daar is onsekerheid oor hoe die foutpatrone in die datastelle die modellering van toekomstige evapotranspirasie en koolstofopberging kan beïnvloed. 'n Verdere navorsingsvraag is hoe die drywers van verandering tussen streke onder verskillende grondbesit, te wete dualistiese of kommersiële stelsels, wissel.

Sistematiese ontleding van grondbedekking en toekomstige modellering is gebruik om die trajek en vloei van grondverandering in die landskap te beskryf. Vloei is beskryf met behulp van (1) 'n aanwyser-gebaseerde benadering, en (2) intensiteitsanalise en veranderingsbegroting. Hipotetiese kaartfoute is vir waargenome en gemodelleerde grondbedekkingskaarte bepaal. Algehele verandering is in kwantiteit, wissel en verskuiwingsverskille en intensiteit opgedeel. Die veranderingsbegroting is per opvanggebied sowel as op plaaslike vlak bereken. Kaartfoute is verder met behulp van 'n plaaslike geografies-geweegde metode ondersoek. Plaaslike geografies-geweegde korrespondensie-matrikse is opgestel om ruimtelik-sensitiewe waarskynlikhede vir veranderinge en foute per opvanggebied en grondbedekkingklas te bepaal. Die totale toekenningsverskilkaarte is geraadpleeg om brandpunte van verandering en waarskynlike foute vir verdere ondersoek te identifiseer. Die tendense in biofisiese veranderlikes wat vanaf afstandswaarneming afgely is, is ontleed om te bepaal hoe verandering in grondbedekking die oppervlakte-energiebegroting en die koolstofsiklus, wat watergebruik en graslandproduktiwiteit verteenwoordig, sou beïnvloed.

Die resultate het getoon dat weiveldagteruitgang, houtagtige indringing, verstedeliking, verhoogde droëlandverbouing en kommersiële bosbou, met laasgenoemde gekonsentreer in die kommersiële opvanggebied, die primêre drywers van grondbedekkingsverandering was. Alhoewel grasland grondbedekking die landskap steeds oorheers, het dit in opvanggebiede onder dualistiese grondbesit afgeneem. Houtagtige indringing is hoofsaaklik in hierdie opvanggebiede opgemerk.

Die algehele akkuraatheid van die inset grondbedekkingskaarte is as >80% gerapporteer, wat teoreties in die konteks van grondbedekkingverandering aan 67-72% gelykstaande is. Landskapverandering het tussen 18% en 42% gewissel, met 19% wat op direkte oorleg van 30 m resolusie grondbedekkingskaarte geraam is. 'n Multi-resolusie-samevoegingstegniek het getoon dat laer resolusie-insetdata minder verandering in die landskap identifiseer, hoofsaaklik omdat die toewysingsfout by laer resolusies verminder. Die akkuraatheid van grondbedekkingskaarte sal verhoog moet word om die akkuraatheid en betroubaarheid van veranderinge te verbeter.

Daar is bevind dat hipotetiese kaartfoute in waargenome grondebedekkingsveranderingskaarte hoër was in opvanggebiede onder dualistiese bestuur vir grondbedekkingsklasse wat toegeneem het, terwyl in die kommersiële opgevanggebied groter foute in grondbedekkingsklasse met afnemende oorgange opgetel is. Die hipotetiese fout was verantwoordelik vir byna 50% van die gemelde verandering. Die gemodelleerde gronddekkingverandering het 'n groter toewysigingsverskil getoon, wat daarop dui dat die grondbedekkingsveranderingsmodel nie baie betroubaar was nie, veral nie vir die kommersiële opvanggebied nie.

Analise van afstandswaarnemingsdataprodukte soos albedo, netto primêre produksie en evapotranspirasie, in kombinasie met grondbedekkingsveranderingsdata, het gelei tot 'n beter begrip van die landskap in die opvanggebiede. Alhoewel die voorspelling is dat grasvelde ten gunste van houtagtige indringerplantspesies en bewerkte lande sal afneem, het hierdie studie slegs 'n afname van onderskeidelik 12% en 6% in die netto koolstofopberging en watergebruik deur plantegroei voorspel. Inligting uit verskeie bronne, beide in kwaliteit en tipe, is geïntegreer om die agteruitgang van die landskapproduktiwiteit beter te verstaan en om die impak van klimaat op grondbestuur in die verskillende opvanggebiede te vergelyk. Die kwantifisering van veranderinge in biofisiese parameters kan wetenskaplikes en bestuurders help om wêreldwye uitdagings die hoof te bied.

TREFWOORDE:

Grondbedekking, grondbedekkingsverandering, landveranderingsmodellering, hipotetiese fout, intensiteitsanalise, geografies geweegde, evapotranspirasie, netto primêre produksie.

ACKNOWLEDGEMENTS

I sincerely thank:

My family, Cecil, Alex, Eric, Laura and Jo-Jo.

My supervisor, Professor Adriaan van Niekerk.

My collaborator and friend, Dr Lesley Gibson.

My godmother and editor, Professor Edith Katzenellenbogen.

Colleagues, Associate Professor Helen de Klerk, Dr Jaco Kemp and Professor Sanette Ferreira.

Perpetua Ifeoma Okoye and Jascha (S.E.) Muller, Centre of Geographical Analysis (CGA), Stellenbosch University for image processing.

Stellenbosch University for the opportunity to study and financial support for tuition.

Water Research Commission Project K5/2520 for financial support.

Water Research Commission Project K5/2400/4 (*Emva kwe dywabasi* — "After the Wattle") for financial support. My gratitude is extended to the project leaders, Dr Sukhmani Mantel and Dr Anthony Palmer, for their continued support.

CONTENTS

FIGURES

TABLES

ACRONYMS AND ABBREVIATIONS

A	Abandonment
AppEEARS	Application for extracting and exploring analysis ready samples
AAT	Annual aggregated time series
AATSR	Advanced along-track scanning radiometer
ANN	Artificial neural network
AUC	Area under the curve
AVHRR	Advanced very high resolution radiometer
BFAST	Breaks for additive seasonal and trend
BR, BRS	Bare rock and soil
BRDF	Bidirectional reflectance distribution function
CD: NGI	Chief Directorate: National Geospatial Information
CI	Confidence interval
CL, CLs	Cultivated land
CLC	Combined location classification
CO_2	Carbon dioxide
CVA	Change vector analysis
D	Deforestation
De	Degradation
Dn	Natural dynamic
DN	Digital numbers
DWA	Department of Water Affairs (formerly known as DWAF)
DWAF	Department of Water Affairs and Forestry
ENVISAT	European Environmental Satellite
EROS	Earth resources observation and science
ESA	European Space Agency
ESRI	Environmental Systems Research Institute
ET	Evapotranspiration
ETM+	Enhanced thematic mapper plus
EVI	Enhanced vegetation index
FB, FITBs	Forest indigenous, thicket bushlands, bush clumps, high fynbos
FP, FPs	Forest plantations (clear-felled, Pine spp., other / mixed spp.)
fPAR	Fraction of photosynthetically active radiation
GIMMS	Global inventory monitoring and modelling system

GIS	Geographic information systems
GEOBIA	Geographic object-based image analysis
GEE	Google Earth Engine
ha	Hectare
Ia	Agricultural intensification
IAPs	Invasive alien plant(s)
IAV	Inter-annual variation
If	Woody encroachment
Iu	Urban intensification
LAI	Leaf area index
LC	Land cover
LC8	Landsat 8 Operational Land Imager
LCC	Land cover change
LCM	IDRISI Land Change Modeller
LE7	Landsat 7 Enhanced Thematic Mapper Plus
LOESS	Local regression
LT5	Landsat 5 Thematic Mapper
LULC	Land use land cover
MAD	Multivariate alteration detection
MERIS	Medium resolution imaging spectroradiometer
MLC	Maximum likelihood classifier
MLP	Multi-layer Perceptron
MODIS	Moderate resolution imaging spectroradiometer
MOLA	Multi-objective land allocation
MR	Maintenance respiration
MSS	Multispectral Scanner
NASA	National Aeronautics and Space Administration
NBAR	Nadir BRDF-adjusted reflectance
NDVI	Normalised difference vegetation index
NDWI	Normalised difference water index
NEE	Net ecosystem carbon exchange
NIAPS	National invasive alien plant survey
NLC	National land cover
NOAA	National Oceanographic and Atmospheric Administration

NPP	Net primary production
OA	Overall accuracy
OBIA	Object-based image analysis
OLI	Operational Land Imager
OLS	Ordinary least squares
PA	Producer's accuracy
PCA	Principle component analysis
PSA	Peak season albedo
PSN	Net photosynthesis
R	Afforestation
R^2	Coefficient of determination
Re	Reclamation
RM	Regression modelling
ROC	Receiver operating characteristics
RS	Remote sensing
SAVI	Soil adjusted vegetation index
SBC	SPOT building count
sd	Standard deviation
se	Standard error
SPOT	Satellite Pour l'Observation de la Terre
STL	Seasonal trend decomposition method
STM	Season-trend model
SUDEM	Stellenbosch University digital elevation model
SVM	Support vector machine
TM	Thematic Mapper
ToA	Top of atmosphere
TRMM	Tropical rainfall measuring mission
UA	User's accuracy
UG	Unimproved (degraded / natural) grassland
UB, UrBu	Urban/built-up (residential, formal township)
USGS	United States Geological Survey
Wb, WB	Water bodies
WfW	Working for Water
Wl, WL	Wetlands

WoE	Weights of evidence
WRC	Water Research Commission

CHAPTER 1: UNDERSTANDING LINKAGES BETWEEN LAND COVER AND ECOSYSTEM SERVICES FOR MANAGING DYNAMIC LANDSCAPES

The competition for land resources and the services provided by the land are increasingly dynamic in response to the high demands of a growing population under a changing climate.
(Verburg et al. 2015: 38)

Land cover and land use dynamics have significant consequences for the natural environment, being important drivers of change in ecosystems and the services they provide (Reyers et al. 2009). Subtle changes in land management and land use practices can have important repercussions (Verburg, Neumann & Nol 2011) as human actions continue to change and exert pressure on the natural environment. To effectively manage complex ecosystems, the processes that create and maintain the environment, whether natural or modified, must be adequately understood and quantified (Bailey 2017). This introductory chapter briefly explores the concepts of landscape dynamics, land cover, and ecosystem services before outlining the significance of investigating the relationships between these concepts. The research problem and related questions are formulated, followed by a statement of the aim and objectives. The research methodology and design are also provided, and the chapter concludes with an outline of the dissertation structure.

1.1 LANDSCAPE DYNAMICS

Many definitions for the term ‘landscape’ exist, but in this study, a landscape is considered a spatially heterogeneous area of interacting ecosystems that function as a unit and can be analysed at any scale. The landscape structure – spatial elements present, their arrangement and spatial extent – determines the heterogeneity of the landscape (Turner & Gardner 2015) and its functioning. The term ‘landscape function’ (Willemen et al. 2010) is used to indicate the capacity of a landscape to provide goods and services. Ecosystem services are then described as the goods and services delivered that benefit humans (Banzahf & Boyd 2005), such as provisioning of food and fibre, regulating and provisioning of water, soil productivity, and use of natural areas for recreation or spiritual purposes (Egoh et al. 2008; 2012).

As interest in landscape function and ecosystem services grow, the need for spatially explicit quantification of landscape dynamics using geo-referenced metrics and GIS-based approaches has increased (Egoh et al. 2012; Lavorel et al. 2017; Martínez-Harms & Balvanera 2012), especially in support of land management (Doré et al. 2011; Grêt-Regamey et al. 2013). For

analysis purposes, landscapes are frequently represented as digital maps (Turner & Gardner 2015).

Complex human-environment interactions determine landscape use and the resulting character (Bastian, Krönert & Lipský 2006; Feranec et al. 2010). The complexity of these human-environment interactions increasingly challenges planners, environmental agencies and policy makers in their decisions on sustainable landscape development (Turner 2009). The effects of human domination over the terrestrial surface of the earth is well documented and evidenced by the 30-50 per cent of the land surface that has been transformed by human activities (Vitousek et al. 1997) and virtually no land surface considered 'pristine' (Turner 2009).

The extent of landscape modifications currently underway and their associated consequences (Steffen et al. 2003) are unprecedented, requiring integrative studies of landscape systems dynamics (Rindfuss et al. 2004). A management decision to exploit a particular landscape function, e.g. cultivation of land, will directly affect the mix of services provided by a landscape (DeFries, Foley & Asner 2004). Consequently, land use and land cover changes may result in production services, e.g. food, a positive service, increasing at the expense of the regulatory service, e.g. soil retention and water quality regulation, the trade-off (Reyers et al. 2009), limiting landscape function. Besides the influence of biophysical factors, land use change can also be affected by economic, social, cultural, political or institutional forces (Verburg et al. 2006), making land use change models important tools to facilitate integrated socio-environmental management (Verburg et al. 2002).

Even though the impact of land use change on ecosystem function is profound, the lack of long-term information regarding the consequences of such change presents a significant obstacle to understanding and managing landscapes (DeFries, Foley & Asner 2004). According to Reyers et al. (2009), land cover change can comprise of land transformation or land degradation, referring respectively to abrupt change versus gradual decline, each with a different effect on the landscape. Since landscapes are complex and dynamic systems, a linear response to land cover change is unlikely (DeFries, Foley & Asner 2004) so that a small change in land use could have large consequences.

Satellite-based Earth observation is a powerful means to monitor changes at the land surface. Not only does remote sensing (RS) provide the basic data to undertake inventory of land (Skidmore et al. 1997), but RS based time series analysis can be used to reveal land surface dynamics and analyse the magnitude of these changes within a defined monitoring time span (Kuenzer, Dech & Wagner 2015; Lasaponara & Lanorte 2012). Land change (systems) science

seeks to understand, explain and project land use and land cover dynamics associated with human-environment interaction (Turner 2009; Turner, Lambin & Reenberg 2007) by integrating information from various research communities (Rindfuss et al. 2004) in support of land management and by inference ecosystem management.

1.2 QUANTIFYING LANDSCAPE FUNCTION

Landscape function (ecosystem services goods and services) can be mapped using landscape indicators that support land cover data and represent a variety of biophysical and socio-economic landscape elements and processes (Willemen et al. 2010). Lavorel et al. (2017) indicated that regulating services have been the most commonly mapped, followed by provisioning services (Lautenbach et al. 2015; Maes et al. 2012; Martínez-Harms & Balvanera 2012; Seppelt et al. 2011). However, the approaches for mapping landscape function are many and varied (Crossman et al. 2013b) as are the definition of what needs to be mapped (Nahlik et al. 2012; Nemec & Raudsepp-Hearne 2013). According to Nemec & Raudsepp-Hearne (2013), an ecosystem process does not produce an ecosystem service unless there is a person as beneficiary (Chan et al. 2006). It is therefore important to distinguish between merely mapping the spatial extent of the landscape structure and function using secondary data as proxy, and quantifying the ecosystem services itself from primary data (Nemec & Raudsepp-Hearne 2013). Hauck et al. (2013) suggest that maps are essential for proper management of ecosystems and their services on regional and landscape levels.

One approach has been to derive information on landscape function directly from land use or land cover maps (Burkhard, Kroll & Müller 2010; Haines-Young, Potschin & Kienast 2012; Lautenbach et al. 2015; Maes et al. 2012; Troy & Wilson 2006; Turner, Lambin & Reenberg 2007), as most ecosystem services cannot be directly quantified. The use of indicators or proxy data for quantification has, therefore, been customary (Andrew, Wulder & Nelson 2014; Egoh et al. 2012). However, attributing fixed values for given land cover types (Lautenbach et al. 2015), based on look-up table approaches, can lead to severe uncertainty in mapped ecosystem services supply from national (Eigenbrod et al. 2010) to landscape (Lavorel et al. 2011) scales, if spatio-temporal patterns and processes (Lavorel et al. 2017) are not accounted for. Grêt-Regamey et al. (2014) demonstrated that finer resolution mapping is required especially in topographically complex areas since spatially explicit information about non-clustered and isolated ecosystem services is lost at coarse resolution.

Many spatially explicit, quantitative estimates of biophysical parameters are currently supported by modern RS, with great relevance to landscape mapping (Andrew, Wulder &

Nelson 2014; Ayanu et al. 2012). RS data products that describe biodiversity, plant traits, vegetation condition, ecological processes, soil properties, and hydrological variables can provide direct estimates of the ecological properties that control ecosystems (Andrew, Wulder & Nelson 2014; Li, Xu & Guo 2014), and may contribute to more effective spatial characterisation of landscape function and ecosystem services in support of integrated land use planning (Bennett et al. 2015).

1.3 CHARACTERISING THE LANDSCAPE

Land cover is one of the most important environmental variables (Foody et al. 2013) and reflects the state of the landscape at a particular point in time (Feranec et al. 2010). Satellite-based Earth observation and geographic information systems (GIS) have been established as the best tools for observation, measurement and monitoring of land cover and associated changes (Bodart et al. 2013; Foody et al. 2013; Foody 2002; Olofsson et al. 2013; Schoeman et al. 2013; Szantoi et al. 2016). Earth observation data provide large area coverage of features on the face of the Earth at near real time. The historical archive of such imagery provides multi-temporal monitoring capability and is therefore well suited to generate thematic land cover maps.

By systematically employing image analysis, useful information is derived from electromagnetic radiation reflected or emitted from the Earth's surface captured in satellite images (Blaschke 2010; Campbell & Wynne 2011). It is important that the quality of these land cover maps derived from remotely sensed data be assessed to understand error and its implications, especially if allowed to propagate through analyses and when linking the maps to other datasets (Foody 2002). This is especially the case when using nationally-produced land cover data products, such as are available in the United Kingdom (Fuller, Smith & Devereux 2003), the United States of America (Homer et al. 2015) and South Africa (Schoeman et al. 2013; Van den Berg et al. 2008). Even though accuracy may be reported for land cover maps, some error and uncertainty, of which the size and location are unknown, is often present (Enaruvbe & Pontius 2015; Estes et al. 2018).

Land cover change can involve anthropogenic actions or alterations in biogeochemical cycles, climate and the hydrology of ecosystems (Reyers et al. 2009) from natural processes that manifest in the landscape and can be captured in a land cover map. Independent classification of RS images from two or more different dates is the most common method of generating a multi-temporal series of maps to identify the difference between land cover categories in maps of different instances (Aldwaik & Pontius 2013; Feranec et al. 2010; Stott & Haines-Young 1998) through land cover change analysis. For ease of quantitative and qualitative evaluation

of the land cover conversions, map categories can be generalised to identify typology of changes by using a land cover conversion label assigned to the intersection of successive land cover maps (Benini et al. 2010). In this way, change trajectories can be represented thematically on a map. The accuracy of land cover change modelling is directly dependent on the accuracy of the input land cover data (Burnicki 2011; Foody 2002; Schoeman et al. 2013).

Classification errors in independently generated land cover maps are compounded in a land cover change analysis, possibly leading to spurious landscape changes (Burnicki 2011; Pontius & Lippitt 2006). For any land cover change analysis, the reliability of the land cover change detected should therefore be assessed in order to explain the certainty with which the change can be considered real or spurious (Fuller, Smith & Devereux 2003; Olofsson et al. 2014; Olofsson et al. 2013; Pontius & Li 2010; Pontius & Lippitt 2006). Aldwaik & Pontius (2012) proposed a method for land cover change analysis, called 'intensity analysis', which computes deviations between observed changes and uniform changes. They proposed a method (Aldwaik & Pontius 2013) to compute the minimum hypothetical error that could account for deviations between observed changes and uniform changes (Teixeira, Marques & Pontius 2016).

While the practice of accuracy assessment is well-established within the RS community (Foody 2002; Strahler et al. 2006), many maps are either not evaluated rigorously or only to a limited extent (Foody 2002). In addition, the image classification accuracy guidelines that exist can provide misleading information on the quality of datasets produced (Foody 2008). Very few published studies make full use of the information obtained from accuracy assessments (Olofsson et al. 2013). In addition, accuracy information is generally reported as a global statistic without spatial context (Foody 2005; McGwire & Fisher 2001) to simplify complex data for decision makers (Comber et al. 2017) with no indication of the spatial distribution of change or error (Comber 2013; Foody 2005; Steele et al. 1998). Although map users and producers are interested in communicating and understanding the quality of land cover change maps, many do not consider accuracy reports (Christ 2017) and need guidance on how to assess accuracy in a consistent and transparent manner, especially when RS products are used for scientific, management, or policy support activities (Olofsson et al. 2014).

Overly simple approaches to quantifying trajectories and flows in a landscape can lead to inaccuracies in landscape mapping and valuation (Bagstad et al. 2014). Land cover mapping and modelling fall into the category of ill-structured problems (Saaty 1978) without a single, correct and convergent answer (Hong 1998). Ill-structured problems cannot be solved with an algorithm or a predefined sequence of operations and can also be referred to as unstructured or semi-structured (Densham 1991; Goodchild & Densham 1990). Such problems may have

multiple solutions, solution paths and criteria (Kitchener & King 1981). Ecosystem services present in the landscape can have complex flow dynamics, operating across differing spatial and temporal scales (Bagstad et al. 2013; Grêt-Regamey et al. 2014; Johnson et al. 2012). Consequently, RS data representing biophysical parameters can be incorporated into quantitative and spatially explicit assessments of landscape functionality (Andrew, Wulder & Nelson 2014; Ayanu et al. 2012; Kuenzer et al. 2014; Lavorel et al. 2017). In particular, RS time series data can be used to investigate seasonal profiles (to characterise intra-annual variability) and temporal trajectories (to characterise changes in state or trends in ecosystem condition above and beyond the range of normal seasonal variability) (Vogelmann et al. 2016) to map and monitor a wide variety of ecosystem properties.

Lavorel et al. (2017) reports on the incorporation of inter-annual variability in agricultural practices derived from moderate resolution imaging spectroradiometer (MODIS) data for modelling crop production ecosystem services. Pasquarella et al. (2016) illustrated how ecosystem properties and dynamics manifest in the Landsat data record, but did not attempt to quantify the patterns observed. By monitoring trends in vegetation greenness, Zhu et al. (2016) integrated land cover change data with Landsat imagery to lay the foundation for quantifying and analysing relationships between time series data, ecosystems and ecological processes. It is clear from the existing literature that cooperation between the biodiversity and RS communities in the field of direct or proxy-driven time series, analysis of habitats and habitat changes is needed to support long-term understanding of climate and human-induced change (Dietterich 2009; Kuenzer et al. 2014).

1.4 IMPACT OF INVASIVE ALIEN PLANTS ON ECOSYSTEM SERVICES IN RURAL EASTERN CAPE

South Africa is regarded as a water-stressed country, with low rainfall and high evaporation. All effort needs to be made to effectively manage resources to ensure water security for both social and economic development (DWA 2013). Water security is mainly reliant on surface (fresh) water and its development. Available water is heavily committed for use; surplus reserves are estimated to represent only 1.4% of total national water availability, and the country as a whole is predicted to experience a 1.7% water deficit by the year 2025 (DWAF 2004). Invasive alien plants (IAPs) are estimated to significantly reduce the yields of dams and runoff-river supply systems (DWA 2013). Areas, such as the Western Cape and parts of the Eastern Cape, have periodically suffered from drought prior to 2012 (DWA 2013), while the whole country has recently experienced water stress (Baudoin et al. 2017). Long-term sustainable

solutions must resort to effective management strategies to sustainably prioritise the remaining water reserves. This requires that the impacts of land use practices on water provision under various land tenure arrangements be quantified and addressed.

In the rural Eastern Cape landscape, communal farming is practised alongside commercial livestock farming. Grazing and crop cultivation are the main land use practices (Kakembo 2001; WRC 2013). The area consists of several land tenure systems, which include former commercial farms north of Maclear and traditional and betterment villages, around Cala, and former Transkei rural areas (Kakembo 2001; Wotshela 2009). Invasive Australian Acacia species continue to spread and cause undesirable impacts, despite a considerable investment into management (Van Wilgen et al. 2012). IAPs contribute to land degradation via soil erosion and reduction of water resources (Le Maitre et al. 2016) affecting available ecosystem services to people and the environment (Van Wilgen et al. 2012). Bush encroachment, the invasion and/or thickening of such aggressive undesired woody species, results in an imbalance of the grass to bush ratio, a decrease in biodiversity and a decrease in livestock carrying capacity (De Klerk 2004). IAPs with relatively high biomass translates to higher evapotranspiration rates and reduced runoff (Turpie, Marais & Blignaut 2008).

Since 1995, the Working for Water (WfW) Alien Plant Clearing Programme, initiated as a poverty relief public works programme, has been clearing IAPs with the primary motivation of water saving (Dye et al. 2008; Turpie, Marais & Blignaut 2008). IAP-induced land cover change also disrupts soil characteristics (De Villiers et al. 2005; Okoye 2016), which requires active restoration to prevent IAP regrowth and fostering of natural vegetation with associated ongoing costs (Gaertner et al. 2012). In addition, native plant invasions are also widespread, independent of local land use changes and driven by global climate (Nackley et al. 2017), with impacts structurally and functionally similar to those of IAPs.

Ngorima & Shackleton (2019) reported that increased rural-urban migration and increase of households supplied with electricity, has reduced the value and use of IAPs as an ecosystem service. Consequently, the cost of IAPs may soon outweigh the benefits. Unless deliberate land management intervention takes place, the IAP invasion in the Eastern Cape would continue to increase (Gouws & Shackleton 2019), which has implications for the WfW programme (Van Wilgen & Richardson 2014). Clearing of the IAPs on their own is not sufficient motivation to proceed with the national WfW programme. There needs to be consideration of the sustainability of the landscape when the activities of WfW are completed, through a process such as rehabilitation. To ensure sustainability of landscape processes for human benefit, it is essential to build stronger links between the control of undesirable woody plants and the derived

benefits to humans occupying the land (Oelofse et al. 2016; Skowno et al. 2017). The capture of carbon by the landscape is the primary driver of livestock and food production in this human-dominated social-ecological system. Understanding the total economic value and water use efficiency (WUE) of these processes requires an empirical assessment of the water cycle (Brantley et al. 2018).

For local farmers reliant on grassland, effective rangeland management would require an understanding of the effect of woody encroachment on grass production, as well how land cover trajectories may impact water sources (Gwate et al. 2016). Land cover maps, such as the South African National Land Cover (NLC) dataset with reported accuracy of 67% (Van den Berg et al. 2008), provide incomplete information about the state of the landscape – despite having a high spatial resolution of 30 m – and therefore does not accurately reflect the processes operating in the landscape (Feranec et al. 2010).

An opportunity exists to characterise land cover and identify change in land cover classes over time to derive change trajectories that will describe processes and flows in the landscape affecting ecosystem services. The intensity analysis framework suggested by Pontius, Shusas & McEachern (2004) has frequently been used to describe categorical changes in land cover (Akinyemi & Pontius 2016; Pontius et al. 2013; Teixeira, Marques & Pontius 2016; Zhou et al. 2014), also in South Africa (Jewitt et al. 2015). Temporal changes among categories can be described as systematic, significant and important (Aldwaik & Pontius 2012). Overall change can be partitioned into difference based on the size of the classes, called quantity difference, and disagreement due to possible misallocation of the classes, called allocation difference (Pontius & Millones 2011). Allocation difference can be partitioned into exchange and shift disagreement based on whether pairs of pixels from two or more land-cover classes have exchanged places (Pontius & Santacruz 2014). Quantity, exchange and shift disagreement statistics (Pontius & Santacruz 2014) have not been applied in land cover change studies in South Africa.

Future land cover changes may result in adjustments to biophysical drivers impacting on net ecosystem carbon exchange (Palmer et al. 2017), catchment water use (Gwate et al. 2018) through evapotranspiration (ET), and the surface energy balance through a change in albedo (Gibson et al. 2018). However, although Gibson et al. (2018) discussed the theoretical value of albedo, spatial and temporal relationships between land cover change and albedo – as metric to monitor potential environmental changes at local scale – have not been explored.

1.5 RESEARCH PROBLEM FORMULATION

The concept of landscape dynamics, landscape function and ecosystem services are increasingly used in support of land use management, urban planning and natural resource management decisions (Cowling et al. 2008; Grêt-Regamey et al. 2013; MEA 2005). While the science for assessing ecosystem services is improving, appropriate methods to address uncertainties in a quantitative manner are still lacking (Grêt-Regamey et al. 2013; Grêt-Regamey et al. 2014). Incorporating phenomenological understanding, derived from RS-estimated ecosystem services proxies (Ayanu et al. 2012) into ecosystem services models, would likely increase reliability and robustness of ecosystem services assessments and maps (Lavorel et al. 2017). Time series satellite data (Forkel et al. 2013; Zhu et al. 2016) have recently been used to quantify changing trends in ecosystem productivity and can provide a continuous view of ecosystem dynamics (Kennedy et al. 2014). However, not many data-driven examples exist that establish its use within the RS temporal domain.

Land cover datasets are frequently used as surrogates of ecosystem services and landscape patterns, while land cover classification followed by change analysis remains one of the most popular uses of RS data (Foody et al. 2013). New approaches have emerged as scientists endeavour to accomplish higher accuracies to better characterise the terrestrial surface of the Earth (Blaschke 2010; Gómez, White & Wulder 2016; Khatami, Mountrakis & Stehman 2016), as this provides insight into the processes that occur and shape our environment. To explain the dynamics of a land change system, observed patterns of land cover change must be linked to the underlying processes that are driving the changes. Association of pattern and process requires an accurate quantification of the spatial characteristics of land cover change (Burnicki 2012). Errors in classified maps are propagated to land cover change maps, which affects our ability to accurately relate pattern to process. Spatial autocorrelation and temporal dependence exist between classification errors in time series maps. Therefore, accuracy of such data is of paramount importance.

According to Le Maitre, O'Farrell & Reyers (2007), the impacts on ecosystem service delivery by different kinds of land use, as well as land use change in the form of land degradation and biodiversity loss, have not been studied extensively in South Africa. The linkages between these factors and human well-being are poorly understood and quantified. In the Eastern Cape, stronger links must be built between the control of undesirable woody plants (including IAPs) and the derived benefits to humans to ensure sustainability of landscape processes for human benefit. Empirical evidence of ecosystem services, such as the water use of every component of the diverse landscape described by land cover, needs to be collected to strengthen such

linkages. Understanding the variability in time and space of land use change linked to ecosystem services change can provide the foundations for effective management of such change. For this to be successful, accurate change maps are required.

Modelling, particularly if performed using a spatially explicit approach, is an important technique for projecting and exploring alternative future scenarios, thereby gaining understanding to quantitatively describe key processes (Lavorel et al. 2017; Veldkamp & Lambin 2001). The following research questions have been formulated towards achieving this:

- *How accurately can transformations in land cover be quantified using existing datasets?*
- *How do trends in biophysical drivers and characteristics of land cover change trajectories differ from one region to another?*
- *How does the pattern of error in land cover change datasets affect modelling of evapotranspiration and carbon storage?*
- *How can ecosystem stress be characterised using Earth observation data and time series analysis?*

1.6 RESEARCH AIM AND OBJECTIVES

The aim of this study is to demonstrate how land cover change, in particular encroachment by woody vegetation, impacts landscape function provided by grasslands in the Eastern Cape. Systematic land cover change and trend analyses of RS-derived biophysical variables will be carried out to determine how land cover change affects the surface energy budget, as well as the carbon cycle.

The following objectives have been identified to achieve these aims:

1. Perform systematic land cover change analyses on existing data products using land cover conversion labels and intensity analysis.
2. Characterise spatial patterns of land change dynamics using land cover conversion labels to represent and interpret transitions.
3. Apply quantitative techniques of intensity analysis to describe and interpret patterns of land change.
4. Characterise the relationship between land cover change and ecosystem stress using RS time series analysis.

Through these objectives the study investigates the use of independent land cover maps for change analysis in a grassland-dominated landscape in the Eastern Cape of South Africa, with the explicit purpose to delineate land cover change trajectories that are crucial to accurately

quantify water and carbon fluxes. Invasion by woody plants as a driver of grassland transformation, which in turn influences rangeland ecosystem services, such as forage production, water supply, habitat, biodiversity, carbon sequestration and recreation, is quantified. The stated aim and objectives were designed to address the identified knowledge gaps by demonstrating how novel geospatial techniques can assist with managing ecosystems. Specifically, solutions will be presented to: (1) determine the accuracy of existing land cover datasets frequently used as surrogates of landscape processes; and (2) model future scenarios by evaluating land cover change trends.

1.7 RESEARCH METHODOLOGY AND AGENDA

In accordance with Van der Merwe & De Necker (2013), a research methodology refers to the theoretical paradigm or framework in which the research was conducted. This research was investigative and experimental in nature and approached from a synoptic perspective. Spatio-temporal analysis of RS data products combined in a modelling framework was used to analyse regional spatial patterns and develop predictions. Concentrating on impacts and drivers of land cover change, the study falls within the emerging interdisciplinary research field of land change science (Verburg et al. 2015).

This dissertation draws on a wide range of technologies and approaches, ranging from land cover classification and land cover change analysis to land change modelling. Spatial patterns of land cover transition-flows are described using an indicator-based approach, intensity analysis and the change budget. Local and global methods are explored to uncover map error. Using trend analysis, the relationship between land cover change, water use and carbon sequestration using satellite products was investigated. The research formed part of Water Research Commission (WRC) funded project (K5/2400/4) *Rehabilitation of grasslands after eradication of alien invasive trees*, with overall project aim to assess, and make recommendations for improving the grass production from areas that have been cleared of wattle. The project was affectionately named *"Emva kwe dywabasi"* by stakeholders, which means "after the wattle" in isiXhosa. The research was performed in a quantitative paradigm, depicted in the research design (Figure 1-1) and comprises four components, each relating to one of the research objectives.

Chapter 3 demonstrates the accuracy of real land cover change as determined by land cover change analysis, while characterising degradation gradients using an indicator-based approach (published as Münch et al. 2017). The chapter consequently addresses Research Objective 1.

Chapter 4 relates to Research Objective 2, as it describes the use of landscape change analysis within the intensity analysis framework (Pontius et al. 2013) to discover the effects of map error and characterise spatial patterns. Chapter 4 also partly addresses Objective 3, given that quantitative techniques, such as the change budget (Pontius & Santacruz 2014), derived by partitioning change into quantity and allocation disagreement and referred to as the disagreement budget, are applied and demonstrated at global and local level.

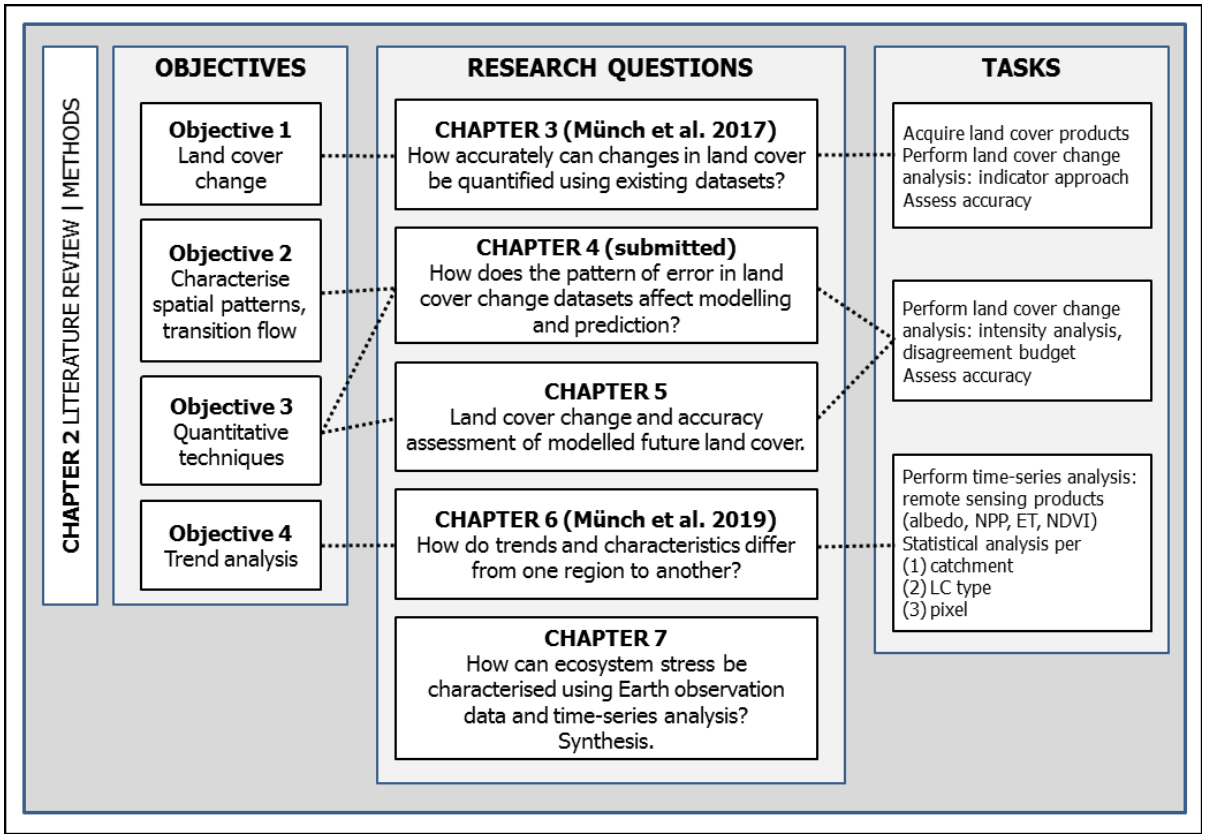

Figure 1-1 Research design

In Chapter 5, land change modelling is described. Land cover was modelled to a future date using predictor variables and land cover change analysis between observed (Chapter 3) and modelled data, as well as the accuracy assessment performed using the same quantitative techniques in a different context. Based on the future model, management principles for the catchments are proposed. Chapter 6 describes the trends in albedo, in support of Objective 4 and research question "*How do trends and characteristics differ among the various catchments and sub-catchments?*" The final chapter (Chapter 7) provides a synthesis of the research and discusses the important role land cover change plays in landscape function mapping and management. To draw the dissertation to a conclusion, Chapter 7 answers the final research question "*Can ecosystem stress be characterised using Earth observation data and time series analysis?*"

Having concluded Chapter 1, which introduced the research problem, aim and objectives, Chapter 2 provides background literature on land cover change analysis methods and terminology, landscape function mapping and trend analysis, especially with the focus on using RS data for the analysis.

CHAPTER 2: A REVIEW OF LITERATURE AND METHODS: LANDSCAPE FUNCTION, DYNAMICS AND MANAGEMENT

... nature is perfect till man deforms it with care.

Alexander von Humboldt (1850: x)
in Meskell (2011: 22)

Land change science addresses the causes and consequences of change in the surface of the Earth and includes observation, monitoring, modelling and projection of that change (Turner 2017). Drawing on the background of the German *Landschaft* traditions introduced by Von Humboldt, Ritter and Ratzel (in Arntz 1999: 297-300), land change science integrates the research interests of the social ecologies, environmental sciences, remote-sensing and GIS and spatial sciences (Chowdhury & Turner 2019; Turner 2017). According to Hartshorne (1939: 23), "…geography was conceived of as a science of relationships between the natural environment and human activities", and concepts and methods to measure the effects of these relationships in the context of land change science, are described in this chapter.

When considering the title of the dissertation: *Towards land change management* using *ecosystem dynamics* and *land cover change*, it makes sense that an objective and critical summary of relevant literature should include a review of literature relating to each of the italicised terms. The literature considered for this review falls within the domains of landscape science and land change science, which are centred on research and implementation challenges for changing land uses/covers in regional social-ecological systems (Robinson & Carson 2013) and will deal with land cover and land cover change in a coupled human-environment system (Turner & Robbins 2008).

In the next section, the emphasis is on ecosystem dynamics and land cover change, and how knowledge acquired about landscape dynamics in analyses, can contribute to land change management. Firstly, the inter-relationship between landscapes and ecosystem dynamics will be explored. Before deliberating on land use and land cover, land cover change and land change modelling, the effect of woody encroachment on the ecosystem services in the grasslands will be discussed, touching on land management. However, different land change management practices will not be covered in detail. Although image processing was undertaken to create land cover data (Chapter 3), this review will not provide exhaustive background on image pre-processing, but merely reflect on image classification techniques for land cover delineation. According to Wulder et al. (2018), the need to undertake pre-processing steps has been

significantly reduced with the availability of well calibrated imagery, analysis ready data and higher-level derived products. Digital maps are often used when investigating landscapes. However, a map is a human construct, merely a model of reality, where scale determines the detail that can be represented. While map error is a universal concern, and the focus of much of this dissertation, it is especially a concern when using classified (i.e. categorical) data due to the potential for misclassifications (Turner & Gardner 2015). Trend analysis, specifically used with remotely sensed data, will be appraised later in this chapter, concluding the literature review.

2.1 LANDSCAPES AND ECOSYSTEMS DYNAMICS

While Hartshorne (1939) defined landscape as a part of the earth's surface with its components as perceived by humans, a more distinct definition of the term landscape was introduced in Chapter 1, namely "a spatially heterogeneous area of interacting ecosystems that function as a unit and can be analysed at any scale" (Chapter 1: 2). According to the American Heritage® Science Dictionary (Editors 2011), a system in which a community of living organisms (biotic) interact with non-living components (abiotic) of their environment, is called an ecosystem, whereas ecosystem dynamics describe the study of how ecosystems change over time. Processes of change can be described as stable linear or rapid non-linear, which can drive the system outside of its normal operating parameters (Chapin, Matson & Vitousek 2011). Change in ecosystems can generally be of seasonal nature and reflect gradual change or be abrupt, caused by disturbances in the landscape. Heterogeneity of the landscape determines interactions among ecosystems (Turner & Gardner 2015). Therefore, it is important to understand the patterns, causes and consequences of spatial heterogeneity for ecosystem function (Chapin, Matson & Vitousek 2011; Lovett et al. 2005).

Ecosystems support human well-being by providing various 'goods and services' to society (Englund, Berndes & Cederberg 2017) based on the capacity of the landscape to deliver the particular function (Bennett et al. 2015; Turner & Gardner 2015). These are termed 'ecosystem services' (Costanza et al. 1997; Daily 1997; Ehrlich & Ehrlich 1981; MEA 2005). The concept of ecosystem services is widely recognised and modelling and mapping approaches for ecosystem services at different spatial and temporal scales have been extensively researched (Burkhard et al. 2013; Crossman et al. 2013b). As most ecosystem services cannot be directly quantified, a clear distinction must be made between mapping the ecosystem service and mapping the landscape within which the ecosystem service operates (Nemec & Raudsepp-Hearne 2013). Indicators or proxy data derived from land cover maps have widely been used

for quantification of ecosystem services (Andrew, Wulder & Nelson 2014; Burkhard, Kroll & Müller 2010; Egoh et al. 2012; Haines-Young, Potschin & Kienast 2012; Lautenbach et al. 2015; Maes et al. 2012; Troy & Wilson 2006; Turner, Lambin & Reenberg 2007).

Egoh et al. (2008) mapped the production of five ecosystem services in South Africa to assess the relationship and spatial congruence between services and evaluate the value of these ecosystem services as a proxy measure compared to primary production. Primary production showed some potential as a surrogate for ecosystem service distribution. Egoh et al. (2012) followed up this work with an extensive review of possible ecosystem services indicators, which was used to provide a methodological framework for mapping and assessing ecosystems and their services at European scale (Maes et al. 2012), thereby going beyond merely using land cover based assessments in policy and decision making.

Extensive research, providing consistent and scientific information for enhanced decision making on various aspects that affect the landscape and their impacts on ecosystem services are now focussed on development of management strategies and land governance (Deininger, Selod & Burns 2011). Under the auspices of the Global Land Programme (https://glp.earth/) (Verburg et al. 2015), land change science has emerged as an interdisciplinary research field, concentrating on both drivers and impacts of land change (Rindfuss et al. 2004; Turner, Lambin & Reenberg 2007).

In the context of land change science, Robinson & Carson (2013) argued that assembling qualitative and quantitative data was the starting point for management of complex non-linear processes that operate at landscape scale. Data for land use and land cover change analyses have been extracted from various sources, including remote sensing (Verburg et al. 2015). Verburg, Neumann & Nol (2011) identified that spatially, temporally and thematically heterogeneous data sources presented various challenges due to intrinsic uncertainties. Moreover, long-term land cover change data have proved to be of great importance in preparation of concrete local, regional and national land management measures, as well as generating management scenarios. Nevertheless, the need exists for sustainable land management practices and policies.

Keesstra et al. (2018) advocated for the use of nature based solutions, implemented in mainstream land management strategies, to assist with restoration of ecosystem services. Egoh et al. (2008) highlighted that for effective management of biodiversity and ecosystem services in a heterogeneous landscape, the focus should be on ecosystem service hotspots that deliver multiple ecosystem services, as the landscape effect varies according to the service being

studied (Duarte et al. 2018). Long & Qu (2018) formulated a theoretical model of regional land use transitions within the framework of natural system-economic system-managerial systems to assist with formulation of land management policies. Mechanisms of mutual feedback were established between land use transition and land management, where land use transitions were affected by land management via economic measures, land engineering, policy and institution; whereas land use transitions contributed to land management via socio-ecological feedback. The authors argued that not only current, but also subsequent future scenarios of land use transitions should be considered. Crossman et al. (2013a) acknowledged that, while human decision making at national to global scale influenced land system changes, likewise local land systems changes feedback on ecosystem services and decision making, concurring with Verburg et al. (2015: 30) that "…land system change is both a cause and consequence of socio-ecological processes". This leads to the next section, where the problem of woody encroachment in the grasslands, the effect on the ecosystems services provided by grasslands and land management of the grasslands, will be deliberated.

2.2 GRASSLANDS, INVASIONS AND ECOSYSTEM SERVICES

In South Africa, grasslands have been affected by degradation and habitat transformation, resulting in most grassland vegetation types being classified as endangered or vulnerable (Reyers et al. 2007). Grasslands provide ecosystem services required to support human well-being, such as below ground carbon storage, surface water supply, water flow regulation, soil accumulation and soil retention (Gwate et al. 2018). In a study to identify spatial priority areas for conserving ecosystem services, Egoh et al. (2011) found that to conserve at least 40% of the soil and water services, preserving only between four and 13 per cent of the grassland biome was required. In contrast, to conserve 40% of the carbon service provided by the grassland, 34% of the grassland biome must be conserved. Due to the moderate to high overlap between priority areas for ecosystem services and biodiversity, a single combined systematic conservation plan was proposed (Egoh et al. 2011).

Land degradation, defined as "… a reduction in the capacity of land to perform ecosystem functions and services that support society and development" (Koohafkan, Lantieri & Nachtergaele 2003: 1), is a major threat to productivity of the grasslands. This is exacerbated by livestock production in the semi-arid Eastern Cape. Land management is characterised by either private ranching under freehold tenure or on a communal basis on land that is under dualistic or bilateral landholding arrangement (Bennett, Palmer & Blackett 2012).

Furthermore, invasive Australian Acacia species continue to spread, despite a considerable investment into management (Van Wilgen et al. 2012) with abandoned cultivated land especially vulnerable to infestation (Blair, Shackleton & Mograbi 2018; De Neergaard et al. 2005; Scorer, Mantel & Palmer 2019). Invasive alien plants (IAPs) contribute to land degradation via soil erosion and reduction of water resources (Gwate et al. 2018; Le Maitre et al. 2016; Palmer et al. 2017) affecting available ecosystem services to people and the environment (Van Wilgen et al. 2012). Bush encroachment, the invasion and/or thickening of aggressive undesired woody species, has been a rangeland management problem since the early 1900s (Skowno et al. 2017). Generally seen as a form of ecological degradation caused by poor land management practices (Hobbs 2016; O'Connor, Puttick & Hoffman 2014), bush encroachment results in an imbalance of the grass to bush ratio, a decrease in biodiversity and a decreased livestock carrying capacity (De Klerk 2004), which potentially threatens food security. Invasions in grazing areas, around riverbanks and homesteads are seen as undesirable, with risk of crime in wattle-infested areas (Shackleton et al. 2007; Shackleton et al. 2016).

Given that South Africa is a water-stressed country, with low rainfall and high evaporation, effective water resources management is required to ensure water security for both social and economic development (DWA 2013). Therefore, agricultural legislation was enacted to address the problem of alien plant invasion and indigenous woody plant encroachment. The Working for Water (WfW) Alien Plant Clearing Programme has also been combatting alien plant invasions since 1995. The primary motivation for IAP clearing was to conserve water provisioning ecosystem services (Dye et al. 2008; Turpie, Marais & Blignaut 2008) as the relatively high biomass of IAPs translates to higher evapotranspiration rates and reduced runoff (Turpie, Marais & Blignaut 2008).

Although soil erosion and soil fertility declines could be attributed to land management practices, such as heavy grazing (Blair, Shackleton & Mograbi 2018), IAP-induced land cover change also disrupts soil characteristics (De Villiers et al. 2005; Oelofse et al. 2016; Okoye 2016). Active restoration is then required to prevent IAP regrowth and facilitate re-establishment of natural vegetation (Gaertner et al. 2012). Continued land management through stewardship and intervention through assisted restoration and thinning of existing trees will be necessary to manage current and new IAPs, as well as native invaders (Nackley et al. 2017; Scorer, Mantel & Palmer 2019).

Nevertheless, should woody plant increase in grassy biomes be a consequence of elevated atmospheric CO_2 in the face of climate change, rangeland managers may need to adopt an adaptive attitude to a different ecosystem state (Case & Staver 2017; Hobbs 2016). A positive

consequence of the increased woody biomass may be increased carbon storage in the landscape (Cai et al. 2016a).

In this section, some of the effects that land cover change due to woody encroachment in the grassland could have on ecosystems services and biodiversity were discussed. The next sections will compare land use and land cover, provide an overview of land cover classification methods and review accuracy assessment, leading into land cover change.

2.3 LAND COVER

Although the terms are often used interchangeably, land use and land cover have some fundamental differences. Anderson et al. (1976) recognised the importance of land use for planning and management, before quoting definition of land use of Clawson & Stewart (1965) as, "man's activities on land which are directly related to the land" while describing land cover as, "the vegetational and artificial constructions covering the land surface" (Burley 1961: 19). Stated simply, land use refers to the purpose the land serves, but does not describe the surface cover on the ground, conversely land cover refers to the surface cover on the ground, but does not describe the use of land. In addition, the land use may be different for land with the same cover type. Land use, and the resulting landscape character (cover), is therefore the result of complex human–environment interactions (Bastian, Krönert & Lipský 2006; Feranec et al. 2010). Since land cover is one of the most important environmental variables (Foody et al. 2013) reflecting the state of the landscape at a specific point in time (Feranec et al. 2010), some of the methods to derive land cover will be described next.

2.3.1 Land cover classification

Satellite-based Earth observation and geographic information systems (GIS) have been established as the best tools to observe, measure and monitor land cover (Bodart et al. 2013; Schoeman et al. 2013; Szantoi et al. 2016). Earth observation is used to capture useful information in satellite images, derived from electromagnetic radiation reflected or emitted from the Earth's surface (Blaschke 2010; Campbell & Wynne 2011) to provide near real time large area coverage of features on the face of the earth. Despite extensive availability of radar-based and thermal infrared satellites, these sources of data are not within the scope of this review, and the focus will be on the use of optical remote sensing. The historical archive of available imagery offers multi-temporal monitoring capabilities. Wulder et al. (2018) elaborated on the fact that, despite the increasing number of sensors available to provide imagery at medium and high spatial resolutions (Belward & Skøien 2015), none have achieved

the temporal depth, radiometric calibration and open access of the Landsat program (Roy et al. 2014; Wulder et al. 2016). However, multi-sensor satellite data from ESA Sentinel and Landsat, could already supply near weekly cloud-free surface observations (Li & Roy 2017) for monitoring.

Analysis of complex landscape objects, captured in remotely sensed imagery, is simplified through land cover classification (Campbell & Wynne 2011). Classification involves grouping similar image pixels into classes, with each pixel evaluated as a discrete unit composed of values in several spectral bands (Campbell & Wynne 2011). Jansen & Gregorio (2002) noted that classification is an abstraction representing reality; it would consequently contain inherent generalisations. A land cover classification system (LCCS), either standardised or project specific, determines the nature and extent of classes and provides the thematic legend (Jansen & Gregorio 2002; Loveland et al. 2000). Producers of land cover data require pure (homogenous) land cover classes that are easily extracted from remote sensing derived data with high classification accuracies, while user requirements are land use driven with land cover only applying to areas covered by natural vegetation (Lück et al. 2010). For planning and management purposes, land use data are more important than land cover data (Wulder et al. 2018), although more difficult to classify.

Petit et al. (2002) suggested that, in the interest of comparing compatible classes between heterogeneous land cover datasets prior to land cover change analysis, levels of thematic content and spatial details must be balanced. This can be achieved by using map generalisation to minimise map inconsistencies, thereby creating a simplified legend. Generally, detailed classes are aggregated under a number of conceptually broader classes (Lück & Diemer 2008). Aldwaik, Onsted & Pontius (2015) warned that, while aggregation could simplify interpretation, it can also influence the sizes and types of changes mapped. Implementing an existing hierarchy (reclassification scheme) to facilitate aggregation may then hide important category dynamics, prompting the use of a behaviour based aggregation algorithm (Aldwaik, Onsted & Pontius 2015).

Both per-pixel and object-based image analysis (OBIA) approaches are used in image classification. In contrast to per-pixel approaches, which manipulate individual pixels, OBIA aims to delineate meaningful spatial units in images based on spatial, structural and hierarchical properties in addition to spectral properties. These units are then classified in an integrated way (Lang 2008). The effect of the change of classification units is that the within-class spectral variation is reduced, removing the so-called salt-and-pepper effects typical of per-pixel classification (Liu & Xia 2011). Common image classification techniques include

unsupervised, supervised and hybrid classification (M Li et al. 2014). Various classification algorithms are available with the maximum likelihood classifier (MLC) being one of the most frequently used algorithms. However, parametric MLC, with its requirement for large training datasets, is not useful for big datasets. Variables (features) derived from satellite data are known to be non-parametric (not normally distributed) and the ranges of targeted classes often overlap (Wulder et al. 2018).

Non-parametric supervised classifiers, such as artificial neural networks (ANN), support vector machines (SVM) and decision tree classifiers, can accommodate complex feature space relationships among classes, and have been shown to be more efficient and accurate than parametric classifiers (Pal & Mather 2005). Furthermore, ensembles of non-parametric classifiers and implementations that apply different random subsets of training data multiple times (Doan & Foody 2007; Friedl et al. 2010; Hansen et al. 2008) have been implemented to improve classification results. For instance, the random forest classifier (Belgiu & Drăguţ 2016) has become one of the most popular ensemble classifiers, especially for large area classifications (Zhang & Roy 2017).

In their review of image classification techniques, M Li et al. (2014) described the use of spatio-contextual information, such as texture extraction (Holobâcă, Ivan & Alexe 2019; M Wang et al. 2018) and Markov random field modelling (Liu & Cai 2012; Moser, Serpico & Benediktsson 2013; Wehmann & Liu 2015), that use the relationship between a pixel and its neighbour in image classification. M Li et al. (2014) concluded that due to their conceptual simplicity and easy implementation, spectral classifiers have remained popular for land cover classification, although the growing realisation that spatial information is important, especially when classifying high resolution imagery, will cause increased popularity of spatio-contextual classifiers.

2.3.2 Map accuracy

Classification accuracy is the direct measure of the quality of maps produced through land cover classification (Foody 2008). No classified map is ever completely correct, it is therefore critical that the accuracy of land cover maps derived from remotely sensed data be assessed to understand error and its implications, especially if allowed to propagate through analyses linking the map to other datasets (Foody 2002). Ideally, a formal accuracy assessment should be completed that involves extensive ground truthing of the map (Turner & Gardner 2015). However, since map error is often unknown (Enaruvbe & Pontius 2015) or a formal accuracy

assessment is beyond the capacity of the analyst (Turner & Gardner 2015), it is important to gain at least a qualitative assessment of map accuracy.

A square contingency table (sequence of categories in rows is the same as in columns) is generally used to show the association between rows representing map categories and columns representing reference categories (Agresti 2019). The contingency table is called an error or confusion matrix in remote sensing land cover classification, with computed estimates typically being overall accuracy (OA), user's accuracy (UA) and producer's accuracy (PA), and commission and omission error percentages (Congalton & Green 2009). The OA represents the percentage of cases correctly allocated to their respective thematic land cover classes (Foody 2002). The PA, of use to the map producer, is a measure of how well a certain area has been classified and indicates the probability of a reference sample being correctly classified (not omitted) (Congalton 2001). The UA, on the other hand, is aimed at the map user, and indicates for a given class how many of the pixels on the map are actually classified correctly (Olofsson et al. 2013). The UA can be computed directly from the sample counts. Criticised by Pontius & Millones (2011), the family of kappa indices have traditionally been used to accommodate for the effects of chance agreement (Foody 2002). AUC (area under the curve) ROC (receiver operating characteristics) curve methods can be used for classification accuracy (Pontius & Schneider 2001). Foody (2008) also recommends the use of confidence intervals computed from the OA using the formula:

$$t\sqrt{\frac{p(1-p)}{n-1}} \qquad \text{Equation 2-1}$$

where p is the proportion of correctly allocated cases (OA);
n is the number of cases used in the assessment; and
t is derived from the *t* distribution at the desired level of confidence.

Statistically defensible and transparent accuracy assessments (Stehman 2009) are essential to ensure user confidence and ensure the integrity of the land cover products (Wulder et al. 2018). While recommendations and good practice guidance have been advocated (Foody 2002; Olofsson et al. 2014), these have not always been followed. Olofsson et al. (2013) gave advice on the content of an accuracy assessment: it should contain a clear description of the sampling design (sample size and scheme); an error matrix; the area of each land cover class according to the map; and descriptive accuracy measures (user's, producer's and overall accuracy). Olofsson et al. (2013) also recommended that mapped areas should be adjusted to eliminate bias caused by map classification error, and confidence intervals must be supplied to quantify the sampling variability of the estimated area, in agreement with Foody (2008).

Accuracy measures estimated from a sample may be subject to uncertainty (Olofsson et al. 2014; 2013; Pontius, Shusas & McEachern 2004). Therefore, a more robust approach would be to report all figures in the estimated error matrix in terms of proportion of area; and estimates of overall accuracy, user's accuracy and producer's accuracy based on the population (Pontius, Shusas & McEachern 2004). Olofsson et al. (2013) also recommended the use of confidence intervals that provide a range of values for the reported parameter, taking the uncertainty of the sample-based estimate into account.

While the practice of accuracy assessment is well-established within the RS community (Foody 2002; Strahler et al. 2006), many maps are either not evaluated rigorously or only to a limited extent (Foody 2002). Very few published studies make full use of the information obtained from accuracy assessments (Olofsson et al. 2013). Although map users and producers are interested in communicating and understanding the quality of land cover maps, many do not consider accuracy reports (Christ 2017) and need guidance on how to assess accuracy in a consistent and transparent manner, especially when RS products are used for scientific, management or policy support activities (Olofsson et al. 2014).

Foody (2005) explained that one of the limitations of the conventional approach to classification accuracy assessment, i.e. using a confusion matrix-based approach, is that it is not spatially explicit (McGwire & Fisher 2001). It yields a single, global (in the sense of relating to the entire classified dataset), estimate of thematic classification accuracy and masks the fact that classification accuracy varies spatially. Only an estimate of the overall accuracy of the entire classification is given. However, this global overall summary statistic simplifies complex data for decision makers (Comber et al. 2017). Moreover, accuracy and error can vary spatially, since misclassifications are typically not randomly distributed over the mapped area, with error concentrated near class boundaries (Congalton 2001; Steele et al. 1998) and/or can be systematically located in relation to issues, such as sensor view angle effects (Foody 2005).

Various authors have explored spatially explicit methods for classification accuracy. Steele et al. (1998) modelled spatial maps of error using kriging interpolation, while McGwire & Fisher (2001) recommended using a Monte Carlo approach. Foody (2005) demonstrated the potential of calculating geographically distributed correspondence matrices and interpolated between them to generate surfaces of error. Comber et al. (2012) used geographically weighted regression to create local correspondence matrices, whereas Tsutsumida & Comber (2015) applied geographically weighted logistic regression to the confusion matrix to address spatio-temporal accuracy for time series land cover data. Comber et al. (2017) recommended the use of geographically weighted correspondence matrices in combination with quantity and

allocation disagreement (Pontius & Santacruz 2015) as a generic spatially explicit approach. Comber et al. (2012) observed that, despite the advances supported by these methods, current validation and accuracy techniques in remote sensing have largely ignored spatially explicit methods.

Generating a land cover map accurately and quantifying the extent of a land cover class require careful selection of reference data for use in both training and validation (Congalton & Green 2009; Foody 2002; MacLean & Congalton 2012; Olofsson et al. 2013). The accuracy of training data will influence the success of the classification, while the validation data, assumed to be correct, are used to perform accuracy assessment (Congalton & Green 2009; Foody 2002). When considering robust methods to generate land cover products for multiple repeat time steps, in preparation for change analysis, Gómez, White & Wulder (2016) recommended the use of novel inputs, such as land cover transitions, improved quality of training samples and combinations of multi-scale, multi-sensor data for improved accuracy.

Kinkeldey (2014) contended that despite accuracy assessment, uncertainty is essentially present in all thematically classified land cover data because boundaries between land cover objects are inherently uncertain due to geometric inaccuracies, ambiguity in classification and vagueness in class definitions (Fisher et al. 2006). Wulder et al. (2018) argued that a common repository of reference data to aid in accuracy assessment activities, such as a global accuracy assessment database for land cover (Khatami, Mountrakis & Stehman 2017), would be invaluable for land cover mapping research as large training sets will potentially increase land cover accuracy and promote scientific development.

2.4 LAND COVER CHANGE

The importance of land cover change as a research topic was confirmed by Google Scholar keyword searches on terms *'land cover change'* and *'remote sensing'* , which yielded scholarly links to more than 77 800 articles, with almost 9 600 articles published since 2018. Land cover change can be caused by anthropogenic actions, such as economic, social, cultural, political or institutional forces (Verburg et al. 2006), or initiated by natural processes, such as alterations in biogeochemical cycles, climate and the hydrology of ecosystems (Reyers et al. 2009). The physical changes that are reflected in the landscape can then be measured by analysing remote sensing products. Jansen & Gregorio (2002) identified that land cover changes could represent conversion from one class to another, or modification within one class, which would have implications for the particular methods selected for both land cover classification and change detection. Various procedures have been developed for comparison of images at different time

steps and has been extensively reviewed (Coppin et al. 2004; Hussain et al. 2013; Lu et al. 2004; Mas 1999; Singh 1989; Tewkesbury et al. 2015).

Based on the transformation procedures and analysis techniques applied, the general approaches to change detection have involved comparison of two or more independent land cover maps, multi-date data classification and image enhancement (Mas 1999; Singh 1989). Lu et al. (2004) identified three phases when performing change detection with remotely sensed data, namely (1) image pre-processing – which includes geometrical rectification as well as image registration, radiometric, atmospheric and topographic correction; (2) change detection technique selection; and (3) accuracy assessment.

2.4.1 Change detection

Tewkesbury et al. (2015) critically summarised change detection techniques from the perspective of several decades of satellite remote sensing. They emphasised that the analysis unit is an important construct to consider in change detection and described commonly used analysis units, such as pixels, objects, and kernels. They also overviewed common change detection techniques such as image analysis overlay, image analysis comparison, multi-temporal image object and polygon vector analyses. The authors compared various analysis units to the fundamental features of image interpretation, as documented by Avery and Colwell (in Campbell 1983: 43), namely size, shape, tone, texture, shadow, pattern and association.

Comprehensive lists of comparison methods during change detection have been presented in previous reviews (Coppin et al. 2004; Hussain et al. 2013; Lu et al. 2004; Mas 1999; Singh 1989). Tewkesbury et al. (2015), however, summarised these methods into six broad groupings (Mas 1999): (1) layer arithmetic; (2) post-classification or map-to-map change detection; (3) direct classification of multi-temporal image stack; (4) data transformation, such as principle component analysis (PCA) and multivariate alteration detection (MAD), applied to a multi-temporal stack; (5) change vector analysis (CVA); and (6) hybrid change detection, often expressed as a layer arithmetic operation, followed by direct classification of changed features (Lu et al. 2004). Hussain et al. (2013) further highlighted the challenges associated with the exponential increase in the image data volume and multiple sensors, especially with the use of very high resolution imagery and object-based methods, suggesting the potential of data mining techniques for change detection (Hussain et al. 2013).

Despite the many and varied comparison methods uncovered, the most common change detection method used to identify the difference between land cover at two time steps, has been independent classification of multi-date RS images (Aldwaik & Pontius 2013; Feranec et al.

2010; Stott & Haines-Young 1998; Tewkesbury et al. 2015). Although all digital change detection methods are affected by spatial, spectral, temporal and thematic restrictions (Coppin et al. 2004), the advantage of this change detection technique is that both the baseline classification and the change transitions are explicitly known (Tewkesbury et al. 2015).

2.4.2 Accuracy and uncertainty

Olofsson et al. (2013) contended that to perform an accuracy assessment effectively, is by no means a trivial task and requires time and resources. Accuracy is defined as the degree to which the map produced agrees with the reference classification (Olofsson et al. 2013). Burnicki (2011) noted that the change detection error matrix is the most reported accuracy assessment tool and is an extension of the single-date classification error matrix (Section 2.3.2), and its related statistics. The error matrix or contingency table (Section 2.3.2) is called a conversion or transition matrix in temporal land cover change analysis (Pontius 2019). Rows represent the initial categories (land cover classes), while columns signify the final categories. Gross loss and gross gain are calculated respectively from the row and column differences and the diagonals of the transition matrix (Comber et al. 2016). Total landscape change is computed as the difference between observed losses and gains.

Ideally, the change accuracy assessment should be performed on the final change map, as done for the single-date input images, since combining accuracy measures produced for the single-date land cover maps may not necessarily indicate the accuracy of the change map (Burnicki 2011). Stratified sampling is, therefore, a common approach to use when sampling for change accuracy assessment (Stehman & Wickham 2006; Stehman, Sohl & Loveland 2003). This is done by dividing the map of change into meaningful strata and conducting sampling separately within each stratum, making sure that all transitions are covered (Burnicki 2011).

Whilst performing land cover classification for the purpose of change analysis, Burnicki (2011) showed that the spatial error structure was comprised of small-scale local error interactions, as well as exhibiting a large-scale trend. In addition, interaction between single-date land cover maps due to temporal dependence increased the expected accuracy of the change map (Burnicki, Brown & Goovaerts 2007). Classification errors in independently-generated land cover maps can be compounded in land cover change analysis, leading to erroneous results in measured landscape change (Burnicki 2011; Pontius & Lippitt 2006). The accuracy of land cover change maps produced from post-classification change detection is therefore directly dependent on the accuracy of the input land cover data (Burnicki 2011; Foody 2002; Schoeman et al. 2013). Under the assumption of temporal independence, the expected OA for a map of

change is estimated by multiplying the individual accuracies for each classified map (Pontius & Li 2010; Pontius & Lippitt 2006). The accuracy and reliability of the land cover change detected should therefore be assessed in order to explain the certainty with which the change can be considered real or spurious (Fuller, Smith & Devereux 2003; Olofsson et al. 2014; Olofsson et al. 2013; Pontius & Li 2010; Pontius & Lippitt 2006).

According to Olofsson et al. (2013), an accuracy assessment of a land cover change map should contain at least estimates of change accuracy and changed area, adjusted for classification error and confidence intervals. The transition matrix, also known as correspondence or confusion matrix, used in the analysis should be included (Pontius 2019). Burnicki (2011), therefore, argues that map accuracy reporting must extend beyond map-wide (global) non-spatial summaries and should include information about the spatial and temporal characteristics of error in a change map. This is in agreement with Comber et al. (2017: 234), who reflected on the "philosophical underpinnings of local rather than global approaches for modelling landscape processes" and that the remote sensing community should engage in more advanced reporting techniques, such as local statistical models.

Uncertainty in land cover change can be quantified from the accuracy assessment (Zhang & Goodchild 2002), from classification confidence (Brown, Foody & Atkinson 2006) or from expert knowledge (Lowry et al. 2008). Similar to Lowry et al. (2008), Kinkeldey (2014) defined a straightforward uncertainty measure for land cover change on the basis of fuzzy membership values, with the complement of the minimum membership value yielding a value for change uncertainty. Kinkeldey (2014) suggests that a potential benefit of using change uncertainty lies in the reduction of falsely detected change.

2.4.3 Change analysis

Change analysis describes further analysis of change detection results, in an attempt to distinguish error from actual change. According to Kinkeldey (2014), change detection outputs are generally thematic datasets that are sensitive to classification error and location error (geometric misregistration or positional error). Carmel & Dean (2004) noted that co-registration errors can occur when using a multi-temporal stack of images and is generally an extension of individual image location errors. To measure both location and classification error, Carmel & Dean (2004) developed the combined location classification (CLC) error model to determine uncertainty in a collection of land cover maps. They reported that the CLC error model could be used to assess overall uncertainty when performing thematic change detection analysis as a good agreement was found between model predictions and simulation results.

Kennedy, Cohen & Schroeder (2007) tested a conceptual approach to change detection for forests using a dense temporal stack of Landsat imagery for a 20-year period. Distinctive temporal progressions prior and post change event caused characteristic temporal signatures in spectral space. The automated method searched for idealised signatures in the entire temporal trajectory of spectral values with overall accuracies ranging between 77-90%.

Benini et al. (2010) devised a method to generalise map categories by identifying typology of change and assigning a conversion label to the intersection of successive land cover maps. This method eases quantitative and qualitative evaluation of land cover conversions by reducing the number of class transitions. In addition, transitions that would be illogical or impossible can be labelled as error. The resultant change trajectories can be represented thematically on a map (Okoye 2016).

A change budget can be constructed by partitioning the overall difference or disagreement between two land cover maps (Section 2.4.2) into quantity and allocation differences, based respectively on correct quantity modelled per class with a given size; and correctly modelled location per class (Pontius & Millones 2011). Aldwaik & Pontius (2012) proposed a method for land cover change analysis, called intensity analysis, which computes deviations between observed changes and uniform changes, and propose a method (Aldwaik & Pontius 2013) to compute the minimum hypothetical error that could account for deviations between observed and uniform changes (Teixeira, Marques & Pontius 2016). Intensity of change is defined as annual rate of change (Aldwaik & Pontius 2012). If the observed intensity is greater than the uniform intensity, then the data show more change than the uniform hypothesis implies, leading to a hypothetical commission error. Hypothetical omission error occurs when the observed intensity is smaller than the uniform intensity. Larger hypothetical errors suggest map error (Aldwaik & Pontius 2012). Intensity analysis has been used particularly when there are more than two categories (Alo & Pontius 2008; Enaruvbe & Pontius 2015; Jewitt et al. 2015; Pontius et al. 2013; Pontius, Huffaker & Denman 2004; Teixeira, Marques & Pontius 2016). Intensity analysis has been applied widely in investigations to improve the understanding of observed land change (Akinyemi & Pontius 2016; Jewitt et al. 2015; Pontius et al. 2013; Zhou et al. 2014). Because the change budget and intensity analysis are applied extensively in this dissertation, a more comprehensive description is required. The formulation of the change budget is provided in the next section, followed by the formulation of intensity analysis.

2.4.4 Change budget formulation

Developed with land change modelling in mind, Pontius (2002) mathematically formulated quantity and allocation disagreement between categorical thematic maps (Pontius & Cheuk 2006; Pontius & Li 2010; Pontius & Millones 2011; Pontius, Shusas & McEachern 2004). Allocation difference, where the location of a land cover class has changed over time, despite the overall quantity at landscape scale remaining the same, can be partitioned into exchange and shift disagreement based on whether pairs of pixels from two or more land cover classes have exchanged places (Pontius & Santacruz 2014). The term disagreement budget therefore seems more appropriate for this method and is used in this text. The formulation of change/disagreement budget is provided in the next section. Equation 2-2 gives the overall difference during time interval *t* for category *j*. In Equation 2-2 to Equation 2-5, the denominator is the product of the study period and the size of the spatial extent, to express change as an annual percentage of the study area extent.

$$d_{tj} = \frac{\{[\sum_{i=1}^{J}(C_{tij} + C_{tji})] - 2 \times C_{tjj}\}100\%}{(Y_{t+1} - Y_t)\sum_{i=1}^{J}\sum_{j=1}^{J} C_{tij}} \qquad \text{Equation 2-2}$$

where

d_{tj}	is the annual difference for category j during interval t;
C_{tij}	is the number of pixels that transition from category *i* to category *j* during interval *t*;
C_{tji}	is the number of pixels that transition from category *j* to category *i* during interval *t*;
C_{tjj}	is the number of pixels that persist in category *j* during interval *t*;
Y_{t+1}, Y_t	are respectively the year at start and end of time interval t;
i, j	are the indices for the categories; and
J	is the number of categories.

Equation 2-3 gives the quantity component during interval t for category j. The quantity component is the absolute change in size of the category.

$$q_{tj} = \frac{\left|\sum_{i=1}^{J}(C_{tij} - C_{tji})\,100\%\right|}{(Y_{t+1} - Y_t)\sum_{i=1}^{J}\sum_{j=1}^{J} C_{tij}} \qquad \text{Equation 2-3}$$

where

q_{tj}	is the annual quantity component for category *j* during interval *t*.

Equation 2-4 gives the exchange between categories *i* and *j* during time interval *t*. Categories *i* and *j* exchange when some locations transition from category *i* to category *j* while other locations transition from *j* to *i*. Equation 2-5 sums the exchanges for category *j* to give the exchange component for category *j*.

$$\varepsilon_{tij} = \frac{2MINIMUM(C_{tij}, C_{tji})100\%}{(Y_{t+1} - Y_t)\sum_{i=1}^{J}\sum_{j=1}^{J} C_{tij}} \; for\; i > j \; and \; \varepsilon_{tij} = 0 \; for \; i \leq j$$ Equation 2-4

$$e_{tj} = \sum_{i=1}^{J}(\varepsilon_{tij} + \varepsilon_{tji}) = \frac{2\{[\sum_{i=1}^{J} MINIMUM(C_{tij}, C_{tji})] - C_{tjj}\}100\%}{(Y_{t+1} - Y_t)\sum_{i=1}^{J}\sum_{j=1}^{J} C_{tij}}$$ Equation 2-5

where ε_{tij} is the annual exchange between categories *i* and *j* during interval *t*;

e_{tj} is the annual exchange component for category *j* during interval *t*;

Equation 2-6 gives the shift component for category *j* during interval *t*. The shift component is the difference minus the quantity component minus the exchange component.

$$S_{tj} = d_{tj} - q_{tj} - e_{tj}$$ Equation 2-6

where S_{tj} is the annual shift component for category *j* during interval *t*;

d_{tj} is the annual difference for category j during interval t;

q_{tj} is the annual quantity component for category *j* during interval *t;* and

e_{tj} is the annual exchange component for category *j* during interval *t.*

Equation 2-3, Equation 2-5 and Equation 2-6 give the three components of difference for an arbitrary category *j*. Equation 2-7 to Equation 2-9 sum the components for each category to give the overall value for the component during time interval *t.* As each location of temporal difference involves two categories, the losing category and the gaining category, division by two is necessary.

$$Q_t = \frac{\sum_{j=1}^{J} q_{tj}}{2}$$ Equation 2-7

$$E_t = \frac{\sum_{j=1}^{J} e_{tj}}{2}$$ Equation 2-8

$$S_t = \frac{\sum_{j=1}^{J} S_{tj}}{2}$$ Equation 2-9

where Q_t is the annual quantity component overall during interval *t*;

E_t is the annual exchange component overall during interval *t*;

S_t is the annual shift component overall during interval *t*;

S_{tj} is the annual shift component for category *j* during interval *t*;

q_{tj} is the annual quantity component for category *j* during interval *t;* and

e_{tj} is the annual exchange component for category *j* during interval *t.*

Equation 2-10 shows how the difference overall (D_t) is the sum of the three components.

$$D_t = \frac{\sum_{j=1}^{J} d_{tj}}{2} = Q_t + E_t + S_t \qquad \text{Equation 2-10}$$

2.4.5 Intensity analysis formulation

Intensity Analysis (Aldwaik & Pontius 2012; Pontius, Shusas & McEachern 2004) is a method that considers maps at multiple instances for the same set of land cover classes, described as categories. The goal of intensity analysis is to account for transitions at interval, category and transition level (Aldwaik & Pontius 2012). Using a transition matrix for each time interval, changes are computed relative to hypothetical uniform change at the interval, category, as well as at the transition level. Interval level can show if the change is large merely because the duration of the interval is long or if the change over time is faster or slower than expected. Category level indicates whether the loss or gain of a particular land cover class is large, because the category is large, thereby identifying classes that are actively losing or gaining. The transition level shows if some transitions are targeting or are targeted by particular land cover classes. By analysing the off-diagonal entries of the confusion matrix, systematic transitions of land cover change can be identified. The method also tests for stationarity of changes across time intervals. Table 2-1 introduces common symbols used in the mathematical equations formulating the intensity analysis framework to reduce duplication.

Table 2-1 Common symbols used in mathematical notation in Equation 2-11–Equation 2-18

Symbol	Meaning
J	Number of categories
i, j	Index for a category, i = initial time point, j = final time point
m, n	Index for the losing (m) and gaining (n) category during transition
C_{tij}	This is the number of pixels that transition from category i to category j during interval t
Y_t, Y_{t+1}	Year at start (t) and end (t+1) of time interval

2.4.5.1 Interval level

Equation 2-11 calculates the overall rate of change during an interval as the size of the change divided by the duration of the time interval expressed as a percentage of the spatial extent at one rate per time interval.

$$S_t = \frac{\text{change during } [Y_t, Y_{t+1}]}{(\text{duration of } [Y_t, Y_{t+1}])(\text{extent})} 100\% = \frac{\sum_{j=1}^{J}\left[\left(\sum_{i=1}^{J} C_{tij}\right) - C_{tjj}\right]}{(Y_{t+1} - Y_t)\left(\sum_{j=1}^{J}\sum_{i=1}^{J} C_{tij}\right)} 100\% \qquad \text{Equation 2-11}$$

where S_t is the annual intensity of change for time interval $[Y_t, Y_{t+1}]$; and

C_{tjj} is the number of pixels that persist in category j during interval t.

Equation 2-12 calculates one uniform rate based on rate of overall change for the entire study period given that the pattern of change were stationary in terms of rate of overall change.

$$U = \frac{\text{area of change during all intervals}}{(\text{duration of all intervals})(\text{extent})}100\% = \frac{\sum_{t=1}^{T-1}\{\sum_{j=1}^{J}[(\sum_{i=1}^{J} C_{tij}) - C_{tjj}]\}}{(Y_T - Y_1)(\sum_{j=1}^{J}\sum_{i=1}^{J} C_{tij})}100\% \qquad \text{Equation 2-12}$$

where U is value of uniform line for time intensity analysis;

C_{tjj} is the number of pixels that persist in category *j* during interval *t*;

T is the number of time points; and

t is the index for the initial time point of interval $[Y_t, Y_{t+1}]$, where t ranges from 1 to *T*-1.

2.4.5.2 Category level

Category level analysis compares observed intensities of loss and gain for each category with uniform intensity of change during each time interval. It identifies the categories for which change is more intensive than the overall change intensity in the spatial extent. At category level, Equation 2-13 computes the annual gross per-category loss intensity during an interval, by dividing the size of the annual gross loss by the size of the category at the start of the interval. Similarly, Equation 2-14 gives the annual gross per-category gain intensity during an interval, this time calculated from the size of the annual gross gain divided by the category size at the end of the interval.

$$L_{ti} = \frac{\text{annual loss of } i \text{ during } [Y_t, Y_{t+1}]}{\text{size of } i \text{ at } Y_t}100\% = \frac{[(\sum_{j=1}^{J} C_{tij}) - C_{tii}]}{(Y_{t+1} - Y_t)\sum_{j=1}^{J} C_{tij}}100\% \qquad \text{Equation 2-13}$$

$$G_{ti} = \frac{\text{annual gain of } j \text{ during } [Y_t, Y_{t+1}]}{\text{size of } j \text{ at } Y_{t+1}}100\% = \frac{[(\sum_{i=1}^{J} C_{tij}) - C_{tjj}]}{(Y_{t+1} - Y_t)\sum_{i=1}^{J} C_{tij}}100\% \qquad \text{Equation 2-14}$$

where L_{ti} is the intensity of annual loss of category *i* during interval *t* relative to size of category *i* at Y_t;

G_{ti} is the intensity of annual gain of category *i* during interval *t* relative to size of category *i* at Y_{t+1};

C_{tjj} is the number of pixels that persist in category *j* during interval *t*; and

C_{tii} is the number of pixels that persist in category *i* during interval *t*.

For category level intensity analysis, the uniform hypothesis states that gross loss and gross gain will occur at the same annual intensity for all categories, which is equal to the speed of change during the interval (*U* from Equation 2-12). The loss of *i* is dormant during interval *t* when annual loss (L_{ti}) < *U*. If G_{tj} < *U*, then the gain of *j* is dormant during interval *t*. Conversely,

if $L_{ti} > U$, then the loss of *i* is active during interval *t*; and gain (G_{tj}) of *j* is active during interval *t* if $G_{tj} > U$.

2.4.5.3 Transition level

For each time interval, transition level of analysis produces two sets of outputs: one for gains of category *n*, and the other for losses of category *m*. The uniform hypothesis at transition level (Equation 2-15) is that during a particular interval, category *n* transitions to all other categories (not-*n*) with the same annual intensity. Equation 2-16 gives the annual transition intensity of the gain of category *n* from another category *i*.

$$W_{tn} = \frac{\text{annual gain of } n \text{ during } [Y_t, Y_{t+1}]}{\text{size of non} - n \text{ at } Y_t} 100\% = \frac{\left[\left(\sum_{i=1}^{J} C_{tin}\right) - C_{tnn}\right]100\%}{(Y_{t+1} - Y_t)\sum_{j=1}^{J}\left[\left(\sum_{i=1}^{J} C_{tij}\right) - C_{tnj}\right]} \quad \text{Equation 2-15}$$

$$R_{tin} = \frac{\text{annual transition from } i \text{ to } n \text{ during } [Y_t, Y_{t+1}]}{\text{size of } i \text{ at } Y_t} 100\% = \frac{C_{tin}100\%}{(Y_{t+1} - Y_t)\sum_{j=1}^{J} C_{tij}} \quad \text{Equation 2-16}$$

where

W_{tn}	is the value of uniform intensity of transition to category *n* from all non-*n* categories at time Y_t during time interval [Y_t, Y_{t+1}];
R_{tin}	is the annual intensity of transition from category *i* to category *n* during time interval [Y_t, Y_{t+1}] where $i \neq n$;
C_{tin}	is the number of pixels that transition from category *i* to category *n* during interval *t*;
C_{tnn}	is the number of pixels that persist in category *n* during interval *t*; and
C_{tnj}	is the number of pixels that transition from category *n* to category *j* during interval *t*.

If the observed transition intensity from *i* (Equation 2-16) is less than the uniform transition intensity (Equation 2-15), then the gain of *n* avoids category *i*, but if the observed transition intensity (R_{tin}) from *i* is greater than the uniform transition intensity (W_{tn}), then the gain of *n* targets category *i*. The transition from *m* to *n* is stationary, given the gain of *n*, if the gain of category *n* either targets category *m* for all time intervals or avoids category *m* for all time intervals.

Equation 2-17 and Equation 2-18 similarly analyse the loss of category *m*.

$$V_{tm} = \frac{\text{annual loss of } m \text{ during } [Y_t, Y_{t+1}]}{\text{size of non} - m \text{ at } Y_t} 100\% = \frac{\left[\left(\sum_{i=1}^{J} C_{tmj}\right) - C_{tmm}\right]100\%}{(Y_{t+1} - Y_t)\sum_{j=1}^{J}\left[\left(\sum_{j=1}^{J} C_{tij}\right) - C_{tim}\right]} \quad \text{Equation 2-17}$$

$$Q_{tmj} = \frac{\text{annual transition from } j \text{ to } m \text{ during } [Y_t, Y_{t+1}]}{\text{size of } j \text{ at } Y_t} 100\% = \frac{C_{tmj} 100\%}{(Y_{t+1} - Y_t) \sum_{j=1}^{J} C_{tij}} \quad \text{Equation 2-18}$$

where

V_{tm}	is the value of uniform intensity of transition to category *m* from all non-*m* categories at time Y_t during time interval $[Y_t, Y_{t+1}]$;
Q_{tmj}	is the annual intensity of transition from category *m* to category *j* during time interval $[Y_t, Y_{t+1}]$ where $j \neq m$;
C_{tmj}	is the number of pixels that transition from category *m* to category *j* during interval *t*;
C_{tmm}	is the number of pixels that persist in category *m* during interval *t*; and
C_{tim}	is the number of pixels that transition from category *i* to category *m* during interval *t*.

If category *m* loses to all other categories in a uniform manner, then $Q_{tmj} = V_{tm}$ for all *j,* and the transition from *m* to *n* is defined as stationary, given the loss of *m*, if the loss of category *m* is either avoided by category *n* or targeted by category *n* of all time steps. Stationary processes will be defined in the next section.

2.4.5.4 Stationarity defined

In statistics, a stationary process is a stochastic process whose joint probability distribution does not change when shifted in time or space. For a stationary process, mean and variance do not change over time or position. In contrast, spatial non-stationarity describes modelled relationships that are not constant across space but are dependent on the absolute location in space (Haining 1993; Jones & Hanham 1995). Miller & Hanham (2011) warn that when underlying processes are non-stationary, global statistics, pattern measurements and model parameters will be inaccurate making any subsequent spatial inferences incorrect. The next section focuses on land change modelling used to simulate future land change.

2.5 LAND CHANGE MODELLING

Spatially explicit modelling is an important technique for projecting and exploring alternative future scenarios, thereby gaining understanding to quantitatively describe key processes (Lavorel et al. 2017; Veldkamp & Lambin 2001). Spearheaded by Verburg et al. (1999) and Pontius, Cornell & Hall (2001), land change modelling (both land cover and land use) entails the simulation of the behaviour of the environmental and social systems in an area over a period of time based on measured land change (Paegelow et al. 2013). A short description of the characteristics of a land change model follows.

Eastman, Van Fossen & Solorzano (2005) noted that land change models must address three main areas, each using a different model: (1) change demand; (2) transition potential; and (3) change allocation, to generate a future land cover scenario. Both change demand and change allocation rely on a transition potential model.

Change demand models are used to estimate the rate of change between each pairwise combination of land cover types using an empirical or theoretical approach (Eastman, Van Fossen & Solorzano 2005). The output is a transition probability matrix that gives a probability estimate for each pixel to either be transformed to another land cover or to persist and be calibrated to an annual time step (Kamusoko et al. 2009). Markov chain analysis is a popular method used in the change demand process.

Transition potential modelling lies at the heart of change modelling and much research has focussed on techniques to generate the transition potential map (Camacho Olmedo, Paegelow & Mas 2013; Eastman, Van Fossen & Solorzano 2005; Mas et al. 2014; Pérez-Vega, Mas & Ligmann-Zielinska 2012). A transition potential map describes the degree to which a location might potentially change in time, and can be created based on probabilities of transitions or on suitability of land cover to be occupied (Eastman, Van Fossen & Solorzano 2005). Various approaches have been suggested to produce transition potential maps. Kolb, Mas & Galicia (2013) used both weights of evidence (WoE) that represents probabilities of change and logistic regression modelling (RM) that expresses suitability for land cover classes, to produce transition potential maps based on identified drivers. Despite low precision identified in the transition potential maps, the evaluated areas of change showed more accurate transition potential maps using WoE. Another popular approach for developing a transition potential map, is the multi-layer perceptron implemented in IDRISI software, which is a back-propagation neural network model (Eastman 2016; Eastman, Van Fossen & Solorzano 2005).

Change allocation techniques produce the spatial patterns of changing landscapes by allocating the amount of changes that have been established with certainty by projecting the historical land cover change across space (Mas et al. 2014). A land change model must predict both the quantity of each land cover type, as well as the location of any change (Pontius, Huffaker & Denman 2004).

The accuracy of the output of an inductive model is a function of both the model itself, namely suitability of algorithms within the model to fulfil the intended purpose, and the accuracy of the input data. Model performance assessment is often based on the spatial coincidence between a simulated map and an observed land cover map. Other methods include expert opinion,

comparison of outputs generated with multiple models or multiple runs with the same model (Mas et al. 2013; 2014).

Simulation of land cover change can follow a prospective approach based only upon past trends or introduce alternative future scenarios (Paegelow & Camacho 2008). However, most land change models follow a data-driven inductive approach (Overmars, De Groot & Huigen 2007), using statistical inferences to find correlations between explanatory factors. The use of a deductive model would allow the operator to include driving factors that may have causal influence on land cover change.

Perera, Sturtevant & Buse (2015) drew attention to the fact that Turner and Gardner had already envisaged spatially explicit simulation of broad-scale ecosystem dynamics as early as 1991 (Turner & Gardner 1991). Verbesselt et al. (2010a) argued that, by detecting and characterising change over time, the first step toward identifying drivers of change and understanding change mechanism is taken. The next step would be to perform spatially explicit modelling to create alternative future scenarios (Mas et al. 2014), as envisaged by Turner and Gardiner. By exploring these scenarios, a better understanding of processes in the landscape can be gained (Veldkamp & Lambin 2001).

The Land Change Modeller (LCM) integrated into IDRISI was used in this study and the approach used by this model is framed here. In LCM, land cover mapped at two time steps (T1 and T2) are used to estimate the patterns and processes of change and for model parameterization / calibration (Mas et al. 2013). LCM uses multi-layer Perceptron (MLP) with explanatory spatial variables to create transition potential maps. Spatial explanatory variables are GIS datasets representing drivers of the observed change (Pérez-Vega, Mas & Ligmann-Zielinska 2012), typically based on biophysical or socioeconomic criteria, used to model the historical change process (Eastman 2016). The potential explanatory power of a variable can be tested using Cramer's V test where the level of association between GIS datasets representing phenomena thought to be drivers in a particular transition and the land cover in question can be determined. Cramer's V is a correlation coefficient that ranges from 0.0, indicating no correlation (discarded variable), to 1.0, indicating perfect correlation (excellent potential variable) (Megahed et al. 2015). Although these values are not regarded as definitive, they can help in deciding whether to include an explanatory variable in creating a transition potential map for a transition by examining whether the explanatory variable explains the transition for a particular land cover. Land cover transitions with similar underlying drivers of change can be grouped into sub-models (Pérez-Vega, Mas & Ligmann-Zielinska 2012). Explanatory spatial variables are assigned to each sub-model on the basis of Cramer's V values.

Cramer's V is the most popular of the chi-square-based measures of nominal association because it gives good norming from 0 to 1 regardless of table size, when row marginal equal column marginal, computed using the formula:

$$V = \sqrt{\frac{\varphi^2}{\min(k-1, r-1)}} = \sqrt{\frac{\chi^2/n}{\min(k-1, r-1)}} \qquad \text{Equation 2-19}$$

where φ is the coefficient of contingency; χ

χ is derived from Pearson's chi-squared test;

n is the grand total of observations;

k is the number of columns; and

r is the number of rows.

Since V has a known sampling distribution it is possible to compute its standard error and significance (Liebetrau 1983).

The transition potential of each sub-model is determined through a knowledge based approach to machine learning in the MLP. The MLP is a feedforward neural network. Data flows in one direction from the input layer through the hidden layers (computational nodes) to the output layer. The nodes are linked by a web of connections that are applied as a set of weights. A back-propagation algorithm is used to train the network by iteratively spreading the errors from the output layer to the input, adjusting weights to minimise the error between the observed and the predicted outcomes (Pérez-Vega, Mas & Ligmann-Zielinska 2012). The training performance is assessed by a precision value expressed in percent. Networks that are too small cannot identify the internal structure of the data and produce lower performance accuracies whereas too large networks overfit the training data (Pérez-Vega, Mas & Ligmann-Zielinska 2012). The aim of the training is to build a model of the data generating process so that network outputs can be predicted from unseen inputs. The network output is then compared with the desired output, the error is computed and then back-propagated through the network to adjust weights. As large quantities of data are required for training, small training samples are unlikely to result in an accurate model. Half of the training data are randomly selected for learning and half for validation. After the MLP has been trained, validation data are used to calculate a "skill measure" (computed as the accuracy of transition prediction minus the accuracy expected by chance) (Mas et al. 2014). The MLP creates time-specific transition potential maps for each of the sub-models (Eastman, 2016). Through cross-tabulation of land cover (Kamusoko et al. 2009) Markov chain analysis develops a transition probability matrix of land cover change between two different dates.

LCM produces two predictors of future land cover: soft prediction and hard prediction. Soft prediction, or potential to transition, is a continuous mapping of vulnerability to change (Eastman 2016). It is calculated by aggregating all the transition potentials and provides an indication of the degree to which the areas have the right conditions to precipitate change. The soft predictor provides a likelihood of a cell to experience land cover change without providing an indication as to what the new land cover will be.

The hard prediction procedure used by LCM is based on IDRISI's multi-objective land allocation (MOLA) module. MOLA determines a compromise solution by maximizing the suitability of lands for each objective given the assigned weights (Eastman 2016). Land allocation conflicts are resolved by allocating the cell to the objective (land cover class) for which its weighted transition potential is highest based on a minimum distance to ideal point rule using the weighted ranks. Finally, the transition probability matrix derived from the Markov chain analysis determines how much land is allocated to a class over a specified *n*-year period.

This section provided a short overview of land change modelling. Land change models are implemented in various software packages and have been used to describe and project the dynamics of land use and land cover to explain how humans are changing the earth's surface. LCMs are used to forecast future land change by computing change demand based on existing and likely future scenarios, developing transition potential and performing change allocation to generate a future land cover scenario. It is a wide, developing topic with an active research community, falling within the context of land change science. In the next section, trend analysis as it pertains to remotely sensed data is reviewed.

2.6 TREND ANALYSIS

By definition, trend analysis is the practice of finding a pattern within collected information. It often relies on a set of statistical techniques that deals with time series data. Time series data refer to data in a series of particular periods or intervals. This discussion focusses specifically on time series analysis of Earth observation data to reveal land surface dynamics and highlight the magnitude of these dynamics within defined monitoring periods (Kuenzer, Dech & Wagner 2015; Lasaponara & Lanorte 2012). In the past, time series analysis was complicated and limited to a small number of expert users, relying on coarse resolution data (Kuenzer, Dech & Wagner 2015). The release of several satellite data archives has led to free access to a large volume of imagery ideal for time series analysis (Lasaponara & Lanorte 2012; Wulder & Masek 2012). This is complemented by the availability of new open source tools and novel techniques

for time series analysis (Kuenzer, Dech & Wagner 2015). This section reviews some of the products and methods applied in trend analysis involving remotely sensed data.

2.6.1 Remotely sensed data available for time series analysis

Accurate estimation of trends depends on the quality of the sensed data, the statistical method used, the length of the time series, as well as the temporal and spatial resolution of the data (Sulkava et al. 2007). Moreover, very few sensors have captured data that span several decades available for time series analysis.

Two of the sensors that have produced the longest available time series of data are the advanced very high-resolution radiometer (AVHRR) sensors, operated by the National Oceanic and Atmospheric Administration (NOAA) that offers coarse resolution daily coverage since 1978. The Landsat archive, operational since 1972, includes Landsat 4 MSS (MultiSpectral Scanner), Landsat 5 TM (Thematic Mapper), Landsat 7 ETM+ (Enhanced Thematic Mapper Plus), and Landsat 8 OLI (Operational Land Imager) consisting of medium resolution imagery at 16-day intervals (Kuenzer, Dech & Wagner 2015; Wulder et al. 2018).

Since the early 2000s, the moderate resolution imaging spectroradiometer (MODIS) sensor (Justice et al. 1998), and the European Environmental Satellite (ENVISAT) sensors, advanced along-track scanning radiometer (AATSR) and medium resolution imaging spectrometer (MERIS) have provided access to coarse and medium resolution data. MODIS was launched on the Terra satellite in 1999 and on the Aqua satellite in 2002, whereas the sensors on board ENVISAT have collected data from 2002 to April 2012. More recently, the European Space Agency (ESA) Sentinel series provides many new multi-sensor options for time series analysis, with global coverage and provided on a free and open basis. The compatibility of Sentinel 2 with Landsat allows measurements from Sentinel 2 to be integrated with Landsat, thereby allowing the Landsat and Sentinel 2 archive to be used for time series analysis in combination (Wulder et al. 2018).

Selected SPOT (Satellite Pour l'Observation de la Terre) VEGETATION data from 1998 onwards at one-kilometre resolution are also available at a daily interval, while higher resolution SPOT multispectral data was made available as part of the SPOT World Heritage Programme (Kuenzer, Dech & Wagner 2015). Lasaponara & Lanorte (2012) comment on the high cost of multispectral SPOT data, which has been prohibitive in assessing its value for time series analysis.

2.6.2 Trend analysis techniques and examples

Temporal vegetation information have been derived from time series of normalised difference vegetation index (NDVI) data since the early 1980s (Malingreau 1986; Tucker, Justice & Prince 1986) and many methods for extracting seasonality and trends have been developed since. For instance, time series satellite data (Forkel et al. 2013; Zhu et al. 2016) have recently been used to quantify changing trends in ecosystem productivity linked to land cover classes and can provide a continuous view of ecosystem dynamics (Kennedy et al. 2014). Trend analysis is not limited to NDVI but can be applied to time series of other satellite-derived data, such as land surface temperature or snow cover (Kuenzer, Dech & Wagner 2015).

All trend estimation methods have limitations that may be more or less critical, depending on the application. Estimation of trends from time series data differs substantially depending on analysed satellite dataset, the corresponding spatio-temporal resolution and the applied statistical method (Forkel et al. 2013). Fensholt et al. (2012) attested that both linear and non-linear development in the time series value, e.g. NDVI, could be detected from time series data. Linear development can be derived using the Pearson Product–moment linear correlation test and Theil-Sen median slope trend analysis (Sen 1968; Theil 1950). However, care must be taken when using linear regression analysis for estimating trends in time series data, as spatial and temporal autocorrelation can violate statistical assumptions, such as the independence of observations (De Beurs & Henebry 2010). Accordingly, De Beurs & Henebry (2010) suggested the application of temporal autocorrelation structures or the use of the non-parametric Mann-Kendall monotonic test for non-linear development, while Neeti & Eastman (2011) proposed using spatial autocorrelation as contextual evidence in the testing of trends based on a modification of the Mann-Kendall statistic, as implemented in IDRISI. The additional contextual information reinforced evidence of neighbouring pixels with similar trends, whereas spurious trends would be removed.

Many studies have calculated trends based on annual time steps, using regression analysis (Eklundh & Olsson 2003), either from annually or seasonally aggregated values, or extracted annual values. Röder et al. (2008) acquired a time series of Landsat data consisting of a single image per year and was able to retrospectively assess rangeland processes and interpret the linear trends in relation to land use practices and previous management interventions. Annual aggregation eliminates the seasonal cycle in a satellite parameter, such as the NDVI time series, removing the seasonal correlation structure that could hamper trend analysis. However, the annual aggregation of time series data reduces the temporal resolution and time series length, which is critical for assessing the statistical significance of the observed trend.

Various methods have been developed to estimate and subtract the seasonal cycle or by modelling the seasonal signal (De Jong et al. 2011; Verbesselt et al. 2010a; Verbesselt et al. 2010b) thereby providing access to the full temporal resolution. Verbesselt et al. (2011) demonstrated that break detection for additive seasonal trend (BFAST) could detect and characterise spatial and temporal changes within the trend component of satellite image time series. BFAST employs the seasonal trend decomposition method (STL) based on a locally weighted regression smoother (LOESS) (Cleveland et al. 1990). Abrupt changes that were not associated with trend or seasonal components of the time series could be identified (Verbesselt et al. 2010b) using BFAST. Method STM (trend estimation based on a season-trend model) described by Forkel et al. (2013) uses this method implemented specifically for remotely sensed data. Method AAT (Forkel et al. 2013) was designed to estimate trends and trend changes based on an annual aggregated time series, with breakpoints estimated using the method of Bai & Perron (2003) and Zeileis et al. (2003). The Mann-Kendall trend test (Mann 1945) was applied to determine significance of trends. To enable detection of long-term trend changes, the observation periods of 48 monthly observations are recommended, while time series segment of a length smaller than eight years are not considered trends (Forkel et al. 2013). Kuenzer et al. (2014) suggested that the residuals, the remainder of the time series after trend and seasonal components were removed, could be relevant for management of natural resources, such as plant disease, fires or natural hazards.

Overall, De Jong et al. (2011) found that trend estimates from the different methods resulted in similar general spatial patterns of the major regional greening and browning trends, but noted substantial spatial pattern variations in areas with weak trends. Vogelmann et al. (2016) advised that gradual changes were best characterised and monitored using time series analysis. Wessels, Van den Bergh & Scholes (2012) identified abrupt changes that were correlated with land cover change and hypothesised error. Similarly, Fensholt et al. (2015) found that patterns of diverging NDVI metric trends could also be used to evaluate the impacts of environmental changes related to land cover change, thereby detecting changes in ecosystem functioning over time. Forkel et al. (2013) developed trend estimation methods specifically applicable to remote sensing data, implemented in R statistical software (R Core Team 2017) package greenbrown (Forkel & Wutzler 2015).

2.7 SUMMARY

This review of literature and methods focussed on the domains of landscape science and land change science but dealt predominantly with land cover and land cover change, land change

modelling and trend analysis. The review commenced with a definition of landscapes as spatially heterogeneous areas of interacting ecosystems functioning together that can be analysed at any scale. While ecosystems support human well-being by providing functions and services, humans also affect ecosystems and their services through socio-ecological processes manifested as land use and land cover change. Ecosystems and their functions and services can be measured using land cover derivatives as proxy. Because of the importance of ecosystem services, development of management strategies and land governance are at the forefront of research priorities in land change science.

Woody encroachment of the grasslands and the effect on ecosystems services delivered by the grasslands were deliberated next. Grasslands are susceptible to both invasion and degradation. Invaders include natural woody vegetation as well as invasive aliens. Degradation is caused by overstocking and overgrazing, often regarded as a management problem. Bush encroachment results in an imbalance of the grass to bush ratio, a decrease in biodiversity, decreased livestock carrying capacity and increased evapotranspiration associated with reduced runoff. Invasive species also affect soil quality. However, if woody plant increase is a consequence of climate change, rangeland managers will have to adopt a different management strategy. This would also be the case for clearing programmes. The effect of different land use management practices is therefore highlighted in Chapters 3 and 5. A positive consequence of the increased woody biomass may be increased carbon storage in the landscape. A large number of scientists are focussing on the ecological effects and management strategies of woody encroachment; however, these were beyond the scope of the project and not covered in detail in this section. Chapters 5 and 6 explore the consequences of land cover change on net ecosystem carbon exchange and the hydrologic functioning of the catchments by investigating trends in albedo, a climate regulating ecosystem service.

A distinction was made between land cover and land use. Land cover was identified as one of the most important environmental variables as it reflects the state of the landscape at a particular point in time and serves as a representative of underlying processes at work. A reflection on image classification techniques for thematic land cover delineation was provided. Object-based image analysis was found to be the preferred classification method. However, digital maps created as classification output are subject to human error, leading into the discussion on map accuracy. Generally, map accuracy is measured in a square contingency matrix by comparing representative reference points with the classified map. Various statistics can be computed from the contingency matrix including overall, producer's and user's accuracy. The family of kappa indices have also been used but have fallen out of favour. Due to the potential for

misclassification when using categorical land cover classes, map error is a universal concern and guidelines exist on what information should be reported from accuracy assessments, both for land cover classification and land cover change. Despite the fact that accuracy reports from the contingency matrix are easy to understand, they are not spatially explicit and therefore do not capture the spatial variation in accuracy and error. Various authors have addressed the lack of spatially explicit methods for classification accuracy since the early 2000s, but these methods do not seem to have had much acceptance. Comber et al. (2017) have suggested the use of geographically weighted contingency matrices to allow mapping of spatially explicit accuracy measurements, both for land cover classification as well as land cover change and forms part of the research activities undertaken in this dissertation.

Land cover change could represent conversion from one class to another, or modification within one class, which would have implications for the particular methods selected for both land cover classification and change detection. Change detection methods have taken the form of image analysis overlay, image analysis comparison, multi-temporal image object and polygon vector analyses. Of these methods, the independent classification of remotely sensed imagery, followed by post-classification change analysis remains the most popular. During change analysis, a square contingency matrix is also used, however, loss and gain is computed from the off-diagonal entries. A popular framework for land cover change accuracy assessment is intensity analysis. The rate of change (intensity) at interval, category and transition level is used to compare if change has occurred faster or slower than uniform. Hypothetical map error can then be identified. By constructing the change budget, change is partitioned into quantity, exchange and shift disagreement. This dissertation therefore uses the terms change budget and disagreement budget interchangeably. The intensity of the change budget components can also be computed. A spatially explicit change budget can also be constructed, as done in Chapter 4.

The next section addressed land change modelling and provided a general overview of the three main areas that a land change model must address, namely change demand, transition potential and change allocation. An in-depth description of the IDRISI Land Change Modeller was given, highlighting strengths and weaknesses of the modelling software. Finally, an overview of trend analysis was given by firstly looking at available remotely sensed data, followed by various trend estimation techniques, that all have limitation. BFAST and the Season-trend model can be used with ease with remotely sensed data. Halmy et al. (2015) argued that remote sensing, and particularly land cover change detection and trend analysis applied to time series satellite images, has become an important tool for ecosystem service monitoring and management.

For the diverse research questions addressed in this study, a very large reading list was required. The paper-based structure of the dissertation lent itself to reporting the bulk of literature in this chapter (Chapter 2) whilst still increasing the body of literature in each separate chapter. Of special interest is that cloud computing platforms are opening new possibilities for generating land-cover maps by applying deep learning algorithms (Azzari & Lobell 2017). To demonstrate this, Midekisa et al. (2017) used high resolution Landsat satellite observations and the Google Earth Engine cloud computing platform to quantify land cover and impervious surface changes in Africa over 15 years at continental scale.

Kuenzer, Dech & Wagner (2015) noted that the greatest challenge to space agencies and data providers over the next decade is the enormous volume of data to be preserved, as well as the amount of data that individual researchers will process in their research endeavours to inform management. This so-called “Big Data” problem has created a demand for cloud-based solutions for data storage and processing, the development of processing algorithms and code-sharing platforms, and the emergence of open source programming languages. The demand for these technologies will grow as more data sources becomes available.

This concludes the formal review of literature. However, each of the subsequent chapters (excluding Chapter 7) has been written in the format of a journal article and therefore includes additional literature pertaining only to the topic addressed by the chapter. The next chapter (Chapter 3) discusses land cover change trajectories in the grasslands in the Eastern Cape, defining woody encroachment as a degradation gradient.

CHAPTER 3: CHARACTERISING DEGRADATION GRADIENTS THROUGH LAND COVER CHANGE ANALYSIS

This chapter[1] overviews a land cover change analysis performed for the agro-ecosystems in the Eastern Cape. The study used land cover change analysis to characterise degradation gradients using an indicator-based approach and to demonstrate the effect of map accuracy on real change that can be measured by the analysis.

3.1 ABSTRACT

Land cover change analysis was performed for three catchments in the rural Eastern Cape, South Africa, for two time steps (2000 and 2014), to characterise landscape conversion trajectories for sustained landscape health. Land cover maps were derived: (1) from existing data (2000); and (2) through object-based image analysis (2014) of Landsat 8 imagery. Land cover change analysis was facilitated using land cover labels developed to identify landscape change trajectories. Land cover labels assigned to each intersection of the land cover maps at the two time steps provide a thematic representation of the spatial distribution of change. The results show that, while land use patterns are characterised by high persistence (77%), the expansion of urban areas and agriculture has occurred predominantly at the expense of grassland. The persistence and intensification of natural or invaded wooded areas were identified as a degradation gradient within the landscape, which amounted to almost 10% of the study area. The challenge remains to determine significant signals in the landscape that are not artefacts of error in the underlying input data or scale of analysis. Systematic change analysis and accurate uncertainty reporting can potentially address these issues to produce authentic output for further modelling.

3.2 INTRODUCTION

Landscape units or land use types encountered in the mesic regions of South Africa are diverse, comprising inter alia irrigation agriculture, dryland cultivation, extensive rangeland and forests, as well as low-density urban areas. Driven by critical water security issues in the country, noteworthy progress has been made towards establishing links between catchment health and especially the effects of invasive alien plants (IAPs) and the provision of hydrological services (Le Maitre, Gush & Dzikiti 2015; Turpie, Marais & Blignaut 2008) within landscape units.

[1]This chapter was originally published as a scientific article (citation below). The manuscript was reformatted to match the guidelines of Department of Geography & Environmental Studies, Stellenbosch University.

Münch Z, Okoye PI, Gibson LA, Mantel S & Palmer AR 2017. Characterising degradation gradients through land cover change analysis in rural Eastern Cape, South Africa *Geosciences* 7:7.

While direct habitat destruction remains the primary threat to biodiversity, IAPs pose an increasing challenge both locally and globally (Driver et al. 2012) and can adversely affect the primary productivity of the natural grasslands in South Africa used for livestock farming (Driver et al. 2012). The reduction in biodiversity heightens ecosystem susceptibility to biological invasions that, in turn, erode ecosystem services (Díaz et al. 2006). Landscape change, by IAPs and other land use approaches, may contribute to land degradation and the reduction of water and other available resources to native species and rural inhabitants (Driver et al. 2012; Le Maitre, Gush & Dzikiti 2015; Turpie, Marais & Blignaut 2008). Therefore, one of the fundamental requirements necessary for evaluating the merit of any land use activity is the ability to accurately quantify ecosystem services associated with such activity (Brown, Bergstrom & Loomis 2007).

Land cover reflects the state of the landscape at a particular point in time (Feranec et al. 2010) arising from processes operating at the terrestrial surface representing elements determined both by natural conditions, as well as by human influence (Bastian, Krönert & Lipský 2006). Land cover change involves alterations in biogeochemical cycles, climate and the hydrology of ecosystems (Reyers et al. 2009) from anthropogenic actions. Land cover dynamics have important consequences for natural resources as drivers of change in ecosystems and their services (Huang & Asner 2009; Reyers et al. 2009), and determining land cover change can provide information about these processes (Feranec et al. 2010). Land cover change analysis identifies the difference between land cover categories in maps of different time points (Aldwaik & Pontius 2013; Feranec et al. 2010; Stott & Haines-Young 1998) and draws conclusions about landscape conversion (Benini et al. 2010; Lambin, Geist & Lepers 2003; Nagendra, Munroe & Southworth 2004).

The ability to quantify the rates and extents of land cover change and develop models that relate changes in land cover to underlying land use processes and environmental effects depends on accurate observations of landscape change (Burnicki 2011; Feranec et al. 2010). The occurrences and mechanisms of these land cover change processes may be difficult to analyse due to a lack of empirical ecological and geospatial data correctly representing the variables driving these changes (Nagendra, Munroe & Southworth 2004). Therefore, to ensure sustained landscape health, change analysis of landscape activities needs to be performed to enable the quantification of the derived benefits to humans occupying the catchment (Cowling et al. 2008).

Satellite-based Earth observation and geographic information systems (GIS) have been established as the best tools for observation, measurement and monitoring of land cover change (Bodart et al. 2013; Schoeman et al. 2013; Szantoi et al. 2016). Earth observation data provide

large area coverage of features on the face of the earth at near real time. The historical archive of such imagery provides multi-temporal monitoring capability and is therefore well suited to generate land cover maps for change analysis. Useful information is derived from electromagnetic radiation reflected or emitted from the earth's surface captured in satellite images, by systematically employing image analysis (Blaschke 2010; Campbell & Wynne 2011).

Independent classification of remote sensing images from two or more different dates is the most common method of generating a multi-temporal series of maps for landscape pattern analysis (Linke et al. 2009). A traditional per-pixel or an object-based approach (Blaschke 2010) can be followed where classes or categories are assigned to each pixel (or object). Common image classification techniques include unsupervised and supervised classification. Various classification algorithms are available, with the most used algorithm being the maximum likelihood classifier (MLC) (Tseng et al. 2007). However, traditional supervised classifiers are often outperformed by classification methods such as artificial neural networks, expert systems and decision trees (DTs) (Pal & Mather 2003).

Accurately generating a land cover map and quantifying the extent of a land cover class or its change over time require careful selection of reference data for use in both training and validation (Congalton & Green 2009; Foody 2002; MacLean & Congalton 2012; Olofsson et al. 2013). The accuracy of training data will influence the success of the classification, while the validation data, assumed to be correct, are used to perform accuracy assessment (Congalton & Green 2009; Foody 2002).

When using land cover data products created from different input datasets, methodologies and legend categories, post-classification editing can be carried out to improve classification accuracies. Minor inconsistencies that would impede direct comparison can also be corrected (Homer et al. 2015). If exact locations of map errors are known, land cover maps can be rectified through post-classification editing to minimise error propagation prior to land cover change analysis. Error can be introduced during sampling if inaccurate land cover classes are assigned or through misclassification during image analysis (Burnicki, Brown & Goovaerts 2007; Pontius & Li 2010).

The accuracy of land cover change modelling is directly dependent on the accuracy of the input land cover data (Burnicki 2011; Schoeman et al. 2013), and thus, classification errors in the independently-generated maps of land cover derived using different methodologies are compounded in an land cover change analysis, possibly leading to spurious results in landscape

change (Burnicki 2011). For any land cover change analysis, the reliability of the land cover change detected should therefore be assessed in order to explain the certainty with which the change can be considered real or spurious (Fuller, Smith & Devereux 2003; Malek, Scolobig & Schröter 2014; Olofsson et al. 2014; Olofsson et al. 2013). A single-date sample-based error matrix, often the endpoint of accuracy assessment prior to land cover change analyses, provides insufficient information to assess the accuracy of gross change (Olofsson et al. 2014; Olofsson et al. 2013). To address the errors introduced by comparison of erroneous input maps, Fuller, Smith & Devereux (2003) proposed a method to measure the level of change with 75% reliability as a function of the accuracy of each input land cover map, the number of classes mapped and the percentage of change detected. Equally, Pontius et al. (Pontius & Li 2010; Pontius & Lippitt 2006) describe measures to determine the probability of error in predicted land change based on erroneous input maps.

This chapter describes the use of independent land cover maps for change analysis in a grassland-dominated landscape in the Eastern Cape of South Africa to delineate land cover change trajectories that are crucial to gain a better understanding of water and carbon fluxes. Invasion by woody plants is a driver of grassland transformation, which influences ecosystem services provided by rangelands, such as forage production, water supply, habitat, biodiversity, carbon sequestration and recreation (Gwate et al. 2016). Therefore, from a rangeland management perspective, understanding the land cover trajectories relating to grass production would be important for local farmers (Gwate et al. 2016). In addition, the success of the Working for Water (WfW) programme (Turpie, Marais & Blignaut 2008), which uses labour-intensive methods to clear invasive woody plants while supporting job creation (Driver et al. 2012), can be evaluated. As IAPs are reported to have a high total incremental water use compared with indigenous vegetation (Clulow, Everson & Gush 2011), clearing could salvage a significant proportion of water to maintain other ecosystem services (Meijninger & Jarmain 2014; Van Wilgen et al. 2008).

The objectives of the chapter therefore are: (1) the post-classification editing and accuracy assessment of the existing national land cover product (Van den Berg et al. 2008); (2) deriving and validating a second land cover map (Okoye 2016) to facilitate change analysis; (3) performing land cover change analysis on these datasets; and (4) delineating important land cover change trajectories. Accurately quantifying the rates and extent of land cover change would be the first step in relating underlying land use processes and the environmental effects thereof to land cover change trajectories involving grassland transformation crucial to the carbon-water nexus.

3.3 MATERIALS AND METHODS

3.3.1 Study area

Three quaternary catchments (T35B, T12A and S50E) situated in the Mzimvubu-Tsitsikamma Water Management Area in the Eastern Cape of South Africa (Figure 3-1) were selected for investigation. The vegetation of the study area is best described as grassland interspersed with thicket, formal plantations and IAPs (Mucina & Rutherford 2006). Grassland is the second largest biome in South Africa comprising almost 29% of the total area (Van Wilgen et al. 2012), of which about 30% has been permanently modified (Mucina & Rutherford 2006). The grasslands comprise not only grass species, but also bulbous perennials that reappear annually (Carbutt et al. 2011). Invasion by woody plants has transformed the grassland, negatively influencing rangeland production. Vegetation diversity and richness have been degraded by poor farming practices such as overgrazing, burning and wood felling. The soils comprise mostly deep clayey loams to rocky soils.

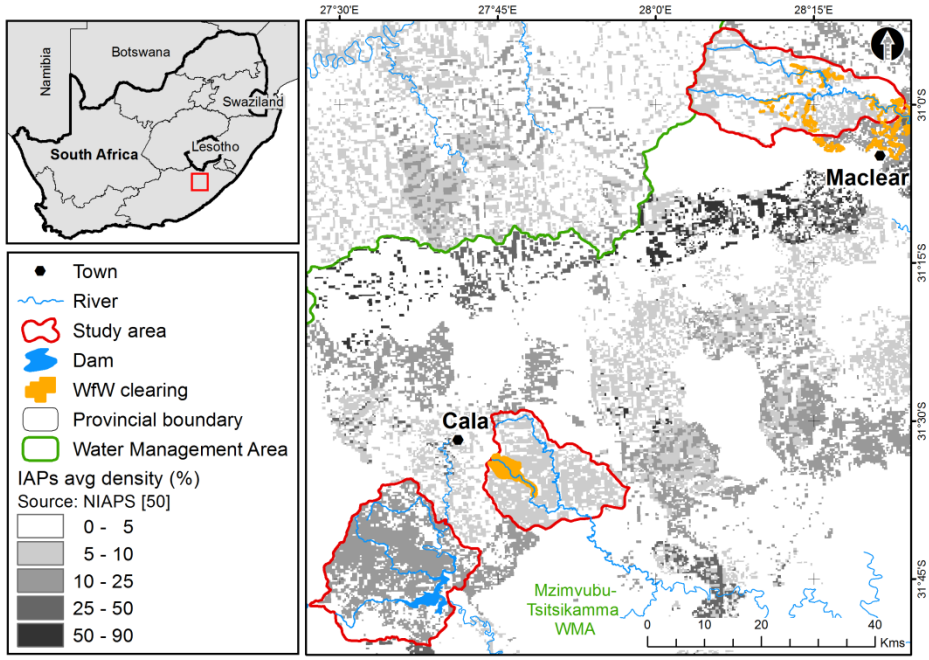

Figure 3-1 Three study sites S50E, T12A and T35B; NIAPS Kotzé et al. (2010)

In this rural landscape, communal farming is practised alongside a strong commercial livestock sector. However, to describe the complexity of the communal farming tenure arrangement in the Eastern Cape more appropriately, the label “dual or bilateral landholding arrangement” was agreed upon by stakeholders, due to the interaction of the components of traditional leadership and the municipal system in land allocation. Grazing and crop cultivation are noticeable as the main land use practices (Kakembo 2001; WRC 2013). The area consists of three different land tenure units namely former commercial farms and traditional and betterment villages, predominantly in T12A and S50E, and former Transkei rural areas (Kakembo 2001; Wotshela

2009). Major users of water and carbon in this socio-ecological system are livestock and alien trees. The local district municipality (Chris Hani) and WfW Alien Plant Clearing Programme have been clearing IAPs in these catchments for the past twelve years, with water saving being the primary motivation (Dye et al. 2008). Location of WfW clearings (Driver et al. 2012) can be seen in Figure 3-1 within T12A and south of T35B (Kotzé et al. 2010).

S50E (31°45'S 27°30'E; 44760 ha), the southernmost catchment, represents an area with high grazing potential, under communal tenure of the local headman, with an eight per cent density of different IAP species (Kotzé et al. 2010). Within the catchment lies the Ncora Dam supplied by the Tsomo River. In close proximity to the east of S50E lies T12A (31°30'S 27°45'E; 27870 ha). Further north, catchment T35B (31°S 28°15'E; 39550 ha) represents commercial/freehold land with many different land usages including forestry, mixed livestock and crop production.

Rainfall in the study area occurs predominantly in summer with highest rainfall measured in January. Figure 3-2 illustrates the annual rainfall variation in the study area derived from Tropical Rainfall Measuring Mission (TRMM) satellite data (Huffman et al. 2010; Huffman et al. 2007) validated with complete weather station data from Cala and Maclear (see Figure 3-1 for location) with median approximately 680mm.

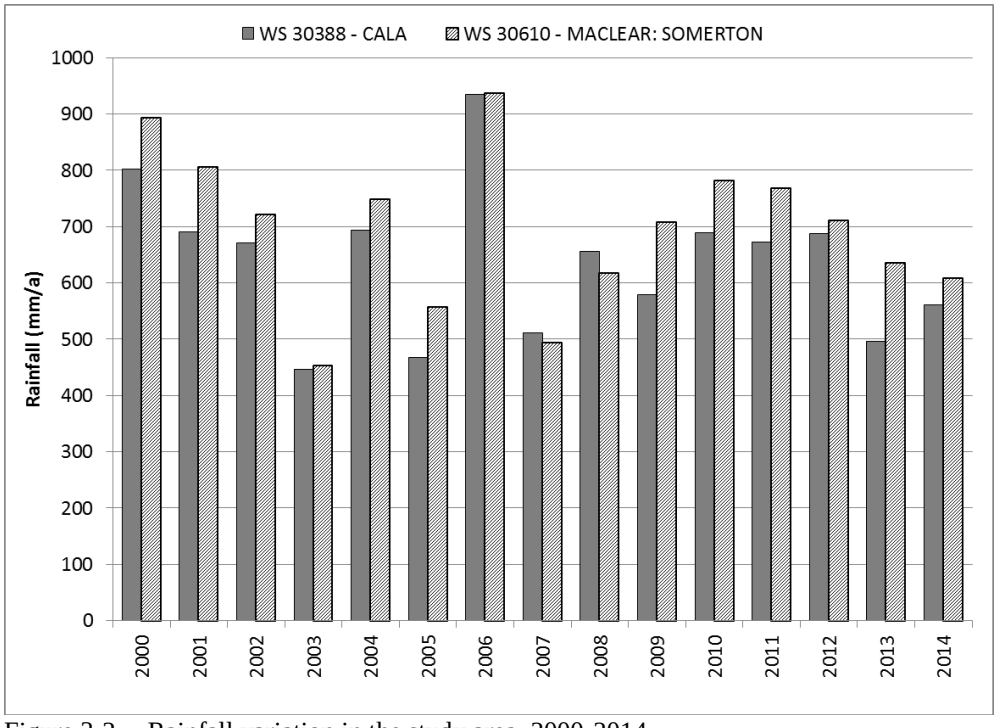

Figure 3-2 Rainfall variation in the study area, 2000-2014

Over the study period, rainfall varied between a low of ~450mm per annum in 2003 to a high of almost 950mm in 2006, a year of extreme rainfall in all of the catchments (NDMC 2007). The rainfall for the two years selected for landscape comparison display significantly different

($p<0.05$) precipitation volumes with 2000 being a relatively wet year (~850mm) in contrast to 2014 when the area received only ~600mm.

3.3.2 Data selection

Two time steps (T1 and T2) were selected for analysis. The first time step (T1) was selected to describe the landscape in 2000, coinciding with the date of the South African National Land Cover (NLC) dataset (Van den Berg et al. 2008). The NLC has commonly been applied in studies requiring land cover as input (Ament & Cumming 2016; Van den Berg, Kotzé & Beukes 2013; Jewitt et al. 2015; Kahinda et al. 2008; Maherry et al. 2010; Munyati & Ratshibvumo 2011; Thomas 2015). This land cover map was classified from multi-temporal Landsat 7 Enhanced Thematic Mapper imagery using primarily conventional per-pixel classifiers based on 2000-2001 conditions (Van den Berg et al. 2008) with a minimum mapping unit of 1-2 ha (Jewitt et al. 2015) and 45 classes (Van den Berg et al. 2008). The year 2000 also corresponds to the launch of the moderate resolution imaging spectroradiometer (MODIS) satellites (Terra and Aqua) providing science quality data with high temporal and spectral resolution, as well as intermediate spatial resolution imagery (Justice et al. 2002). This data was used in other modelling and comparison studies in this project (Gwate et al. 2016).

In the interest of comparing compatible classes between land cover datasets T1 and T2, a revised land cover classification scheme (legend) comprising eight classes (Table 3-1) was developed, by aggregating detailed classes (Aldwaik, Onsted & Pontius 2015; Petit et al. 2002) under a number of conceptually broader classes (Lück & Diemer 2008).

Table 3-1 Modified land cover legend compared to original legends

Conceptual class*	Final legend	Abbreviation
Natural, terrestrial non-vegetated bare areas	Bare Rock and Soil (natural)	BRS
Cultivated and managed terrestrial primarily vegetated areas	Cultivated land	CLs
	Forest Plantations (clear-felled, Pine spp, Other / mixed spp)	FPs
Natural and semi-natural terrestrial primarily vegetated areas	Unimproved (Degraded / Natural) Grassland	UG
	Forest Indigenous, Thicket Bushlands, Bush Clumps, High Fynbos	FITBs
Artificial, terrestrial primarily non-vegetated areas	Urban/Built-up (residential, formal township)	UrBu
Natural or artificial primarily non-vegetated aquatic or regularly flooded water bodies	Water bodies	Wb
Natural and semi-natural aquatic or regularly flooded vegetated areas	Wetlands	Wl

* Chief Directorate National Geospatial Information (CD: NGI) hierarchical structure (Lück & Diemer 2008: 7).

For this study the conceptual class “Cultivated and managed terrestrial primarily vegetated areas” was divided into “cultivated” (CLs) and “managed” (FPs) vegetation, while “Natural and semi-natural terrestrial primarily vegetated areas” was separated into grassland and low

shrubs (UG) and wooded vegetation (FITBs) based on the original NLC land cover legend (Table 3-1). Due to the low reported overall accuracy (65.8%) of the selected T1 dataset (Van den Berg et al. 2008), it was systematically updated using the revised legend (Table 3-1) with aggregated land cover classes, subsequently referred to as ENLC 2000 for T1. Some tracts, labelled "Degraded Unimproved (natural) Grassland", were recognised as subsistence farming and re-allocated to "CLs", while some parcels were re-allocated to "Urbu" after identification as rural villages. Accuracy assessment was performed on the edited dataset using stratified random sample points generated using ArcMap 10.4 (Environmental Systems Research Institute (ESRI), ESRI 2016). Classes were assigned from aerial photography (dated July 2000: Chief Directorate: National Geospatial Information (CD: NGI)) using the eight-class land cover legend (Table 3-1). In addition, a new land cover dataset was generated through image processing to represent the second time step (T2) for 2014, 15 years later (Okoye 2016) corresponding to collection of field data (Gwate et al. 2016).

3.3.3 Image processing[2]

Various steps were taken to generate the land cover dataset for 2014 (T2). These included developing supplementary datasets, image pre-processing and image classification (Okoye 2016). An object-oriented supervised approach using geographic object-based image analysis (GEOBIA) was selected for classifying imagery in eCognition Developer (Definiens 2003). A rule-based decision tree classification with defining threshold conditions was implemented to categorise object-features into respective classes.

Various supplementary datasets were developed to inform the decision tree classification. Stratified random sample points were generated from the existing land cover map (NLC 2000) and buffered by 30m to capture land cover areas. A new label, according to the new eight-class land cover legend (Table 3-1), was then assigned to each area by visually interpreting 2014 aerial photographs. In excess of 5000 points per catchment were generated in this manner, with more points selected for land cover classes with greater geographical extent e.g. UG. Field (in-situ) data collected during field visits in 2014 (less than 100 points) were included in the training dataset. Density estimation was performed on the SPOT Building Count (ESKOM SBC) (Mudau 2010) data to delineate urban areas (UrBu). Digitised boundaries of cultivated land (for CLs) and forest plantations (FP) were rasterised and slope was derived from a digital elevation model (SUDEM) (Van Niekerk 2013).

[2] Image processing was carried out by PI Okoye (Okoye 2016) assisted by SE Muller (CGA).

Two suitable cloud-free Landsat 8 images (scenes LC81690812014121LGN00 and LC81700822014160LGN00, dated 2014-05-01 and 2014-06-09 respectively) covering the spatial extent of the study area were downloaded for analysis. Images for the dryer winter season were selected to enhance the possibility of detecting greener IAPs within dry grasslands (Huang & Asner 2009). The Landsat scenes were atmospherically corrected by normalising the solar radiance through conversion of spectral radiance to atmospheric reflectance. This was done in ATCOR 2 (Richter & Schlapfer 2013) using radiance-conversion-to-top of atmosphere (ToA) reflectance model by converting digital numbers (DN) to radiance using the gain and bias values found in the metadata of each image file. The Landsat scenes had little or no cloud cover. Haze removal was performed using the ToA reflectance correction method to eliminate atmospheric effect that can cause image contamination and obscure ground features (Richter & Schlapfer 2013). This was followed by scene sharpening in PCI Geomatica (Nikolakopoulos 2008) to improve spatial resolution of the multi-bands in order to separate interspersed land cover classes by extracting small feature objects (Laliberte, Fredrickson & Rango 2007).

Spectral and vegetation indices were derived from the stacked Landsat dataset to improve the decision tree construction. These included the normalised difference vegetation index (NDVI), enhanced vegetation index (EVI), normalised difference water index (NDWI), soil adjusted vegetation index (SAVI) and tasselled cap brightness. NDVI was selected to separate indigenous forest from grasslands. NDVI is affected by soil brightness (Carlson & Ripley 1997) and saturates in high biomass areas (Huete et al. 2002; Wang, Liu & Huete 2002), EVI was consequently calculated as it shows greater sensitivity to vegetation change and reduces atmospheric effects on vegetation index values (Huete et al. 2002). NDWI was used to improve delineation of wetlands, owing to its sensitivity to changes in liquid water content of vegetation canopies (Gao 1996). SAVI (Haboudane 2004) was computed as a corrective index on soil brightness for areas with low vegetation cover (<40%) and exposed soil surface. The brightness algorithm (Crist & Cicone 1984; Kauth & Thomas 1976) was calculated to represent the reflectance intensity of bare rocks and soils, among other features, sharing similar spectral radiance.

Image pixels with relative homogeneity were clustered using multi-resolution segmentation (MRS) algorithm (Jiang et al. 2008; X Li et al. 2014). MRS is an ascending area-merging technique where smaller objects are progressively merged into larger objects. The advancement in heterogeneity is controlled with three input parameters, namely scale, shape and compactness (Laliberte, Fredrickson & Rango 2007). Shape and compactness were weighted at 0.1 and 0.5, respectively. Scale, referred to as “window of perception” (Marceau 1999) is a unit-less

parameter that regulates the size and homogeneity of image objects. Scale was set to two due to accommodate the land cover heterogeneity in the study area. All layers were given equal importance in the segmentation settings, except the near infrared and red bands that received double weighting to increase their response signal to vegetation greenness. A minimum mapping unit of 1825 m^2 (3X3 pan-sharpened pixels (Blaschke 2010; MacLean & Congalton 2012) was selected to accommodate small fragmented land cover classes.

A decision tree is defined as a classification procedure that recursively partitions a dataset into smaller subdivisions according to a decision framework defined by a tree structure (Friedl & Brodley 1997). Not only are decision trees non-parametric and do not require assumptions regarding the distributions of the input data, but the classification structure is explicit and easy to interpret, making the method intuitive. Using training classes derived from aerial photographs with eight land cover classes (Table 3-1), a preliminary decision tree was generated in the classification and regression trees (CART) software (Salford Predictive Modeller 7.0) from which the final rule-set was constructed (Laliberte, Fredrickson & Rango 2007). The shadows class was incorporated into the surrounding vegetative cover class, validated by visual assessment from aerial photographs. The land cover maps (one for each Landsat scene) were combined into a single dataset hereafter referred to as DLC 2014 (T2).

3.3.4 Accuracy assessment

Since accuracy measures, estimated from a sample, are subject to uncertainty (Olofsson et al. 2014; Olofsson et al. 2013; Pontius, Shusas & McEachern 2004), a more robust approach is to report the estimated error matrix (Section 2.3.2) in terms of proportion of area and estimates of OA, UA and PA based on the population (Pontius, Shusas & McEachern 2004). An associated confidence interval provides a range of values for the reported parameter which takes the uncertainty of the sample-based estimate into account. Accuracy assessment of both ENLC 2000 for T1 and DLC 2014 for T2 was performed by cross tabulating estimated area of observed reference classes vs. predicted classes. Stratified random sample points were generated per land cover class using ArcMap 10.4. Reference land cover classes were assigned to these sample points from aerial photography of the same year. The estimated proportion of area for each cell of the error matrix was calculated (Olofsson et al. 2013). Accuracy measures calculated from this error matrix includes OA (proportion correctly classified) PA accuracy (the probability that a reference land cover is correctly classified) and UA (the probability of pixels matching the sample) (Congalton 2001). A 95% confidence interval was computed from the standard error of the estimated area (Olofsson et al. 2014).

3.3.5 Change analysis

The comparative approach the most commonly used land cover change detection method (Section 2.4.1). In this approach categorical land cover maps generated independently at different time steps are compared using a transition matrix to identify the most important transitions (Marceau 1999; Mas 1999). The basis for this method is an accurate land cover map at each time step. Errors in these land cover maps will be propagated to the change map, with overall expected error greater than in either of the maps from which it originated (Stott & Haines-Young 1998).

Land cover change analysis was performed by comparing the reference dataset ENLC 2000 from time step 1 (T1) to the classified dataset DLC 2014 from time step 2 (T2) in a transition matrix. Rows in the transition matrix represent the land cover at T1, while columns represent land cover at T2. From the transition matrix, net gain and loss per class was calculated. The accuracy of the resulting land cover change map was quantified (Section 2.4.2). The pattern of error observed in the land cover change map will reflect the errors in the individual input classified maps and their interactions (Nagendra, Munroe & Southworth 2004) if the classification errors are independent (Fuller, Smith & Devereux 2003). This is unlikely as locations that were difficult to classify correctly at T1 would also be difficult to classify correctly at T2 even if different methodologies are used (Congalton 2001).

The probability of a particular class transition occurring can be calculated from the user's accuracies for each land cover map (Pontius & Li 2010), which give the conditional probability that a pixel transitioned from the land cover class in its row to the class in its column. Theoretical (D), upper (U), middle (M) and lower (L) bounds for estimates of change were calculated (Pontius & Li 2010) from the user's accuracy per land cover class for each input map (T1 and T2) and reported in a transition matrix. Matrix D assumes the land cover maps from T1 and T2 to be perfectly accurate. Matrix M assumes possible error in all pixels. Matrix U considers error only in areas that correspond between T1 and T2, whereas matrix L considers error in places that differ between T1 and T2 and assumes no error in pixels that match (Pontius & Li 2010).

Figure 3-3, adapted from Fuller, Smith & Devereux (2003), shows the level of change that can be measured with 75% reliability when performing change analysis between pairs of maps with two and eight classes, with map accuracies ranging from 75 to 99%. The level of change between 2000 and 2014 that can be measured with 75% reliability (75% of the observed difference between the maps is real change), was subsequently calculated as a function of the

accuracy of each input land cover map, the eight classes mapped and the percentage change detected according to Figure 3-3 (Fuller, Smith & Devereux 2003).

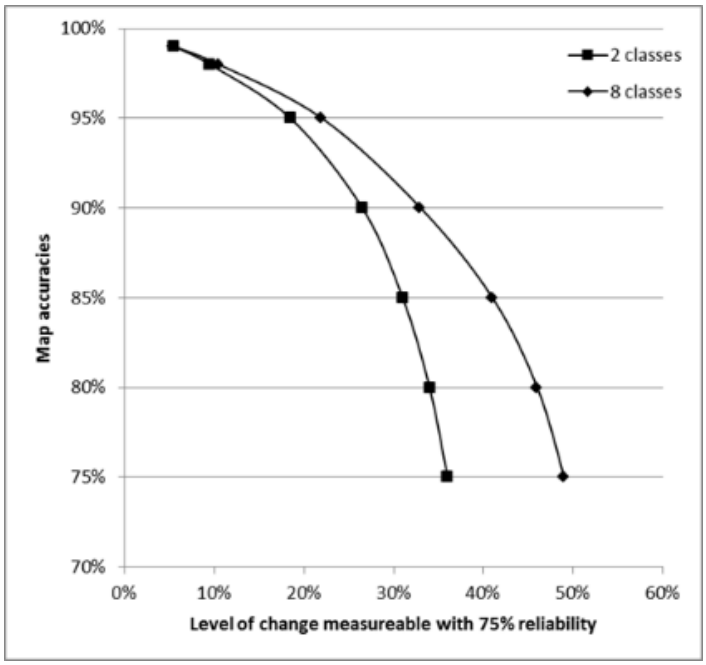

Adapted from Fuller, Smith & Devereux (2003)

Figure 3-3 Level of change with 75% reliability when mapped using pairs of maps with 2 and 8 classes and with map accuracies ranging from 75 to 99%

3.3.6 Land cover change trajectories

Seven main flows or trajectories of aggregated land cover change were identified (Feranec et al. 2010; Stott & Haines-Young 1998) and are listed in Table 3-2 (highlighted with grey background). These trajectories include: (1) persistence, where no land cover change has occurred; (2) intensification, which represents the transition of a lower intensity to a higher intensity usage; (3) afforestation representing the planting of trees; (4) deforestation, which involves the clearance of trees; (5) extensification where higher intensity usage is converted to a lower intensity usage; (6) natural dynamics to represent seasonal conversions; and (7) exceptionality associated with potential map errors. In the context of this study, these seven categories were subdivided to account for specific changes in this landscape (Table 3-2). As part of persistence (P), Pf indicates areas where woody vegetation (including indigenous forest and IAPs) has persisted while Pu describes areas where settlements have persisted over time. Of particular importance are areas where forests (indigenous or alien) and other woody areas have disappeared or been removed (reclamation, deforestation) or another land cover has potentially been replaced by IAPs (FITBs intensification). Due to the resolution of the satellite imagery used in the generation of the land cover classes, it was not possible to determine change in the intensity of agricultural activities, but conversion to agricultural practices can be

identified (agricultural intensification). Exceptionality indicates where an improbable conversion occurs such as to wetland, which may be used to identify classification errors.

Table 3-2 Labels and descriptions for conversion patterns and trajectories

Land cover conversion label	Description
Persistence	
P – Persistence	Areas with no change in land cover
Pf – FITBs persistence	Areas where woody natural and artificial vegetation persists
Pu – Urban persistence	Areas where settlements persist over time
Intensification	
If – FITBs intensification	Areas where woody natural and artificial vegetation substitutes previous land cover
Iu – Urban intensification	Areas converted to urban
Ia – Agricultural intensification	Areas where agricultural activities substitute previous land cover
Afforestation	
R – Afforestation	Areas where other land cover is converted into plantation
Deforestation	
D – Deforestation	Plantation converted to other land cover
Extensification	
Re – Reclamation	Woody natural and artificial vegetation areas converted to grassland and bare area
De – Degradation	Shrub areas converted to grassland or bare areas
A – Abandonment	Urban and agricultural areas converted to grassland and bare areas
Natural dynamics	
Dn – Natural dynamics	Areas where natural changes occurred
Exceptionality	
E – Exceptionality	Unusual conversion–Not expected / possible misclassification / active intervention

The use of a land cover conversion label not only allows a thematic representation of the spatial distribution of change (Aldwaik & Pontius 2013), but also provides information about the processes (flows) in the landscape that can be represented on a map to simplify the evaluation of land cover change (Section 2.4.3). From the intersection of the two land cover layers, a square transition matrix was created where rows show the classes from 2000 (T1), columns show the same classes from 2014 (T2). The table entry indicates the intersection created by the overlay of the successive land cover maps. A land cover conversion label (Table 3-2) was assigned to each intersection representing process flow depicted in Table 3-3.

Table 3-3 Land cover conversion labels representing conversion trajectories between T1 and T2

		2014 (T2)							
Class label		**UG**	**FITBs**	**BRS**	**Wb**	**Wl**	**CLs**	**FPs**	**UrBu**
2000 (T1)	UG	P	IF	De	Dn	Dn	Ia	R	Iu
	FITBs	Re	Pf	Re	E				
	BRS	Dn	IF	P					
	Wb			Dn	P				E
	Wl				Dn	P			Iu
	CLs	A		A	E	E	P		
	FPs	D		D			Ia	P	
	UrBu	A		A				R	Pu

UG: Unimproved Grassland; FITBs: Forest Indigenous Thicket Bushlands; BRS: Bare Rock and Soil
Wb: Water bodies; Wl: Wetlands; CLs: Cultivated Land; FP: Forest Plantations; UrBu: Urban built-up

This conceptual schema of using land cover conversion labels (Benini et al. 2010) for change analysis was developed to describe patterns and trajectories both qualitatively and quantitatively. The area for each land cover conversion label was calculated and expressed as a percentage of the total area of each of the catchments (Section 2.4.3).

3.4 RESULTS

3.4.1 Accuracy assessment of datasets for T1 and T2

The accuracy assessment for the land cover map ENLC 2000 for Time Step 1 (T1) obtained after updating the existing NLC dataset (Van den Berg et al. 2008) based on sample counts, is presented in Table 3-4, while Table 3-5 illustrates the accuracy expressed as the estimated per cent of the study area (the population). Rows represent map categories, while reference categories are given in the columns. Table 3-4 also reports the area for each map category and the per cent of the study area to the nearest integer, where a zero means a positive number less than one half and a dash means that no pixels were observed. Table A-1 in Appendix A provides the detail at the catchment level. Accuracy measures, OA, UA and PA are presented with a 95% confidence interval (Olofsson et al. 2013).

Table 3-4 Summarised accuracy assessment of land cover map ENLC 2000 (T1) based on sample counts

Class	UG	FITBs	BRS	Wb	Wl	CLs	FP	UrBu	Total	Map Area Ha	Map Area %
UG	3544	269	59	13	77	190	71	60	4283	78370	70
FITBs	90	1360	2	6	0	26	31	0	1515	10367	10
BRS	1	0	0	0	0	0	0	0	1	19	0
Wb	1	0	0	448	1	3	0	0	453	1402	1
Wl	41	0	0	1	155	62	22	0	281	1427	1
CLs	79	33	0	1	17	1488	15	21	1654	12089	11
FP	13	253	0	0	2	1	1125	1	1395	4991	4
UrBu	68	12	0	0	1	55	1	418	555	3506	3
Total	3837	1927	61	469	253	1825	1265	500	10137	112172	100

UG: Unimproved Grassland; FITBs: Forest Indigenous Thicket Bushlands; BRS: Bare Rock and Soil
Wb: Water bodies; Wl: Wetlands; CLs: Cultivated Land; FP: Forest Plantations; UrBu: Urban built-up

Table 3-5 Summarised accuracy assessment of ENLC 2000 (T1) expressed as the estimated proportion of area

Class	UG	FITBs	BRS	Wb	Wl	CLs	FP	UrBu	Total	UA	PA	Overall
UG	58	4	1	0	1	3	1	1	70	83±1	97±1	84±1
FITBs	1	8	0	0	-	0	0	-	9	90±2	60±2	
BRS	0	-	-	-	-	-	-	-	0	0±50	0±1	
Wb	0	-	-	1	0	0	-	-	1	99±1	83±4	
Wl	0	-	-	0	1	0	0	-	1	55±6	34±6	
CLs	1	0	-	0	0	10	0	0	11	90±2	72±2	
FP	0	1	-	-	0	0	4	0	4	81±2	70±3	
UrBu	0	0	-	-	0	0	0	2	3	75±4	68±4	
Total	60	14	1	1	2	14	5	3	100			

UG: Unimproved Grassland; FITBs: Forest Indigenous Thicket Bushlands; BRS: Bare Rock and Soil
Wb: Water bodies; Wl: Wetlands; CLs: Cultivated Land; FP: Forest Plantations; UrBu: Urban built-up
UA: User's Accuracy; PA: Producer's Accuracy

Based on the sample counts (Table 3-4) and estimate of the population (Table 3-5), the OA of the T1 dataset (ENLC 2000) is 84% with a 95% confidence interval of 1% based on the calculated standard error. This is almost 20% more than the uncorrected NLC 2000 dataset (Van den Berg et al. 2008).

A summary of the accuracy assessment performed on the DLC 2014 dataset, which was derived through classification of Landsat 8 imagery for time step T2, is presented in Table 3-6. Catchment level results are reported in Table A-2 of Appendix A. The descriptions for abbreviations used as column headings can be found in Table 3-1. The rows represent the map categories, while columns represent reference categories. The areas computed from the map categories, as well as the per cent of total area, are also shown in Table 3-6. Similar to Table 3-5, Table 3-7 illustrates the accuracy of the T2 dataset based on Table 3-6 data expressed as the estimated proportion of area (the population) reported as the per cent, where a zero means a positive number less than one half and a dash means that no pixels were observed.

Table 3-6 Summarised accuracy assessment of DLC 2014 (T2), based on sample counts

Class	UG	FITBs	BRS	Wb	Wl	CLs	FP	UrBu	Total	Map Area ha	Map Area %
UG	3282	363	8	16	170	64	12	42	3957	75968	68
FITBs	75	1475	0	1	1	9	37	0	1598	9861	9
BRS	5	1	24	0	0	1	0	1	32	193	0
Wb	4	2	0	173	6	0	0	0	185	1319	1
Wl	26	6	0	17	121	0	2	0	172	538	1
CLs	91	32	6	4	35	1577	0	25	1770	13089	12
FP	15	2	0	0	0	0	541	3	561	4175	4
UrBu	39	6	0	0	2	5	0	393	445	7030	6
Total	3537	1887	38	211	335	1656	592	464	8720	112172	100

UG: Unimproved Grassland; FITBs: Forest Indigenous Thicket Bushlands; BRS: Bare Rock and Soil
Wb: Water bodies; Wl: Wetlands; CLs: Cultivated Land; FP: Forest Plantations; UrBu: Urban built-up

Table 3-7 Summarised accuracy assessment of DLC 2014 (T2) expressed as the estimated proportion of area

Class	UG	FITBs	BRS	Wb	Wl	CLs	FP	UrBu	Total	UA	PA	Overall
UG	56	6	0	0	3	1	0	1	68	83±1	97±1	85±1
FITBs	0	8	-	0	0	0	0	-	9	92±1	55±2	
BRS	0	0	0	-	-	0	-	0	0	75±17	42±17	
Wb	0	0	-	1	0	-	-	-	1	94±4	76±6	
Wl	0	0	-	0	0	-	0	-	0	70±7	10±3	
CLs	1	0	0	0	0	10	-	0	12	89±2	90±2	
FP	0	0	-	-	-	-	4	0	4	96±2	90±3	
UrBu	1	0	-	-	0	0	-	6	6	88±3	86±3	
Total	58	15	0	1	4	12	4	6	100			

UG: Unimproved Grassland; FITBs: Forest Indigenous Thicket Bushlands; BRS: Bare Rock and Soil
Wb: Water bodies; Wl: Wetlands; CLs: Cultivated Land; FP: Forest Plantations; UrBu: Urban built-up

Wetlands (Wl) were poorly predicted with a low PA (Section 2.3.2) of 36% based on sample counts, which means that more than 60% of the reference samples were omitted from the classification (error of omission). The PA calculated from the area proportion is as low as 10% ± 3%, reflecting the uncertainty in the classification. Based on the reference data, the

stratified area for land cover class Wl can be calculated as 3981 ± 492 ha, more than seven-times the mapped area. An error-adjusted estimate of the area covered by Wl (±95% confidence interval) confirms the need to adjust the map area obtained from pixel counting to account for the large omission error. FITBs and bare rock and soil (BRS) also showed low producer's accuracies.

The FITB class showed a UA (Section 2.3.2) of greater than 90%, but a PA of only 55% ± 2%. The OA based on reference point data, computed as correctly classified divided by the total, ranged between 83% (T35B) and almost 90% (S50E) (Table A-2 in Appendix A) using sample points (Table 3-6), but did not differ much when using the proportion of estimated area (Table 3-7). The OA (Section 2.3.2) for T35B was 83% ± 1% and for S50E slightly lower at 87% ± 1%. The OA for the study area was calculated as 85% ± 1% (Table 3-7).

3.4.2 Land cover change: ENLC 2000 vs. DLC 2014

A post-classification comparison of the overlaid land cover maps for 2000 (T1) and 2014 (T2) was made using a transition matrix (Section 2.4.2). Table 3-8 shows the transition from one land cover class to another as a per cent of the study area. Four values are reported per land cover change combination. The left entries in the cells represent D, assuming each input land cover map to be completely accurate; the upper right entries are the upper bound (U) where error exists in corresponding areas; the middle right entries (M) assume possible error in all pixels; and the lower right entries (L) assume no error in matching pixels. Descriptions of class labels can be found in Table 3-1. The rows represent the T1 (2000) land cover classes, while the T2 (2014) land cover classes are found in the columns. The diagonal entries (light grey in Table 3-8) indicate the persistence of land cover classes, while the off-diagonal entries indicate a change from one land cover class to a different class. The Total T1 column shows the land cover totals at 2000, and the Total T2 row shows the land cover totals at 2014 expressed as a per cent of the total study area. The column on the right (Loss T1) indicates loss by land cover class, and the row at the bottom (Gain T2) indicates gain by land cover class. The total change as a proportion of the total study area is given in the entry in the bottom row of column Loss T1. The columns UA and PA reflect the product of the user's and producer's accuracy for each individual land cover map (T1 and T2) providing a theoretical accuracy for the transition per class.

Grassland (UG) still dominated the study area in 2014 with 68% of the total area being classified as such when measuring change without considering error (accuracy 84% × 85% = 71%). Although UG has the highest theoretical PA of 94%, the remaining UG could be as low as 58%

when considering possible error in all pixels (matrix M). Net losses were noted for UG and FP, with gains in UrBu. No change was calculated for Wb. For classes FITBs, BRS and CLs, the net gain or loss was dependent on the method for calculating land change (matrix D, M, U or L). CLs showed a net gain of 1% when no error is considered, but up to 2% loss when possible error in all pixels is considered (M). The low PA for CLs of 63% confirms large differences between map and ground conditions. In addition, the theoretical accuracy of the resulting land cover change maps, computed as the product of the overall accuracies of the individual land cover maps at T1 and T2 (Aldwaik & Pontius 2013; Fuller, Smith & Devereux 2003; Mas 1999), ranged between a low 67% for T35B to 76% for T12A (Table A-3 in Appendix A). This leaves a hypothetical error in landscape transition of up to 30% based on error propagation from contributing land cover maps. The total change, computed from loss at T1 and gain at T2, varies between 18% and 42% calculated from the lower (L) and upper (U) bounds of change (lower right cell, Table 3-8) with 19% computed from the overlay of the T1 and T2 maps.

Table 3-8 Transition matrix for the 2000 (T1)–2014 (T2) change

Class		2014 (T2)								Total	Loss	UA	PA
		UG	FITBs	BRS	Wb	Wl	CLs	FP	UrBu	T1	T1		
2000 (T1)	UG	42 60 42 61	8 3 7 2	0 0 0 0	0 0 0 0	2 0 2 0	4 2 3 2	1 1 1 1	4 3 3 2	61 70 60 69	19 9 17 8	69	94
	FITBs	7 4 6 3	4 5 5 5	0 0 0 0	0 0 0 0	0 0 0 0	0 0 1 0	1 0 1 0	0 0 0 0	13 9 14 10	9 4 9 4	83	33
	BRS	1 0 1 0	0 0 0 0	0 0 0 0	0 0 0 0	0 0 0 0	0 0 0 0	0 0 0 0	0 0 0 0	1 0 1 0	1 0 1 0	0	0
	Wb	0 0 0 0	0 0 0 0	0 0 0 0	1 1 1 1	0 0 0 0	0 0 0 0	0 0 0 0	0 0 0 0	1 1 1 1	0 0 0 0	92	63
	Wl	2 1 1 0	0 0 0 0	0 0 0 0	0 0 0 0	0 0 0 0	0 0 0 0	0 0 0 0	0 0 0 0	2 1 2 1	2 1 2 1	39	3
	CLs	4 1 4 1	1 0 1 0	0 0 0 0	0 0 0 0	0 0 0 0	7 9 7 9	0 0 0 0	1 0 1 0	13 11 14 11	6 2 6 3	80	64
	FP	2 1 2 1	0 1 1 1	1 0 0 0	0 0 0 0	0 0 0 0	0 0 0 0	2 3 2 3	0 0 0 0	5 4 5 4	3 2 3 2	78	63
	UrBu	1 0 1 0	0 0 0 0	0 0 0 0	0 0 0 0	0 0 0 0	0 0 0 0	0 0 0 0	2 3 2 3	3 3 3 3	2 0 2 0	67	58
Total T2		58 68 58 67	13 9 15 9	1 0 0 0	1 1 1 1	3 0 4 1	12 12 12 12	4 4 4 4	7 6 6 6				
Gain T2		17 7 16 6	9 4 10 4	1 0 0 0	0 0 0 0	3 0 3 1	5 3 4 3	2 1 2 1	5 4 5 3		42 19 40 18		

Note: The left entries in the cells represent matrix D, the upper right entries matrix U, the middle right entries matrix M and the lower right entries matrix L. All entries express the per cent of the study area

Assuming that map errors are independent, and changes are mapped correctly within the area of overlap, the accurately-mapped difference due to change (c), as well as those changes that are hidden, can be calculated (Fuller, Smith & Devereux 2003). Areas with no change

(persistence) can also be identified. Table 3-9 assesses the likely differences due to change and those due to error (Fuller, Smith & Devereux 2003). Where the land cover change map reflects the true situation (change or persistence), the cell text in Table 3-9 is shown in bold; true change hidden by errors is given in italic text; and the cells are shaded where the map records a difference (change or error).

Table 3-9 A comparison of T1 and T2 to assess the differences due to change or error

Proportional accuracy of T1 (2000)		a_1	0.84				
Proportional accuracy of T2 (2014)		a_2	0.85				
Number of classes		N	8				
Indicative proportion of change		C					
Areas of change (c)		c = 0.19			c = 0.40		
		a_2	$1 - a_2$	Totals	a_2	$1 - a_2$	Totals
a_1		**0.14**	0.02	0.16	**0.29**	0.04	0.33
			0.00	0.00		*0.01*	0.01
$1 - a_1$		0.02	0.00	0.03	0.05	0.01	0.05
		0.00	*0.00*	0.00	*0.01*	*0.00*	0.01
	Totals	0.16	0.03	0.19	0.34	0.06	0.40
Areas with no change (1 − c)		a_2	$1 - a_2$	Totals	a_2	$1 - a_2$	Totals
a_1		**0.58**	0.10	0.68	**0.43**	0.08	0.50
$1 - a_1$		0.11	0.02	0.13	0.08	0.01	0.09
			0.00	0.00		0.00	0.00
	Totals	0.69	0.12	0.81	0.51	0.09	0.60
				c = 0.19			c = 0.40
Maps show different classes (sum of shaded cells)				41%			55%
Maps show the same classes (sum of unshaded cells)				59%			45%
Real change as a proportion of mapped difference				40%			54%
Proportion of change which is correctly shown as such				96%			96%

Note: Cell text in bold reflects true change or persistence; true change hidden by errors is given in italic text; and cells are shaded where the map records a difference (change or error).

With the change of 19% calculated from Table 3-8 and the levels of accuracy estimated for T1 (Table 3-5) and T2 (Table 3-7), there would only be a 59% agreement between the two land cover maps, and 41% of the combined map area would record differences. Of the 41% difference, ~18% would be real change, and ~23% would have arisen through errors. With a change of 40% (matrix M from Table 3-8), there would only be an agreement of 45% between the maps and 55% difference. Although there is substantial over-estimation of changed areas in both scenarios, 96% of all change could be mapped (Table 3-9).

3.4.3 Land cover conversion dynamics

Using the conceptual schema of land cover conversion labels (Table 3-2 and Table 3-3) in analysing the change matrix statistics, landscape transition between the two time periods was quantified. Transitions from and to land cover classes BRS and Wl were not characterised according to Table 3-3, but were added to land cover conversion label E (exceptionality) due to the low UA and PA for these two classes. Table 3-10 summarises the conversion dynamics

by area and per cent of catchment area to the nearest integer, where zero indicates a positive number less than one half, and a dash means no transitions were observed.

Table 3-10 Land cover conversion (area and percentage) described using land cover labels

Land cover label (Land cover change trajectory)		Conversion between Time Step T1 and T2 (2000-2014)							
		T35B		T12A		S50E		Overall	
		ha	%	ha	%	ha	%	ha	%
Pf:	FITB persistence	683	2	1984	7	2746	6	5413	5
If:	FITB intensification	916	2	1466	5	2066	5	4448	4
Re:	Reclamation	2394	6	652	2	1275	3	4321	4
Pu:	Urban persistence	28	0	1133	4	1892	4	3054	3
Iu:	Urban intensification	49	0	1582	6	2343	5	3975	4
P:	Persistence	31488	80	19364	70	30843	69	81694	73
Ia:	Agricultural intensification	671	2	865	3	1869	4	3405	3
R:	Afforestation	1121	3	54	0	91	0	1265	1
D:	Deforestation	356	1	136	1	572	1	1064	1
De:	Degradation	-	-	-	-	-	-	-	-
Dn:	Natural dynamic	779	2	15	0	187	0	981	1
A:	Abandonment	533	1	555	2	720	2	1808	2
E:	Exceptionality	530	1	60	0	155	0	745	1

Figure 3-4 provides the spatial distribution of these land cover conversions using the indicator-based approach (land cover labels) to visualise change trajectories.

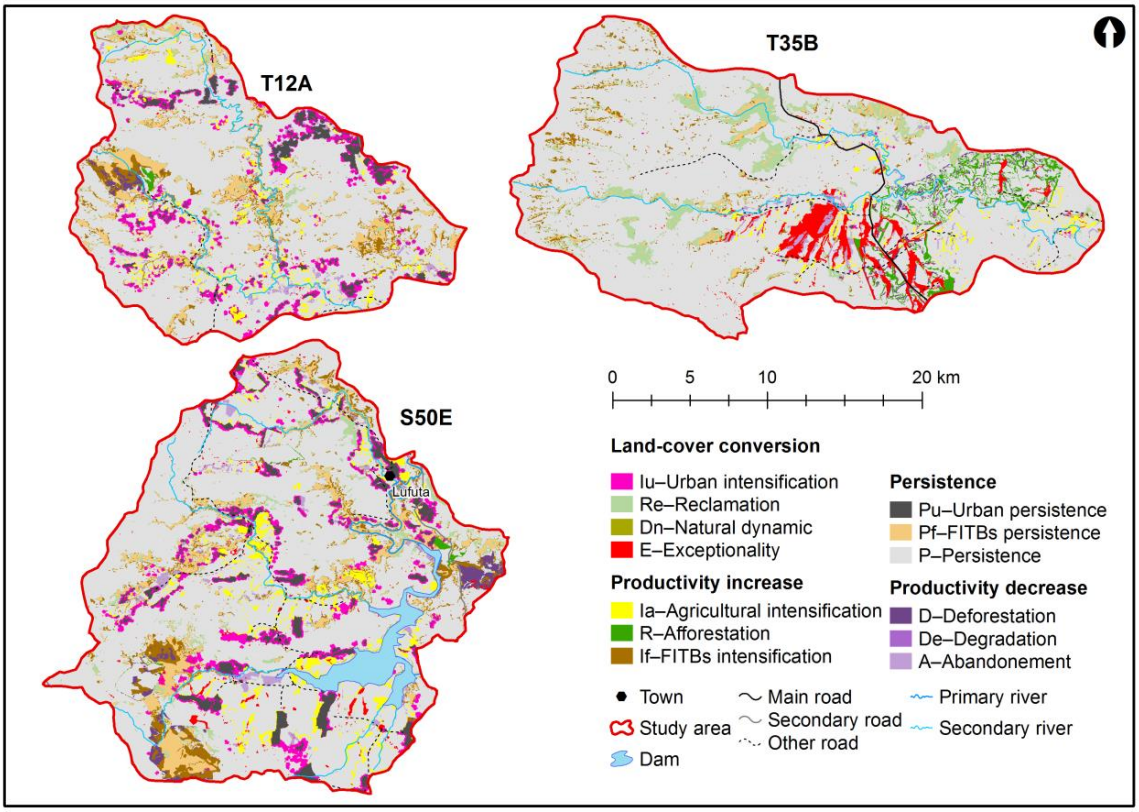

Figure 3-4 Indicator-based approach for land cover conversion.

Land use patterns in all three catchments are characterised by persistence (Figure 3-4 land cover labels P, Pu and Pf) with more than 70% of the total area showing no change. Conversions between classes represent small fragmented areas of less than six per cent within the

catchments. Intensification of woody vegetation, where class FITBs have substituted previous land cover, averaged at four per cent, while reclamation (Re) to grassland was four per cent over all three catchments. Transitions from plantation, labelled deforestation (D), covered one per cent of the study area extent, while afforestation (R) mostly affected T35B. Degradation (De) linked to conversion to bare soil was not represented due to the low accuracy of land cover class BRS. Exceptionality (E), indicating possible classification errors and land cover classes with high uncertainty (BRS and Wl), represented one per cent of land transformation. The highest exceptional trajectories were found in catchment T35B, caused by the high presence of Wl.

3.5 DISCUSSION

This study describes the challenges encountered while performing change analysis to determine landscape conversion dynamics between two time steps, represented by two datasets derived using different methods. The original input dataset proposed for Time Step 1 (T1) proved unsatisfactory based on OA and was subsequently improved using manual methods. The T1 dataset was derived from a national level dataset frequently used for studies that require land cover as input, such as the quantification of runoff and infiltration for a particular land cover unit (Thomas 2015). Users often do not consider the low reported accuracy. As this dataset coincides with the availability of high temporal resolution MODIS data, it is frequently used as a starting point for area-based spatial analysis studies.

The dataset for Time Step 2 (T2) is the output of the object-based classification of Landsat 8 data. The OBIA approach was able to deal with the problem of the salt-and-pepper effect (Section 2.3.1), common in classification outcomes using traditional per-pixel approaches (Blaschke 2010). The rule-based expert system provided robust land cover classifications for a highly fragmented catchment landscape and precision in delineating boundaries of the various vegetation types despite the coarser Landsat 8 resolution (Blaschke 2010; Radoux & Defourny 2007). The OA for this land cover dataset (T2) using single-date imagery was deemed acceptable based on the OA value of greater than 85% ± 1% (Table 3-7). Sufficient ground truth data are required for definite mapping of alien plants and other cover classes, such as wetlands.

As land cover classification is fraught with uncertainty, it is important to accurately report on the uncertainty inherent in data created through spatial modelling (Olofsson et al. 2014; Olofsson et al. 2013), which starts with an effective sampling design of ground truth data (Olofsson et al. 2014). Estimates of OA, user's accuracy and PA based on the population

(Pontius, Shusas & McEachern 2004) can be reported. A confidence interval can be computed, to describe the uncertainty of the sample-based estimates. In addition, the construction of a meaningful land cover legend through categorical aggregation in a manner that gives insights concerning categorical change over time (Aldwaik, Onsted & Pontius 2015) that can accommodate these wooded classes must be investigated. However, it must be noted that category aggregation may decrease the error in the individual land cover maps, as well as the difference between land cover maps at T1 and T2 (Pontius & Malizia 2004).

In this study, land cover change detection was performed using a transition matrix to compare the categorical land cover maps from the two time steps. The method (D) assumes that the probability of error in the two independently classified maps (T1 and T2) is randomly distributed, which is unlikely, as error is affected by autocorrelation (Pontius & Lippitt 2006). Upper (U), middle (M) and lower bounds of land cover change were also reported. Method U assumes that error only exists where land cover maps match; therefore, more error is associated with higher estimated change, up to 42% in this study area. Simulated errors cause a shift of values from the diagonal to the off-diagonal entries of the transition matrix (Pontius & Li 2010). In contrast, method L considers that error exists only in areas of change, therefore more error with less estimated change (Pontius & Li 2010). As some classes are easier to classify than others, and such regions are frequently clustered (Congalton 2001); the error may exhibit spatial autocorrelation. This would cause large homogenous classes, such as UG, to exhibit small errors compared to fragmented small classes, such as woody outcrops with many edges around small patches. This is clear from the high PA for the UG class (Table 3-5 and Table 3-7) and low PA for FITBs. Error may also be temporally autocorrelated, such as classes on flat slopes that persist over time, which may be easier to classify (Pontius & Lippitt 2006). Future studies should therefore consider investigating the spatial and temporal correlation of error within the input land cover maps prior to land cover change analysis, to reduce error propagation (Burnicki, Brown & Goovaerts 2007). The accuracy for the land cover change map was derived from the overall accuracies of the individual land cover maps (84% and 85%, respectively) resulting in a low OA of 71% for the change map. From Figure 3-3, the level of change that can be recorded with 75% reliability on maps with 2, 3, 10 and 30 classes with a particular accuracy can be determined (Fuller, Smith & Devereux 2003). For instance, to map a change of 19% (Table 3-8), input land cover maps would need to be about 96% accurate, assuming 75% reliability. Should greater reliability be required, map accuracies need to approximate 99% (Kiruki et al. 2017), a near-impossible operational requirement. Theoretical accuracy of greater than 70% was achieved for the land cover change maps for the southern catchments (T12A and

S50E) with T35B showing greater uncertainty at 67%. Individual classes BRS and Wl displayed low producer's accuracies, which caused conversion trajectories involving these classes to be flagged as exceptionality and excluded from the trajectory analysis.

This study used a framework for change analysis (Benini et al. 2010; Feranec et al. 2010; Mas 1999) based on change trajectories derived from land cover labels (Table 3-3) categorising combinations of land cover change into seven main flows or trajectories. When this framework was applied to the land cover change maps, the persistence of land cover classes (>70% from Table 3-10) was noted with grassland remaining the majority cover in the three catchments. Both urban persistence (Pu) and FITB persistence (Pf) are clearly visible in catchments T12A and S50E (Figure 3-4) with the expansion of urban areas (Iu, urban intensification) in these two southern catchments predominantly at the expense of grassland (UG) and agriculture (CLs), demonstrating the natural development of urban areas. Urban intensification is also highest in these catchments where subsistence farming is practised. This apparent intensification may possibly be attributed to the T1 dataset classification strategy that identified formal townships but failed to delineate traditional villages practising subsistence farming, as encountered in these areas. Accordingly, agricultural activities intensified (Ia) by four per cent in S50E, attributed to conversion from grassland (UG) when no error is considered, but up to 2% loss when possible error in all pixels is considered (M), associated with low user's and producer's accuracies for CLs in land cover classification.

Considering that the class FITBs contains indigenous forest, thicket, bushland, bush clumps, high fynbos and alien plants that are spectrally similar and could not be separated using Landsat imagery, it is not surprising that T12A, with persistent remnants of indigenous forest, has the highest percentage of the class FITB persistence (Pf). The high persistence of FITBs (Pf) in S50E is likely attributed to the presence of *Pinus* spp. (Mucina & Rutherford 2006) on the southwest of the catchment. Interestingly, despite T12A being a focus area for WfW with the aim of eradicating alien trees, there is still a prominent presence of such vegetation. In both the T1 and T2 datasets, the low PA for FITBs highlights the uncertainty associated with this transition. In order to provide a better distinction between different wooded classes, higher spatial resolution data need to be considered to distinguish between spectrally homogenous vegetation types (Wang, Liu & Huete 2002).

Since scientists want to identify the dominant signals of land change, the varying dynamics between the three catchments must be noted. Accounting for approximately four per cent of the study extent, agricultural intensification (Ia) and afforestation (R) can be regarded as an increase in the productivity of the landscape, with land use intensification associated with a productivity-

driven landscape. Conversely, the persistence and intensification of FITBs (Pf + If) may be regarded as a degradation gradient existing in the landscape, when IAPs included in the FITBs class affect biodiversity and ecosystem services. T12A and S50E have similar trajectories of this degradation gradients (Pf + If), which may reflect real change or be an artefact of the classification and land cover change detection. After persistence, this is the strongest conversion trajectory within these two catchments. It can be postulated that the FITB persistence and intensification noticeable in T12A and S50E may be attributed to IAPs, known to affect grassland veld types (Carbutt et al. 2011).

The context of reclamation (Re) in this study designates the potential extent of anthropogenic rehabilitation, where areas classified as FITBs (invaded by IAPs and other woody vegetation) have been replaced with grassland and bare rocks. Despite reported WfW activity, reclamation (Re) in T12A and S50E was less than three percent. In T35B, six per cent of FITBs have been returned to grassland, an area of almost 2400 ha. This, however, may be an artefact associated with the low accuracy of the land cover change map for T35B (Table A-3 in Appendix A). Spatial analyses of the locational factors, which may be driving the land cover change trajectories (Ariti, Van Vliet & Verburg 2015; Kiruki et al. 2017; MacFadyen et al. 2016), are envisaged for future research.

3.6 CONCLUSIONS

This study described the use of independent land cover maps for change analysis in a grassland-dominated landscape for three catchments in the Eastern Cape of South Africa. Land cover maps were derived from an existing national land cover dataset data (2000-T1) and through OBIA (2014-T2) of Landsat 8 imagery. A revised land cover legend comprising eight classes was developed by aggregating detailed classes under a number of conceptually broader classes to create a common land cover scheme for comparing compatible classes between land cover datasets T1 and T2.

The land cover change analysis has revealed an increase of agricultural intensification, urbanisation and infrastructural development across the three catchments over the 15-year period. Land cover class FITBs in the guise of natural vegetation or alien plants have persisted and intensified chiefly at the periphery of river channels, as well as around agricultural areas and human inhabited regions. While some land cover classes, such as grassland and water bodies, have maintained approximate states of persistence, land degradation resulting from land use intensification and FITBs (possibly IAPs) infestations has been identified.

Landscape units associated with clearly identified persistent or degradation trajectories can be used in future studies to characterise water use and carbon fluxes for sustained landscape health from remote sensing products allowing models of ecosystem stress to be developed. The persistence and intensification of natural or invaded wooded areas were identified as such a degradation gradient within the landscape. The challenge remains to determine significant signals in the landscape that are not artefacts of the underlying input data, different classification schemes and aggregation methods, the experience of operators or the scale of analysis. Through systematic analysis of changes and accurate reporting of uncertainty, this can be addressed to produce output that authentically reflects the landscape dynamics in order to accurately quantify the effect of landscape transitions on the ecosystem services in the catchments.

3.7 SPATIAL PATTERNS OF ERROR

The land cover change analysis described in this chapter was performed on land cover maps derived specifically for this study. This means that relatively good accuracy assessment data was available and accurate reporting could be done on the inherent uncertainty associated with land cover classification. This study highlighted the effect of poor accuracy results on the reliability of land cover change results, stressing the importance of high accuracies for operational purposes. In the next chapter (Chapter 4), further systematic analysis of changes and potential map error are explored in the quest to produce output that authentically reflects landscape dynamics. Landscape units associated with clearly identified persistent trajectories can then be used in future studies (Chapter 6) to characterise water use and model future scenarios (Chapter 5) to demonstrate effect of land cover change on water use and carbon storage in the study areas. Chapter 4 describes the use of intensity analysis (Pontius et al. 2013; Pontius, Shusas & McEachern 2004) to identify non-uniform change (Aldwaik & Pontius 2012; Aldwaik & Pontius 2013), either faster or slower than expected. To complement these global change statistics, local geographically weighted measures are applied to report spatially explicit change statistics (Comber et al. 2017).

CHAPTER 4: GLOBAL AND LOCAL PATTERNS OF LANDSCAPE CHANGE ACCURACY

Processes of change can only effectively be identified after spatial land transition has been revealed and patterns of change quantified (Macleod & Congalton 1998). In Chapter 3, the effect that accuracy of existing land cover products has on land cover change analysis, was uncovered using an indicator-based approach. This chapter[3] describes how the minimum hypothetical error in imperfect land cover maps can be revealed at landscape level using intensity analysis (Aldwaik & Pontius 2012; Pontius, Shusas & McEachern 2004) to measure landscape change.

4.1 INTRODUCTION

Land cover maps are increasingly used in research to study social and environmental processes, patterns and change (Estes et al. 2018). Most often image classification of satellite data is performed to produce land cover maps (Foody et al. 2013; Foody 2008) that are used in the subsequent analyses of change and causal process. Land cover change analysis provides evidence of the spatial dynamics and intensity of processes (Puertas, Brenning & Meza 2013). Change detection outputs, however, are sensitive to misclassification and misregistration of imagery (Kinkeldey 2014; Pontius & Cheuk 2006). As evidenced by Tobler's first law of geography (Tobler 1970), spatial autocorrelation lies at the heart of many landscape processes and land cover errors show a distinctive spatial distribution (Tsutsumida & Comber 2015). In addition, Foody (2008: 3137) laments that "image classification accuracy typically adopted in remote sensing may often be unfair, commonly being rather harsh and misleading", while maps with relative low accuracy produced by other communities are often used unquestioningly.

A common problem with land cover maps is that even though accuracy is reported, some error and uncertainty, of unknown size and location, remains (Enaruvbe & Pontius 2015; Estes et al. 2018). Despite land cover data being such a crucial reference dataset (Foody et al. 2013), informing a wide variety of activities Olofsson et al. (2013, 2014) reported that the practice of providing accuracy assessment and uncertainty accounting has not consistently been adopted in the remote sensing community. Typically, insufficient description is provided of sampling strategies or how accuracy assessment was conducted (Olofsson et al. 2014; Stehman 2014). In addition, the information provided in the confusion matrix, generally used for accuracy reporting in remote sensing land cover classification, is a global statistic without spatial context

[3] Submitted to ISPRS Journal of Photogrammetry and Remote Sensing

(Foody 2005; McGwire & Fisher 2001). This global overall summary simplifies complex data for decision makers (Comber et al. 2017) but gives no indication of the spatial distribution of change or error (Comber 2013; Foody 2005; Steele et al. 1998) masking local variations thereby possibly limiting the understanding of the spatial process and statistical relationships under investigation (Comber et al. 2017).

Aldwaik & Pontius (2012) introduced the 'intensity analysis' framework to analyse land change in maps over several points in time. The framework compares land cover change intensity with uniform or random change (Section 2.4.3), characterising change as persistence, gain or loss (Aldwaik & Pontius 2012). Intensity analysis has been applied widely in investigations to improve the understanding of observed land change (Akinyemi & Pontius 2016; Jewitt et al. 2015; Pontius et al. 2013; Zhou et al. 2014). The effect of hypothetical map error in explaining deviations from uniform land change (Aldwaik & Pontius 2013; Enaruvbe & Pontius 2015; Teixeira, Marques & Pontius 2016), especially faced with unknown map error as in maps for historical time points can be studied. Even when highly accurate classified datasets with reported accuracy are used, about half of the observed change could be explained by error (Pontius & Lippitt 2006; Chapter 3). Inconsistent results may thus provide insight into the processes that created the land cover change pattern (Pontius & Li 2010). A change budget (Section 2.4.4) can be constructed by partitioning the overall difference between two land cover maps into quantity and allocation differences (Pontius & Millones 2011). Although spatio-temporal results can be obtained by partitioning the study area domain (Quan et al. 2018), the reported change is not spatially explicit (Comber et al. 2017).

Various authors have explored spatial characteristics of classification accuracy, such as modelling spatial maps of error using kriging interpolation (Steele et al. 1998) and Monte Carlo approaches (McGwire & Fisher 2001). Foody (2005) demonstrated the potential of calculating geographically distributed correspondence matrices and interpolated between them to generate surfaces of error. Comber et al. (2012) focussed on using geographically weighted regression to create local correspondence matrices for variations in the accuracy of both (crisp) Boolean and (soft) fuzzy land cover classes and applied geographically weighted logistic regression to the confusion matrix (Comber 2013) to also address spatio-temporal accuracy for time series land cover data (Tsutsumida & Comber 2015). In describing the use of geographically weighted correspondence matrices as a generic spatially explicit approach, Comber et al. (2017:242) lament the lack of research into local statistical models of land cover, which would "accommodate the spatial autocorrelation found in remotely sensed data and analyses of many landscape processes".

In the semi-arid grasslands of South Africa, land cover change, manifested as degradation or transformation, has important consequences for natural resources, significantly affecting ecosystem processes and services (Egoh et al. 2011; Reyers et al. 2009). Conversion of grassland to woody vegetation results in increased leaf area and rooting depth and consequently higher actual evapotranspiration, thereby reducing water yield (Zhang, Dawes & Walker 2001). In addition, consistent with global trends, grasslands have displayed an increasing trend in actual evapotranspiration and reduction in water use efficiency (Gang et al. 2016; Gwate et al. 2018). Even with land cover maps providing a simple approach to derive information on ecosystem services (Burkhard et al. 2013; Egoh et al. 2012; Kandziora, Burkhard & Müller 2013; Maes et al. 2012), a combination of other factors, including land management and global forces related to warming, may be at work. The availability of the medium resolution Landsat series archive provides a temporal record of more than 40 years of space-based surface observations (Roy et al. 2014) offering scientists the opportunity to document and compare land cover. However, it is difficult to obtain accurate ground information to validate land cover maps produced from historical data (Enaruvbe & Pontius 2015).

Chapter 3 described a recent land cover change study in the Eastern Cape of South Africa. In this study (Chapter 3) independently created land cover maps for 2000 and 2014 revealed a theoretical accuracy for the resulting land cover change maps of just over 70%, with a hypothetical error in landscape transition of up to 30% based on error propagation from the contributing land cover maps. Land use patterns were characterised by persistence with more than 70% of the total area showing no change. Despite the relatively high accuracies for the independently mapped land cover maps, 37% of the combined map area recorded differences with ~19% real change and ~19% arising from error (Chapter 3). Despite substantial over-estimation of changed areas, 96% of all change could be mapped (Fuller, Smith & Devereux 2003). However, map error was evident as the total change, computed from loss at T1 and gain at T2, varied between 18% and 42% with only 19% computed from the direct overlay of the T1 and T2 maps, which assumes the unlikely probability that map error (in T1 and T2) is randomly distributed. Although overall land cover change between 2000 and 2014 was quantified and described in Chapter 3, only global statistics were presented, and the spatial distribution of errors was not determined.

The aim of this chapter is to describe how map error would influence measurement of land cover change, as derived from imperfect input data; and how that could affect modelling of landscape processes. In particular, this chapter will focus on the spatial distribution of map error. Using the transition matrix, the change budget (Section 2.4.4) and change intensity

(Section 2.4.5), are extracted at various spatial scales and global scale statistics are reported. Geographically weighted correspondence matrices (Section 2.3.2) are developed (Brunsdon, Charlton & Harris 2016; Comber et al. 2017; Pontius & Santacruz 2015) to capture local, spatially explicit statistics. Spatially distributed estimates of change are explored to support interpretation of results from maps that have known error of which the size and location are unknown.

4.2 MATERIALS AND METHODS

4.2.1 Study area and data

The illustrative case study area selected is quaternary catchment S50E (448 km^2) in the Eastern Cape, South Africa, located around 27°35′E 31°45′S (Figure 4-1). A single Landsat scene covers the catchment, minimising potential error from image pre-processing, such as atmospheric correction and pan sharpening. S50E is administered under a dual land tenure system where land allocation is jointly managed by traditional leadership and the municipal system. Mixed farming is practised, and the catchment is under pressure from land cover change affecting ecosystem services of carbon sequestration and water production. Invasive alien plants (IAPs) represent a known threat in this catchment. Despite an active clearing programme, a density of between five and 25% has been recorded (Kotzé et al. 2010).

Land cover maps independently derived from Landsat at three time steps (1990, 2000 and 2014) were used. A revised land cover legend (Table 4-1) with eight classes was developed (Chapter 3) by combining detailed classes to enable comparison of the three land cover maps.

Table 4-1 Land cover legend with eight aggregated classes

Conceptual class*	Classes included	Aggregated class	Abbreviation
Natural and semi-natural terrestrial primarily vegetated areas	Unimproved Grassland; Degraded Grassland; Shrubland and Low Fynbos	Grassland	UG
	Indigenous Forest; Thicket, Bushland, Bush Clumps, High Fynbos; Dense bush; Woodland/Open bush	Forest indigenous	FITBs
Natural, terrestrial non-vegetated bare areas	Bare Rock and Soil; Mines and Quarries	Bare Rock and Soil	BRS
Cultivated and managed terrestrial primarily vegetated areas	Cultivated, permanent, commercial, irrigated; temporary, commercial, dryland; temporary, subsistence, dryland	Cultivated	CLs
	Forest Plantations; Woodlots	Forest Plantations	FP
Artificial, terrestrial primarily non-vegetated areas	Urban / Built-up (residential, formal township)	Urban / Built-up	UrBu
Natural or artificial primarily non-vegetated aquatic or regularly flooded water bodies	Waterbodies	Waterbodies	Wb
Natural and semi-natural aquatic or regularly flooded vegetated areas	Wetlands	Wetlands	Wl

Aggregation of classes generally increases accuracy (Strahler et al. 2006) by removing error caused by confusion of classes with similar spectral characteristics. The simplified land cover for the three time steps is shown in Figure 4-1. The dataset for 1990 (GeoTerraImage 2016) was created as a commercial venture following the success of the 2013-14 National Land cover map (NLC) (GeoTerraImage 2015). Due to absence of historical validation data, no accuracy assessment was performed. However, since the same mapping and modelling methodologies were applied as for the 2013-14 NLC (GeoTerraImage 2015),but using Landsat 5 instead of Landsat 8 data (GeoTerraImage 2016), the accuracy is reported to be similar at 82.53±0.6%. Thirty-three land cover classes were combined to match the aggregated eight-class legend (Table 4-1). The dataset for the year 2000 (Chapter 3) is based on the South African NLC dataset (Van den Berg et al. 2008) for the same year. After applying the revised legend (Table 4-1), this dataset was systematically updated to increase the low reported overall accuracy of 66% (Chapter 3) to 85.5±0.01%.

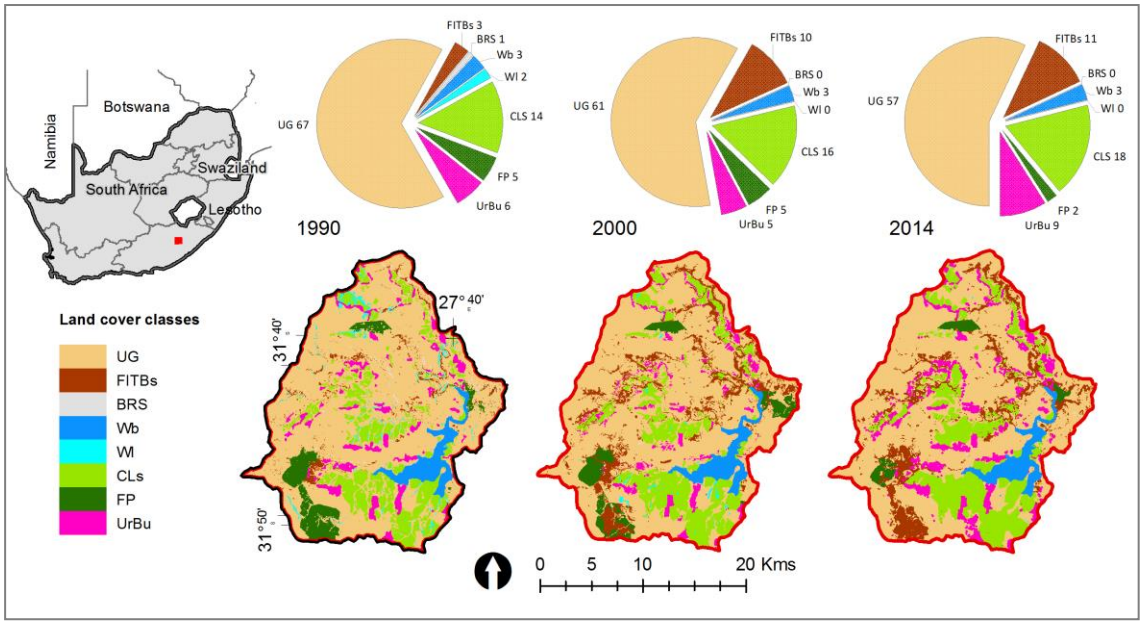

Figure 4-1 Study area showing simplified land cover for 1990, 2000 and 2014

The 2014 dataset was classified from Landsat 8 data using object-based image processing[4] (Chapter 3) using the same revised land cover legend comprising eight classes (Table 4-1) with an overall accuracy of 89.9±0.01%. Overall accuracy (Section 2.3.2) is the proportion of the spatial extent that has agreement between the map and the ground, combined over all categories (Teixeira, Marques & Pontius 2016).

$NDVI_{3g}$.v0, the third generation global inventory monitoring and modelling system (GIMMS) normalised difference vegetation index (NDVI) data from the National Oceanographic and

[4] Image processing was carried out by PI Okoye (Okoye 2016) assisted by SE Muller (CGA).

Atmospheric Administration (NOAA) advanced very high resolution radiometer (AVHRR) sensor, has been used to map and monitor vegetation changes since 1981 (Pinzon & Tucker 2014; Tucker et al. 2005). $NDVI_{3g}$.v0 is compatible with moderate resolution imaging spectroradiometer (MODIS) NDVI (MOD13Q1) as the same dynamic range is used (Brown et al. 2006; Tucker et al. 2005). The GIMMS archive is considered the best dataset available for long-term NDVI trend analysis (Beck et al. 2011). For comparison, $NDVI_{3g}$.v0 (8 km resolution), MOD13Q1 (250 m resolution) and NDVI derived from Landsat 5 TM, Landsat 7 ETM and Landsat 8 OLI, available via Google Earth Engine (GEE), were extracted and aggregated to monthly time steps in the GEE code editor. A monthly time series for 1990-2014 was constructed from which trend analysis (Section 2.6.2) was performed in package greenbrown (Forkel & Wutzler 2015) in R statistical software (R Core Team 2017). Trends were computed based on annual aggregated time series (method AAT) and on a season-trend model (method STM) (Section 2.6.2). Trend and breakpoint estimation in method STM explains the time series by a piecewise linear trend and a seasonal model in a regression relationship following the decomposition formulation used in BFAST (Verbesselt et al. 2010b; Verbesselt et al. 2011).

4.2.2 Landscape level change analysis

Land cover change maps T1 (1990-2000) and T2 (2000-2014) were constructed from the three land cover maps by overlaying pairs of these maps in ArcGIS software (ESRI 2016). Transition matrices were constructed to summarise the spatial intersection of all pixels for T1 and T2, serving as a record for land cover class changes (Section 2.3.2). The methods used in the subsequent catchment scale change analysis (Section 2.4.3) is overviewed in Figure 4-2.

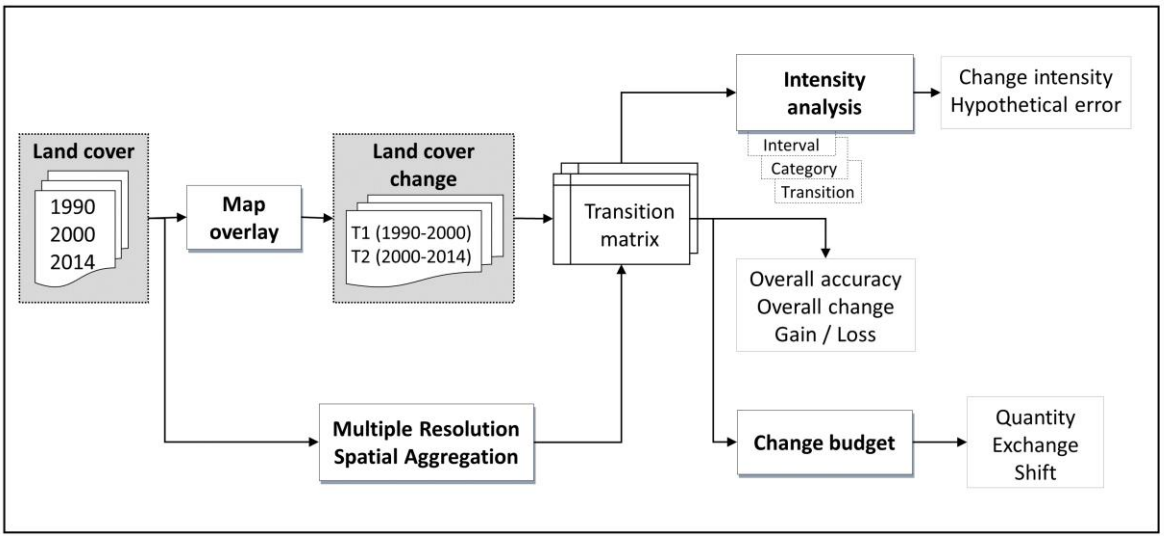

Figure 4-2 Flow diagram of methods applied in change analysis

Accuracy for the change maps at catchment scale was calculated as the product of the OAs of the individual contributing maps (Pontius & Li 2010; Pontius & Lippitt 2006) based on the reported accuracies. Losses and gains (area and class percentage) were derived from the row and column marginal totals and the diagonals of the transition matrix (Section 2.4.2). Total landscape change was computed as the difference between observed losses and gains.

By analysing the off-diagonal entries of the confusion matrix, systematic transitions of land cover change were identified. Following the *intensity analysis* framework (Section 2.4.5), hypothetical omission and commission error intensities were calculated from the transition matrices for each time step (Aldwaik & Pontius 2012). The *change budget* (Section 2.4.4) was computed by deconstructing the total landscape change during each time interval into quantity, exchange and shift disagreement. Pontius (2019) showed how intensive exchange components could signal possible confusion of categories with each other. Intensity analysis was therefore also applied to change budget components quantity, exchange and shift (Pontius 2019). The intensity of each component was calculated per land cover class, after which the overall intensity of each component was computed. Component intensities not only facilitate comparison of each category with other categories but also with overall difference.

A *multi-resolution spatial aggregation* procedure (Pontius & Cheuk 2006; Pontius 2002) was applied to each of the two land cover change datasets (T1 and T2) to determine the effect of geographic distance over which land change transitions occur on the change budget. Coarser grid cells that have partial (fuzzy) membership in each of the land cover classes were produced by aggregating a cluster of four neighbouring pixels. The membership in each class is the proportion of finer resolution cells of each class that constitute the coarser cell. As resolution becomes coarser, the specification of location becomes less precise. However, using a composite operator (Pontius & Cheuk 2006), the proportion of each land cover class remains constant in the landscape, thereby preventing aggregation bias. The differ package (Pontius & Santacruz 2015) was used to compute multi-resolution location (exchange and shift) and quantity disagreement in the land cover maps (T1 and T2) in eleven multiples of the finest resolution (Pontius 2002) ranging from 30 m to 29 km.

4.2.3 Geographically weighted change budget

Since the transition matrix-based approach only indicates the overall, or global, accuracy of the change maps, local measures of correspondence (Section 2.3.2) were computed from subsets of the full datasets in a geographically weighted change analysis approach. Local correspondence matrices were constructed at predefined locations (Comber et al. 2017) to

describe the spatial variation in the agreement between two datasets and generate spatially distributed measures of error. A sample of 5000 points were selected on a hexagonal lattice over the catchment using spsample (sp package) (Pebesma et al. 2018). A centric systematic grid (Milne 1959) was generated, which when clipped to catchment boundaries, yielded 4325 locations. At each location, a subset of the data falling under a bi-square kernel were weighted by their distance to that particular location, to be used for construction of a local transition matrix using the gwxtab package (Brunsdon, Charlton & Harris 2016). The bi-square kernel uses a distance-decay weighting function (Equation 4-1), but gives null weights to observations at a distance greater than the set bandwidth (Gollini et al. 2015).

$$f(d) = \begin{cases} \left(1 - \left(\frac{d}{h}\right)^2\right)^2 & \text{if } d < h; \\ 0 & \text{otherwise.} \end{cases} \qquad \text{Equation 4-1}$$

where d is the distance of the data point to the kernel centre; and

h is the bandwidth.

An adaptive bandwidth of the nearest 15% data points, as well as fixed bandwidths at 1 km, 3 km and 5 km were explored (Comber et al. 2017), as bandwidth affects the degree of smoothing and the sensitivity of the analyses to the data distribution. Spatially distributed quantity and allocation (exchange and shift) disagreement values were calculated by integrating functionality from the gwxtab (Brunsdon, Charlton & Harris 2016) and diffeR (Pontius & Santacruz 2015) packages. Three locations, representing different change trajectories based on bandwidth, were selected to illustrate local geographically weighted transition cross tabulations and the effect of bandwidth. Location of points are illustrated in Figure 4-3. Shannon`s diversity index (SHDI) (Ortiz-Burgos 2016) was selected as an indicator of landscape patch diversity for comparison at local level, calculated using package vegan (Oksanen et al. 2018) in R using the following Equation 4-2:

$$SHDI = \sum_{i=1}^{m} (p_i ln p_i) \qquad \text{Equation 4-2}$$

where p_i is the proportion of the landscape occupied by land cover change type *i*; and

m is the number of land cover change types in the given landscape.

All instances of persistence were counted as a single type. SHDI is sensitive to the diversity and heterogeneity of the landscape at T1 and T2. Higher values of SHDI indicate higher degree of fragmentation in the land cover change pattern and therefore higher spatial heterogeneity. The relationship between the SHDI and the change budget both at catchment and the selected

locations at local scale were analysed to verify the spatial variation in the change budget at local scale.

4.3 RESULTS

Figure 4-3 shows persistence of land cover (in grey) over the entire study period between 1990 and 2014. Persistent classes in T2 (2000-2014) are shown in green. Areas with persistence in T1 (1990-2000) appear in orange while areas of change in both periods are indicated in red in Figure 4-3. For each period (T1 / *T2*), Figure 4-3 shows land cover change as loss of land cover at time step 1 (1990 / 2000) and gain of land cover at time step 2 (2000 / 2014).

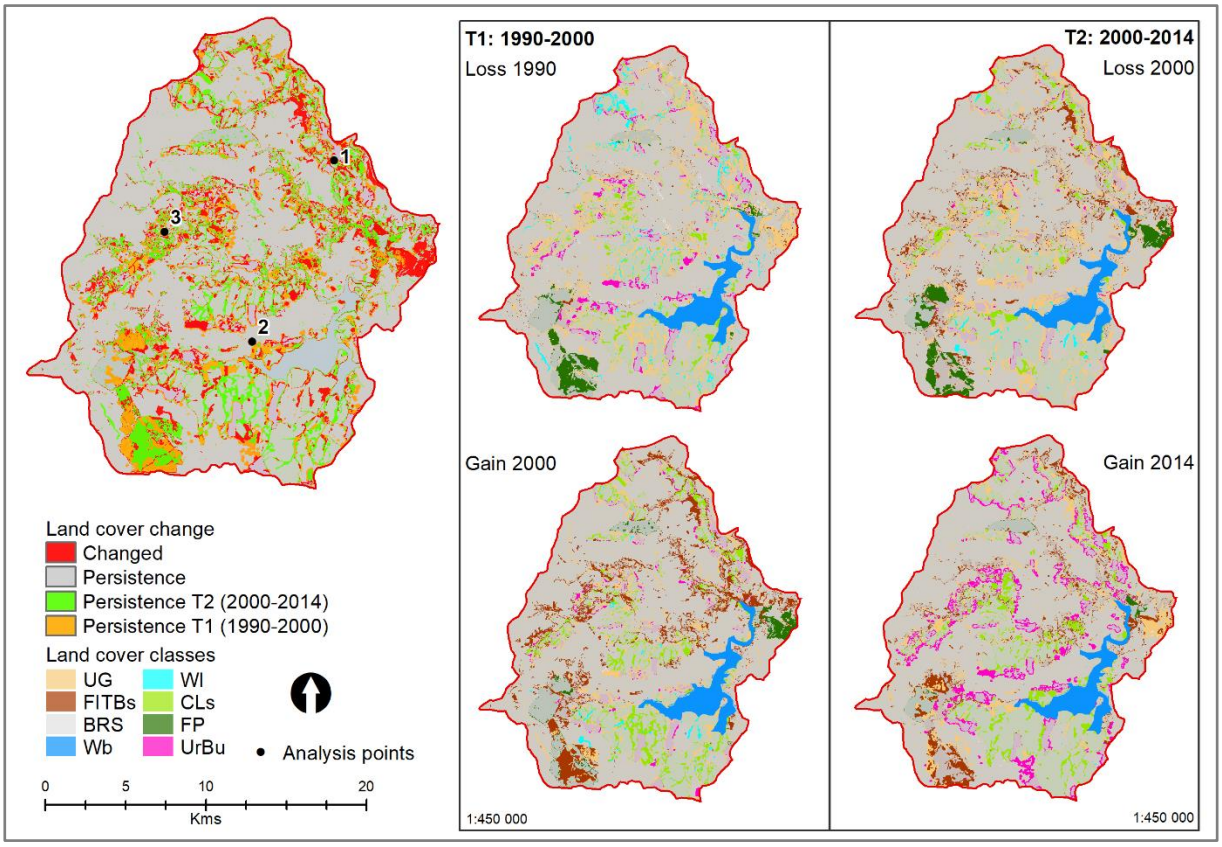

Figure 4-3 Land cover change partitioned into persistence, loss and gain

Land cover classes that have remained the same are indicated in grey as persistence.

4.3.1 Intensity analysis at landscape level

Based on the product of the overall accuracies of the individual contributing land cover maps, land cover change accuracies varied between 70 and 72%, with accuracies for T1 (1990-2000) lower than for T2 (2000-2014). Figure 4-4 shows the sizes of observed changes and hypothetical commission and omission errors to the left and the intensity of the change compared to uniform on the right.

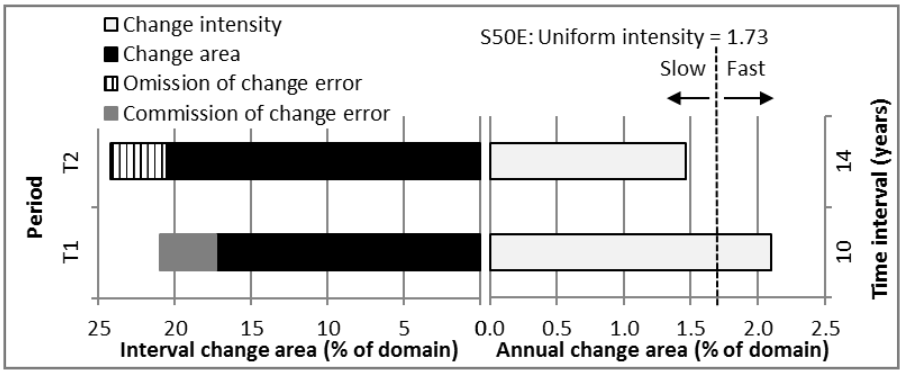

Figure 4-4 Intensity analysis at interval level

Interval level change of approximately 20% of the study area domain was observed. Over the ten-year period of T1, this translates into an annual rate of change of ~ 2%, while during T2 (14 years) an annual change of approximately 1.5% was exhibited. Land cover change during T1 was categorised as fast (greater than uniform annual change of 1.73%). In contrast, during T2 land cover change was categorised as slow, being less than uniform. Four per cent hypothetical commission error in T1 suggests that change was mapped while the uniform hypothesis implies persistence (Aldwaik & Pontius 2013). Conversely, for T2 the omission error indicates persistence while the uniform hypothesis implies change. Both the trend in the annual aggregate NDVI time series (AAT) and the seasonal trend (STM) at catchment scale was captured with NDVI3g.v0 for the entire study period (1990-2014) and with MOD13Q1 for T2 (2000-2014) in Figure 4-5. Slope (m) and significance (p) of trends are reported at the top of the graph for AAT and at the bottom of the graph for STM.

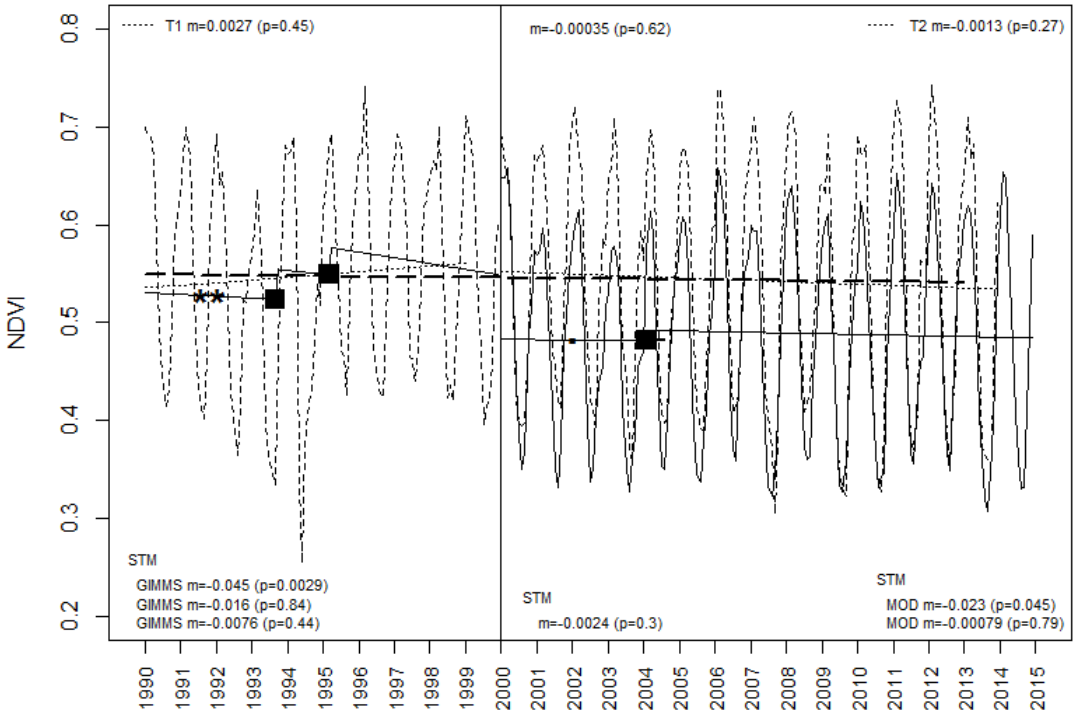

Figure 4-5 Landsat NDVI time series at catchment scale

The AAT demonstrated a gradual and non-significant (m=-00035; p=0.62) decreasing trend (thick dashed black line). In period T1, AAT on NDVI3g.v0 showed an increase while T2 showed a decrease, however, not significant in either period. The ordinary least squares (OLS)-based moving sum (MOSUM) test on the NDVI3g.v0 time series detected two significant structural breaks (p=0.01) in T1 during 1993 and 1995, but none in T2. A significant downward trend was detected prior to the breakpoint in 1993 (Figure 4-5) with non-significant negative trends between and after the breakpoint. The MOD13Q1 time series (T2 only) indicated a significant structural break in 2004, significant downward trend prior to the breakpoint and non-significant negative trend after the breakpoint.

Over the entire period (1990-2014), the mean NDVI (NDVI3g.v0) remained constant with seasonal fluctuations, but no significant overall trend. MOD13Q1 values were consistently lower, but followed a similar trend, in agreement with findings that the GIMMS3g dataset shows statistically significant increases in vegetation productivity (Guay et al. 2014) compared to MODIS.

Figure 4-6 provides a graphic summary of the **category level** change, namely per land cover class, for T1 and T2 computed from the transition matrix. Gross loss (T1 Loss 1990, T2 Loss 2000) was calculated from the row difference, while gross gain (T1 Gain 2000, T2 Gain 2014) was computed from the column differences in the transition matrices.

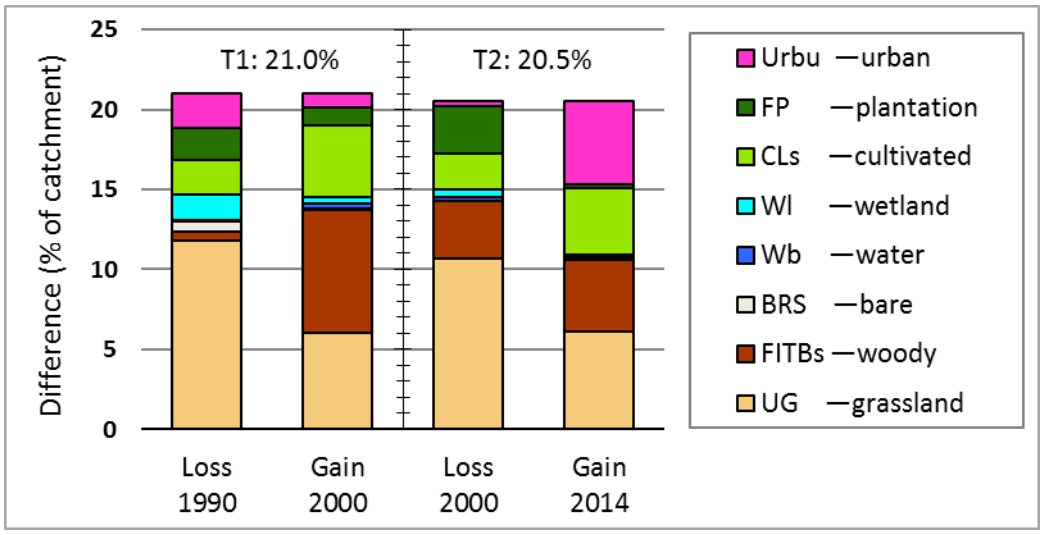

Figure 4-6 Loss and gain per land cover class

Grassland (UG), the largest class by area, is involved in many of the transitions in the landscape and a nett loss was recorded for both T1 and T2 of respectively 6% and 5%. Especially prominent in Figure 4-6 is the gain in FITBs in T1 (7% gain in 2000) at the expense of UG. Large gains were also noted for CLs (2% in each period) and UrBu (5% in T2) as reported in Chapter 3, which focussed only on T2 (2000-2014). Persistence was measured in almost 80%

of the catchment area. Graphically (Figure 4-6), the results at category level indicate large losses of grassland, UrBu in T1, but gains in FITBs in T1, CLs in both periods and UrBu in T2, as also reported in Chapter 3.

Detailed results from intensity analysis at category level are illustrated in Table 4-2. The observed size of gain and loss per land cover class (in per cent of study area) are presented per time step. Hypothetical error per class is shown as either omission or commission error.

Table 4-2 Hypothetical error in input data contributing to error in land cover change

	Gain T1 (1990-2000)				**Loss T1 (1990-2000)**			
	Observed	**Omission Error**	**Commission Error**	**Gain Intensity**	**Observed**	**Omission Error**	**Commission Error**	**Loss Intensity**
UG	6.0	8.7	0	1.0	11.8	2.9	0	1.8
FITBs	**7.7**	**0**	**7.2**	**8.0**	**0.6**	**0**	**0.1**	**2.3**
BRS	0	**0**	**0**	**10.0**	**0.7**	**0**	**0.7**	**10**
Wb	0.4	0.3	0	1.2	0	0.7	0	0.1
Wl	**0.4**	**0**	**0.4**	**8.6**	**1.6**	**0**	**1.6**	**9.6**
CLs	**4.5**	**0**	**1.3**	**2.7**	2.2	0.9	0	1.6
FP	**1.2**	**0**	**0.3**	**2.6**	**1.9**	**0**	**1.1**	**3.7**
UrBu	0.8	0.2	0	1.8	**2.2**	**0**	**1.2**	**3.7**
Total change	21.0				21.0			
Hypothesised Error	9.2				4.5			
	Gain T2 (2000-2014[1])				**Loss T2 (2000-2014[1])**			
	Observed	**Omission Error**	**Commission Error**	**Gain Intensity**	**Observed**	**Omission Error**	**Commission Error**	**Loss Intensity**
UG	6.1	7	0	0.8	10.7	2.4	0	1.2
FITBs	**4.5**	**0**	**2.9**	**3**	**3.6**	**0**	**2**	**2.6**
BRS	**0.1**	**0**	**0.1**	**7.1**	**0**	**0**	**0**	**7**
Wb	0.1	0.6	0	0.2	0.2	0.5	0	0.5
Wl	**0.1**	**0**	**0.1**	**6.7**	**0.4**	**0**	**0.4**	**7.1**
CLs	**4.2**	**0**	**0.6**	**1.6**	2.3	1.3	0	1
FP	0.2	0.2	0	0.8	**2.9**	**0**	**2.5**	**4.6**
UrBu	**5.2**	**0**	**4.1**	**3.9**	0.3	0.8	0	0.5
Total change	20.5				20.5			
Hypothesised Error	7.8				5.0			

UG: Unimproved Grassland; FITBs: Forest Indigenous Thicket Bushlands; BRS: Bare Rock and Soil

Wb: Water bodies; Wl: Wetlands; CLs: Cultivated Land; FP: Forest Plantations; UrBu: Urban built up

Table 4-2 also shows the change intensity (as per cent of the class) for each class in each period. Categories more active than uniform are marked in bold. Note that the uniform intensity at category level for the study periods T1 and T2 were computed as 2.1% and 1.5% respectively. Hypothesised error from gains amounted to 9% for T1 and 8% for T2, whereas hypothesised error from losses was approximately 5% in each period.

Hypothesised error from gains amounted to 9% for T1 and 9% for T2, whereas hypothesised error from losses was approximately 5% in each period. Since hypothesised error of omission (Table 4-2) in one class will be counted as error of commission in another class, omission errors identified in some classes (such as UG, Wb and UrBu in T1) were balanced by commission errors in other classes (FITBs, BRS, Wl, CLs and FP). Overall UG, a large dormant class (Aldwaik & Pontius 2012) with loss and gain in both periods below the calculated hypothetical uniform change, showed the highest omission error. The flow matrix (Table 4-3) expresses the annual land change at transition level during each time interval, with initial time in the rows and end time in the columns.

Table 4-3 Flow matrix in hectares per year (ha.a^{-1}) where the upper number is T1 (1990-2000) and the lower number (*in italics*) is T2 (2000-2014).

S50E		**End time 2000 / *2014 (columns)*** UG	FITBs	BRS	Wb	Wl	CLs	FP	**UrBu**	**1990 / *2000* Loss**
Initial time 1990 / *2000 (rows)*	UG		255^{T}	0.8	12	13^{T}	168	47	**32**	**527^{d}**
			78^{A}	*3^{T}*	*2*	*2^{T}*	*113*	*2^{A}*	***142^{T}***	***342^{d}***
	FITBs	20		-	0.1^{A}	0.1^{A}	0.4^{A}	5^{T}	**0.3^{A}**	**26^{a}**
		92^{T}		*0.2*	*0.5*	*0.1^{A}*	*5^{A}*	*5^{T}*	***12***	***114^{a}***
	BRS	22^{T}	5^{T}		3^{T}	-	-	0.2^{A}	**-**	**30^{a}**
		0.5	*0^{A}*		-	-	*0^{A}*	*0^{T}*	***0.4^{T}***	***1.0^{a}***
	Wb	0.9^{A}	0.5	-		-	0^{A}	0.1	**-**	**2^{d}**
		3.9^{A}	*0.5^{A}*	-		-	*3*	-	***0.1^{A}***	***8^{d}***
	Wl	44	7	0^{A}	1.4		18^{T}	0.2^{A}	**1**	**72^{a}**
		8	*0.1^{A}*	-	-		*6^{T}*	-	***0.2^{A}***	***14^{a}***
	CLs	89	4^{A}	-	0.1^{A}	3^{T}		0^{A}	**3^{A}**	**100^{d}**
		48^{A}	*13*	*0.1*	*0.4^{A}*	*0.1*		*0^{A}*	***11***	***73^{d}***
	FP	19^{A}	67^{T}	0	0.1^{A}	0^{A}	0.1^{A}		**0.6^{A}**	**87^{a}**
		41	*51^{T}*	*0.8^{T}*	-	*0^{A}*	*0.1^{A}*		***0.4^{A}***	***94^{a}***
	UrBu	76^{T}	7^{A}	0.5^{T}	0^{A}	0.2^{A}	13^{A}	0.1^{A}		**96^{a}**
		3^{A}	*0.4^{A}*	*0.1*	-	-	*8^{T}*	*0.1^{A}*		***11^{d}***
2000 / *2014*	**Gain**	271^{d}	345^{a}	1.4^{a}	16^{d}	17^{a}	200^{a}	52^{a}	**37^{d}**	**939**
		196^{d}	*143^{a}*	*4^{a}*	*3^{d}*	*2^{a}*	*134^{a}*	*7^{d}*	***167^{a}***	***656***

Note: ^{a}Active at category level. ^{d}Dormant at category level. ^{T} Targets at transition level. ^{A} Avoids at transition level.
UG: Unimproved Grassland; FITBs: Forest Indigenous Thicket Bushlands; BRS: Bare Rock and Soil
Wb: Water bodies; Wl: Wetlands; CLs: Cultivated Land; FP: Forest Plantations; UrBu: Urban built-up

The flow matrix gives the annual area of each transition, annual losses and gains for each category, including annual overall change in hectares (Runfola & Pontius 2013). Where losses are greater than gains, the numbers in column 'Loss' underlined. Similarly, if gains are greater than losses, the numbers in row 'Gain' are underlined. At category level, for Loss and Gain, superscript ^{a} means active (greater than uniform) while superscript ^{d} means dormant (less than uniform). At transition level, systematic transitions (Aldwaik & Pontius 2013) are indicated in Table 4-3 where superscript ^{T} means the gaining category in the column targets the initial

category in the row while the losing category in the row targets the initial category in the column. Similarly, superscript ^{A} means the gaining category in the column avoids the initial category in the row, while the losing category in the row avoids the category in the column. The size of overall change slowed down to 656 ha.a^{-1} in T2, decreasing from 939 from ha.a^{-1} in T1, confirming T2 change as slower than uniform (Figure 4-4). The largest simultaneous annual transitions in size were pairs of transitions from UG to CLs at some locations and from CLs to UG at other locations, with UG avoiding CLs in T2. Systematically targeting transitions for both periods were found between FITBs and FP, also seen in Figure 4-3. Not only was high loss intensity noted for UrBu in T1 (Table 4-2), but Table 4-3 shows UrBu was systematically targeted by UG in T1. In contrast in T2, high gain intensity of UrBu was at the expense of UG (Table 4-3).

4.3.2 Global change budget

The global change budget, divided into quantity, exchange and shift disagreement expressed as a percentage of catchment size for both periods, is reported at interval level (Figure 4-7B) and category level for T1 (Figure 4-7A) and T2 (Figure 4-7C). The red minus (-) indicates a net loss per class while the green plus (+) shows net gain for the class in the particular interval. Quantity, exchange and shift intensities per class are shown at category level (Figure 4-7D, F) and interval level (Figure 4-7E).

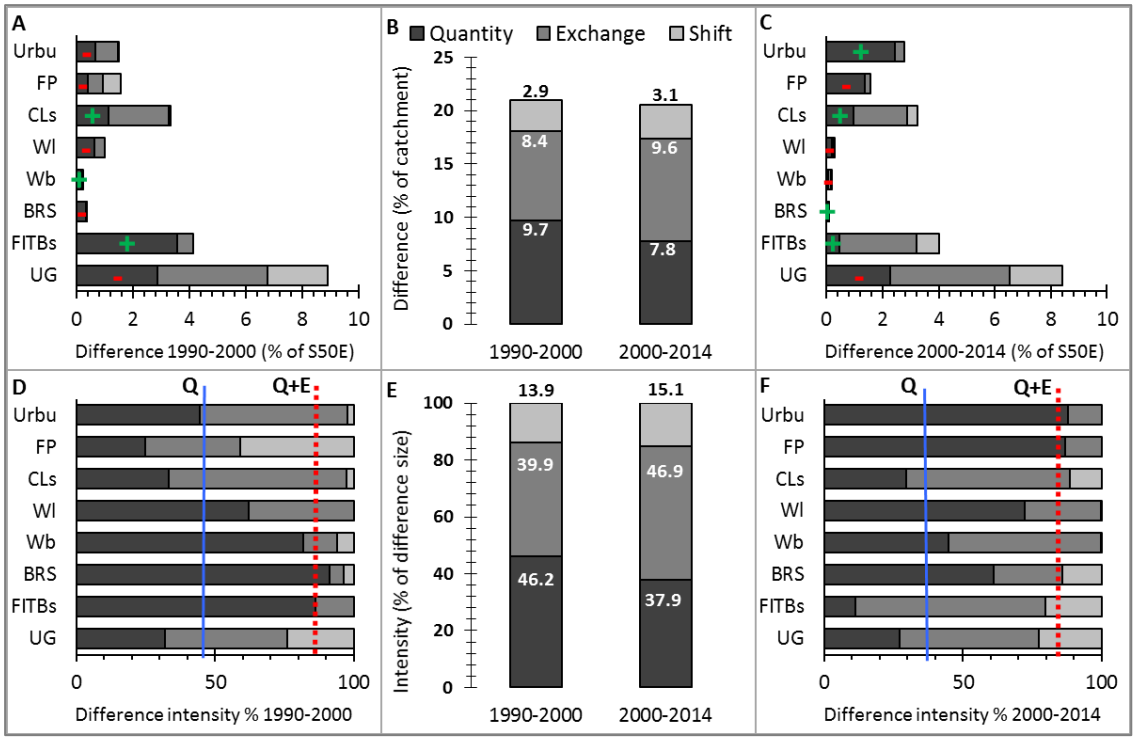

Figure 4-7 Global change budget size and intensity at interval level (B, E) and category level for T1 (A, D) and T2 (C, F)

Quantity difference, also referred to as Net change (Pontius & Millones 2011) from gain and loss, amounts to almost 10% for T1 and 8% for T2 (Figure 4-7B). Figure 4-7E interprets the quantity size as an intensity of 46% of total change for T1, specified by the Q line in Figure 4-7D. Allocation (exchange + shift) from Urbu, FP, CLs and UG (Figure 4-7D) contribute to the change during T1. The intensity of quantity change is lower in T2 than in T1 at 38% (vertical line Q in Figure 4-7F), with UG, FITBs and CLs having less intensive quantity components relative to the quantity component overall. Allocation intensity (exchange plus shift) amounted to 54% for T1 and more than 60% for T2, in agreement with sensitivity analysis findings by Pontius & Lippitt (2006).

4.3.3 Resolution and the global change budget

The effect of increasing pixel resolution on the allocation disagreement (exchange plus shift) is shown in Figure 4-8 for T1. The horizontal axis depicts pixel resolution in geometric increments (1, 2, 4, 8…), while the vertical axis shows the percentage change. Table 4-4 summarises the data for the change budget at multiple resolutions.

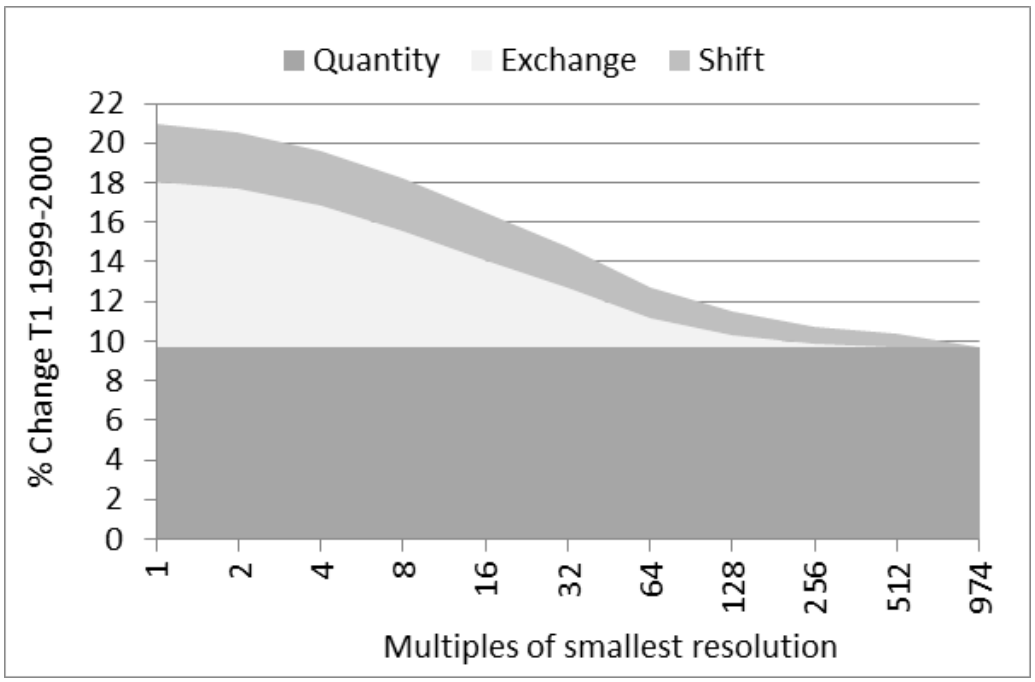

Figure 4-8 Effect of multiple resolution spatial aggregation on allocation error at catchment level

In the aggregation routine based on the composite operator (Pontius & Cheuk 2006), the quantity change stays constant with resolution (Pontius 2002), in this case 9.7% for T1 and 7.8% for T2 (Table 4-4). However, the allocation error (exchange + shift components) diminishes at coarser resolutions. At catchment resolution, only quantity plays a role in the overall change percentage.

Table 4-4 Change budget at multiple resolutions for T1 and T2

Multiples	Resolution (m)	T1 (1990-2000) Quantity	Exchange	Shift	Overall	T2 (2000-2014) Quantity	Exchange	Shift	Overall
1	30	9.7	8.4	2.9	21.0	7.8	9.6	3.1	20.5
2	60	9.7	8.0	2.9	20.5	7.8	9.3	3.1	20.1
4	120	9.7	7.1	2.8	19.6	7.8	8.4	3.0	19.2
8	240	9.7	5.9	2.6	18.2	7.8	7.1	2.9	17.8
16	480	9.7	4.4	2.4	16.5	7.8	5.5	2.8	16.1
32	960	9.7	3.0	2.1	14.8	7.8	3.7	2.7	14.2
64	1920	9.7	1.5	1.6	12.7	7.8	2.0	2.5	12.3
128	3840	9.7	0.6	1.2	11.5	7.8	0.3	2.2	10.3
256	7680	9.7	0.2	0.9	10.8	7.8	0.1	1.6	9.5
512	15360	9.7	0.0	0.7	10.4	7.8	0.0	0.3	8.1
974	29220	9.7	0.0	0.0	9.7	7.8	0.0	0.0	7.8

At the finest resolution, error due to location accounts for 11% of the landscape in T1 but at a resolution of 1 km (960 m in Table 4-4) the error due to location accounts for only 5% of the landscape. Allocation error in T2 is higher than T1, with almost 13% error attributed to land cover classes that have changed position at the finest resolution in T2.

4.3.4 Change budget at local scale

The effect that the selected bandwidth may have on the outcome of the geographically weighted analysis is illustrated in Figure 4-9. Overall allocation difference (overallAllocD) computed at 4325 locations within the specified bandwidth (adaptive, fixed 1, 3 and 5 km) is expressed as a normalised value between 0 and 1 representing the probability of the particular error occurring (Comber et al. 2017). Labelled points 1, 2 and 3 are superimposed on the bandwidth maps in Figure 4-9.

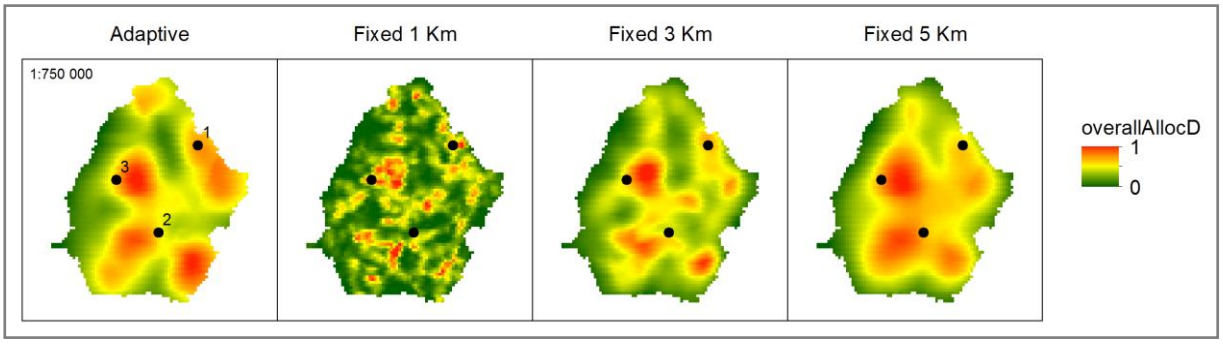

Figure 4-9 Effect of bandwidth on local analysis

Bandwidth affects the degree of smoothing (Gollini et al. 2015), but as yet, the gwxtab package does not include bandwidth optimisation. A fixed bandwidth of 5 km yields clusters that cannot easily be distinguished from each other, possibly not representative of processes in the landscape. In contrast many small local clusters are found with a bandwidth of 1 km. Figure 4-10 maps the variation of overall comparative measures (quantity, exchange and shift)

computed from the geographically weighted transition matrices extracted for points 1, 2 and 3 (Figure 4-9) using adaptive and fixed bandwidth (1, 3 and 5 km) values.

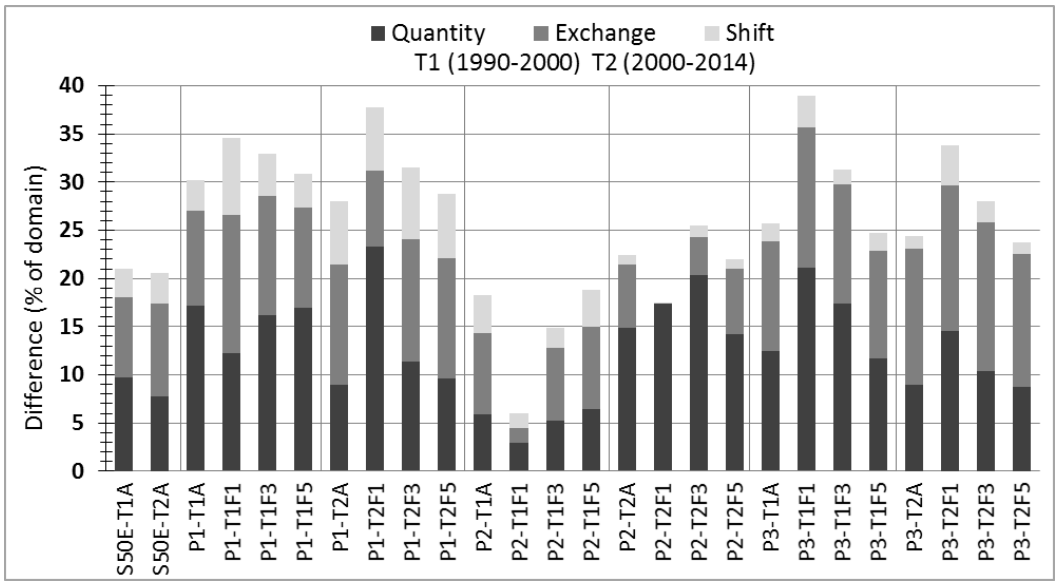

Figure 4-10 Localised quantity, exchange and shift disagreement calculated at three selected points for two time steps and four different bandwidths.

The local change budget at Points 1, 2 and 3 (Figure 4-10) identify clear spatial differences in how change has occurred in the catchment, both in terms of quantity and allocation. Persistence surrounds Point 2 (SHDI 0.5-0.9) where quantity error remains fairly constant for T1, and in T2 the allocation error only increases at the largest bandwidth. At this point (P2) the overall change is less than catchment average. Points 1 (SHDI 1.1-1.4) and 3 (SHDI 0.9-1.4) show much higher spatial heterogeneity with change higher than 35% within a fixed bandwidth of 1km. Table 4-5 tabulates the SHDI corresponding to the change budget results in Figure 4-10.

Table 4-5 Localised quantity, exchange and shift disagreement calculated at three selected points for two time steps and four different bandwidths, with Shannon index (SHDI) for overall catchment and fixed bandwidths

Period	Location	S50E	Point 1				Point 2				Point 3			
T1	Bandwidth	Adap-tive	Adap-tive	Fixed 1 km	Fixed 3 km	Fixed 5km	Adap-tive	Fixed 1 km	Fixed 3 km	Fixed 5km	Adap-tive	Fixed 1 km	Fixed 3 km	Fixed 5km
	Quantity	9.7	17.1	12.3	16.2	17.0	5.8	2.9	5.3	6.5	12.4	21.1	17.4	11.7
	Exchange	8.4	9.8	14.3	12.4	10.4	8.5	1.6	7.5	8.5	11.4	14.6	12.4	11.2
	Shift	2.9	3.3	8.1	4.3	3.5	4.0	1.5	2.1	3.9	1.8	3.3	1.5	1.9
	SHDI	1.0		1.4	1.2	1.1		0.5	0.8	0.9		1.3	1.0	0.9
T2	Bandwidth	Adap-tive	Adap-tive	Fixed 1 km	Fixed 3 km	Fixed 5km	Adap-tive	Fixed 1 km	Fixed 3 km	Fixed 5km	Adap-tive	Fixed 1 km	Fixed 3 km	Fixed 5km
	Quantity	7.8	8.9	23.3	11.4	9.7	14.9	17.3	20.4	14.0	8.9	14.5	10.4	8.8
	Exchange	9.6	12.5	7.9	12.7	12.4	6.5	0.0	3.9	6.8	14.1	15.1	15.4	13.8
	Shift	3.1	6.5	6.6	7.4	6.7	1.0	0.0	1.1	1.0	1.3	4.2	2.2	1.2
	SHDI	1.0		1.4	1.1	1.1		0.8	0.9	0.9		1.4	1.1	0.9

The SHDI and change budget (Figure 4-10, Table 4-5) confirm that Point 2 experienced less change than the entire catchment in T1, while Points 1 and 3 present change greater than catchment level. Exchange and shift disagreement at Point 2 occured at distances larger than 3

km. Spatially explicit overall comparative measures (quantity, exchange and shift) were extracted and are presented in Figure 4-11 for 1 km bandwidth. Figure B-1 in Appendix B shows the spatially explicit disagreement budget for the 3 km bandwidth.

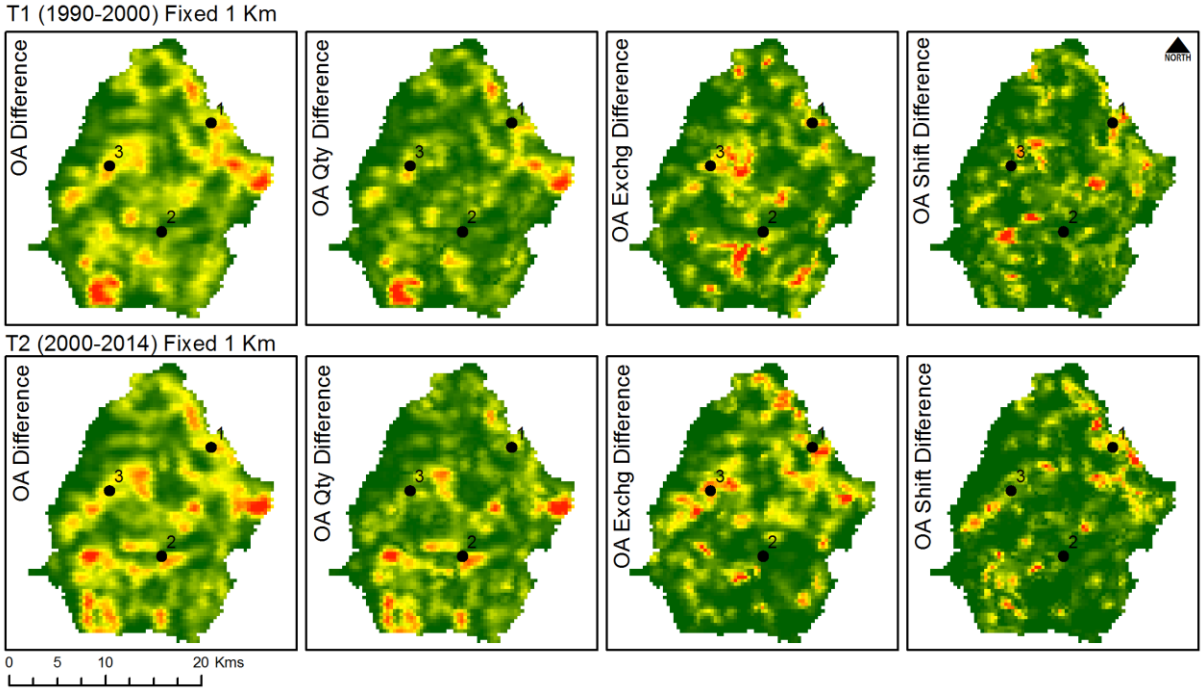

Figure 4-11 Spatial distribution of overall difference, quantity, exchange and shift difference computed at 1 km bandwidth

The overall difference map shows hotspots of change and probable error within the study area. Of particular importance would be areas affected in both periods. The spatial distribution of the change budget elements (quantity, exchange and shift) per land cover class was computed for all bandwidths. Figure 4-12 shows each of the components for T1 at 1 km bandwidth in rows, while land cover classes (UG, FITBs, CLs, FP and UrBu) are represented in columns, expressing the probability of land cover change in graduated colours, white to black. Black represents the highest probability of change, while white represents the lowest probability. Period T2 is similarly illustrated in Figure 4-13.

Spatial variation in quantity disagreement in Figure 4-12 can be related to loss and gain as illustrated in Figure 4-3. The exchange disagreement identified for UG and CLs in Figure 4-7A, D (~3%) can be identified in Figure 4-12 E: UG and E: CLs. In Figure 4-12, shift is most prominent in UG and, as the largest dormant class, is most likely involved in many transitions. Figure 4-7D indicates the highest shift difference intensity for FP in T1, which is also visible in Figure 4-12 S: FP.

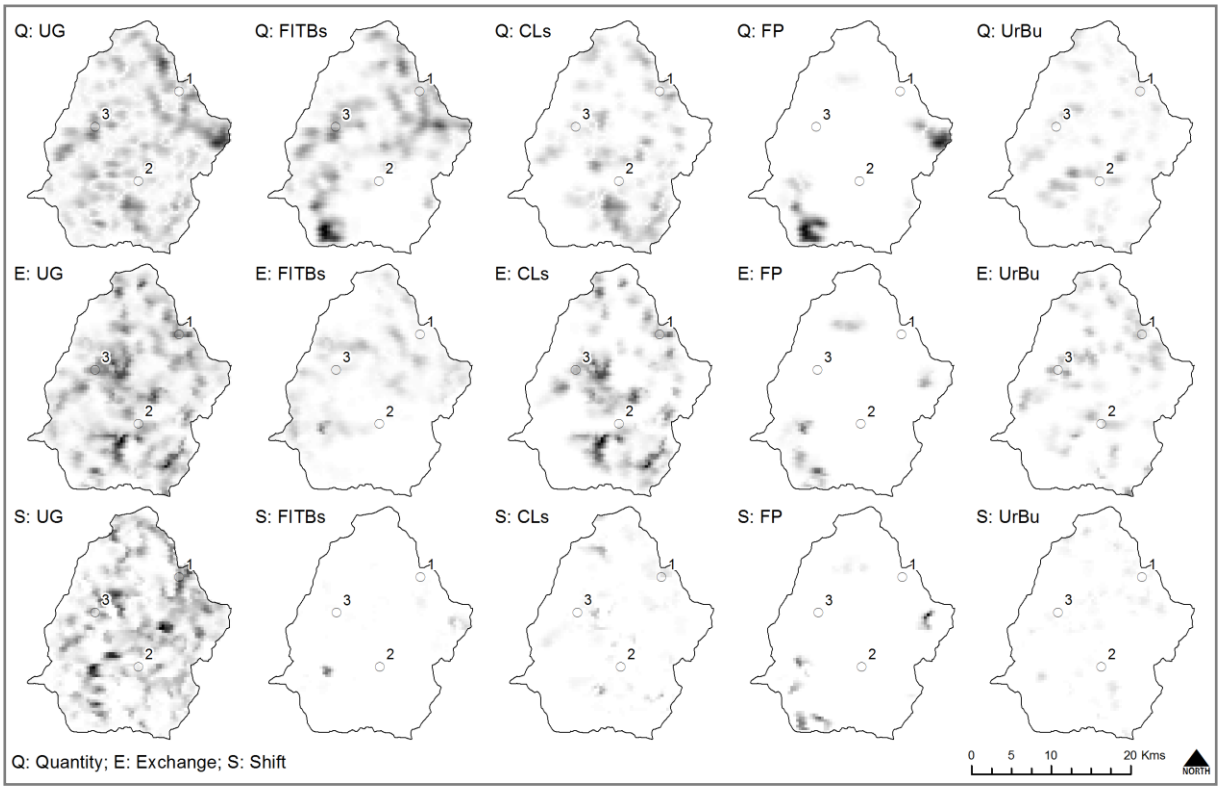

Figure 4-12 Spatial distribution of quantity, exchange and shift difference per land cover class for T1 computed at 1 km bandwidth.

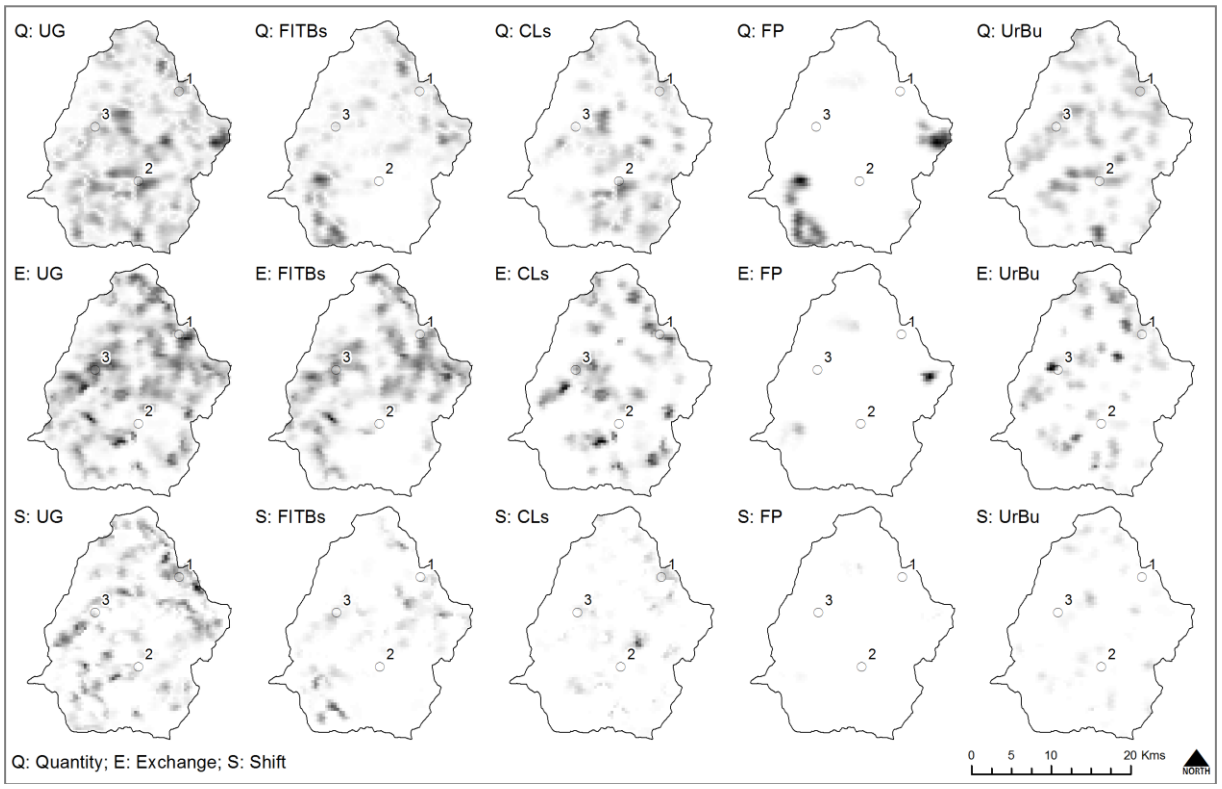

Figure 4-13 Spatial distribution of quantity, exchange and shift difference per land cover class for T2 computed at 1 km bandwidth

4.4 DISCUSSION

This study set out to describe the influence of map error on measurement of land cover change that could affect modelling of landscape processes; and explore techniques to find and describe the error. Following on from Chapter 3, the temporal setting for this study includes a land cover dataset from the near past (1990) that was retrospectively classified (GeoTerraImage 2016) but for which no suitable historical ground truth data was available. Reported accuracy (82.53%, Kappa 0.81) is based on the premise that the same mapping and modelling procedures and image formats were used as for a later dataset SA-land cover (GeoTerraImage 2015) for which field data was collected, and which performed well in terms of accuracy in comparison to other national scale land cover products (Estes et al. 2018). As overall accuracy for the 2000 dataset was improved from 67% (Van den Berg et al. 2008) to 84% (Chapter 3), the T1 land cover change output map could have a theoretical accuracy of 56-69% based on the product of the two input land cover maps (Aldwaik & Pontius 2013; Fuller, Smith & Devereux 2003; Mas 1999). The accuracy of the T2 land cover map is reported as 72% (Chapter 3), but could be as low as 58% if a more detailed land cover classification system (LCCS) was employed. Pontius & Malizia (2004) noted that category aggregation may decrease the error in individual land cover maps as classes that are spectrally similar, would likely be aggregated. This in turn would also affect the land cover change maps by reducing error while increasing uncertainty. To this end Aldwaik, Onsted & Pontius (2015) suggested the use of behaviour based categorical aggregation to construct a meaningful LCCS.

Intensities higher than the uniform value indicate that gains (or losses) are more intensive than the landscape in general. This is found within all classes except UG and Wb (Table 4-2). If the observed intensity for a particular class, for example FITBs in T2 (2000-2014), is greater than the hypothesised intensity of 1.5%, then change in the class is active and the observed change is the sum of uniform change and commission error. The commission error reflects the false positives, number of pixels allocated in a predicted class that do not belong to that class in reality. Similarly, if the observed intensity for a class, for instance UG in T1 (1990-2000), is less than the hypothesised intensity 2.1%, then the class is seen as dormant and the hypothesised change is the sum of observed change and omission error. An omission error is a measure of false negatives and occurs for example when grassland pixels are not classified as grassland but erroneously as another class. Despite displaying the highest change intensity (both gain and loss) in Table 4-2, land cover classes Wl and BRS cover a very small part of the catchments and presented low producer's accuracies (Chapter 3). Both Wl and BRS are strongly affected by natural processes and climate and exhibit seasonal variation. Of concern to note is that in

1990, 2% of the study area comprised Wl (Figure 4-1). This may be an artefact from the image classification. The decline in wetlands due to agricultural intensification close to river courses over the 24-year study period, exacerbated by low rainfall, is cause for concern.

The flow matrix (Table 4-3) expresses transition level annual land change and confirms T2 change as slower than uniform (Figure 4-4). The size of overall change slowed down to 656 $ha.a^{-1}$, decreasing from 939 from $ha.a^{-1}$ in T1. The largest simultaneous annual transitions in size were pairs of transitions from UG to CLs at some locations and from CLs to UG at other locations, with UG avoiding CLs in T2. Distinguishing between cropland (CLs) and surrounding land cover classes, in particular grassland and savanna, is an ongoing research question in agricultural remote sensing. Ozdogan & Woodcock (2006) showed that sensor resolution should be finer than average field size to accurately determine cropland area and location, especially in areas, such as S50E, where smallholder fields are smaller (Samberg et al. 2016). Residual trees in these rural farming communities cause classifiers to have difficulty with distinguishing grassland and savannas from the smallholder fields (Debats et al. 2016; Estes et al. 2016; Sweeney et al. 2015). Figure 4-12 (E: UG and E: CLs) shows the highest probable locations of these pairs of transitions derived from the geographically weighted transition matrix. Although local statistical models and spatially dependent methods better reflect the understanding of local spatial processes and relationships, they are difficult to construct (Comber et al. 2017), however the ability to reflect such statistics in maps make them potentially more widely usable. Global statistics, such as overall accuracy from the confusion matrix, are easy to understand, but are not spatially explicit.

Systematically targeting transitions for both periods were found between FITBs and FP (Table 4-3, Figure 4-3 and Figure 4-12). This is likely an indication of some classification error in the original land cover datasets, as the spectral signatures of plantation (FP) and indigenous forest (FITBs) are similar (Chapter 3). FITBs show higher than uniform gain and loss intensities for both periods (Table 4-2) ascribed to woody encroachment by alien or native vegetation (Nackley et al. 2017; Skowno et al. 2017) as a consequence of elevated atmospheric CO_2 (Hobbs 2016; Skowno et al. 2017) on the one hand, and clearing on the other. The affected area in both catchments is between 5-7% of the catchment area. Not only was high loss intensity noted for UrBu in T1 (Table 4-2), but Table 4-3 shows UrBu systematically targeted by UG in T1. In contrast in T2, high gain intensity of UrBu was at the expense of UG (Table 4-3). This is a clear case of error in the 2000 map as loss of UrBu in T1 in Figure 4-3 is clearly matched with gain in UrBu in T2 (in the centre of the map). Though not as clear as for the previous examples, local exchange disagreement for urban in Figure 4-12 shows high probabilities

distributed over the map. In this setting, rural villages are easily confused with cropland or rangeland due to widely spaced dwellings interspersed with bare soil and occasional trees. It is likely that the occurrence of mixed pixels introduced error in the land cover classification (Ozdogan & Woodcock 2006).

At the finest pixel resolution (30 m), error due to allocation accounts for 11% of the study area in T1, but at a resolution of 1 km this error accounts for only 5% of the study area (Figure 4-8). Allocation error in T2 is higher than T1, with almost 13% error attributed to land cover classes that have changed position at the finest resolution in T2. The aggregation routine, based on a composite operator, causes quantity to stay constant (Pontius & Cheuk 2006), while allocation diminishes. In this scenario, half of the location errors occur over distances less than 1 km. If woody encroachment occurs in one cell and clearing occurs in the neighbouring cell, then the pair of cells constitutes a swap in the FITBs category. At a slightly coarser resolution, the invaded cell and the cleared cell are aggregated into the same coarse cell, causing the swap to disappear, resulting in diminished swap at coarser resolutions. At the coarsest resolution (29 km) only quantity plays a role and the increase in agreement is equal to the allocation error. When using coarse resolution satellite imagery to extract biophysical parameters to measure changes in NDVI, ET or NPP, along with land cover change maps derived from medium to high resolution satellite imagery, quantity disagreement should thus be considered as the overall change in the landscape.

The potential of using geographically weighted local measures of change reporting was explored in this chapter to complement the global statistics derived from the transition matrix. Local statistics not only support the identification of potential map error, but provides a spatially explicit manner to dynamically visualise accuracy and to characterise error in maps and models. Spatial distribution of overall allocation difference (Figure 4-11) over time can help to identify hotspots of change. However, the geographically weighted methods are sensitive to bandwidth selection (Gollini et al. 2015) and finding the optimal degree of smoothing has not yet been implemented into gwxtab (Brunsdon, Charlton & Harris 2016). The implementation is currently available as an R package and runs prohibitively long on the Windows platform. However, the geographically weighted framework based on correspondence tables supports understanding of spatial processes and statistical relationships (Comber et al. 2017).

4.5 CONCLUSION

This chapter described how map error could be determined and reported, both at global scale (from the transition matrix) and at local scale (by constructing a geographically weighted

transition matrix). Processing was done on imperfect input data with known error of which the size and location was unknown. Using the intensity analysis framework and local correspondence matrices, spatially explicit probabilities of error could be constructed. It was found that at coarser resolutions, quantity disagreement would provide the total change in the landscape as allocation disagreement disappears with composite aggregation.

Concluding with the sentiment of Foody (2008) – that image classification accuracy is often viewed negatively, and simplistically – a greater awareness of the problems encountered in accuracy assessment and potential of spatially explicit accuracy assessment may reduce unfair criticism of thematic maps derived from remote sensing. Spatially explicit approaches such as the geographically weighted correspondence matrices can accommodate the spatial autocorrelation found in remotely sensed data and address the spatial non-stationarity of processing within such data for improved modelling of landscape processes.

The next chapter focuses on land change modelling to derive a land cover dataset for a point in the future from landscape units associated with clearly identified persistent trajectories of change which will then be used in Chapter 6 to characterise the relationship between biophysical parameters and land cover change. In Chapter 5 intensity analysis and the change budget will again be explored as tools to validate a dataset for which there is no field data.

CHAPTER 5: ACCURACY OF MODELLED FUTURE LAND COVER

In Chapter 3, land cover change from 2000 to 2014 was analysed for the study area, while Chapter 4 investigated spatially explicit measures of patterns of landscape change over a larger time horizon, by considering 1990 through to 2014 to establish trends in land cover change. Five primary drivers of landscape modification were identified, comprising rangeland degradation, woody encroachment, urbanisation, increased dryland cultivation and commercial afforestation. Bearing a similar period in mind, future land cover scenarios for catchments S50E and T35B are explored in this chapter. Since the two catchments under investigation are examples of different management practices, a comparison of potential future land cover can guide land management decision making. S50E hosts mixed farming practices of livestock grazing and crop cultivation, with land allocation managed collaboratively by traditional leaders and the municipal system. The label "dualistic or bilateral landholding arrangement" was agreed upon by stakeholders to describe the complexity around this land management system. Conversely, in T35B the land tenure is predominantly freehold, representative of a commercial farming system.

This chapter[5] focuses on Objective 3 (Figure 1-1) in describing quantitative techniques used in accuracy assessment of the modelled future land cover, of intensity analysis and in particular the disagreement budget (Pontius & Santacruz 2014), in order to describe and interpret patterns of land change to inform management. Land use land cover change modelling (subsequently referred to as land change modelling) entails the simulation of the behaviour of the environmental and social systems in an area over a time period in such a way that it relates to the measured land change (Paegelow et al. 2013). The chapter will provide a brief overview of the land change modelling performed before describing the validation of the future scenario, used for modelling biophysical variables in Chapter 6.

5.1 LAND CHANGE MODELLING

Land change models (Section 2.5) generally address change demand, transition potential and change allocation (Eastman, Van Fossen & Solorzano 2005). Most land change models follow a data-driven inductive approach, attempting to draw correlations between the multitudes of explanatory factors involved using statistical inferences (Overmars, de Groot & Huigen 2007).

[5] Components of this chapter have been published as a scientific article (citation below). The chapter contains excerpts from the manuscript but has been adapted extensively and was reformatted to match the guidelines of Stellenbosch University, Department of Geography & Environmental Studies.

Gibson LA, Műnch Z, Palmer AR & Mantel S 2018. Future land cover change scenarios in South African grasslands - implications of altered biophysical drivers on land management *Heliyon* 4:e00693.

Simulation of land cover change can be carried out using a prospective approach based only upon past trends or by introducing alternative future scenarios (Paegelow & Camacho 2008). Deductive models would allow the inclusion of relevant driving factors assumed to have causal influence on land cover change, such as political change or climatic disasters. Both change demand and change allocation rely on a transition potential model. According to Veldkamp & Lambin (2001), an inductive pattern-based top-down approach can be used to build on spatial distribution of past land cover change to develop a mathematical model to estimate change potential along with spatial explanatory variables, the so-called drivers of change (Kolb, Mas & Galicia 2013) often embedded in GIS (Castella & Verburg 2007).

Transition potential maps can be created based on probabilities of transitions or on suitability of land cover to be occupied (Eastman, Van Fossen & Solorzano 2005), describing the degree to which locations might potentially change in time. Various approaches have been suggested to produce transition potential maps. These include weights of evidence (WoE), a modified form of Bayesian analysis (Bonham-Carter 1994) to represent the probabilities of dominant change processes; logistic regression modelling (RM) that shows the suitability regarding the different land cover classes; or back-propagation neural network models as implemented in IDRISI's multi-layer perceptron (Eastman, Van Fossen & Solorzano 2005; Kolb, Mas & Galicia 2013).

Change demand models estimate the rate of change between each pairwise combination of land cover types, summarising the results in a transition probability matrix. Empirical or theoretical approaches have been used (Eastman, Van Fossen & Solorzano 2005). Through cross tabulation of land cover, Markov chain analysis develops a transition probability matrix of land cover change between two different dates and provides a probability estimate for each pixel to either be transformed to another land cover or to persist and be calibrated to an annual time step (Kamusoko et al. 2009).

Change allocation involves techniques to allocate the amount of certain changes, established through the projection of the historical land cover change across space, to produce the spatial patterns of changing landscapes (Mas et al. 2014). A land change model must predict both the quantity of each land cover type, as well as the location of any change (Pontius, Huffaker & Denman 2004). The accuracy of the output of an inductive model is a function of both the model itself, namely suitability of algorithms within the model to fulfil the intended purpose, and the accuracy of the input data. Thus, to anticipate where possible inaccuracies may be entering into modelled output, assumptions within the model can be examined, as can accuracies of input data (Gibson et al. 2018). Model performance assessment is often based on the spatial

coincidence between a simulated map and an observed land cover map. Other methods include expert opinion, comparison of outputs generated with multiple models or multiple runs with the same model (Mas et al. 2013; 2014).

The aim of this chapter is to perform land change modelling to project land cover change trends to a future time step. The disagreement budget (Pontius & Santacruz 2014), which separates change into quantity, exchange and shift disagreement, will be used to validate the future land cover model. This will be used to gain an understanding of the implications on biophysical parameters (Chapter 6) that in turn can guide land management strategies.

5.2 MATERIALS AND METHODS

Land change modelling[6] was used to create transition potential maps for each transition, a projected potential for transition map (soft prediction) and a predicted land cover map for 2030 (T_3) for S50E and T35B following the flowchart in Figure 5-1.

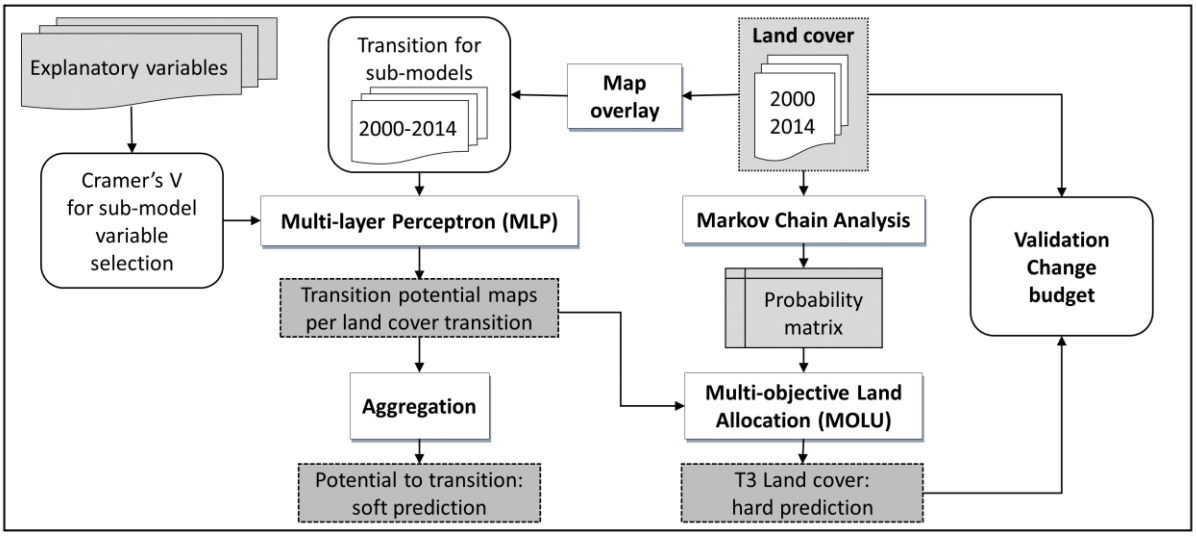

Figure 5-1 Land Change Modeller (LCM) method for land cover change prediction

The soft prediction is a continuous mapping of potential to transitionwith no final land cover predicted while the hard prediction (change allocation) shows the individual land cover classes predicted by the model (Section 2.5). Though limited when developing alternative scenarios (Pérez-Vega, Mas & Ligmann-Zielinska 2012), the Land Change Modeller (LCM), integrated into IDRISI Terrset 18.08 software (http://www.clarklabs.org/), was selected as it provides extensive tools for the assessment and projection of land cover change (Eastman, 2016). Historical land cover change maps were used to determine all possible transitions of land cover classes. Explanatory variables were identified that could influence future land cover change (Gibson et al. 2018).

[6] Land change modelling was performed by Dr Lesley Gibson.

5.2.1 Transition sub-models

Overlay of land cover maps for T_1 (2000) and T_2 (2014) at 30 m pixel resolution (Okoye 2016) were used to determine transitions for sub-models to feed into the multi-layer Perceptron (MLP) in IDRISI. A transition label was given to all possible transitions of land cover using an identical common land cover legend (Chapter 3). The land cover classes involved in transition are grassland (UG); woodland, indigenous and invasive (FITBs); bare (BRS); waterbodies (Wb); wetland (Wl); cultivated (CLs); plantation (FP); and urban (UrBu) (Chapter 3). Land cover transitions with common underlying drivers were identified and grouped into sub-models (Pérez-Vega, Mas & Ligmann-Zielinska 2012). Six sub-models were identified as (1) Intensification representing the transition of a lower intensity to a higher intensity usage and includes increase in cultivation, woody encroachment or invasion and urban expansion. Afforestation (2) refers to the planting of commercial trees and (3) Deforestation refers to the clearance of trees. Any conversion to grassland or bare areas are characterised as (4) Reclamation, Degradation and Abandonment, while seasonal conversions not explained through anthropogenic change are labelled as (5) Natural dynamics. Exceptionality (6) is associated with potential map errors (Chapter 3). Table 5-1 displays the labels, transitions and description for each sub-model. Small transitions (less than 10 ha) were removed from the analysis to minimise exceptionalities.

Table 5-1 Transition sub-models and descriptors for catchment S50E and T35B

Transition sub-model	Description	Land cover transitions*++
If: FITBs intensification (↑FITBs)	Woody natural and artificial vegetation substitutes previous land cover	UG to FITBs; FP to FITBs; CLS to FITBs
Ia: Agricultural intensification (↑Agric)	Agricultural activities substitute previous land cover	UG to CLS; FITBs to CLS; **Wb to CLS***; Wl to CLS; UrBu to CLS; *FP to CLS*+
Iu: Urban intensification (↑Urban)	Urban activities substitute previous land cover	UG to UrBu; **CLS to UrBu***; FITBs to UrBu
R: Afforestation (↑Forest)	Other land covers are converted to plantations	UG to FP; FITBs to FP; *WL to FP++; CLS to FP++*
D: Deforestation (↓Forest)	Plantations converted to other land covers	FP to UG; **FP to BRS***; *FP to Wl++*
A: Abandonment (Abandon)	Urban and agricultural areas converted to grassland and bare areas	CLS to UG; UrBu to UG; *CLS to Wl++*
Dn: Natural dynamic (Natural)	Areas where natural changes occurred	UG to Wb; UG to Wl; Wb to UG; Wl to UG; *FITBs to Wl++*
De: Degradation (Degrade)	Shrub area converted to grassland and bare areas	UG to BRS
Re: Reclamation (Reclaim)	Woody natural and artificial vegetation areas converted to grassland and bare area	FITBs to UG

Note: *Bold text shows transitions that occurred in S50E only; ++italics show transitions that occurred only in T35B
UG: Unimproved Grassland; FITBs: Forest Indigenous Thicket Bushlands; BRS: Bare Rock and Soil
Wb: Water bodies; Wl: Wetlands; CLs: Cultivated Land; FP: Forest Plantations; UrBu: Urban built-up

Areas of potential woody encroachment, where another land cover class has potentially been replaced by IAPs (FITBs intensification), were identified as a dominant driver in the study area. A change from any other land cover class to urban (with the exception of waterbodies and wetlands) were labelled Iu (Urban intensification). It was not possible to determine change in the intensity of agricultural activities due to image resolution, but conversion to agricultural practices was identified (Agricultural intensification). Where forests (indigenous or alien) and other woody areas have disappeared or have been removed, the labels Reclamation and Deforestation were assigned. Due to the low accuracy reported in Chapter 3, all transitions involving land cover classes bare soil (BRS) and wetlands (Wl) were labelled as potential classification error. In reality, as indicated in Table 5-1, not all possible transitions occurred between 2000 and 2014 in both S50E and T35B.

5.2.2 Explanatory variables

GIS datasets were identified to describe the potential transitions (Table 5-1). Typical explanatory variables are slope and distance to roads and settlements and land tenure (Mas et al. 2014). Within the context of this study, IAP intensification is more likely to occur in close proximity to existing infestation through the process of seed dispersal and afforestation close to existing plantations based on existing infrastructure. Topographic variability can affect certain transitions, for example water bodies will not expand into areas with positive slope and certain vegetation may not grow at higher altitudes. In addition, vegetation distribution is influenced by access to water, therefore the Euclidean distance from rivers was used as a proxy for water availability (Gibson et al. 2018). Geoprocessing was performed to represent the particular process and abbreviations were assigned to each processed spatial dataset. Each derived explanatory dataset was tested for suitability using Cramer's V (Section 2.5), where higher values represent stronger relationships between the variable and a particular transition with values higher than 0.4 regarded as good, while values higher than 0.15 are 'useful' (Megahed et al. 2015). For transitions with low Cramer V values, evidence likelihood (EV) was computed as an additional explanatory variable. EV calculates the relative frequency of pixels that belong to the different classes within the areas of change (Eastman 2016).

5.2.3 Land Change Modeller

Explanatory spatial variables were combined with transition sub-models in the MLP in IDRISI to create transition potential maps following Figure 5-1. A transition probability matrix was generated using Markov chain analysis to assign probability of change by projecting historic change to the future. The transition probability matrix and transition potential maps were

combined in IDRISI's multi-objective land allocation (MOLU) module to present the land cover scenario for 2030 (T_3), a hard prediction with explicit predicted land cover classes. Individual transition potential maps were aggregated to create a soft prediction map indicating the propensity of the landscape to experience change. Soft prediction, or potential to transition, is a continuous mapping of vulnerability to change (Eastman 2016). Model performance was evaluated using the accuracy rate and skill measure provided in IDRISI (Eastman 2016). The skill measure compares the number of correct predictions, minus those attributable to random guessing, to that of a hypothetical set of perfect predictions and so measures the applicability of the explanatory variables to past land cover change. Therefore, the skill measure is not an evaluation of performance of the model, but rather a gauge of how well the explanatory variables explained change in the past.

5.2.4 Validation of future land cover dataset

Since the result of this model is a future scenario, typical land cover validation methods could not be employed. Other indicators were thus employed to assess the prediction. While visual examination reveals spatial patterns, it is subjective and can be misleading. Disagreement statistics, in the form of quantity, exchange and shift disagreement (Pontius & Santacruz 2014), were used to provide an indication of the quality of the future scenario map. Quantity difference is defined as the amount of difference between the predicted map and a comparison map, in this case the 2014 land cover map, where the proportions of the classes do not match. Allocation disagreement occurs where the quantity per class remains the same, but the spatial distribution of the class changes and can be separated into exchange and shift, involving two or more classes respectively (Pontius & Santacruz 2014). Even though the disagreement budget is applied to different land cover maps than proposed (Pontius & Chen 2006; Pontius & Millones 2011), it provides a novel approach to compare the measured land cover maps and the future scenario for which there is no validation data.

Land cover change analysis was performed by overlaying the land cover dataset from T_2 (2014) and the modelled dataset (T_3–2030) to produce a transition matrix. Rows in the transition matrix represent the land cover at T_2, while columns represent land cover at T_3. Land cover change from the transition matrix was matched to the sub-models (Table 5-1) representing the six main trajectories (Feranec et al. 2010; Stott & Haines-Young 1998) of specific changes in the landscape, and land cover labels were assigned. The disagreement budget, including quantity and allocation disagreement for the land cover change analysis was extracted, and analysed.

5.3 RESULTS

5.3.1 Explanatory variables

A description of the explanatory variables, geoprocessing performed to create the layers, as well as the overall Cramer's V values used for sub-model selection are shown in Table 5-2.

Table 5-2 Description of potential explanatory variables and their overall Cramer's V value

Variable	Geoprocessing	Data source	Scale	Cramer V S50E	Cramer V *T35B*
Elev	Elevation	United States Geological Survey (USGS) SRTM 1 Arc-Second (USGS, 2004)	~30m cell resolution	0.268	*0.207*
Asp	Aspect computed from Elev			0.213	*0.089*
Slope	Slope computed from Elev			0.259	*0.167*
D_FP	Euclidian distance from FP (T_1)	Land cover 2000 (Chapter 3)	30m cell resolution	0.200	*0.275*
D_FITBs	Euclidian distance from FITBs (T_1)			0.181	*0.087*
D_riv	Euclidian distance from rivers	National Geo-Spatial Information vector data	1: 50 000 vector scale converted to 30m cell resolution	0.098	*0.105*
D_rd	Euclidian distance from roads			0.172	*0.128*
D_res	Euclidian distance from settlements			0.230	
EV	Evidence likelihood				*0.408*

Cramer V values larger than 0.15 at variable level were used for sub-model selection. Explanatory variables selected for each sub-model are shown in Appendix C, Table C-1 for S50E and Table C-2 for T35B.

5.3.2 Transition potential

The skill measure and accuracy rate of each sub-model calculated through MLP (Figure 5-2) are recorded in Table C-1 (S50E) and Table C-2 (T35B). The skill measure, based on the 2000 and 2014 land cover maps, compares the number of correct predictions, minus those attributable to random guessing, to that of a hypothetical set of perfect predictions.

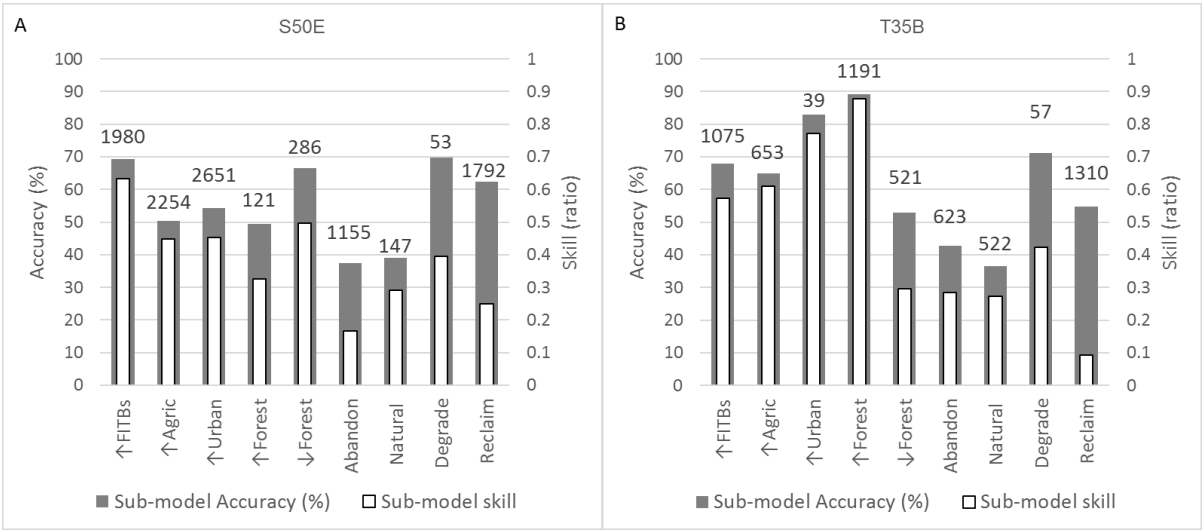

Figure 5-2 Sub-model accuracy and skill measure from multi-layer Perceptron for (A) S50E and (B) T35B [Figures above bars depict the number of pixels in each sub-model]

In S50E, accuracy varies between 37% and 70%, with a correlation of 0.5 between accuracy and number of pixels involved in transition (Table C-1). Higher sub-model accuracies were achieved in T35B, particularly for the afforestation sub-model. Abandonment (A) and Natural dynamics have lowest accuracies. Anomalies are ascribed to low user's and producer's accuracies (Chapter 3) for land cover classes Wetlands (Wl) (in sub-model Dn) and Bare rock and soil (BRS) (in sub-model De) affecting the MLP outcome. However, this could also be an indication that change is not totally controlled by the drivers selected to be used in the models. Low accuracies for transitions that involve a small number of pixels should be regarded as being of low importance.

5.3.3 Change demand

The probability of a land cover persisting (diagonal shaded grey) and of each class transitioning to every other class from the Markov matrix are presented in Table 5-3.

Table 5-3 Markov matrix probability of land covers in S50E (bold) and T35B (italics) transitioning or persisting

Class	UG	FITBs	BRS	Wb	Wl	CLS	FP	UrBu
UG	**0.80** *0.91*	**0.05** *0.03*	**0.00** *0.00*	**0.00** *0.00*	**0.00** *0.01*	**0.07** *0.02*	**0.00** *0.03*	**0.08** *0.00*
FITBs	**0.34** *0.82*	**0.58** *0.10*	**0.00** *0.00*	**0.00** *0.00*	**0.00** *0.01*	**0.02** *0.03*	**0.02** *0.03*	**0.04** *0.00*
BRS	**0.43** *0.25*	**0.05** *0.00*	**0.00** *0.00*	**0** *0*	**0.00** *0.01*	**0.02** *0.11*	**0.01** *0.62*	**0.49** *0.00*
Wb	**0.03** *0.56*	**0.00** *0.01*	**0** *0.00*	**0.93** *0.07*	**0** *0.16*	**0.04** *0.13*	**0** *0.06*	**0.00** *0.00*
Wl	**0.52** *0.68*	**0.01** *0.01*	**0.00** *0.00*	**0.00** *0.00*	**0.00** *0.06*	**0.43** *0.12*	**0** *0.13*	**0.03** *0.00*
CLS	**0.11** *0.24*	**0.03** *0.01*	**0.00** *0.00*	**0.00** *0.00*	**0.00** *0.03*	**0.84** *0.69*	**0.00** *0.02*	**0.03** *0.00*
FP	**0.34** *0.16*	**0.42** *0.00*	**0.00** *0.00*	**0** *0*	**0.00** *0.02*	**0** *0.01*	**0.24** *0.82*	**0.00** *0.00*
UrBu	**0.03** *0.46*	**0.00** *0.04*	**0.00** *0.00*	**0** *0.00*	**0** *0.02*	**0.05** *0.27*	**0.02** *0.02*	**0.92** *0.19*

UG: grassland; FITBs: woodland; BRS: bare; Wb: waterbodies; Wl: wetlands; CLS: cultivated; FP: plantation; UrBu: urban

The probability estimate for each UG pixel to persist is approximately 80% in S50E and 90% in T35B with probability of loss to FITBs in both catchments. Although a much higher probability of loss of FITBs to UG is predicted, the number of pixels that can in reality transition are limited. Waterbodies have a high probability of persistence in S50E, given the presence of the Ncora dam. The probability of persistence of FP is low in S50E, but high in T35B where commercial forestry is practised. Classes Wl and BRS show a very low probability of persisting.

5.3.4 Prediction

The output from the LCM is reported in Figure 5-3. The soft prediction map derived from the aggregated individual transition potential maps is shown in Figure 5-3A and B, while the change allocation predicted by IDRISI's MOLU module is presented in Figure 5-3C and D.

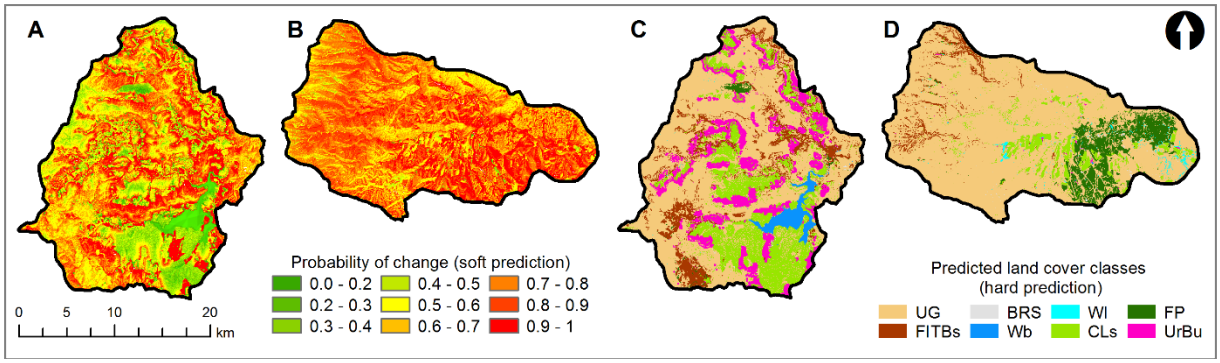

Figure 5-3 Projected potential to transition map (A-S50E, B-T35B), Predicted land cover for 2030 (C-S50E, D-T35B)

The soft prediction (Figure 5-3A, B) is a continuous mapping of vulnerability to change with no final land cover predicted while the hard prediction, the output from change allocation (Figure 5-3C, D) shows the individual land cover classes predicted by the model.

5.3.5 Evaluating prediction

A map of the land cover change, with transition labels assigned to the intersection of each class pair representing the sub-models for the land cover change modelling, is presented in Figure 5-4.

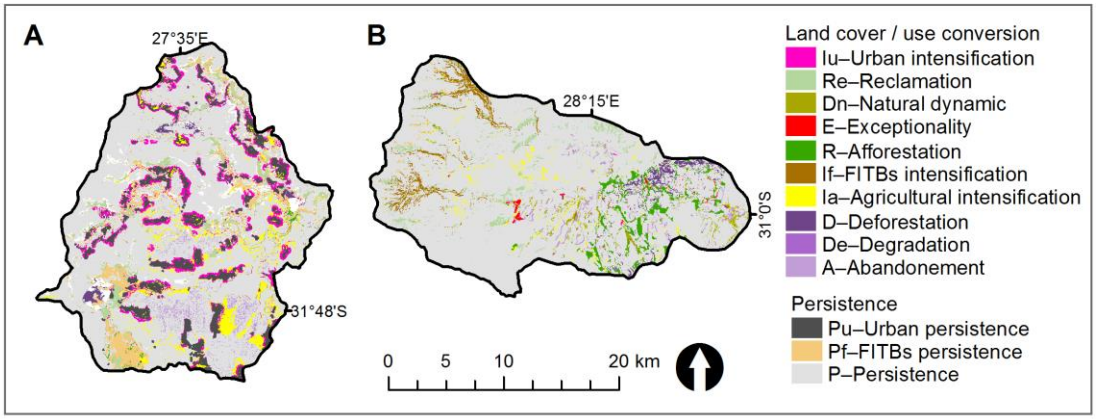

Figure 5-4 Land cover conversion / persistence for S50E (A) and T35B (B)

The transition matrix derived from the overlay between the 2014 (T2) and LCM 2030 (T3) is presented in Table 5-4 as a percentage of the catchment. Net gain and loss of a particular land cover class over the period 2014-2030 is shown with land cover labels from Figure 5-4 representing the transition in Table 5-4.

Table 5-4 Modelled land cover change as a percentage of the study area for S50E (bold) and T35B (italics). Land cover labels are provided as superscript to S50E values at class intersect

Change	UG	FITBs	BRS	Wb	Wl	CLs	FP	UrBu	Total 2014	**Loss**	**Net**
UG	**44.7** ^{P}	**3.2** ^{If}	**0.1** ^{De}	**0.1** ^{Dn}	**0.1** ^{Dn}	**4.0** ^{Ia}	**0.1** ^{R}	**4.7** ^{Iu}	**56.9**	**12.0**	***-4.8***
	72.7	*2.7*	*0.1*	*-*	*0.5*	*1.3*	*2.6*	*0.1*	*79.9*	*7.2*	*-0.2*
FITBs	**4.0** ^{Re}	**5.5** ^{Pf}	**0.0** ^{Re}	**0.0** ^{E}	**0.0** ^{Dn}	**0.3** ^{Ia}	**0.2** ^{R}	**0.5** ^{Iu}	**10.5**	**5.1**	***-0.6***
	3.3	*0.4*	*-*	*-*	*0.0*	*0.1*	*0.1*	*0.0*	*4.0*	*3.6*	*-0.9*
BRS	**0.0** ^{Dn}	**0.0** ^{If}	**0.1** ^{P}	**-** ^{E}	**-** ^{Dn}	**0.0** ^{Ia}	**0.0** ^{R}	**0.0** ^{Iu}	**0.1**	**0.1**	**0.1**
	-	*-*	*0.2*	*-*	*-*	*-*	*-*	*-*	*0.2*	*0.0*	*0.1*
Wb	**0.1** ^{Dn}	**0.0** ^{If}	**-** ^{Dn}	**2.6** ^{P}	**-** ^{Dn}	**0.1** ^{Ia}	**-** ^{R}	**0.0** ^{E}	**2.9**	**0.3**	***-0.2***
	0.0	*-*	*-*	*0.0*	*-*	*-*	*-*	*-*	*0.0*	*0.0*	*0*
Wl	**0.0** ^{Dn}	**-** ^{If}	**0.0** ^{Dn}	**-** ^{Dn}	**0.0** ^{P}	**0.0** ^{Ia}	**-** ^{R}	**0.0** ^{Iu}	**0.1**	**0.1**	***-0.01***
	0.8	*-*	*-*	*-*	*0.1*	*0.1*	*0.2*	*-*	*1.2*	*1.1*	*-0.3*
CLs	**2.2** ^{A}	**0.5** ^{If}	**0.0** ^{A}	**0.0** ^{E}	**0.0** ^{E}	**15.0** ^{P}	**0.0** ^{R}	**0.7** ^{Iu}	**18.2**	**3.4**	**1.7**
	1.5	*0.1*	*-*	*-*	*0.2*	*4.3*	*0.2*	*-*	*6.2*	*1.9*	*-0.2*
FP	**0.6** ^{D}	**0.7** ^{If}	**0.0** ^{D}	**0.0** ^{E}	**-** ^{E}	**0.0** ^{Ia}	**0.4** ^{P}	**0.0** ^{Iu}	**1.8**	**1.4**	***-1.1***
	1.3	*-*	*-*	*-*	*0.1*	*0.0*	*6.8*	*-*	*8.3*	*1.5*	*1.5*
UrBu	**0.3** ^{A}	**0.1** ^{If}	**0.0** ^{A}	**0.0** ^{E}	**0.0** ^{E}	**0.6** ^{Ia}	**0.0** ^{R}	**8.5** ^{Pu}	**9.5**	**1.0**	**4.9**
	0.1	*-*	*-*	*-*	*0.0*	*0.1*	*0.0*	*0.1*	*0.2*	*0.1*	*0*
Total 2030	**52.1**	**9.9**	**0.2**	**2.7**	**0.1**	**20.0**	**0.7**	**14.4**			
	79.7	*3.1*	*0.3*	*0.0*	*0.9*	*6.0*	*9.8*	*0.2*			
Gain	**7.4**	**4.4**	**0.1**	**0.1**	**0.1**	**5.1**	**0.3**	**5.9**		**23.4**	
	7.0	*2.7*	*0.1*	*-*	*0.8*	*1.7*	*3.0*	*0.1*		*15.5*	
Change per year									**S50E**	**1.5**	
									T35B	*1.0*	

If: FITBs intensification; Ia: Agricultural intensification; Iu: Urban intensification; R: Afforestation; D: Deforestation; A: Abandonment; Dn: Natural dynamic; De: Degradation; Re: Reclamation

Assuming a map accuracy for the modelled map similar to that of the observed map, the cross tabulation of current and future land cover classes (Table 5-4) shows for future period 2014-2030 a 23% total change (gain and loss) for catchment S50E. This compares favourably with the 21% change for the periods 1990-2000 (Chapter 4) and 2000-2014 (Chapter 3; Chapter 4). Since the future scenario model mimics patterns of past measured change, the change intensity, defined as the change per year, remained constant at 1.5% per year for S50E.

In T35B, the total change (gain and loss) in the landscape over all land cover classes was only 15.5% for prediction period 2014 to 2030, compared with 18.2% for the period between 2000 and 2014 (Chapter 3). The change intensity decreased from 1.3% to less than 1% for this catchment. The disagreement between the actual land cover maps 2014 (T2) and 2000 (T1), as well as between modelled land cover classes (T3) and 2014 land cover classes (T2), is provided in Table 5-5.

Table 5-5 Comparison between transitions for 2000 to 2014 (T1-T2) and 2014 to 2030 (T2-T3) for S50E and T35B. Columns are labelled Q for Quantity, E for Exchange and S for Shift disagreement.

	S50E						T35B					
	2000–2014			2014–2030			2000–2014			2014–2030		
Class	**Q**	**E**	**S**	**Q**	**E**	**S**	**Q**	**E**	**S**	**Q**	**E**	**S**
UG	4.5	***8.9***	4.0	4.8	***12.0***	2.8	4.3	***9.3***	2.7	0.2	***11.6***	2.5
FITBs	0.8	5.9	1.8	0.6	7.5	1.4	4.3	4.6	0.0	0.9	5.4	0.0
BRS	0.1	0.0	0.0	0.1	0.1	0.0	0.2	0.0	0.0	0.1	0.0	0.0
Wb	0.2	0.2	0.0	0.2	0.2	0.0	0.0	0.1	0.0	0.0	0.0	0.0
Wl	0.4	0.1	0.0	0.0	0.1	0.0	1.9	1.4	0.1	0.3	1.5	0.1
CLS	1.9	4.0	0.7	1.6	6.3	0.5	0.1	2.6	0.6	0.2	3.0	0.3
FP	2.7	0.4	0.0	1.1	0.5	0.0	1.8	2.1	0.0	1.5	3.0	0.0
UrBu	4.9	0.8	0.0	4.9	2.0	0.0	0.0	0.2	0.1	0.0	0.2	0.0
Overall	7.7	10.3	3.3	6.7	14.4	2.4	6.3	10.1	1.8	1.7	12.4	1.4

Q: Quantity; E: Exchange; S: Shift
UG: grassland; FITBs: woodland; BRS: bare; Wb: waterbodies; Wl: wetlands; CLS: cultivated; FP: plantation; UrBu: urban

Table 5-5 reveals the classes that account for the largest exchanges and therefore possibly the largest model errors. In both measured and modelled transitions, UG had the highest exchange percentage with approximately 9% for the 2000-2014 transition and ~12% for the modelled transition (in bold italics). In the measured data (2000-2014), the similarity between categories with similar spectral signatures could cause exchange error, which would be propagated to the predicted land cover change model. Figure 5-5 shows the overall disagreement of the catchment at the two time steps for the two catchments.

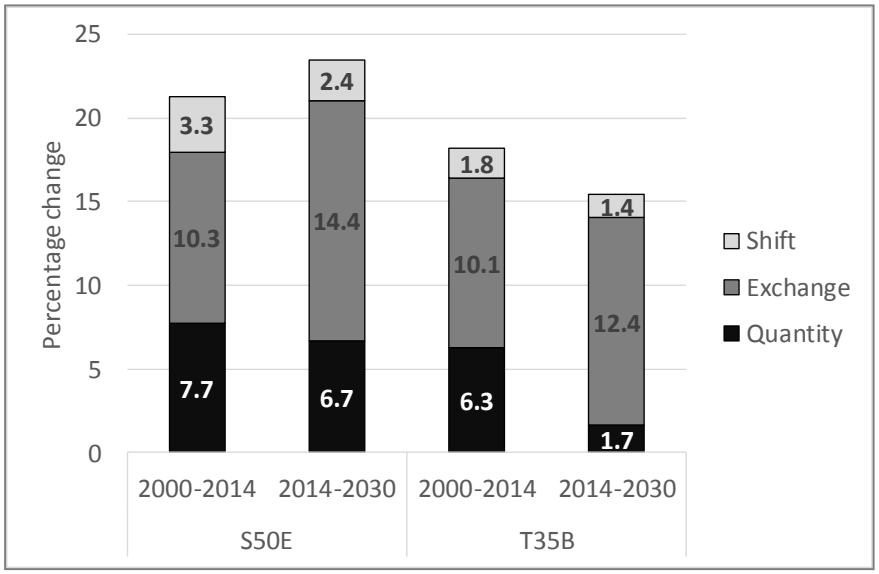

Figure 5-5 Quantity, exchange and shift disagreement

There is a marked increase in exchanged pixels in the predicted model for 2030, with lower quantity disagreement, particularly in T35B. The similarity in quantity disagreement between measured and modelled scenarios implies that for S50E, the correct number of pixels were allocated to a class. The high exchange disagreement for classes UG, FITBs and CLs, as well

as FP in T35B suggests that these classes were probably not modelled accurately in the 2030 land cover map and that certain transitions were incorrectly predicted. This was to be expected based on the model accuracies reported for S50E (Table C-1, Appendix C) with none of the sub-models having an accuracy level higher than 70%. For T35B (Table C-2, Appendix C), sub-models for urban intensification (Iu) and afforestation (R) provided accuracies of higher than 80%. The disagreement budget for these classes in the two time periods is also similar. The sub-models for abandonment (A) and natural dynamics (Dn) presented accuracies lower than 50%, but very few pixels were associated with these transitions.

5.4 DISCUSSION

The aim of this research was to guide land management strategies by performing land change modelling to project land cover change trends into the future. A land change model must predict not only the quantity of each land cover type, but also the location of any change (Pontius, Huffaker & Denman 2004). Since the LCM follows an inductive approach, past land cover maps are used to empirically model change as a function of explanatory spatial variables (Mas et al. 2014). The accuracy of the output of an inductive model is a function of both the model itself, specifically suitability of algorithms within the model to fulfil the intended purpose, and the accuracy of the input data. Errors in the individual input land cover maps will be propagated through the model and produce errors in all model outputs, including the probability matrix, transition potential map and future land cover map (Figure 5-1). Gibson et al (2018) evaluated the LCM based on two modelling assumptions. Firstly, rates of change are assumed to be constant, which implies that external forces remain constant, as implemented in the Markov process of change demand. Secondly, the drivers of change (explanatory spatial variables) are assumed to act identically to create the propensity for change maps in change allocation. Selection of explanatory spatial variables are at the discretion of the operator. This implies that a single model can produce different outputs based on the user's choice of model parameters. Therefore, there can be greater variation within the outputs of a single model than between the outputs of different models (Camacho Olmedo et al. 2015). Consequently, the ability to capture the non-linear behaviour of land cover change processes in variables and model in algorithms is a limitation of LCM (Camacho Olmedo et al. 2015; Paegelow et al. 2013).

Despite the limitations of the LCM output, land cover change analysis was performed between the observed land cover map of 2014 and the modelled land cover map for 2030 to identify landscape dynamics and identify trends that may continue into the future given the set of explanatory variables used. The overall accuracy for the input land cover maps, T_1 (2000) and

T_2 (2014), was reported as respectively **83%** *(81%)* and **87%** *(83%)* for **S50E** *(T35B)*, equating to a land cover change accuracy of **72%** *(67%)*. Assuming similar map accuracies between the modelled map and the observed map T_2, the accuracy of the land cover change map for the modelled scenario would be **76%** *(69%)*. This may appear low, but if higher change accuracies are required, for example change mapped with 75% reliability, the accuracy of input land cover maps at T_1 and T_2 would need to be about 90% (Fuller, Smith & Devereux 2003). This is a seldom achievable accuracy level when mapping land cover from medium resolution satellite imagery. Hypothetical map errors for the 2000-2014 transition amounted to **8%** *(5%)* for gains in **S50E** *(T35B)* and **5%** *(10%)* for losses (Chapter 4). Similarly, hypothetical errors computed for the 2014-2030 period was **6%** *(6%)* for gains and **5%** *(6%)* for losses.

It was found that in 2014, grasslands represented **57%** *(80%)* of the total **S50E** *(T35B)* area with this figure modelled to decrease to **52%** *(80%***)** by 2030 with losses likely to favour a gain in woody plants and cultivated land. The results show that the total change (gain and loss) in the study area over all land cover classes was **21%** *(18%)* for the period between 2000 and 2014 and **23%** *(16%)* from 2014 up to the future scenario for 2030, with the change intensity remaining constant at **1.5%** *(<1%)* per year. It was determined that the probability of grasslands persisting is around **80%** *(>90%)* with the highest probability of grasslands being lost to woody encroachment **~5%** *(3%)* and cultivation **~7%** *(<2%)*.

Grassland, the largest class, showed the largest measured and modelled loss. A slightly higher loss intensity was modelled for this large dormant class (+0.1%). In contrast to the measured change, a net loss was modelled for woody plants and shrubs. However, the predicted loss falls within the 30% hypothetical error in landscape transition ascribed to error propagation from contributing land cover maps calculated in Chapter 3, making the result acceptable. Net change in woody plants for 2000 to 2014 varied between -0.5% to +1% of total catchment area. In T35B, plantations showed a small net gain, potential of expansion of forestry. Intensification of woody plants were modelled in the upper reaches of the Pot River and Little Pot. Intensity analysis (Aldwaik & Pontius 2012) determined that, while woody plants systematically target grassland (transition If), clearing of woody plants also systematically result in grassland (Re–reclamation), albeit degraded, with a net loss of woody plants over the modelled period. Afforestation (increased plantation) was the strongest trajectory in T35B showing a net gain of 1.5% with plantation targeting wetlands. This transition is likely be the result of the low accuracy of the wetland class (Wl) in the 2014 input land cover dataset.

5.5 FUTURE LAND COVER EFFECTS

Grasslands are vital in supporting agriculture and providing ecosystem services (Gwate et al. 2018), such as forage production, habitat, carbon sequestration and water supply. Consequences of loss of grassland include loss of grazing for livestock through degradation or transformation affecting rural livelihoods (Skowno 2018). In addition, loss of grasslands to agriculture and woody encroachment, will result in higher catchment evapotranspiration (ET) linked to catchment water use (Gwate et al. 2018), with T35B being most impacted (Gibson et al. 2018). Conversion of grassland to woody vegetation (indigenous and invaders) results in increases in biophysical attributes, such as leaf area and rooting depth, causing higher actual ET, which reduces runoff and consequently water yield from the catchment (Gwate et al. 2018; Palmer et al. 2017). However, such transitions can result in more carbon storage, the benefits of which may be offset by greater water demands from leafy vegetation. Changes in proportions and composition of land cover across the catchment will therefore affect the net ecosystem carbon exchange (NEE) (Lei et al. 2016) and influence the hydrologic functioning of a catchment affecting the climate system (Bright, Cherubini & Strømman 2012).

LCM models future scenarios based on trends of historic change and consequently the results represent a future scenario based on no intervention deviating from past interventions. The impact of the different land management practices in S50E (dualistic farming system) and T35B (commercial system) can be identified in the historic land cover change trends, as well as in the future scenario. It is apparent that under the dualistic farming system, degradation is taking place at a more rapid rate than in T35B, where over 90% of current grassland is expected to persist to 2030. For those involved in planning in these rural catchments, there should be greater sensitivity amongst policy makers towards the negative effects of further afforestation and uncontrolled invasion of IAPs. The results therefore suggest that rehabilitation and land management initiatives should be targeted in catchments under a dualistic farming system, rather than those that are predominantly commercial systems.

5.6 MODELLING LANDSCAPE FUNCTION

This chapter illustrated that future land cover changes will likely result in adjustments to biophysical drivers impacting on net ecosystem carbon exchange, catchment water use through evapotranspiration, and the surface energy balance through a change in albedo. Subsequently, the next chapter (Chapter 6) explores the relationship between the regulating ecosystems service, albedo, and land cover change, considering that a pattern of error may exist. The analysis will compare trends in albedo, evapotranspiration (ET) and net primary production

(NPP), using the current (2014) and future land cover derived in this chapter (2030), to model water use and carbon storage for a future date to describe how ecosystem stress can be characterised from Earth observation date by employing time series analysis.

CHAPTER 6: MONITORING EFFECTS OF LAND COVER CHANGE ON BIOPHYSICAL DRIVERS IN RANGELANDS USING ALBEDO

In this chapter[7], the relationship between land cover change and albedo is explored as the latter has shown to be a regulating ecosystems service (Anderson et al. 2011; Betts 2001; Lutz & Howarth 2014). Trends in albedo are described at catchment and land cover change trajectory level. Links are established to landscape processes of carbon storage and water use — through net primary production (NPP) and evapotranspiration (ET) respectively — to serve as indicators of future carbon storage and water use potential in the carbon-water nexus. The chapter thus addresses Objective 4 and responds to the research question: *How do trends in biophysical drivers and characteristics of land cover change trajectories differ among the various catchments?*

6.1 ABSTRACT

This chapter explores the relationship between land cover change and albedo, recognised as a regulating ecosystems service. Trends and relationships between land cover change and surface albedo were quantified to characterise catchment water and carbon fluxes, through ET and NPP respectively. Moderate resolution imaging spectroradiometer (MODIS) and Landsat satellite data were used to describe trends at catchment and land cover change trajectory level. Peak season albedo was computed to reduce seasonal effects. Different trends were found depending on catchment land management practices and satellite data used. Although not statistically significant, albedo, NPP, ET and normalised difference vegetation index (NDVI) were all correlated with rainfall. In both catchments, NPP, ET and NDVI showed a weak negative trend, while albedo showed a weak positive trend. Modelled land cover change was used to calculate future carbon storage and water use. According to the results, a decrease in catchment carbon storage and water use is expected. Grassland, a dominant dormant land cover class, was targeted for land cover change by woody encroachment and afforestation, causing a decrease in albedo, while urbanisation and cultivation caused an increase in albedo. Land cover map error of fragmented transition classes and the mixed pixel effect affected the results, suggesting the use of higher resolution imagery for NPP and ET and albedo as a proxy for land cover.

[7] This chapter was originally published as a scientific article (citation below). The manuscript was reformatted to match the guidelines of Stellenbosch University, Department of Geography and Environmental Studies.

Münch Z, Gibson LA & Palmer AR 2019. Monitoring effects of land cover change on biophysical drivers in rangelands using albedo. *Land*, 8, 33; doi:10.3390/land8020033.

6.2 INTRODUCTION

Changes in land use and land cover (LULC) cause bio-geophysical changes to the land surface that disturb the earth's surface energy balance (Betts 2001), which have noticeable impacts on ecological and environmental systems. Biophysical characteristics associated with land cover types are not only responsible for carbon storage in the landscape, but also affect water use of vegetation driven by eco-hydrological processes (Gwate et al. 2018), such as in grasslands in water scarce catchments in South Africa. Ecosystem changes can be detected and quantified using biophysical parameters derived from multi-temporal satellite observations of the land surface (Forkel et al. 2013). Primary drivers of change within the rural catchments in the Eastern Cape have been linked to woody encroachment, commercial afforestation, urbanisation, increased dryland cultivation and rangeland degradation to the detriment of native grasslands (Chapter 3). Conversion of grassland to woody vegetation results in higher actual evapotranspiration (ET) due to increases in biophysical attributes, such as leaf area and rooting depth. In turn, higher ET has the effect of reduced water yield from the catchment (Gwate et al. 2018; Palmer et al. 2017). Changes in proportions and composition of LULC across the catchment will affect the net ecosystem carbon exchange (NEE) (Lei et al. 2016) and influence the hydrologic functioning of a catchment affecting the climate system (Bright, Cherubini & Strømman 2012).

Surface albedo, the proportion of solar radiation reflected relative to the total incident radiation, can vary considerably depending on the character of the landscape and the vegetation present (Lutz & Howarth 2014). Land surface albedo has long been recognised as a radiative force from LULC change (Bonan 2008; Bright, Cherubini & Strømman 2012) and plays a key role in climate change (Bonan 2008; Georgescu, Lobell & Field 2011), while climate modelling studies have confirmed albedo as a climate regulating ecosystem service (Lutz & Howarth 2014). Afforestation reduces surface albedo by absorbing more solar radiation and increasing surface temperature (Bonan 2008; Swann, Fung & Chiang 2012), while deforestation may activate either radiative forcing, due to surface albedo change, or non-radiative forcing due to change in evapotranspiration efficiency and surface roughness (Davin et al. 2010). In addition, invasion by woody alien species changes the landscape composition and affects soil properties, even after clearing (Oelofse et al. 2016). Thus, for each land cover transition, the shift in surface albedo should also be considered. Commercial afforestation, invasive alien plants (IAPs) (like *Acacia mearnsii* [black wattle]) and native woody plant encroachment (like *Vachelia karroo*) all result in an increase in the total aboveground woody standing biomass (Gouws & Shackleton

2019; O'Connor, Puttick & Hoffman 2014) with associated increase in leaf area index (LAI) and consequently a possible reduction in surface albedo.

The higher level of green water in these land cover classes is a good absorber of heat, and this may result in further global heating (Bonan 2008; Swann, Fung & Chiang 2012), possibly discounting the positive consequences of carbon sequestration (Lutz & Howarth 2014). In contrast, urban communities, such as those found in the rural Eastern Cape, South Africa, with widely spaced dwellings interspersed with bare soil, may result in higher albedo. Similarly, degraded rangeland, with lower fractional canopy cover, may also have higher albedo (Rotenberg & Yakir 2010). Betts (Cunha et al. 2018) found surface albedo to be an accurate proxy for land cover change in a semi-arid region in Brazil, due to its sensitivity to seasonal phenological variation (Cunha et al. 2018; Wang et al. 2017) and landscapes affected by land management practices (Cai et al. 2016b). Land cover change projections in the Eastern Cape of South Africa have highlighted the importance of focusing land and water resources management interventions on rehabilitation in catchments under dualistic[8] farming systems (Chapter 5). Consequently, it is vital to consider surface albedo within a range of different land cover classes, and recommend policies that will change albedo to promote improvements offered by carbon offsets.

Remote sensing is a key tool for monitoring long-term environmental change from space. High spatial resolution Landsat (Wulder & Masek 2012) and high temporal resolution gridded moderate resolution imaging spectroradiometer (MODIS) vegetation indices have been used to characterise land cover dynamics for climate change assessment, mitigation and adaptation (Friedl et al. 2014; Ganguly et al. 2010). Furthermore, the recent launch of the Google Earth Engine (GEE) cloud-based platform facilitates systematic large-scale processing of geospatial data through ease of access to data archives (Hansen & Loveland 2012) and shared algorithms (Gorelick et al. 2017).

Due consideration must be given to the scale at which analyses should be conducted since spatial resolution and the extent of analysis can have major effects on results, especially when categorical land cover maps are derived that provide information about patterns and processes in the landscape (Estes et al. 2018). A common problem in spatial analysis of heterogeneous landscapes is the two-fold modifiable areal unit problem (MAUP) (Openshaw & Taylor 1979). Not only can the shape and placement of non-overlapping units used to extract map values (such

[8] To describe the complexity around the communal farming tenure arrangement in the Eastern Cape, the label "dualistic or bilateral landholding arrangement" was agreed upon by stakeholders, due to the interaction of the components of traditional leadership and the municipal system in land allocation.

as land cover classes) influence analyses of those values, but also the dimensions of arbitrary aggregation units (such as pixels in remote sensing imagery) do not match the characteristic shapes and scales of natural features in the heterogeneous landscape, affecting subsequent analyses (Dark & Bram 2007). Estes et al. (2018) suggested that higher resolution imagery could address this problem. However, map error may be responsible for incorrect interpretations of land cover change (Pontius & Lippitt 2006). Lack of adequate reference data or imperfect reporting of accuracy results affect the explanations of the processes depicted in land cover change maps (Estes et al. 2018; Olofsson et al. 2014; Olofsson et al. 2013).

Various studies have been conducted to gain an understanding of rangeland dynamics in the mesic regions of the Eastern Cape, using a combination of remote sensing and field data. For instance, Gwate et al. (2016) described the invasion of the rangelands by black wattle and the effect on soil properties (Okoye 2016). In Chapter 3 (Münch et al. 2017) derived land cover change trajectories and associated error from land cover maps, while Palmer et al. (2017) determined the fraction of photosynthetically active radiation (fPAR) and LAI for several land cover classes. Modelled evapotranspiration (ET) was used to highlight the effect of land cover change on the catchment evaporative fraction (Gwate et al. 2018). In Chapter 5 (Gibson et al. 2018) future land cover changes were modelled based on observed land cover change maps and future change trajectories derived. However, the effect of land cover change, both observed and modelled, on surface albedo and consequently the surface energy balance, has not been explored in this region. Additionally, the link between modelled landscape change, surface albedo and changes in catchment water and carbon fluxes have not been investigated. Recently, surface albedo was extracted from satellite data per land cover class for calibration of land surface models (LSM) in climate modelling (Duveiller et al. 2018; Duveiller, Hooker & Cescatti 2018), while other authors have investigated the potential of albedo in land cover (De Oliveira Faria et al. 2018) and land cover change analyses (Cunha et al. 2018).

The aim of this chapter is to quantify trends and relationships between land cover change, surface albedo, NPP and ET to characterise catchment water and carbon fluxes and postulate consequences on ecosystem services provided by grasslands. Trends in surface albedo are described at catchment and trajectory level for observed land cover change. Links are established to quantify future carbon storage and water use — through respectively NPP and ET — in response to modelled land cover change. The benefits of using albedo as a proxy for land cover change are highlighted.

6.3 MATERIALS AND METHODS

Located in the Eastern Cape Province, South Africa (Figure 6-1), the quaternary catchments S50E and T35B are dominated by grassland, interspersed with woody IAPs (Mucina & Rutherford 2006). The Ncora Dam, supplied by the perennial Tsomo River, lies within the S50E catchment, while T35B, drained by the Pot and Little Pot Rivers, has no large dams. The mean annual rainfall for the area is ~800 mm (Schulze 2007), with the majority falling in summer particularly during January.

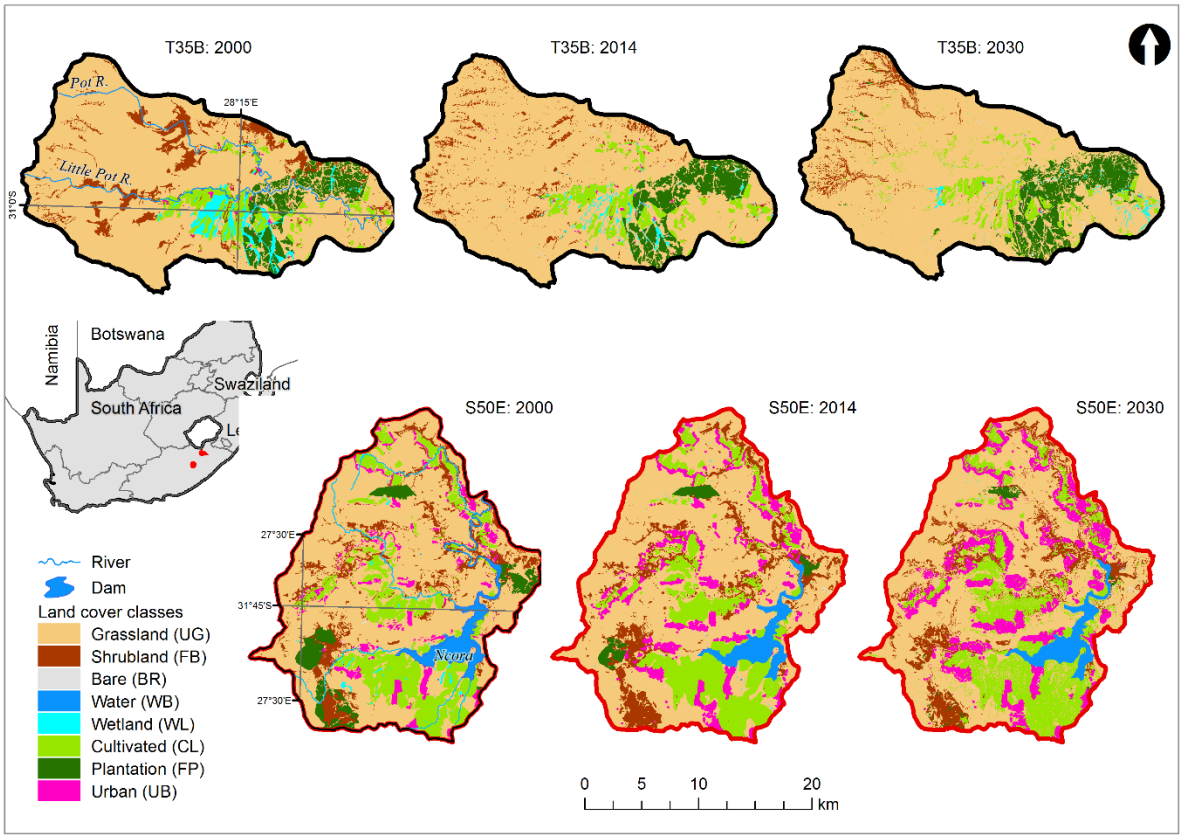

Figure 6-1 Study area with land cover classification for 2000, 2014 and 2030

Mixed farming, with livestock grazing and crop cultivation practised under dualistic land tenure (Kakembo 2001) is practised in S50E with its high grazing potential. In this catchment, farming practices such as overgrazing, burning and wood felling have contributed to grassland transformation resulting in degraded vegetation diversity and richness. In contrast, T35B represents commercial/freehold land with several different land usages, including forestry, mixed livestock and crop production. Non-clustered rural and urban settlements are found in both catchments.

Invasion by woody plants, particularly black wattle (*Acacia mearnsii*), silver wattle (*Acacia dealbata*) and poplar (*Populus* spp.), has transformed the grasslands (Gouws & Shackleton 2019; Oelofse et al. 2016), affecting rangeland production. Coordinated efforts of clearing IAPs (Van Wilgen & Wannenburgh 2016) that have higher water use relative to indigenous

vegetation (Clulow, Everson & Gush 2011) are underway to increase the proportion of water available to maintain other ecosystem services provided by rangelands (Meijninger & Jarmain 2014; Van Wilgen et al. 2008). Figure 6-2 provides an overview of the processing steps described in this section to perform trend analysis and characterise carbon fluxes (NEE) and water use in the catchments.

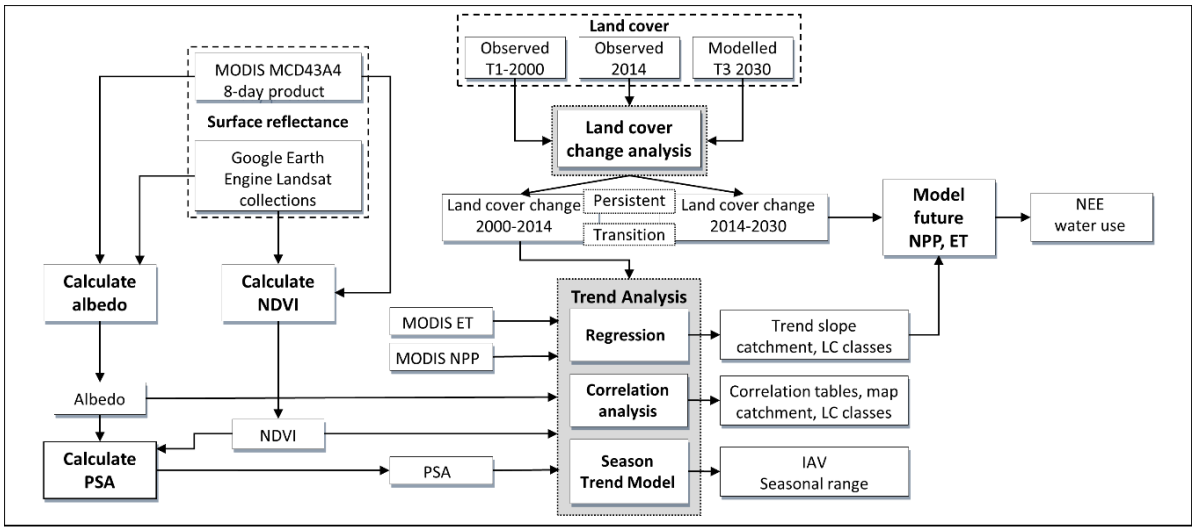

Figure 6-2 Processing flow to model albedo relationship with land cover

6.3.1 Land cover change

Observed land cover maps for 2000 (T1) and 2014 (T2) (Münch et al. 2017) and modelled land cover for 2030 (T3) (Gibson et al. 2018) at 30 m pixel resolution were selected for land cover change analysis. Land cover classes included grasslands (UG), shrublands, indigenous as well as invasive trees and bushes (FB), bare soils (BR), water bodies (WB), wetlands (WL), croplands (CL), forests (FP) and urban, built-up (UB). As described in Chapter 3 and Chapter 5, the existing South African national land cover map for 2000 (Van den Berg et al. 2008) was adapted to these eight classes through aggregation to conceptually broader classes (Lück & Diemer 2008) and manual editing (Chapter 3). Supervised object-based image analysis using a rule-based decision tree classification of Landsat 8 imagery was implemented to generate the 2014 land cover maps (Chapter 3). The overall accuracy achieved for these maps was 84 ± 1% and 85 ± 1% for 2000 and 2014 respectively. Land cover changes between T1 and T2 were analysed along with explanatory variables to generate transition potential maps. Markov chain analysis was used to assign probabilities to potential changes to derive the future land cover map for 2030 (Chapter 5) presented in Figure 6-1.

Post-classification change analysis was performed through overlay of (1) T1 and T2, and (2) T2 and T3 land cover maps and used to construct a transition matrix for the intersection of each pair of land cover maps (Chapter 3; Chapter 5). Observed historical land cover change of 21%

and 18% in, respectively, S50E and T35B were reported for 2000–2014 (Chapter 3). Projected land cover change, modelled from the 2014 and 2030 land cover maps, amounted to 23% and 16% of the catchment for S50E and T35B respectively (Chapter 5). Nine land cover change trajectory labels were assigned to specific land cover transitions to relate land cover change to specific landscape processes (Chapter 3). Landscape changes in the study area were grouped into three land change categories (Verbesselt et al. 2011; Vogelmann et al. 2012).

Table 6-1 shows the land cover class transitions identified by trajectory labels with expected albedo change direction for each class transition, based on literature values (De Oliveira Faria et al. 2018; Henderson-Sellers & Wilson 1983; Matthews et al. 2004) for similar land cover classes, provided in brackets: (↑) to signify increase, (↓) decrease or (-) no change. The land change category is also specified as abrupt (highlighted in light grey), seasonal (dark grey) or gradual ecological change (no background).

Table 6-1 Land cover change trajectories with expected albedo change direction for each class transition provided in brackets: (↑) to signify increase, (↓) decrease or (-) no change

Land cover trajectory (label)	**Land cover transitions (expected albedo change)**	**Land change category**
Woody encroachment (If^{g})	UG->FB(↓); FP->FB(↑); CL->FB(↓)	Gradual ecological change
Abandonment (A^{g})	CL->UG(↓); UB->UG(↓)	
Degradation (De^{g})	UG->BR(↑)	
Reclamation (Re^{g})	FB->UG(↑)	
Increased cultivation (Ia^{a})	UG->CL(↑); FB->CL(↑); WB->CL(↑); WL->CL(↑); UB->CL(↓)	Abrupt change
Urban expansion (Iu^{a})	UG->UB(↑); CL->UB(↑); FB->UB(↑)	
Afforestation (R^{a})	UG->FP(↓); FB->FP(↓)	
Deforestation (D^{a})	FP->UG(↑); FP->BR(↑)	
Natural dynamic (Dn^{s})	UG->WB(↓); UG->WL(↓); WB->UG(↑); WL->UG(↑)	Seasonal change

UG: grasslands, FB: shrublands, BR: bare, WB: water bodies, WL: wetlands, CL: croplands, FP: forest/plantation, UB: urban

Gradual ecological change (superscripted with g) describes landscape changes associated with the woody intensification of grassland, abandonment of agriculture, degradation of grassland and agriculture, as well as reclamation of grassland from IAPs. When a lower intensity use transitions to a higher intensity use, such as bushland encroachment into grassland, or increase in agriculture, it is considered intensification in the landscape. Although an increase in agriculture is intensification of the landscape, it is categorised as an abrupt change (superscripted with a), along with afforestation, deforestation and urban intensification due to the time scale over which the change occurs. Deforestation, degradation and reclamation, resulting in expected albedo increase, as well as abandonment, with expected albedo decrease, describe transitions to grassland and bare areas. Seasonal change (superscripted with s) can account for natural dynamics of seasonal conversions not explained through anthropogenic

change that may result in albedo fluctuations. As trajectory labels identified in the study area (Table 6-1) define transitions from multiple land covers to a single land cover, or to multiple land covers, there may be opposing albedo change directions within the same trajectory. These opposing vectors may have a confounding effect on the results and require further work to untangle the influence of each land cover transition.

The land cover trajectory labels (Table 6-1), subsequently called transition classes, were applied to the transitions between 2000–2014 and 2014–2030 (Chapter 5). In addition to these transitions, exceptionality, associated with potential map errors (Chapter 3) was noted in the study area, but excluded from analysis (<1% of T35B, 2.8% of S50E). Persistent classes, defined as pixels that represent the same thematic land cover class in 2000 as in 2014, where no land cover change was measured, may represent a measure of seasonality, degradation or long-term background change not associated with class transition. Both transition and persistent classes were used for further analysis.

6.3.2 Satellite data

6.3.2.1 Albedo

A strong agreement exists between Landsat surface reflectance (SR) and MODIS nadir–bidirectional reflectance distribution function (BRDF)–adjusted reflectance (NBAR) implying that the Landsat archive, prior to the MODIS era, can be used to obtain results of a similar quality to MODIS (Wang et al. 2017). To maintain this integrity, the same methodology to estimate albedo was applied to both the Landsat and MODIS collections. Albedo for each time step was calculated from MODIS and Landsat using the formula suggested by (Liang et al. 2003; Liang 2001) with constant values referred to in Equation 6-1 provided in Table 6-2.

$$albedo = c0 + c1r1 + c2r2 + c3r3 + c4r4 + c5r5 + c7r7, \quad \text{Equation 6-1}$$

where *r1*, *r3*, *r4*, *r5*, *r7* are the surface reflectance derived from MODIS and Landsat bands 1, 3, 4, 5, and 7 respectively, while *r2* is excluded for Landsat but represents MODIS band 2.

Table 6-2 Constant values used in calculation of albedo from moderate resolution imaging spectroradiometer (MODIS) and Landsat

Sensor	c0	c1	c2	c3	c4	c5	c7
MODIS	-0.0015	0.160	0.291	0.243	0.116	0.112	0.018
Landsat	-0.0018	0.356	0	0.13	0.373	0.085	0.072

The MODIS 500 m BRDF/NBAR/albedo product (MCD43A) (Schaaf et al. 2002; Z Wang et al. 2018) standardises MODIS directional reflectance to a nadir view at the illumination of local solar noon to eliminate the angular effect on biophysical related parameters. A 15-year time series of MODIS data were extracted using the National Aeronautics and Space Administration (NASA) application for extracting and exploring analysis ready samples (AppEEARS) interface (https://lpdaacsvc.cr.usgs.gov/appeears/). This time series was made up of 690 8-day surface reflectance (MCD43A4 nadir reflectance band 1-7, version 5) and albedo band quality (MCD43A2 BRDF albedo band quality, version 5) data from 18 February 2000 (8-day composite beginning on ordinal day 49) to 10 February 2015 at 500-m resolution. To cover 15 years, each year-long period is defined as beginning on ordinal day 49 and ending on day 41 containing 46 data points (Loarie et al. 2011).

Landsat imagery was selected from the Google Earth Engine image collections (USGS Earth Resources Observation and Science (EROS) Center, Sioux Falls, United States of America) (Gorelick et al. 2017) for the same period as the MODIS data. Sixty three Landsat 5 Thematic Mapper (LT5), 243 Landsat 7 Enhanced Thematic Mapper Plus (ETM+, LE7) and 49 Landsat 8 Operational Land Imager (LC8) images were selected. These selected images that had already been (1) calibrated to a consistent radiometric scale and (2) atmospherically corrected to represent surface reflectance, were filtered for pixel quality and catchment geography (image path/row 169/082 for T35B and 170/082 for S50E). Equation 6-1 was applied to each image in the LT5 and LE7 image collections as the band specifications on Landsat TM and Landsat ETM+ are identical. For the LC8 collection, the parameters *r1, r3, r4, r5, r7* in Equation 6-1 are the surface reflectance values derived from equivalent LC8 bands 2, 4, 5, 6 and 7 respectively (Holden & Woodcock 2016). The separate LT5, LE7 and LC8 albedo collections, sorted by date, were merged into a new albedo image collection in GEE.

6.3.2.2 Normalised difference vegetation index (NDVI) and peak season albedo

As surface albedo is sensitive to vegetation cover change, especially during the growing season (Zhai et al. 2015), peak season albedo (PSA) was extracted. PSA, defined as the albedo when the maximum NDVI value per year occurs, could limit seasonal vegetation fluctuation in the data thereby reflecting the relationship between inter-annual albedo variations with land cover change.

For MODIS, NDVI was calculated from MCD43A4 (NASA EOSDIS Land Processes DAAC, USGS EROS Center, Sioux Falls, United States of America) surface reflectance band 1 (red) and band 2 (near infrared) at 500 m spatial resolution for every pixel in each annual time series

and the relative position of the maximum NDVI was marked. The albedo value for the particular position, representing the PSA, was extracted from the MCD43A4 time series (Zhai et al. 2015).

The same method to derive PSA was applied to the Landsat data in GEE. However, only growing season images between September and May were considered as the lower temporal resolution and images with cloud cover may confound albedo at an annual time step. Cloudy pixels were masked out using the quality assessment bands that identify pixels exhibiting adverse instrument, atmospheric, or surface conditions, supplied with Landsat surface reflectance products. The relative position of maximum NDVI during the peak growing season for each year was used to extract the albedo from the merged Landsat albedo image collection. NDVI was calculated from red and near infrared surface reflectance bands – bands 3 and 4 respectively for LT5 and LE7 and bands 4 and 5 respectively, for LC8. Mean PSA values for persistent and transition classes in each study area were extracted from the MODIS and Landsat PSA using a zonal statistics function in R statistical software (R Core Team 2017).

6.3.2.3 Moderate resolution imaging spectroradiometer (MODIS) net primary production (NPP) and evapotranspiration (ET)

NPP (MOD17A3, version 5, 1 km) (Running & Mu 2015) and ET (MOD16A2, version 5, 1 km) (Mu et al. 2007; Mu, Zhao & Running 2011) products, were extracted to represent carbon and water fluxes, respectively. The MOD17A3 product provides information about annual (yearly) NPP at 1 km pixel resolution. Although the new 500 m, version 6 product (Running & Mu 2015) was considered, uncharacteristically high NPP values were observed for 2000 and 2001, and the coarser resolution 1 km product was, therefore, selected instead.

Not only does ET play an important role in the terrestrial water cycle through precipitation return, but as user of more than half of the total solar energy absorbed by land surfaces, ET is an important energy flux (Trenberth et al. 2009). The MOD16 product uses a physical model based on the Penman–Monteith logic (Monteith 1965) to calculate ET (Cleugh et al. 2007; Mu et al. 2007; Mu, Zhao & Running 2011). Although uncertainties were noted in both measured (Savage et al. 2004) and remotely sensed data (Mu, Zhao & Running 2011; Ramoelo et al. 2014; Zhao et al. 2005), MOD16A2 data was previously used in catchment S50E (Gwate et al. 2018) to investigate the influence of land cover change on ET.

Annual NPP (MOD17A3) and ET (MOD16A2) were extracted for the period 2000 to 2014 to visualise the trend of these variables in the catchments. Non-parametric least squares regression was performed in localised subsets to fit a smooth “LOcal regression” (LOESS) curve

(Cleveland 1979). Mean NPP and ET per-pixel were calculated. Summary statistics were computed from the gridded datasets for each land cover transition class using zonal statistics.

6.3.3 Trend analysis

Linear correlation analysis was performed on annual PSA time series for MODIS and Landsat using linear least square regression to identify significant linear trends ($p<0.05$) at catchment, land cover trajectory and pixel level. The slope of the regression, which describes the direction of change, was also extracted. PSA percentage change (slope of linear correlation analysis multiplied by study period) was computed per-pixel. Mean values for catchment and trajectory level analyses were extracted by applying zonal statistics.

Per-pixel linear regression was performed between PSA, NPP, ET and NDVI to characterise the relationships between PSA and (1) NPP, (2) NDVI and (3) ET. The coefficient of determination (R^2), correlation coefficient and the direction of the trend was extracted from the slope of the linear regression. Percentage change was applied to model future change as a function of land cover change using the linear regression equations developed for persistent classes applied to modelled land cover.

A season-trend model (STM) (Forkel et al. 2013) based on a classical additive decomposition model as formulated in breaks for additive seasonal and trend (BFAST) software (Verbesselt et al. 2010b) was applied to the 8-day MODIS albedo time series with package greenbrown (Forkel & Wutzler 2015) in R statistical software (R Core Team 2017). The full temporal resolution albedo time series was explained by a piecewise linear trend and a seasonal model in a regression relationship (Forkel et al. 2013), to identify trends, inter-annual variation (IAV) and significant breakpoints at pixel level. The method uses ordinary least squares (OLS) regression fitting linear and harmonic terms to the original time series to estimate time series segments based on significant trend slope. The significance of the trend in each segment is estimated from a t-test. A maximum of three breakpoints with significant structural changes ($p \leq 0.05$), were selected. Time series properties (mean, trend, inter-annual variability, seasonality and short-term variability) were estimated from the 8-day MODIS albedo product (Forkel et al. 2013).

6.4 RESULTS

6.4.1 Catchment level peak season albedo (PSA), NPP, ET and NDVI

Figure 6-3 shows the spatial and statistical distribution of the PSA trend, computed as the pixel level slope of PSA regression over the study period for T35B and S50E for both MODIS (Figure 6-3A, B, E, F) and Landsat (Figure 6-3C, D, G, H).

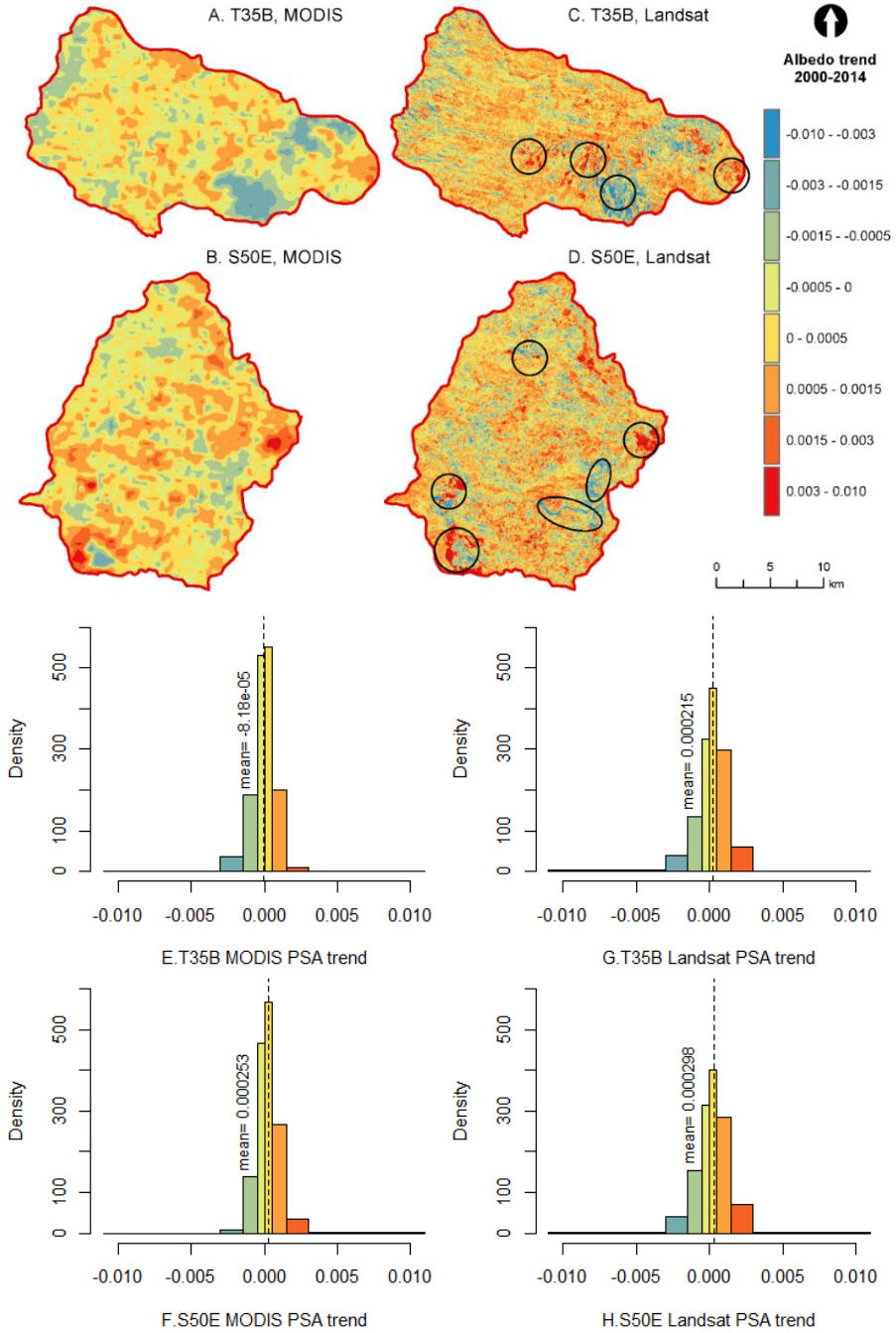

Figure 6-3 Peak season albedo (PSA) trend (top) and histogram of trend (bottom) measured with MODIS and Landsat for T35B and S50E between 2000–2014

Although similar spatial patterns are observed, it is clear from Figure 6-3C and D that there are some extreme changes that are not captured at coarser MODIS resolution. This is borne out by

the larger range for Landsat displayed on the x-axes in Figure 6-3G and H. The slope for MODIS pixels varied between -0.003 (blue pixels) in both catchments with maximum increase of 0.005 for S50E and 0.0026 for T35B (red pixels). Measured from Landsat PSA, greater variation of values between −0.01 (blue pixels) and 0.011 (red pixels) was calculated. Locations where Landsat PSA trend is either higher than the maximum MODIS trend or lower than the minimum trend are indicated with circles in Figure 6-3C and D. At catchment scale the mean change (mpc) in PSA was less than one per cent ±10 standard deviations (sd) for MODIS and ±5 sd for Landsat.

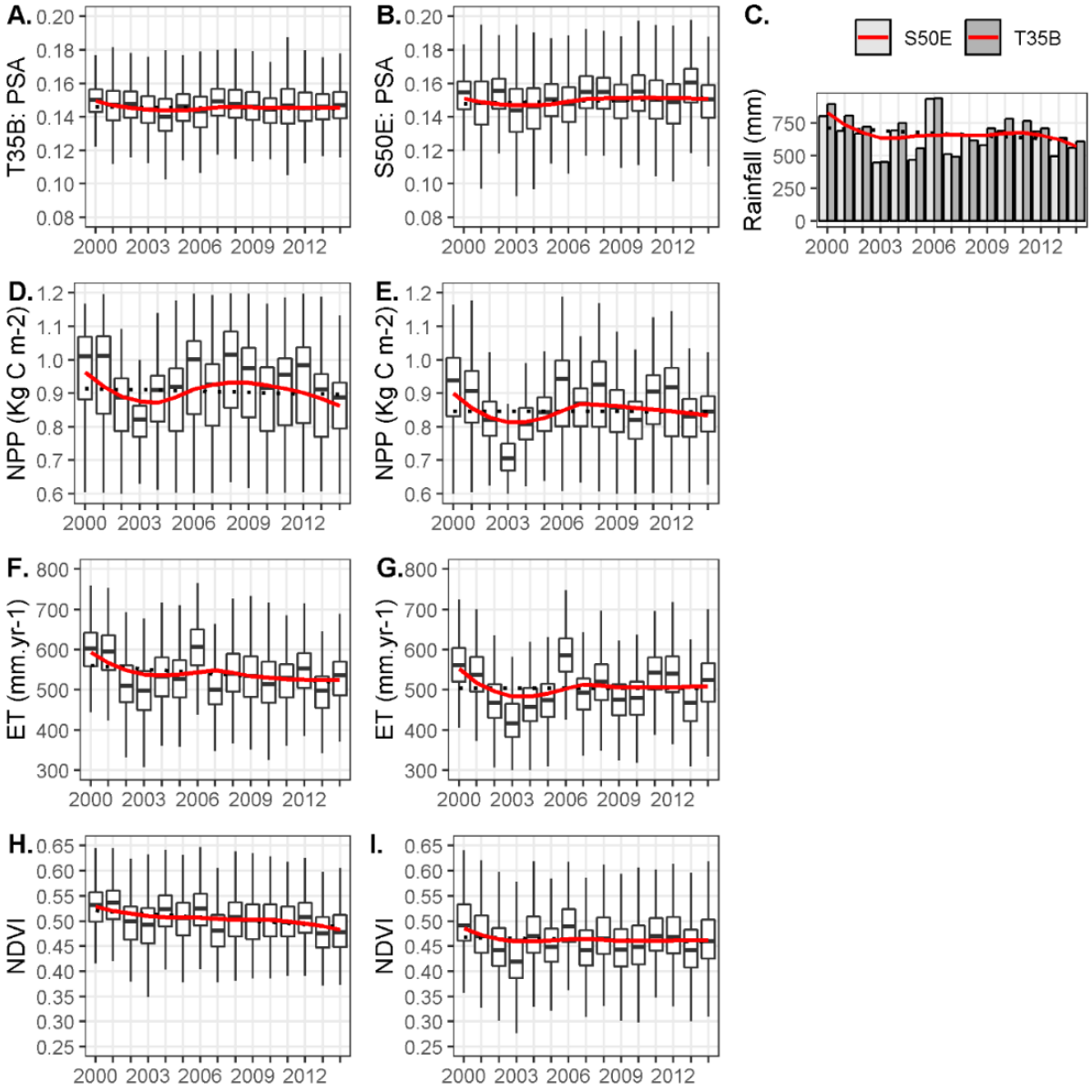

Figure 6-4 Mean annual PSA (A, B), net primary production (NPP) (D, E), evapotranspiration (ET) (F, G) and normalised difference vegetation index (NDVI) (H, I) values respectively for T35B (left) and S50E (right), with bar plot of annual rainfall (C)
[LOcal regression (LOESS) curve in red, linear regression curve in dotted lines]

Over the study period, mean MODIS PSA values of 0.145±0.011 and 0.150±0.014 were obtained for catchment T35B and S50E respectively, with mean Landsat PSA values significantly lower ($p<0.05$) at 0.143±0.022 for T35B and 0.140±0.022 for S50E. The boxplots in Figure 6-4 illustrate mean annual PSA (Figure 6-4A, B), NPP (Figure 6-4D, E), ET (Figure 6-4F, G) and NDVI (Figure 6-4H, I) trends for the observed study period extracted from MODIS data. Mean annual rainfall (Agricultural Research Council weather station data, Tropical Rainfall Measuring Mission satellite data) is shown in the bar plot in Figure 6-4C. WS 30388 represents the rainfall in S50E at Cala, while WS 30149 represents the rainfall for T35B at Ugie. The linear trend is shown with a dotted line while the LOESS curve indicates the local trend.

While similar spatial patterns were observed for mean MODIS PSA at coarser resolution and mean Landsat PSA, linear correlation between Landsat pixels, scaled to MODIS resolution, shows an R^2 of only 0.718 for T35B and 0.723 for S50E. In addition, the mean PSA in both S50E and T35B did not change significantly over the 15-year study period ($p>0.05$). However, by fitting a median-based linear model (Sen 1968; Siegel 1982; Theil 1950), the S50E slope showed a slight increase ($\beta_{1M} = 0.00023$; $\beta_{1LS} = 0.0003$; $p>0.05$), which would cause a net increase of 0.003 (*0.004*) in PSA. In contrast, mean PSA trend in T35B was negative with MODIS ($\beta_{1M} = -00009$) but positive with Landsat ($\beta_{1LS} = 0.0004$), translating to PSA change of −0.001 (*+0.006*). Non-significant trends at catchment scale were confirmed with a Mann-Kendall (MK) test ($p > 0.05$) for both catchments. Mean albedo values and trend were also calculated from the 8-day MODIS product (T35B-σ = 0.135±0.017, $\beta_{1M8} = 0.0001$; S50E-σ= 0.146±0.001, $\beta_{1M8} = 0.00004$).

PSA generally followed an increasing trend in response to reduced rainfall, and a decreasing trend in response to increased rainfall, when comparing Figure 6-4A and B with Figure 6-4C. The high rainfall in 2006, categorised as a flood (NDMC 2007), caused a drop in PSA reflected in 2006. Although a relationship between albedo and rainfall is suggested, neither the linear, nor non-linear trend (Theil-Sen slope, measured with MK-test) was significant ($p>0.5$) at catchment scale. NPP, ET and NDVI in T35B (Figure 6-4) have higher mean values (0.892 kg.C.m^{-2}; 542 mm.yr^{-1}; 0.54) compared to S50E (0.802 kg.C.m^{-2}; 508 mm.yr^{-1}; 0.49) and are statistically different ($p<0.05$), measured with the Wilcoxon signed rank test for non-parametric data. Although the trends appear strongly related to that of the rainfall pattern in Figure 6.4C, there is only a weak negative linear trend ($p>0.1$). Lower NPP, ET and NDVI were noted for 2003 in both catchments confirming the inflection point in 2004, which Gwate et al. (2018) associated with extreme low rainfall in 2003 (Figure 6-4C). Even though the LOESS

curve (in red) indicates a local downward trend, the linear trend is not significant (p>0.05) in any of the catchments.

The correlation between mean PSA, NPP, NDVI and ET is reported in Table 6-3. Complete cases, where a value existed for each of the four datasets for the pixel in question, were extracted for every pixel within the two catchment extents for comparison. A positive correlation indicates the extent to which one variable, like PSA, increases or decreases in parallel with another variable, while a negative correlation indicates the extent to which one variable increases as the other decreases.

Table 6-3 Catchment level correlation between PSA, NPP, NDVI and ET

T35B	**1**	**2**	**3**	**4**
1. PSA	-	*−0.01*	*−0.35*	*−0.22*
2. NPP	0.13	-	*0.51**	*0.71**
3. NDVI	−0.28	0.31	-	*0.60**
4. ET	−0.08	0.64*	0.57*	-

Note: Correlations for S50E (n = 2407) are presented above the diagonal in italics, and correlations for T35B (n = 2162) are presented below the diagonal. *p < 0.05.

In both the catchments, the strongest correlation was found between NPP and ET with 0.64 in T35B (n=2162) and slightly higher at 0.71 for S50E (n=2407). Correlation between NDVI and ET was ~0.6 in both catchments, while NDVI showed a stronger relationship with NPP in S50E. A weak negative correlation was found between PSA, NPP and ET. In T35B, PSA had a weak positive correlation with NPP, but none in S50E. Detail of the correlations computed per land cover class and transition trajectory are provided in supplementary material, Appendix D, Table D-1. In contrast to the catchment results, the strongest correlation at land cover class and transition level was between NDVI and ET (>0.79). Only persistent forest/plantation (n=42; 0.55) and trajectory deforestation (n=35; 0.75) in S50E showed a significant correlation between NPP and ET. Intensification of agriculture showed a similar strong positive NDVI–ET correlation (0.87) response in both catchments, but a negative PSA–NDVI correlation, only the correlation between albedo and NDVI was stronger in T35B (n=41; −0.54) as compared to S50E (n=117; −0.45). Contrary to expectation, deforestation in T35B showed a positive correlation (n=23; 0.7) between albedo and NPP. Afforestation in S50E (n=6; −0.56) displayed a negative correlation between albedo and NPP, but a positive correlation in T35B (n=60; 0.63). The aggregated catchment correlation masks some of the per class correlations, resulting in Simpson's paradox where groups of data show one particular trend, which is reversed when groups are aggregated (Comber et al. 2016). Common in spatial analysis of heterogeneous landscapes, this is an example of MAUP (Dark & Bram 2007) where the sample size (n) is dictated by the arbitrary land cover aggregation units.

The spatial distribution of the correlation between PSA and each of the variables NPP, NDVI and ET are shown in Figure 6-5 for T35B (top) and S50E (bottom). Only significant correlations ($p<0.05$) are symbolised, while $p>0.05$ is shown in grey. 'No data' values (white) are visible in Figure 6-5D and F where the NPP and ET algorithms did not calculate a value for the Ncora dam in S50E.

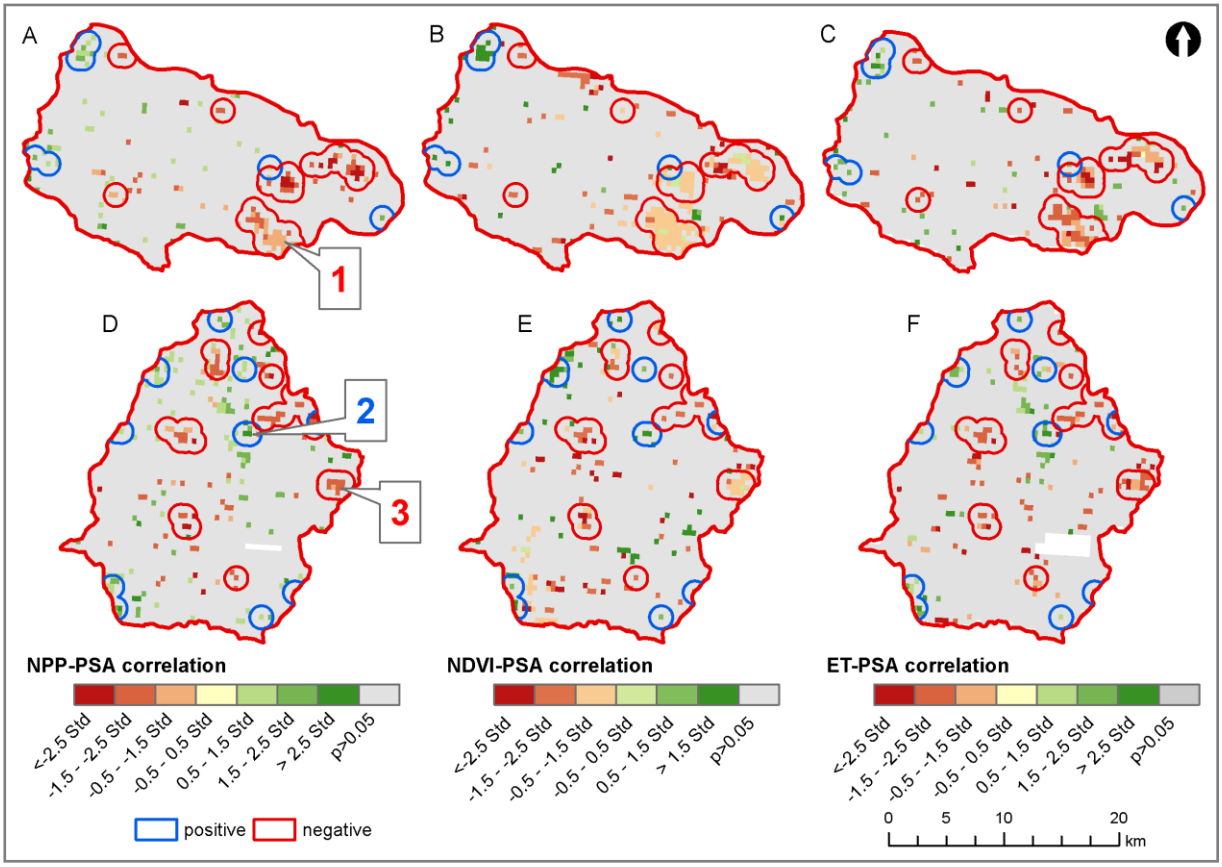

Figure 6-5 Spatial distribution of albedo correlation with NPP, NDVI and ET

Negative values (brown) show negative correlation where one variable increases as the other decreases. Positive values (green) show positive correlation where variables increase in parallel. Pixels where all three variables are significantly correlated with PSA, are highlighted with blue (+PSA+ET+NDVI+NPP or –PSA-ET-NDVI-NPP) and red (+PSA-ET-NDVI-NPP or -PSA+ET+NDVI+NPP) buffers to indicate the direction of the correlation.

Labels 1, 2 and 3 in Figure 6-5 indicate the spatial location of three points where pixel values were extracted to further illustrate the correlation between PSA, NPP, ET and NDVI at local scale, linked to specific land cover trajectories. Point 1 represents an area with high negative albedo trend (Figure 6-5A), in contrast to Point 3 with a high positive albedo trend (Figure 6-5B). Point 2 was selected as the middle ground with almost no trend (Figure 6-5B). In the case of Points 1 and 3, negative correlation was noted, while for Point 2 positive correlation was measured between PSA and NPP, ET and NDVI. It is important to note that each of the

variables (NPP, ET and NDVI) can show either positive or negative correlation with PSA at different spatial locations.

6.4.2 Land cover trajectories

Table 6-4 compares published albedo values to similar land covers as those found in the study area.

Table 6-4 Study area albedo values compared to literature

Land cover		S50E		T35B		Literature value
		Landsat	Mean MODIS	Landsat	Mean MODIS	
UG	grasslands	0.142	0.152	0.146	0.147	0.17 (Matthews et al. 2004)
FB	shrublands (indigenous & invasive trees & bushes)	0.113	0.133	0.138	0.144	0.17 (Matthews et al. 2004)
BR	bare	0.163	-	-	-	0.20–0.33 (Henderson-Sellers & Wilson 1983)
WB	water bodies	0.126	0.134	0.043	-	0.05–0.20 (Henderson-Sellers & Wilson 1983)
WL	wetlands	0.120	-	0.126	0.147	0.10-0.195 (Blok et al. 2011; Carrington, Gallimore & Kutzbach 2001)
CL	Croplands	0.146	0.155	0.163	0.154	0.163 (De Oliveira Faria et al. 2018)
FP	forest/plantation	0.105	0.117	0.113	0.124	0.11 (Matthews et al. 2004)
UB	urban, built-up	0.166	0.163	0.177	0.157	0.1 – 0.9 (Small 2005)

No persistent bare soil was observed in T35B, while the extent of bare soils and water bodies was too small to extract mean MODIS PSA. Similarly, in S50E, mean MODIS PSA could not be evaluated for bare soils and wetlands. In this study, UG refers to herbaceous vegetation (grassland, savannas and degraded grassland), while in other databases found in literature, such as the CORINNE database (Pérez-Hoyos, García-Haro & San-Miguel-Ayanz 2012), grassland may refer to greener pastures with a lower albedo value. Similarly, in the case of shrublands it is probable that the albedo measured by Matthews et al. (2004) are leafier and thus have a higher LAI and lower albedo than in this study area. Pérez-Hoyos, García-Haro & San-Miguel-Ayanz (2012) observed that class names used in land cover classification systems are often descriptive without providing detail on the criteria used to define these classes. Water bodies and croplands fall within the literature ranges, while forest/plantation lies within 0.01 of published values for this land cover class, although lower than reported by De Oliveira Faria et al. (2018).

Table 6-5 summarises significant PSA change (trend slope $p < 0.05$) and the percentage area per catchment occupied by persistent land cover classes and transition trajectory classes, measured using both MODIS and Landsat. Significant PSA change is divided into decrease in albedo (negative change) and increase in albedo (positive change), given both in percentage of catchment area as well as PSA change. PSA change is calculated as the trend slope multiplied

by the study period (15 years) to give the expected increase or decrease in PSA per land cover class or transition and is highlighted in light grey. Equally, the detail per land cover class is presented in supplementary material, Appendix D, Table D-2 and Table D-3.

Table 6-5 Total and significant change in land cover classes per catchment, reported in percentage of catchment and change in albedo [highlighted in light grey]

Study area	Total catchment				Significant change				Negative sig. change				Positive sig. change			
	% area		PSA change		% area		PSA change		% area		PSA change		% area		PSA change	
Land cover	MOD	*LS*	MOD	*LS*	MOD	*LS*	MOD	*LS*	MOD	*LS*	MOD	*LS*	MOD	*LS*	MOD	*LS*
T35B			−0.001	0.003	11.1	11.3	−0.013	0.004	7.9	4.3	−0.026	−0.039	3.2	7.0	0.019	0.031
P	82.7	81.0	−0.001	0.004	7.4	8.4	−0.011	0.007	5.0	2.8	−0.025	−0.039	2.4	5.6	0.018	0.03
T	17.6	17.8	−0.004	0.001	3.4	2.8	−0.017	−0.002	2.7	1.4	−0.027	−0.04	0.7	1.4	0.023	0.036
S50E			0.004	0.004	8.5	16.1	0.016	0.017	1.9	4.1	−0.018	−0.026	6.6	12.0	0.026	0.032
P	75.4	75.5	0.004	0.004	5.4	10.9	0.013	0.013	1.3	2.9	−0.023	−0.027	4.1	8.0	0.025	0.027
T	20.6	21.1	0.007	0.009	3.0	5.0	0.023	0.029	0.5	1.1	−0.020	−0.027	2.5	3.9	0.032	0.045

MOD=MODIS LS=Landsat P=Persistent classes T=Transition classes

As expected, with persistent classes comprising 82% of T35B, the mean change (MODIS, *Landsat*; −0.001, *0.004*) for these classes was similar to that of the entire catchment (−0.001, *0.003*). Significant change (9%, 10%) was noted with similar trend directions.

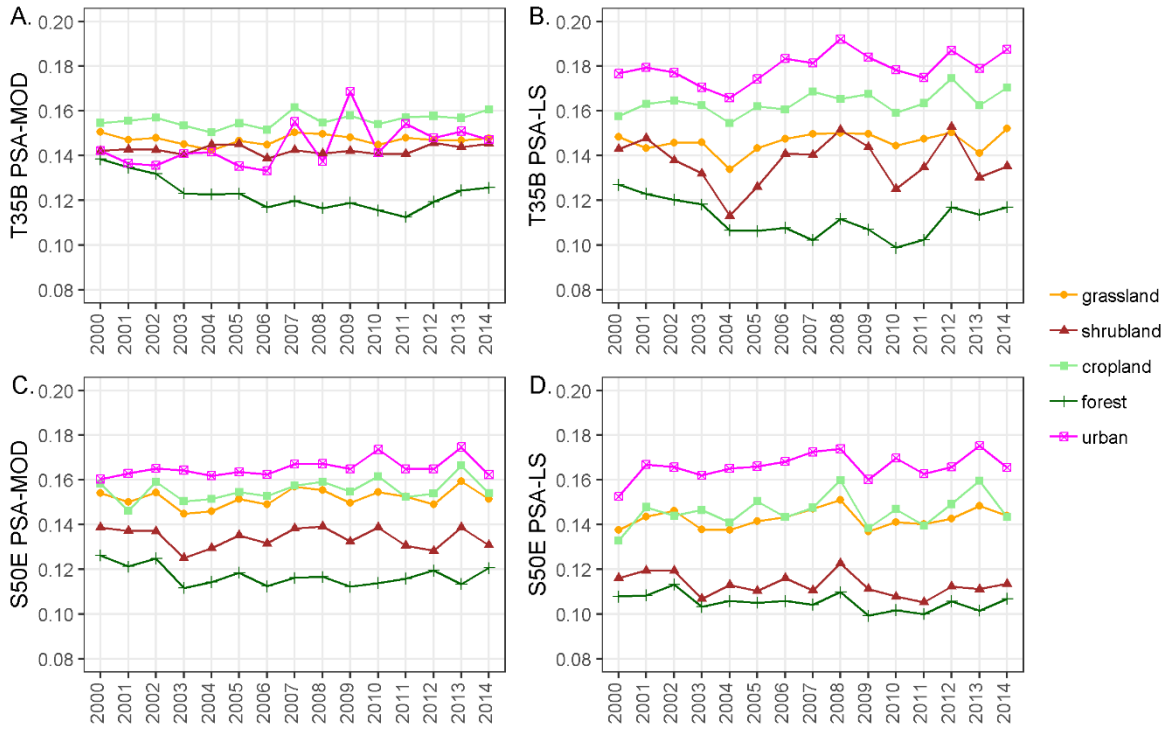

Figure 6-6 Peak season albedo (PSA) in persistent land cover classes over the study period

Negative trends amounted to a larger negative change to lower albedo values, however, the positive change measured with Landsat covered a larger area. For S50E, persistent classes covered 75% of the landscape with a mean change in PSA over the study period of 0.004

measured by both MODIS and Landsat. Although the area mapped as persistent is almost the same among the data sources, the area of significant change ($p<0.05$) is almost double when Landsat is used. Figure 6-6 illustrates the mean PSA for each persistent land cover class measured with MODIS and Landsat for T35B (A, C) and S50E (B, D) for the study period. In S50E, persistent urban land cover displayed the highest PSA, measured with either sensor (Figure 6-6C, D). In contrast, MODIS PSA in urban land cover (Figure 6-6A), showed an anomalous result for T35B owing to the fragmented nature of the urban class (n=3; Appendix D, Table D-2), representing only 0.1% (n=3) of the catchment area (Appendix D, Table D-2, D-3). The urban sites in this catchment have a longer history of human occupation, and are characterised by considerably more woody vegetation than rural villages in S50E that are under communal tenure arrangements. Shrubland in T35B shows an unexplained trough between 2002–2006 and 2009–2011 in Figure 6-6B. This could be related to variation in rainfall, IAP clearing activities and regrowth.

Transition classes (Table 6-1) account for 18% in T35B and 21% in S50E (Münch et al. 2017) at Landsat resolution. These transition classes measured with MODIS and *Landsat* respectively showed smaller changes in T35B (-0.004, *0.001*) compared to S50E (0.007, *0.009*). Total area of transition in T35B is almost 4% larger when measured with Landsat, while there is only 2% difference in S50E, implying more local scale and fragmented transition in T35B.

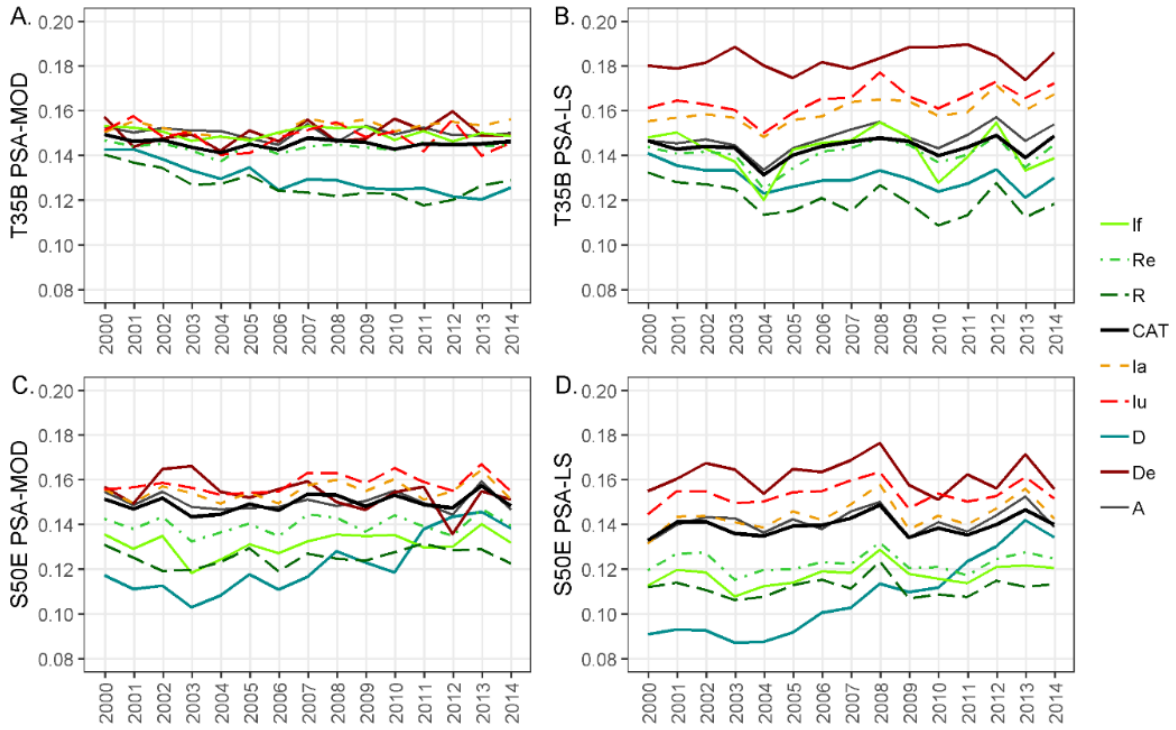

Figure 6-7 Peak season albedo (PSA) in transition classes over the study period [If-woody encroachment, Re-reclamation, R-afforestation, CAT-catchment average, Ia-increased cultivation, Iu-increased urban, D-deforestation, De-degradation, A-abandonment]

Between 2000 and 2014, gradual ecological change (woody encroachment, abandonment, degradation and reclamation) caused a positive significant increase in albedo for all Landsat-based classes (Supplementary material, Appendix D, Table D-2 and D-3), however, the affected area covers less than 2% of the two catchments.

In contrast, when MODIS data was used, only woody encroachment and reclamation caused increases in albedo. Therefore, it is clear that the detail of change in the landscape is not effectively captured using only MODIS data. Figure 6-7 illustrates the relationship between the transition classes and PSA from MODIS and Landsat compared with the catchment average PSA (black line). Degradation, urban intensification, increased cultivation and abandonment all have higher than catchment average PSA. These classes are all associated with increased bare surfaces with higher albedo. Increased cultivation also results in a higher albedo, due to clearing of existing vegetation to establish crops, the fraction of bare ground between standing rows or desiccation in fallow fields. In both catchments, the effect of degradation (De) is much larger when PSA is measured using Landsat, but the percentage is low (0.1% in both catchments). Deforestation (D) shows the expected increase in PSA in S50E, but not in T35B where it follows the afforestation (R) curve, possibly indicative of a classification error in the land cover products due to replanting of young trees.

6.4.3 Season-trend model

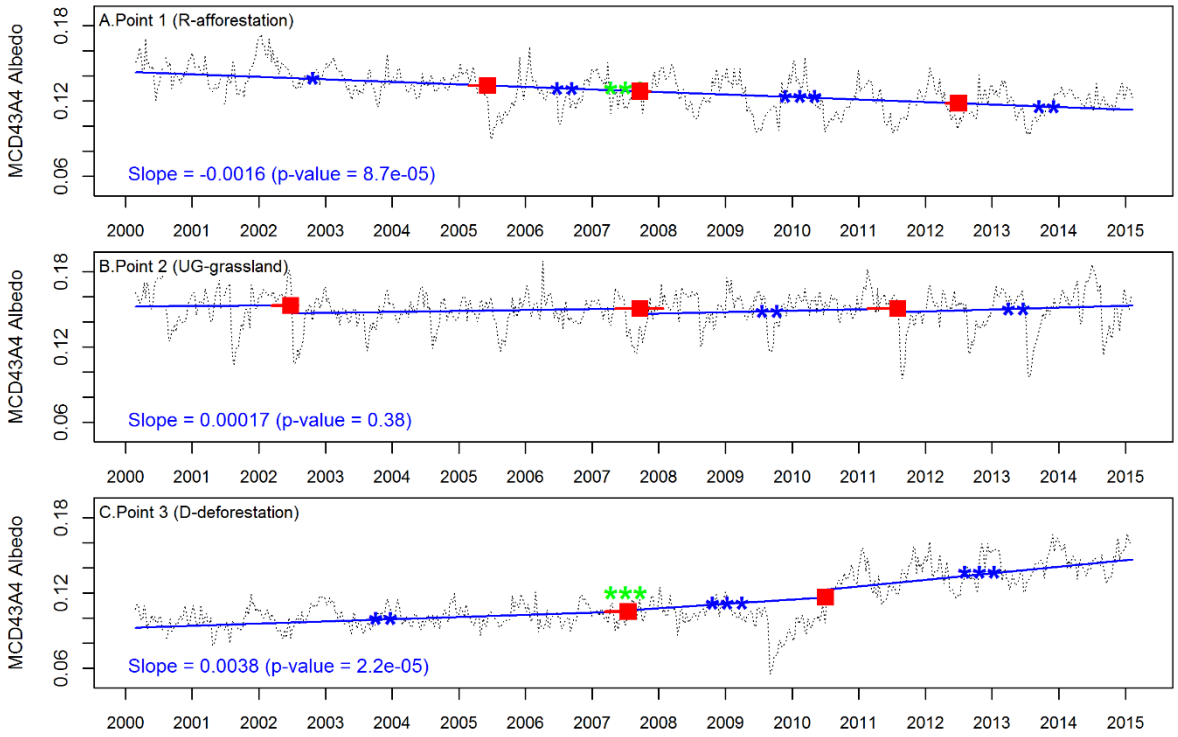

Figure 6-8 Estimated trends on three selected points decomposed using season-trend model (STM) in package greenbrown in R [Red squares indicate structural breaks, while blue and green stars indicate significance of trend segments]

The estimated trend and breakpoints from the deconstructed 8-day albedo time series using the STM method (Forkel et al. 2013), extracted for Points 1, 2 and 3 (Figure 6-5) are depicted in Figure 6-8. Significant structural breakpoints (95% CI) are indicated by red squares and horizontal red lines. The trend line on 8-day time series, between significant breaks, is added in blue. The significance of the trend line segments is indicated by blue stars to show the p-value (*** p<=0.001, ** p<=0.01, * p<=0.05). The slope and significance of the trend line on annual aggregate is added in blue text, with the p-value illustrated with green stars on the trend line.

Trend for Point 1, with persistent forest/plantation (FP) and trajectory afforestation (R^a), shows a significant overall decrease of albedo (p<=0.001 green *) with three significant breakpoints, each with significant trend (blue *). The overall slope indicates a small but significant negative change. Point 3 indicates the opposite trajectory with D^a (deforestation) resulting in an increase of albedo (p<=0.001). Two breakpoints are indicated with three significant segments (p<=0.01). Point 2 is an example of persistent grassland (UG) where the overall trend shows a very small, insignificant increase. Structural changes occurred at all three points in 2007.

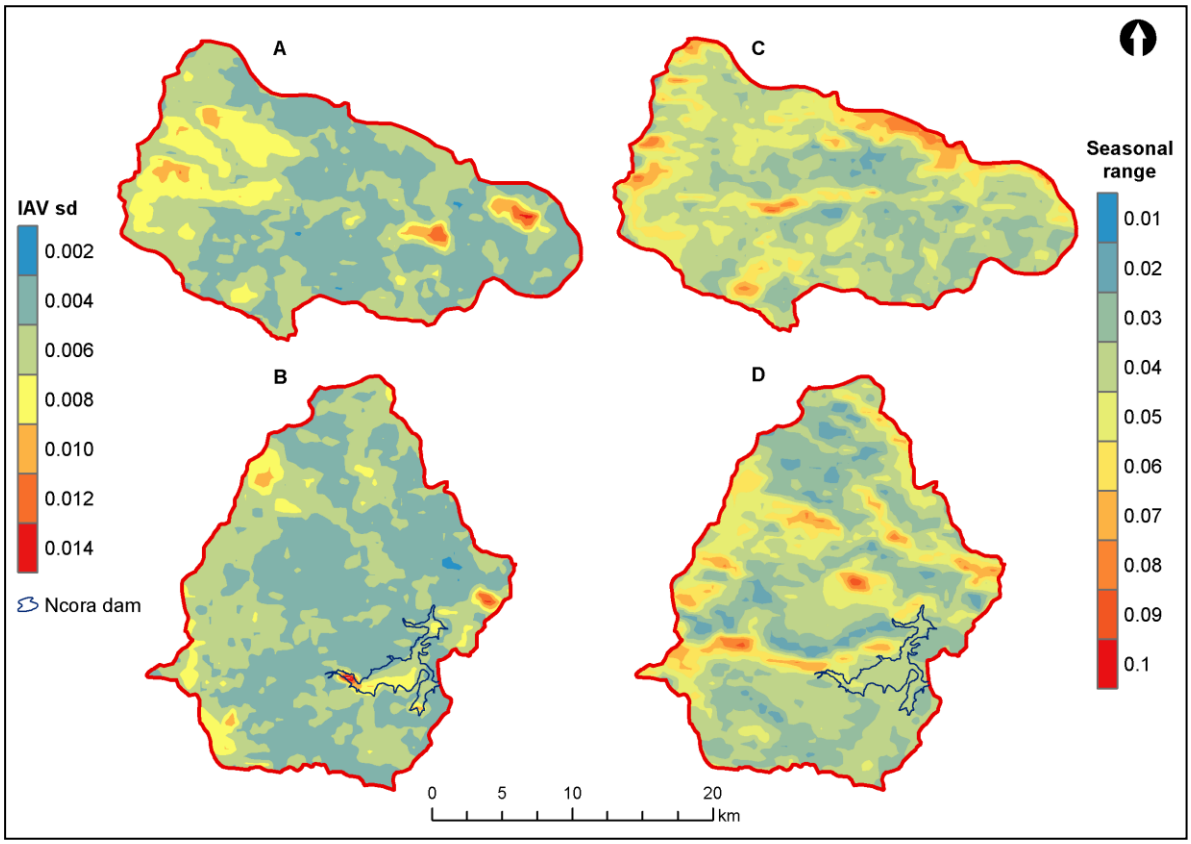

Figure 6-9 Inter-annual variability standard deviation (IAV sd) (A-T35B, B-S50E) and seasonal range (C-T35B, D-S50E) of albedo measured on all pixels from the 8-day MODIS product

Estimated IAV (annual anomalies) and seasonality (mean seasonal cycle) are shown in Figure 6-9 for all pixels in the catchments, not only those with significant change. In Figure 6-9, the IAV is shown in the left panel, while the seasonal range is shown in the right panel for T35B

(top; A, C) and S50E (bottom; B, D). Over the study period of 15 years, albedo in S50E fluctuated annually with a mean of 0.0041, very similar to the mean of 0.0045 in T35B. However, the IAV for the two catchments were found to be significantly different ($p<0.001$; Wilcoxon rank sum test). The highest frequency of pixels varied with standard deviations (sd) between 0.003 and 0.005. Similarly, the mean seasonal cycle in the two catchments — based on 8-day MODIS albedo values — are significantly different ($p<0.001$; Mann-Whitney U test for non-parametric data). The albedo can vary between 0.01 and 0.08. Distinct spatial patterns are noted in the maps in Figure 6-9.

6.4.4 Modelling ET and NPP

In Table 6-6, the area percentage for modelled persistent land cover classes in 2030 are compared with the size of these land cover classes in 2014. Table 6-6 also includes the net change, as well as the mean trend calculated from MODIS. Based on the mean MODIS PSA change and relationships with NPP and ET, three scenarios for future NEE and water use were calculated: (1) lower mean albedo indicating proliferation of woody vegetation; (2) mean albedo, the status quo persists; and (3) higher mean albedo, with conversion to agriculture and urban intensification dominating future transitions.

Table 6-6 Modelled net ecosystem carbon exchange (NEE) and water use for persistent land cover classes in S50E (bold) and T35B (italics)

Land cover class		**UG (grassland)**		**FB (woody encroachment)**		**CL (croplands)**		**FP (forest/plantation)**		**UB (urban)**	
Catchment		*T35B*	S50E	*T35B*	S50E	*T35B*	S50E	*T35B*	S50E	*T35B*	S50E
% area 2014		*79.9*	56.9	*4.0*	10.5	*6.2*	18.2	*8.3*	1.8	*0.2*	9.5
% area 2030		*79.7*	52.1	*3.1*	9.9	*6*	20.0	*9.8*	0.7	*0.2*	14.4
Net %change		*-0.2*	-4.8	*-0.9*	-0.6	*-0.2*	1.7	*1.5*	-1.1	*0*	4.9
PSA trend		*†*	†	*	*	*†*	††	***	**	**	††
%Persistence		*72.7*	44.7	*0.4*	5.5	*4.3*	15.0	*6.8*	0.4	*0.1*	8.5
NEE (10^3 kg C)	2014	*2027*	1633	*53*	213	*138*	408	*206*	71	*2*	129
	High	*2021*	1323	*12*	181	*124*	392	*238*	17	*2*	236
	Med	*2690*	1739	*17*	237	*169*	521	*292*	21	*2*	316
	Low	*4605*	2832	*28*	383	*291*	843	*358*	23	*4*	518
ET (10^3 m^3)	2014	*1437*	1182	*36*	156	*96*	303	*127*	37	*1*	94
	High	*1403*	855	*8*	122	*85*	263	*144*	10	*1*	152
	Med	*1520*	1007	*9*	140	*93*	316	*170*	12	*1*	185
	Low	*1714*	1163	*10*	160	*105*	378	*190*	14	*1*	219

Negative trend= *** <-0.0005 ** <-0.0002 * <-0.0000 Positive trend=† >0.0000 †† >0.0002 ††† >0.0005

In the higher albedo scenario, the total modelled NEE in 2030 for persistent classes in T35B could reduce by 1% when compared with 2014. Should a low albedo scenario ensue, an increase of more than 80% could be obtained with a catchment mean of 3.2×10^6 kg C based on the

mean time series NPP. Similarly, water use could decrease by almost 3% or increase by up to 19% for persistent classes. In T35B, the total change (gain and loss) in the landscape over all land cover classes was 15.5% for modelled period 2014 to 2030 (Gibson et al. 2018), compared with 18.2% for the period between 2000 and 2014 (Münch et al. 2017). Trajectory labels indicating gradual and abrupt changes are responsible for the difference between persistence and the total modelled NEE and water use in the catchment. Trajectories abandonment, reclamation and degradation increase grasslands, woody encroachment boosts shrublands, increased cultivation, afforestation and urban expansion respectively, result in higher croplands, forest/plantation and urban. Afforestation was the strongest modelled trajectory in T35B showing a net gain of 1.5% and a strong negative albedo trend. These changes could produce an additional 0.5–1.1 × 10^6 kg C and 0.3–0.4 Mm^3 ET.

For S50E, the total change over all land cover classes was 23% for the same modelled period (Gibson et al. 2018). By comparison, the period between 2000 and 2014 exhibited 21% change (Münch et al. 2017), assuming a similar map accuracy for the modelled map. The modelled NEE for persistent classes varies between 2.1 and 4.6 × 10^6 kg C, with modelled water use varying between 1.4 and 1.9 Mm^3. In 2014, these values were 2.5 × 10^6 kg C and 1.8 Mm^3 respectively (Table 6-6). Changes to the landscape could account for NEE of 0.7–1.6 × 10^6 kg C and water use of 0.5–0.7 Mm^3. The expected scenario for S50E is increased PSA due to intensification of agriculture, lower NEE and water use, depending on which land cover class is replaced.

6.5 DISCUSSION

6.5.1 Land cover change and trend analysis

Land use and land cover change in the selected catchments have affected ecosystem services provided by land cover classes, particularly grasslands. Although land use patterns are characterised by relatively high persistence (Figure 6-1), it is clear that human activities are having an increasing impact on the size of the rangelands and consequently, the productivity of the landscape. The availability of dense time series satellite images enables degradation to be assessed not merely in terms of land cover change vectors but with more sophistication through identifying trends or catastrophic changes across the time series. As was shown in this study, land cover change analysis using only categorical land cover maps can neither identify a decline in the productivity of grasslands nor minor intrusions of shrubs and woody vegetation into the landscape. However, transitions can be identified and from analysing time series data in these

transition classes, from which a more nuanced understanding of long-term changes can be gained.

The results have shown that important transitions that have occurred from 2000 to 2014 (Münch et al. 2017) are likely to continue into the future (Gibson et al. 2018) with alien invasion, afforestation, rehabilitation, and increased livestock production identified as factors that could affect water use and carbon storage either positively or negatively. Analysis of the characteristics of albedo trends, linked to catchments and land cover change trajectories, provide a deeper understanding of how these changes may influence NPP and ET, precursors to future carbon storage and water use potential in the carbon-water nexus.

Despite being actively targeted in many of the transitions in the catchment, grassland (UG) remains the dominant cover, and has the greatest effect on the catchment albedo, remaining constant over the study period (Figure 6-6). As LAI and fPAR measured for shrubland (Figure 6-6 and If in Figure 6-7) and croplands (Figure 6-6) in the catchments (Palmer et al. 2017) are higher than that measured for grassland, conversion would result in a potential gain in carbon storage (NEE), but a higher water demand by vegetation. When considering mean Landsat and MODIS albedo values (Table 6-4), conversion from shrubland presenting a lower mean albedo than grassland, should cause a gradual decrease in albedo of ~0.03 (Table 6-4). Contrary to expectation, the grassland to cropland transition shows an increase in albedo. This reason for the increase is two-fold: (1) the land tenure system, where farming is interspersed with rural housing gives rise to an increase in degraded surfaces with associated higher albedo, and (2) due to lower rainfall, agricultural production decreases with dry bare soil for parts of the year post-harvest increasing the mean albedo for this class. These factors result in higher inter-annual variation (Figure 6-7). Continuous grazing by livestock also contributes to rangeland degradation and increase of albedo due to reduction in the basal cover of herbaceous plants (mainly grasses) (Bennett, Palmer & Blackett 2012). Urban expansion and intensification increased the albedo when natural woody areas were replaced by housing.

Similar spatial patterns of PSA were observed when comparing mean MODIS PSA with Landsat PSA (Figure 6-3), although the values differ significantly ($p < 0.05$). It was noted that the coarser MODIS resolution causes spatial smoothing that masks the detail captured at higher Landsat resolution, especially for small fragmented land cover classes, where coarse pixels with mixed land cover classes will be dominated by greener vegetation (Zhang et al. 2017). The spatial smoothing may then in turn result in misleading temporal patterns when analysing the MODIS derived data. On the other hand, although Landsat has superior spatial resolution and despite the long record of the freely available Landsat data archives (Hansen & Loveland 2012),

MODIS offers a higher temporal resolution lending itself to a more dense time series and, as a result, a more detailed temporal analysis.

As a consequence of lower temporal frequency, calculation of PSA using Landsat can become problematic when limited cloud-free images are available for the growing season. For example, a lower mean albedo may be calculated, from which could be concluded that more carbon can be sequestered than may happen in reality, and thus translating into higher expected water use. Forkel et al. (2013) demonstrated that the performance of trend estimation methods decreased with increasing inter-annual variability. Zhai et al. (2015) recommended reducing seasonal variation by using PSA. Seasonal effects on the time series analysis are illustrated by high inter-annual variability (Figure 6-9) at, for example the Ncora dam inflow, the perennial Nququ River in the west and the Tsomo River in the north of S50E and the confluence of Pot and Little Pot Rivers in T35B. The range of the seasonal cycle (Figure 6-9) was largest in areas of steep slope (>25%), usually classified as persistent grassland. Therefore, the use of PSA rather than full time series albedo would reduce overall time series variation and likely increase the performance of trend estimations.

The main land cover change trajectories recorded in the catchments are reflected in the measured NDVI, NPP and ET patterns. Changes in carbon storage and water use can be related to: (1) alien invasion and afforestation that decrease albedo but increase water use and carbon storage and (2) livestock production that increases water use, but could result in grassland degradation with increased albedo, and rehabilitation (reclamation) that reduces water use and carbon storage. Given the reliance of NPP, ET and NDVI on water availability, as expected these MODIS calculated variables displayed a positive correlation with rainfall (as rainfall increased, each of these variables increased). Confirming this reliance on precipitation, lower NPP, ET and NDVI were measured in 2003 when lowest rainfall was recorded. Similarly, 2006 stands out as a year with high rainfall and high NPP and ET in both catchments, although NDVI did not increase significantly (Figure 6-4). However, a weak negative trend across the period of study was detected as less rainfall over time was recorded. S50E, the catchment under dualistic land tenure, was more affected by the low rainfall, with lower NPP, ET and NDVI (Figure 6-4).

6.5.2 Catchment differences

Correlation analysis between PSA and the variables NPP, ET and NDVI at catchment scale (Table 6-3), showed similar trends with negative correlations between PSA and NDVI, and PSA and ET. A positive correlation was determined between PSA and NPP in T35B, but with

no significance in S50E. However, significant positive correlations were recorded between ET and NDVI in all persistent land cover classes and transitions, namely greener vegetation associated with higher water use (supplementary material, Appendix D, Table D-1). Intensification of wooded areas revealed different patterns in the two catchments, where the increase of woody biomass should increase NPP and ET, while albedo decreases. Transition trajectories that describe conversions from multiple land cover classes, such as deforestation (removal of forest to be replaced by other land cover) or afforestation (gradual ecological change to plantations from either grassland or previously wooded areas) encapsulates opposing trajectories, which may affect the correlation results especially in transition classes smaller than the MODIS footprint. The results of transition correlations may also be confounded by the difference in resolution of land cover data and biophysical parameters. This illustrates the effect of scale on spatial analysis, where the size, shape and placement of arbitrary aggregation units, such as categorical land cover maps may lead to incorrect interpretation of results in heterogeneous landscapes (Comber et al. 2016; Estes et al. 2018).

In T35B, the commercial agriculture catchment, intensification of woody invaders in the upper reaches of the Pot River and Little Pot River is offset by reclamation to grassland (possibly degraded) in the lower reaches (Figure 6-1). The transition from shrubland to grassland is expected to increase albedo in this catchment based on mean MODIS and Landsat values extracted (Table 6-4). However, persistence of shrubland may be accompanied by densification of woody vegetation, which would not be noticed in the land cover change analysis as the land cover class remains constant. While afforestation (R in Figure 6-7) is the strongest trajectory in T35B, conversion to forest/plantation from all other classes will result in lowering of albedo. It is likely that the decrease in surface albedo could result in an increase in the absorption of energy, leading to higher temperatures (Rotenberg & Yakir 2010). Higher NPP was noted for T35B than in the dualistic catchment S50E, with declining patterns of NPP observed in both catchments (Figure 6-4). However, mean MODIS albedo trend decreased, with Landsat showing a positive increasing trend in PSA (Table 6-5).

The net carbon storage for persistent classes in 2014, modelled from mean NPP values, was 3.2×10^6 kg C, giving a higher carbon value than extracted directly from the MODIS product for 2014. This leads to the conclusion that using the time series mean for modelled values may overestimate the NEE (and ET) in 2030. Although land cover change modelling predicted an increase in commercial forestry, with associated increase in NPP, grassland is still the largest land cover class, contributing less to catchment carbon sequestration. In 2030, the expected carbon storage based on 2014 figures would, therefore, be no higher and could even decrease.

However, using mean MODIS NPP values, an increase of 30% in NEE was modelled. Water use in the catchment is expected to vary between −3% and +19% with water use efficiency (WUE) remaining constant at approximately 1.5 kg.m^{-3}.

For S50E a positive albedo change trend over the 2000–2014 study period was observed (Table 6-5). When considering a scenario where mean albedo prevails and the positive trend does not continue, net carbon storage for persistent classes could increase by 15% to 2.88 x10^{6} kg C by 2030 based on land cover change. However, a more likely scenario is an increase in albedo due to degradation and decrease of grasslands, intensification of agriculture and urbanisation resulting in a decrease of 12% in modelled NEE, mirroring the decline in NPP over the period of the study (Figure 6-4E). In 2014, 1.8 Mm^3 of water was used by persistent classes in S50E recorded as ET, resulting in WUE of 1.4 kg.m^{-3}. Total catchment ET for persistent classes could decrease by 6% in 2030 based on mean time series ET values, and may reduce to as low as 1.4 Mm^3, resulting in a reduction of 21%. However, should albedo decrease, ET could increase by 9% in persistent land cover classes.

6.5.3 Implications

Land cover change brought about by woody encroachment of grassland and in particular the densification of existing patches (Gouws & Shackleton 2019; Gwate et al. 2016) will typically alter carbon sequestration and cycling (Hughes et al. 2006; Oelofse et al. 2016). Although technically regarded as a degradation gradient in the landscape (Münch et al. 2017) due to the effect on biodiversity and ecosystem services, this land cover change (woody encroachment and densification) can potentially act as a carbon sink (Oelofse et al. 2016) due to an increase in woody biomass (Scholes & Archer 1997). Invasion of grassland by IAPs can also reduce productivity due to a loss of rangeland productivity for livestock production. *Acacia* spp. are effective in utilising available resources more efficiently and may therefore outcompete native species by altering local conditions (Lorenzo et al. 2016; Rodríguez-Echeverría et al. 2013; Sholto-Douglas et al. 2017). However, the value and use of IAPs as an ecosystem service is reducing in the study areas due to increased rural–urban migration and the increase in the number of households supplied with electricity (Ngorima & Shackleton 2019). The cost of IAPs in the study areas will soon outweigh the benefits, resulting in a net negative trade-off. Gouws & Shackleton (2019) suggested that IAP invasion would continue to increase in the Eastern Cape unless deliberate land management intervention takes place. This has implications for national-scale invasion management strategies such as the Working for Water programme in South Africa (Van Wilgen & Richardson 2014). Though grasslands are predicted to decrease

in favour of woody invasive plant species and cultivated land, this study predicted a decrease of 12% and 6% respectively in net carbon storage and water use by vegetation. This is in contrast to expectation where previous studies (Palmer et al. 2017), measuring LAI and fPAR, indicated that woody encroachment would represent a gain in both catchment net ecosystem carbon exchange and evapotranspiration.

The novelty of this study lies in the application of dense time series analysis of 15 years of data on surface energy balance, water and carbon sequestration parameters for catchments under two different land management regimes. The study uses previous land cover change and future scenario analyses, combined with the season-trend model output to quantify carbon sequestration and water use, both for areas of no change (persistent classes) and areas that have transitioned from one land cover to another. The release of satellite image archives and the possibility of online bulk processing through platforms such as Google Earth Engine are allowing more subtle yet refined analyses of land cover changes. Not only can the changes themselves be quantified in terms of categorical land cover maps, but persistence and transition between and within classes has become possible.

Analysing remotely sensed data products such as albedo, NPP and ET can lead to a better understanding of trends in the functioning of catchments generally and rangelands specifically. Declining trends, as seen in albedo, NPP and ET (Figure 6-4) may be caused by regional climate trends. Information from multiple sources, both quality and type, can contribute to an enhanced understanding of degradation in rangeland productivity (Eddy et al. 2017), relating degradation to the impact of climate versus land management by investigating dual catchments with similar climate regimes but clearly different management practices (Eddy et al. 2017). Quantifying the changes in these biophysical parameters can assist scientists and managers in addressing the global challenges of our times.

6.6 CONCLUSIONS

It was found that the spatial and temporal characteristics of the different sensors are useful for highlighting differing aspects of change in the study area: Landsat's resolution is well suited for highlighting spatial change, but MODIS temporal resolution is ideal for a complete long-term dense time series. The presence of many small and fragmented land cover classes in these catchments suggest that analysis of albedo, NPP and ET derived from satellite data with similar resolution would be ideal. Further research is recommended to explore the use of higher resolution satellite data to effectively model carbon storage and water use. The Google Earth Engine platform provides shared geoprocessing algorithms (Gorelick et al. 2017) and access to

long-term data (Hansen & Loveland 2012), that can be used to generate detailed maps (Forkel et al. 2013) to model future scenarios.

Furthermore, the advent of new sensors, such as the European Space Agency's Sentinel-2 satellites, with 5-day revisit time and up to 10 m spatial resolution, may provide a better alternative for time-series analysis. In particular, the red-edge bands will allow determination of rangeland quality (Ramoelo et al. 2015). However, since Sentinel-2B was only launched in March 2017, it will take time before this data can be used for long-term studies. In the meantime, taking an ensemble approach with Landsat and MODIS allows for the benefits of each sensor to be exploited.

Based on trend analysis, the study revealed little change in catchment mean albedo at the time of peak vegetative growth. This implies little to no change in either carbon capture potential or WUE of each catchment at the peak of the growing season. However, since inter-annual variation can affect the accurate calculation of trends (Forkel et al. 2013), the PSA was used to minimise these effects in this study.

As expected, a strong positive correlation between ET and NDVI was found, as greener vegetation is associated with higher water consumption and a decrease in albedo is correlated with an increase in ET and NDVI. Some transitions, however, include opposing albedo change vectors, confounding correlation analysis between these variables. Consequently, it is recommended that separate transition classes be analysed for opposing vectors.

Although the comparison of ET in grassland performed by Gwate et al. (2018) found lower values prior to 2003, this may be ascribed to the different method used to extract values from land cover maps with potential uncertainty, especially for grassland, a large dormant class. This confirms the importance of accurate land cover maps for modelling (Estes et al. 2018) as the reliability of downstream analyses can be impacted with substantial risk of error magnification (Scholes & Archer 1997).

It is probable that a decrease in precipitation leads to desiccation of vegetation and soil, thus resulting in a higher albedo. The cause and effect of a positive correlation between PSA and rainfall (increased PSA with increased rainfall as seen in 2006–2007) is yet to be established and it may be that, at local scale, increased albedo is driving a decrease in rainfall, as suggested by Doughty, Loarie & Field (2012) and Loarie et al. (2011).

Finally, predicted land cover for the year 2030 was used to postulate consequences of the change on catchment water and carbon fluxes. The expected decrease in net carbon storage and

water use by vegetation confirms recommendations for land and water resources management interventions in catchments under dualistic farming systems (Chapter 5), such as S50E.

Accurate land cover classes and change trajectories are required to successfully model scenarios for future land cover change that may affect ecosystem services. Even though map errors in land cover maps affect the understanding of socioeconomic and environmental patterns and processes in landscapes, such maps remain an essential resource in describing and quantifying such processes (Estes et al. 2018). Higher quality input datasets would provide higher confidence levels in the overall observed change. A large dominant class, such as grasslands, may be easier to classify and exhibit smaller errors than highly fragmented classes, such as woody outcrops (FB) or wetlands (WL) due to spatial and temporal autocorrelation (Congalton 2001; Pontius & Lippitt 2006). This research has demonstrated that albedo can be an effective parameter for the detection of environmental change. Albedo could be considered a proxy for land cover and land cover change in studies investigating ecosystems services, capturing changes in productivity.

This concludes the reporting of the empirical results of this dissertation. The next chapter provides a summary and reflective restatement of the research.

CHAPTER 7: SYNOPSIS — Emva kwe dywabasi

As part of project "Emva kwe dywabasi[9]", this study set out to demonstrate how land cover change, in particular, encroachment by woody vegetation, impacts landscape function delivered by grasslands in the Eastern Cape. Land cover change has arguably the greatest effect on climate change and landscape function globally and is triggered primarily by anthropogenic land use change. As a result, land use and land cover change affect biophysical characteristics at the earth's surface and can be measured using remote sensing. Woody encroachment into the grasslands of the Eastern Cape of South Africa have been a threat to the function and productivity of rangelands and is threatening rural livelihoods, exacerbated by rising CO_2 levels associated with climate change.

In this study, systematic land cover change analysis and future modelling were performed to determine land cover change trajectories and flows in the landscape. Trends in remote sensing-derived biophysical variables were analysed to determine how land cover change would affect the surface energy budget and the carbon cycle, providing local communities with a better understanding of future water use and rangeland productivity. This research sought to address the following research questions:

How accurately can transformations in land cover be quantified using existing datasets?

How does the pattern of error in land cover change datasets affect modelling of evapotranspiration and carbon storage?

How do trends in biophysical drivers and characteristics of land cover change trajectories differ from one region to another?

How can ecosystem stress be characterised using Earth observation data and time series analysis?

Four main objectives were set to address these questions. These objectives were addressed in Chapters 3 to 6 (Figure 1-1). Each chapter has been written as a freestanding article and the main findings from the particular experiment were summarised within the respective chapters, titled:

- Chapter 3: Characterising degradation gradients through land cover change analysis;
- Chapter 4: Global and local patterns of landscape change;
- Chapter 5: Accuracy of modelled future land cover; and

[9] After the wattle in isiXhosa (Section 1.7)

- Chapter 6: Monitoring effects of land cover change on biophysical drivers in rangelands using albedo.

The next section provides a synthesis of the research findings in response to each of the research questions, followed by the contribution of this research to knowledge. This leads to a discussion on the study limitations and recommendations for future research, before making some concluding remarks.

7.1 SYNTHESIS OF FINDINGS IN RESPONSE TO RESEARCH QUESTIONS

Change in land cover were detected for different combinations of periods from four time steps (1990, 2000, 2014 and 2030) and over three quaternary catchments (S50E, T12A and T35B) under different land tenure systems (bilateral and freehold). Existing land cover datasets (1990, 2000), modified (2000) and newly generated products (2014, 2030) were used for the analyses. The following subsections reflect on each of the research questions and critically evaluate to what extent this research has addressed each.

7.1.1 How accurately can transformations in land cover be quantified using existing datasets?

Concentrating on Objectives 1[10] and 2[11], Chapter 3 (Münch et al. 2017) described the land cover classification and subsequent change analysis performed for three grassland-dominated quaternary catchments (S50E, T12A and T35B) in rural Eastern Cape, South Africa. Data from two time steps (2000 and 2014) were selected to characterise land cover, namely (1) existing land cover data for 2000 and (2) land cover map for 2014 generated using object-based image analysis (Chapter 3). Grappling with Objectives 1[10] and 3[12], Chapter 4 explored the quantitative frameworks of intensity analysis and the change/disagreement budget to describe land cover change analysis in S50E for two periods: (1) 1990-2000, by introducing an existing dataset from 1990; and (2) 2000-2014, by using the same datasets as in Chapter 3. The square contingency table (confusion matrix or transition matrix) is at the centre of these analyses, from which statistics about classification accuracy and land cover change were calculated.

Theoretical accuracy of a land cover change map was computed as the product of the input map accuracies. Theoretical accuracies for the land cover change maps varied between 56% and 76% (Chapter 3, Table A-3; Chapter 4, Discussion). If change maps with reliability higher than 75% were required, the map accuracies for input land cover datasets would have to be improved

[10]Perform systematic land cover change analyses on existing data products using LC conversion labels and intensity analysis.
[11]Characterise spatial patterns of land change dynamics using LC conversion labels to represent and interpret transitions.
[12] Apply quantitative techniques of intensity analysis to describe and interpret patterns of land change.

to ~99% (Chapter 3). Achieving these levels of accuracies at Landsat resolution is unlikely, suggesting that some uncertainty in both the classification results and the change results must be accepted.

Land cover change detection was performed by image overlay using a transition matrix for change analysis. Four different scenarios of location of map error were considered, specifically, (1) randomly distributed error; (2) error that can occur at all places; (3) error that exists only in places that match; and (4) error that exists only in places that differ. Land cover change ranging from 18–42% was computed. A change of 19% was calculated from direct overlay of land cover maps with 30 m resolution pixels, assuming random error (Chapter 3). Furthermore, the intensity analysis framework (Chapter 4) was used to analyse land cover change in maps at interval, category and transition level, by comparing change intensity (rate of change per year) with uniform or random change. The land cover change was then characterised as persistence, gain or loss at each level and important transitions were identified.

Hypothetical error that could account for land cover change was computed by comparing the observed change intensity with random change (Chapter 4). Larger values for hypothetical error are indicative of probable map error. Land cover class transitions with highest hypothetical error were identified. As expected, land cover classes Bare Soil (BRS) and Wetlands (Wl) showed the highest hypothetical error (Chapter 4) in the change analysis. These classes were also highlighted in Chapter 3 as having poor user's and producer's accuracies during land cover classification. Woody plant encroachment (FITBs) showed a high commission error in both size and intensity for 1990–2000 analysis, likely due to map error in the 2000 dataset (Chapter 4). Land cover change was also deconstructed into a change budget of quantity, exchange and shift disagreement from the transition matrix. Despite the ease of understanding, these results obtained from the transition matrix are not spatially explicit.

By performing hierarchical multi-resolution spatial aggregation, it could be demonstrated that at coarser resolutions, exchange and shift disagreement disappeared, while quantity disagreement could provide a realistic value for the total change in the landscape. This result could be attributed to land cover classes that changed position at the finest resolution. In sensitivity analyses of detected change, Pontius & Lippitt (2006) found that about half of the observed difference over time could be explained by error. This finding was supported by the allocation change intensity of greater than 50% computed for the two periods (Chapter 4).

To gain a clearer understanding of the location of hypothetical error, Chapter 4 described how the change budget could also be computed at local scale by constructing a geographically

weighted transition matrix. Spatially explicit probabilities of error per land cover class were constructed by combining components of the intensity analysis framework with local correspondence matrices. The overall allocation difference maps highlighted hotspots of change and probable error for further investigation (Chapter 4), leading to the conclusion that the suggested combination of global and especially local analyses from the transition matrix, should be used to accurately quantify map error in existing land cover datasets.

Results from Chapter 3 and 4 indicated that map error in input land cover classification datasets had the greatest effect on the accuracy of measured land cover change. Lack of adequate reference data or imperfect reporting of accuracy results affect the explanations of the processes depicted in land cover change maps. By implementing a change budget, quantity disagreement could be used as a reliable measure of minimum change in the landscape, which would be valid at multiple scales. Change budget maps produced from geographically weighted contingency tables could be used to provide spatial context to map error.

7.1.2 How do trends in biophysical drivers and characteristics of land cover change trajectories differ from one region to another?

7.1.2.1 Spatial patterns of land change dynamics

The study followed two different approaches in understanding land cover change dynamics. Firstly, an indicator approach was designed based on process flows in the landscape; and secondly, direct transitions between land cover classes from time step 1 and time step 2 were compared with each other, analysed using the intensity analysis framework and change budget.

Seven main flows or trajectories were identified in the landscape. *Persistence* generally dominates the landscape and can be described as areas where no land cover change has been measured. *Intensification* represents the transition of a lower intensity to a higher intensity usage, such as transitions from grassland to woody vegetation or agriculture. Clearance or planting of trees, with particular reference to plantations, were characterised respectively as *deforestation* and *afforestation*. In areas where higher intensity usage was converted to a lower intensity usage, such as degradation of grasslands or reclamation where woody encroachment was cleared or has disappeared, the flow was described as *extensification*. The term *natural dynamics* was used to represent seasonal conversions. *Exceptionality* describes improbable land cover conversions that could not exist in reality and could potentially be used to identify classification errors.

Land cover change labels, developed to identify landscape change trajectories, were assigned to each intersection of the land cover maps at the two time steps. These land cover labels provide a thematic representation of the spatial distribution of change and simplify understanding of the processes involved (Chapter 3). Sub-models for future land change modelling (Chapter 5) were subsequently developed using these land cover labels. However, for some of these land cover labels, opposing albedo change directions were found under the same label (Chapter 6), which may have had a confounding effect on the results. Some of the trajectory labels defined transitions from multiple land covers to a single land cover, or to multiple land covers with different characteristics (Chapter 6). Nonetheless, homogenous landscape units associated with clearly identified persistent trajectories were used to characterise water use and carbon fluxes for sustained landscape health from remote sensing products (Chapter 6).

While land cover patterns were characterised by high persistence (77%) in all three catchments, the landscape trajectories classified as rangeland degradation, woody encroachment, urbanisation, increased dryland cultivation and commercial afforestation were identified as drivers of landscape modification affecting landscape function. Considering that the class describing woody encroachment (FITBs) contained a large variety of vegetation types, including indigenous forest, thicket, bushland, bush clumps, high fynbos and alien plants that are spectrally similar and could not be separated using Landsat imagery, it is not surprising that this class demonstrated a low producer's accuracy (Chapter 3) and high hypothetical map error (Chapter 4). Despite the uncertainty associated with this transition, persistence and intensification of wooded areas, by native or invasive species, were recognised as a degradation gradient within the landscape, amounting to almost 10% of the study area. The presence of invasive alien plants, included in the Woody encroachment class, is known to affect biodiversity and landscape function (Chapter 3).

Urban intensification was measured in the catchments where subsistence farming is practised (S50E and T12A) with expansion around existing villages (Chapter 3). In contrast, no urban intensification was measured in the commercial catchment T35B. However, commercial agriculture (4% of study extent) emerged as increased productivity of the landscape, with land use intensification associated with a productivity-driven landscape (Chapter 3). Notwithstanding, net carbon storage in the catchment, measured by the MODIS net primary production product, did not increase significantly between 2000 and 2014 (Chapter 6).

Due to the ongoing work of Working for Water in the area, and grassland rehabilitation plans for the project at large, the study placed a great emphasis on reclamation. However, less than three per cent reclamation was noted in T12A and S50E, the catchments under bilateral tenure.

In contrast, in T35B, freehold tenure, the six per cent of woody encroachment returned to grassland, was partly attributed to the low accuracy of the land cover change map (Chapter 3).

The intensity analysis framework is commonly used to describe categorical changes between two datasets, summarised in a square contingency table. Though the total change in area constituted approximately 20% of the S50E catchment, the change intensity over the ten-year period from 1990-2000 was reported as faster than uniform at interval level. A four per cent hypothetical commission error was computed implying that change was mapped, while the hypothesis suggested persistence. Conversely, observed change was slower than uniform during 2000-2014, with the implication that some change was omitted. At interval and category level, the computed hypothetical map error pointed to an unusual amount of error associated with the 2000 land cover dataset (Chapter 4). Partitioning the change budget into quantity, exchange and shift intensities indicated that 46% of change for 1990–2000 could be assigned to change in quantity, while for 2000–2014 only 38% of change was associated with quantity. This was is in agreement with the findings in Chapter 3. Error due to change in location of classes amounted to almost 10% of the total area of change for 2000–2014 (Chapter 4).

7.1.2.2 Trends in biophysical drivers

Based on persistent landscape units, trends in biophysical drivers were described (Chapter 6) using Landsat and MODIS satellite data, in support of Objective 4[13]. Landsat resolution was found to be best suited to highlight spatial change. However, obtaining a dense time series of cloud-free Landsat imagery proved to be difficult. Conversely, the temporal resolution of MODIS imagery was ideal for obtaining a complete long-term dense time series. Based on the analyses it was found that, owing to the presence of many small fragmented land cover change classes in the catchments, imagery with spatial resolutions similar to Landsat and temporal resolutions similar to MODIS would provide the best results, potentially eliminating the risk of Simpson's paradox (Chapter 6).

Based on the 2000–2014 trend analysis, Chapter 6 revealed little change in catchment mean albedo at the time of peak vegetative growth, which was analysed to minimise the effect of inter-annual variation. The stable albedo trend was linked to little or no change in either carbon capture potential or water use efficiency of each catchment at the peak of the growing season. Trends in biophysical variables describing carbon storage (NPP), water use (ET) and vegetation vigour (NDVI), though strongly related to that of the rainfall pattern, showed only a weak negative linear trend. As expected, a strong positive correlation between ET and NDVI was

[13] Characterise the relationship between LC change and ecosystem stress using RS time series analysis.

found as greener vegetation is associated with higher water consumption and a decrease in albedo is correlated with an increase in ET and NDVI. T35B demonstrated statistically higher mean values of NPP, ET and NDVI compared to S50E, reflecting not only the difference in land management and tenure, but also climate variation. Predicted land cover for the year 2030 was used to model consequences of land cover change on catchment water and carbon fluxes. From the model, a decrease in net carbon storage and water use by vegetation is expected (Chapter 6).

> *The study found significant differences between the catchments with different land management practices. Land management and land use in the study area affected spatial patterns of land cover change and map error. Variations in biophysical drivers net primary production (NPP) and evapotranspiration (ET) were also associated with the land tenure of the catchments as a result of the land use. In addition, the difference in climate gradient could also have contributed to these differences (see rainfall difference in Figure 6-4C). This is in agreement with the statement by Verburg et al. (2015:30) that "…land system change is both a cause and consequence of socio-ecological processes".*

7.1.3 How does the pattern of error in land cover change datasets affect modelling of evapotranspiration and carbon storage?

Accurate land cover classes and change sub-models are required to successfully model future land cover change scenarios. Following an inductive approach using selected explanatory spatial variables, the land change model (Chapter 5) predicted not only the quantity of each land cover type, but also the location of all changes. Grassland (UG), as the dominant cover in the study area, had the greatest effect on catchment albedo. Conversion of grassland to woody shrubland and cropland cultivation was expected to decrease albedo and cause a potential gain in carbon storage (NEE), but a higher water demand by vegetation. However, contrary to expectation, the grassland to cropland transition showed an increase in albedo, possibly related to the land tenure system, as farming interspersed with rural housing gave rise to an increase in degraded surfaces. Continuous grazing by livestock contributed to rangeland degradation and increased albedo. Similarly, urban expansion and intensification increased the albedo when natural woody areas were replaced by housing. Increased albedo was associated with a loss in carbon storage, but also a decrease in the demand for water by vegetation. Consistent with global trends, grasslands have displayed an increasing trend in water use and reduction in water use efficiency (Gang et al. 2016; Gwate et al. 2018).

The model output relied on the suitability of the algorithms within the model, as well as the accuracy of the input data. Errors in the individual input land cover maps were propagated through the model and produced errors in all model outputs. Therefore, higher quality input datasets, with smaller map error, would offer higher confidence levels in the overall output model. Given that the selection of explanatory spatial variables to define the drivers of change are at the discretion of the operator, a single model can produce different outputs based on a different selection of model parameters. The ability to capture the non-linear behaviour of land cover change processes, especially those that may not yet exist within the current context, is thus a shortcoming of inductive land change models.

> *The pattern of error observed in the modelled land cover change map reflects the errors of the individual input maps even if the classification errors are independent. This pattern of error therefore affected modelling of carbon storage and water use. It was also noted that the coarser moderate resolution imaging spectroradiometer (MODIS) resolution caused spatial smoothing that masked the detail captured by the higher resolution Landsat imagery. This was especially the case for small fragmented land cover classes, where coarse pixels with mixed land cover classes would be dominated by greener vegetation. The spatial smoothing could also result in misleading temporal patterns when analysing the MODIS derived data. However, the lower temporal resolution of the Landsat imagery, especially in the growing season, is a confounding factor.*

7.1.4 How can ecosystem stress be characterised using Earth observation data and time series analysis?

This section elaborates on the implications of understanding where error can occur in land cover datasets derived through Earth observation. Such an understanding will increase the confidence of using remote sensing derived data products for land cover change analysis.

Grasslands are vital in supporting rural livelihoods and providing landscape function, such as water supply and carbon sequestration, forage production and habitat. Consequences of loss of grassland include loss of grazing for livestock through degradation or transformation. Chapters 3 and 4 describe the decline in the size of grassland, elaborating on the transitions between classes. In Chapter 5, land cover change was modelled to a future date using predictor variables and historical land cover change. Despite certain limitations of the inductive land change model applied, the future scenario modelled a further decrease in grasslands with a >80% probability of persistence. However, grassland, the biggest class, showed the largest measured and

modelled loss, favouring a gain in woody plants and cultivated land. In T35B, modelled plantations showed a small net gain, a possible opportunity for expanded commercial forestry.

The consequences of loss of grasslands to afforestation and woody encroachment would be increased leaf area and rooting depth, higher catchment evapotranspiration (ET) linked to increased catchment water use, reduction of runoff with lower water yield from the catchment. Conversely, these transitions can result in higher carbon storage, the benefits of which may be offset by greater water demands from leafy vegetation. In contrast, dryland agriculture and urbanisation would cause an increase in albedo. Changes in proportions and composition of land cover across the catchment thereby affect the net ecosystem carbon exchange (NEE) and influence the hydrologic functioning of the catchments, disturbing the climate system.

Chapter 6 described how biophysical parameters (NPP and ET) could be measured using coarse resolution MODIS imagery. Relationships between albedo at the time of peak vegetative growth, NPP, ET and NDVI were established to highlight areas of significant change that can be related to specific land cover changes.

The impact of the different land management practices in S50E (dualistic farming system) and T35B (commercial system) were identified in the historic land cover change trends, as well as in the future scenario. It is apparent that under the dualistic farming system of S50E, degradation is taking place at a more rapid rate than in T35B, where over 90% of current grassland is expected to persist to 2030. However, there is greater uncertainty associated with the T35B model, with high allocation intensity error (Chapter 5). The results, therefore, suggest that rehabilitation and land management initiatives should target catchments under dualistic farming systems, rather than those that have predominantly commercial systems. However, land management policy is required to determine the feasibility of clearing programmes in the light of continued alien and native encroachment assisted by climate change.

The implications are that woody encroachment of grassland, and particularly densification of existing patches, will typically alter carbon sequestration and cycling. Although technically regarded as a degradation gradient in the landscape due to the effect on biodiversity and ecosystem services, woody encroachment and densification can potentially act as a carbon sink due to increase in woody biomass (Scholes & Archer 1997). Invasion of grassland by IAPs reduces productivity for livestock production due to decreased rangeland productivity. Invasive species are known to alter local conditions and use available resources more efficiently, thereby outcompeting native species. In addition, the previously perceived value of IAPs as an ecosystem service is reducing due to increased rural–urban migration and the increase in

number of households supplied with electricity. Therefore, the cost of IAPs in the study areas will soon outweigh the benefits, resulting in a net negative trade-off, which has implications for national-scale invasion management strategies, such as the Working for Water programme in South Africa. Though grasslands are predicted to decrease in favour of woody invasive plant species and cultivated land, this study predicted a decrease of 12% and 6% respectively in net carbon storage and water use by vegetation.

Changes in land cover will affect the net ecosystem carbon exchange (NEE) and analysis of remotely sensed data products, such as NDVI, NPP and ET provides insight into patterns of landscape function such as browning, carbon storage and water use. Local knowledge can be used in combination with time series data to provide an enhanced understanding of degradation in rangeland productivity, relating degradation either to the impact of climate or to land management practices. Potential consequences of land cover change, especially on the net ecosystem carbon exchange, can be mapped and modelled using satellite derived albedo. The availability of dense time series satellite images enables degradation to be assessed not merely in terms of land cover change vectors but with more sophistication by identifying trends or abrupt changes across the time series.

7.2 CONTRIBUTION TO KNOWLEDGE

Various authors have conducted research on the grasslands of the Eastern Cape, e.g. investigating black wattle encroachment (Oelofse et al. 2016) and woody expansion into the grassy biome (Skowno et al. 2017). Others have monitored rangeland conditions (Yapi et al. 2018), ET dynamics (Gwate et al. 2018) or drought dynamics and vegetation productivity in different land management systems (Graw et al. 2017), predominantly following an ecological landscape perspective (Gouws & Shackleton 2019). None has, however, approached ecosystems dynamics and land management through the lens of land cover change analysis, land change modelling and time series analysis using remote sensing.

This research developed land cover change trajectories using a land cover label (Benini et al. 2010) to match process flows in the landscape. However, since map error may be responsible for incorrect interpretations of land cover change (Pontius & Lippitt 2006), various methods of quantifying map error were applied in this study area. The first method (Chapter 3) considered location of map error to compute a range of map error values based on probability (Pontius & Li 2010) while the second method (Chapter 3) used proportional accuracy and areas of change (Fuller, Smith & Devereux 2003). Chapter 4 presents hypothetical error to derive map error by

comparing change intensity with uniform change (Aldwaik & Pontius 2013). This popular intensity analysis framework has been used extensively for studies world-wide but has not yet been applied in the Eastern Cape. In response to critique by Comber et al. (2017) on the interpretation of the change budget components, Pontius (2019) introduced formulae to compute quantity, exchange and shift intensity (Chapter 4) that have not yet been applied and published elsewhere. Finally, the application of geographically weighted contingency matrices (Comber et al. 2017) specifically for use in change analysis, implements a novel method of mapping spatially explicit quantity, exchange and shift disagreement (Chapter 4).

Chapter 5 describes land change modelling for a future time step. The change/disagreement budget was applied on the land cover change between the current land cover and the future land cover. Even though the change/disagreement budget is applied to different land cover maps than proposed (Pontius & Chen 2006; Pontius & Millones 2011), it provides a novel approach to compare the measured land cover maps and the future scenario for which there is no validation data.

Prior to the present study, the effect of land cover change, both observed and modelled, on surface albedo and consequently the surface energy balance, has not been explored in this region before (Chapter 6). Additionally, the link between modelled landscape change, surface albedo and changes in catchment water and carbon fluxes have not been investigated previously. The novelty lies in the analysis of a dense time series consisting of 15 years of data to improve our understanding of surface energy balance, water and carbon sequestration parameters for catchments under two different land management regimes. The study uses previous land cover change and future scenario analyses, combined with the season-trend model output to quantify carbon sequestration and water use, both for areas of no change (persistent classes) and areas that have transitioned from one land cover to another. The study combined the use of traditional and cutting-edge remote sensing techniques (e.g. using Google Earth Engine) to develop peak season albedo from Landsat, while scientifically robust techniques (implemented in R software) were used to process MODIS data.

7.3 LIMITATIONS OF THE STUDY

As with most studies, this research was limited by several factors. The quality of available data was a major limiting factor. Some inherent limitations found with using the existing input data include:

(1) Imperfect input data was available, however the size and location or these errors were unavailable due to lack of sample data;

(2) No accuracy assessment had been done on the 1990 land cover dataset, but accuracy was reported to be similar to another dataset for which comparable processing and modelling had been used (Chapter 4);

(3) The reported accuracy of the 2000 land cover dataset was extremely low (67%) and though the quality of this dataset was improved through post-classification editing (Chapter 3), some errors may have been overlooked or systematic errors may have been introduced;

(4) The 2014 land cover dataset was classified from a single-date image (Chapter 3), therefore, not capturing seasonal variation;

(5) A new aggregated land cover classification system was used to accommodate the different land cover legends of each dataset (Chapter 3), which could have led to generalisations; and

(6) The datasets were created by different operators and may thus have been affected by operator bias.

Each of these factors increased the uncertainty of the land cover change products. Additionally, the future land cover dataset could not be validated.

Various shortcomings were identified in the land change modelling (Chapter 5). These included the selection of the particular model, the explanatory variables used, and the process followed. A prospective approach based only upon past trends was used while more value would be gained by introducing alternative future scenarios (Paegelow & Camacho 2008). In addition, it was found that the Land Change Modeller in IDRISI is limited when developing alternative scenarios (Pérez-Vega, Mas & Ligmann-Zielinska 2012).

For some land cover labels used to describe landscape transitions, opposing albedo change directions were found under the same label (Chapter 6) that may have a confounding effect on the results. Further work is required to untangle the influence of albedo within each land cover transition.

7.4 RECOMMENDATIONS FOR FUTURE RESEARCH

This study found that, in order to provide a better distinction between different wooded classes, higher spatial resolution imagery need to be considered, especially to distinguish between spectrally homogenous vegetation types. The introduction of new sensors, such as the European Space Agency's Sentinel-2 satellites, with higher temporal, spatial and spectral resolution, may provide a more suitable option for such analyses in the future.

Some land cover change transitions showed opposing albedo change vectors that confounded correlation results among these variables. Therefore, it is recommended that separate transition classes be analysed for opposing vectors.

Using geographically weighted local measures of change showed much potential. Local statistics not only supported the identification of potential map error, but also provided a spatially explicit manner to dynamically visualise accuracy and characterise error in maps and models. Spatially explicit approaches can accommodate spatial autocorrelation found in remotely sensed data and address the spatial non-stationarity directly, which will improve modelling of landscape processes. It is recommended that software implementing these methods be expanded to include bandwidth smoothing optimization. Such software should be made available to the wider remote sensing community.

The availability of analysis ready satellite data and cloud computing platforms provide new possibilities for generating land cover maps. Applying deep learning algorithms, spatio-contextual information and novel inputs, such as land cover transitions and combinations of multi-scale, multi-sensor data, can improve map accuracies. This avenue of research is strongly recommended.

Further research is recommended to explore the use of higher resolution satellite data to effectively model carbon storage and water use. The Google Earth Engine platform provides shared geoprocessing algorithms (Gorelick et al. 2017) and access to long-term data (Hansen & Loveland 2012), that can be used to generate detailed maps (Forkel et al. 2013) to model future scenarios.

7.5 CONCLUDING THOUGHTS

This narrative has confirmed that land cover and land use dynamics have significant effects on the natural environment and are important drivers of change in the landscape and its function. Human activities continue to change and exert pressure on the natural environment, triggering changes in land management and land use practices. To facilitate changes in these practices, adequate knowledge of the processes at play in the landscape are essential. One of the main drivers of grassland transformation was identified as encroachment by woody plants of indigenous or invasive origin, which exerts a major influence on ecosystem services that the landscape can provide, specifically for water supply and carbon storage, as well as function such as feed production for food security.

This study used existing, independent land cover maps and modelled future land cover maps to determine land cover change trajectories in a grassland-dominated landscape in the Eastern Cape of South Africa. The main land cover change trajectories investigated were those that are crucial to quantify water and carbon fluxes. In the remote sensing community, image classification accuracy is a required and stringent process, while maps with relative low accuracy are often generated and used unquestioningly by those investigating ecosystem services. This points to the importance of a simple method to identify map error. If higher reliability of change results should be required for operational purposes, accuracies of 99% for each independently mapped land cover dataset must be obtained. This is unlikely, and therefore some uncertainty in both the classification results and the change results must be accepted. Although map error was present in the land cover maps and was subsequently propagated in the modelling, change analysis using (1) an indicator approach and (2) the intensity analysis framework, provide bounds of accuracy at global scale, which is useful to assess the confidence of derived results. In addition, hot spots of map error could be determined through local spatially explicit change analysis performed using geographically weighted contingency matrices.

This study confirmed that land cover dynamics have significant consequences for the natural environment. The expected decrease in net carbon storage and water use modelled from a land cover change scenario confirms the impact of land cover change on ecosystems and the services they provide. Land management practices in the two tenure systems (freehold versus communal) have important repercussions. As human actions continue to change and exert pressure on the natural environment, the modelling results suggest that rehabilitation and land management initiatives should be targeted in catchments under a dualistic farming system, rather than those that are predominantly commercial systems. To effectively manage complex ecosystems, accurate change maps are required to explain and quantify both drivers and impacts of land change. As interdisciplinary research and land change science seek to understand, explain and project land use and land cover dynamics associated with human-environment interaction, integrating information from various research communities is essential to support land management.

REFERENCES

Agresti A 2019. Categorical data analysis. In *Wiley Series in Probability and Statistics*, 400. John Wiley & Sons.

Akinyemi FO & Pontius RG 2016. Land change dynamics: Insights from intensity analysis applied to an African emerging city. *Journal of Spatial Science* 8596, September: 1–15.

Aldwaik SZ & Pontius RG 2012. Intensity analysis to unify measurements of size and stationarity of land changes by interval, category, and transition. *Landscape and Urban Planning* 106, 1: 103–114.

Aldwaik SZ & Pontius RG 2013. Map errors that could account for deviations from a uniform intensity of land change. *International Journal of Geographical Information Science* 27, 9: 1717–1739.

Aldwaik SZ, Onsted JA & Pontius RG 2015. Behavior-based aggregation of land categories for temporal change analysis. *International Journal of Applied Earth Observation and Geoinformation* 35, PB: 229–238.

Alo CA & Pontius RG 2008. Identifying systematic land cover transitions using remote sensing and GIS: The fate of forests inside and outside protected areas of Southwestern Ghana. *Environment and Planning B: Planning and Design* 35, 2: 280–295.

Ament JM & Cumming GS 2016. Scale dependency in effectiveness, isolation, and social-ecological spillover of protected areas. *Conservation Biology* 30, 4: 846–855.

Anderson JR, Hardy EE, Roach JT, Witmer RE & Peck DL 1976. *A land use and land cover classification system for use with remote sensor data (Vol. 964). A revision of the land use classification system as presented in U.S. Geological Survey Circular 671 964*.

Anderson RG, Canadell JG, Randerson JT, Jackson RB, Hungate BA, Baldocchi DD, Ban-Weiss GA, Bonan GB, Caldeira K, Cao L, Diffenbaugh NS, Gurney KR, Kueppers LM, Law BE, Luyssaert S & O'Halloran TL 2011. Biophysical considerations in forestry for climate protection. *Frontiers in Ecology and the Environment* 9, 3: 174–182.

Andrew ME, Wulder MA & Nelson TA 2014. Potential contributions of remote sensing to ecosystem service assessments. *Progress in Physical Geography: Earth and Environment* 38, 3: 328–353.

Ariti AT, Van Vliet J & Verburg PH 2015. Land use and land cover changes in the Central Rift Valley of Ethiopia: Assessment of perception and adaptation of stakeholders. *Applied Geography* 65: 28–37.

Arntz K 1999. Landscape: A forgotten legacy. *Area* 3, 1: 297–300.

Ayanu YZ, Conrad C, Nauss T, Wegmann M & Koellner T 2012. Quantifying and mapping ecosystem services supplies and demands: A review of remote sensing applications. *Environmental Science and Technology* 46, 16: 8529–8541.

Azzari G & Lobell DB 2017. Landsat-based classification in the cloud: An opportunity for a paradigm shift in land cover monitoring. *Remote Sensing of Environment* 202: 64–74.

Bagstad KJ, Semmens DJ, Waage S & Winthrop R 2013. A comparative assessment of decision-support tools for ecosystem services quantification and valuation. *Ecosystem Services* 5: 27–39.

Bagstad KJ, Villa F, Batker D, Harrison-Cox J, Voigt B & Johnson GW 2014. From theoretical to actual ecosystem services: Mapping beneficiaries and spatial flows in ecosystem service assessments. *Ecology and Society* 19, 2: 64.

Bai J & Perron P 2003. Computation and analysis of multiple structural change models. *Journal of Applied Econometrics* 18: 1–22.

Bailey CJ 2017. Scaling patterns and drivers of species richness and turnover across the Afrotropics. Master's thesis. Stellenbosch: Stellenbosch University.

Banzahf S & Boyd J 2005. The architecture and measurement of an ecosystem services index. Discussion Paper

DP-05-22 (54 pp.). Washington, DC: Resources for the Future.

Bastian O, Krönert R & Lipský Z 2006. Landscape diagnosis on different space and time scales – A challenge for landscape planning. *Landscape Ecology* 21, 3: 359–374.

Baudoin M-A, Vogel C, Nortje K & Naik M 2017. Living with drought in South Africa: Lessons learnt from the recent El Niño drought period. *International Journal of Disaster Risk Reduction* 23: 128–137.

Beck HE, McVicar TR, Van Dijk AIJM, Schellekens J, De Jeu RAM & Bruijnzeel LA 2011. Global evaluation of four AVHRR–NDVI datasets: Intercomparison and assessment against Landsat imagery. *Remote Sensing of Environment* 115, 10: 2547–2563.

Belgiu M & Drăguţ L 2016. Random forest in remote sensing: A review of applications and future directions. *ISPRS Journal of Photogrammetry and Remote Sensing* 114: 24–31.

Belward AS & Skøien JO 2015. Who launched what, when and why: Trends in global land cover observation capacity from civilian Earth observation satellites. *ISPRS Journal of Photogrammetry and Remote Sensing* 103: 115–128.

Benini L, Bandini V, Marazza D & Contin A 2010. Assessment of land use changes through an indicator-based approach: A case study from the Lamone river basin in Northern Italy. *Ecological Indicators* 10, 1: 4–14.

Bennett EM, Cramer W, Begossi A, Cundill G, Diaz S, Egoh BN, Geijzendorffer IR, Krug CB, Lavorel S, Lazos E, Lebel L, Martín-López B, Meyfroidt P, Mooney HA, Nel JL, Pascual U, Payet K, Harguindeguy NP, Peterson GD, Prieur-Richard AH, Reyers B, Roebeling P, Seppelt R, Solan M, Tschakert P, Tscharntke T, Turner BL, Verburg PH, Viglizzo EF, White PCL & Woodward G 2015. Linking biodiversity, ecosystem services, and human well-being: Three challenges for designing research for sustainability. *Current Opinion in Environmental Sustainability* 14: 76–85.

Bennett JE, Palmer AR & Blackett MA 2012. Range degradation and land tenure change: Insights from a 'released' communal area of Eastern Cape Province, South Africa. *Land Degradation & Development* 23, 6: 557–568.

Betts RA 2001. Biogeophysical impacts of land use on present-day climate: Near-surface temperature change and radiative forcing. *Atmospheric Science Letters* 2, 1–4: 1–8.

Blair D, Shackleton CM & Mograbi PJ 2018. Cropland abandonment in South African smallholder communal lands: Land cover change (1950–2010) and farmer perceptions of contributing factors. *Land* 7, 4: 121.

Blaschke T 2010. Object-based image analysis for remote sensing. *ISPRS Journal of Photogrammetry and Remote Sensing* 65, 1: 2–16.

Blok D, Schaepman-Strub G, Bartholomeus H, Heijmans MMPD, Maximov TC & Berendse F 2011. The response of Arctic vegetation to the summer climate: relation between shrub cover, NDVI, surface albedo and temperature. *Environmental Research Letters* 6: 35502–35511.

Bodart C, Brink AB, Donnay F, Lupi A, Mayaux P & Achard F 2013. Continental estimates of forest cover and forest cover changes in the dry ecosystems of Africa between 1990 and 2000. *Journal of Biogeography* 40, 6: 1036–1047.

Bonan GB 2008. Forests and climate change: forcings, feedbacks, and the climate benefits of forests. *Science (New York, N.Y.)* 320, 5882: 1444–1449.

Bonham-Carter GF 1994. *Geographic Information Systems for Geoscientists: Modelling with GIS*. New York, NY: Pergamon.

Brantley ST, Vose JM, Wear DN & Band L 2018. Planning for an uncertain future: Restoration to mitigate water scarcity and sustain carbon sequestration. In Kirkman LK & Jack SB (eds) *Ecological restoration and management of longleaf pine forests*, 291–309. Boca Raton, FL: CRC Press.

Bright RM, Cherubini F & Strømman AH 2012. Climate impacts of bioenergy: Inclusion of carbon cycle and albedo dynamics in life cycle impact assessment. *Environmental Impact Assessment Review* 37: 2–11.

Brown KM, Foody GM & Atkinson PM 2006. Deriving thematic uncertainty measures in remote sensing using classification outputs. In Caetano M & Painho M (eds), *Proceedings of the 7th International Symposium on Spatial Accuracy Assessment in Natural Resources and Environmental Sciences*, Lisbon, Portugal, July 5–7. Lisbon, Portugal. Painho, Instituto Geográfico Português.: 5–7. [online]. Available from: http://spatial-accuracy.org/system/files/Brown2006accuracy.pdf [Accessed 23 June 2019].

Brown ME, Pinzón JE, Didan K, Morisette JT & Tucker CJ 2006. Evaluation of the consistency of long-term NDVI time series derived from AVHRR, SPOT-vegetation, SeaWiFS, MODIS, and landsat ETM+ sensors. *IEEE Transactions on Geoscience and Remote Sensing* 44, 7: 1787–1793.

Brown TC, Bergstrom JC & Loomis JB 2007. Defining, valuing, and providing ecosystem goods and services. *Natural Resources Journal* 47: 329–376.

Brunsdon CF, Charlton M & Harris P 2016. Geographically weighted cross tabulation. [online]. Available from: https://github.com/chrisbrunsdon/gwxtab [Accessed 19 November 2018].

Burkhard B, Crossman N, Nedkov S, Petz K & Alkemade R 2013. Mapping and modelling ecosystem services for science, policy and practice. *Ecosystem Services* 4: 1–3.

Burkhard B, Kroll F & Müller F 2010. Landscapes' capacities to provide ecosystem services: A concept for land cover based assessments. *Landscape Online* 15: 1–22.

Burley TM 1961. Land use or land utilization? *Professional Geographer* 16, 6: 18–20.

Burnicki AC 2011. Spatio-temporal errors in land cover change analysis: Implications for accuracy assessment. *International Journal of Remote Sensing* 32, 22: 7487–7512.

Burnicki AC 2012. Impact of error on landscape pattern analyses performed on land cover change maps. *Landscape Ecology* 27, 5: 713–729.

Burnicki AC, Brown DG & Goovaerts P 2007. Simulating error propagation in land cover change analysis: The implications of temporal dependence. *Computers, Environment and Urban Systems* 31, 3: 282–302.

Cai H, Di X, Chang SX, Wang C, Shi B, Geng P & Jin G 2016a. Carbon storage, net primary production, and net ecosystem production in four major temperate forest types in northeastern China. *Canadian Journal of Forest Research* 46, 2: 143–151.

Cai H, Wang J, Feng Y, Wang M, Qin Z & Dunn JB 2016b. Consideration of land use change-induced surface albedo effects in life-cycle analysis of biofuels. *Energy and Environmental Science* 9, 9: 2855–2867.

Camacho Olmedo MT, Paegelow M & Mas JF 2013. Interest in intermediate soft-classified maps in land change model validation: Suitability versus transition potential. *International Journal of Geographical Information Science* 27, 12: 2343–2361.

Camacho Olmedo MT, Pontius RG, Paegelow M & Mas JF 2015. Comparison of simulation models in terms of quantity and allocation of land change. *Environmental Modelling & Software* 69: 214–221.

Campbell JB 1983. *Mapping the Land: Aerial Imagery for Land Use Information*. Washington, DC, DC: Association of American Geographers. [online]. Available from: https://files.eric.ed.gov/fulltext/ED235078.pdf [Accessed 24 June 2019].

Campbell JB & Wynne RH 2011. *Introduction to Remote Sensing*. 5th ed. New York, NY: The Guilford Press.

Carbutt C, Tau M, Stephens A & Escott B 2011. The conservation status of temperate grasslands in southern Africa. *Grassroots* 11, 1: 17–23.

Carlson TN & Ripley DA 1997. On the relation between NDVI, fractional vegetation cover, and leaf area index. *Remote Sensing of Environment* 62, 3: 241–252.

Carmel Y & Dean DJ 2004. Performance of a spatio-temporal error model for raster datasets under complex error patterns. *International Journal of Remote Sensing* 25, 23: 5283–5296.

Carrington DP, Gallimore RG & Kutzbach JE 2001. Climate sensitivity to wetlands and wetland vegetation in mid-Holocene North Africa. Climate Dynamics 17: 151–157.

Case MF & Staver AC 2017. Fire prevents woody encroachment only at higher-than-historical frequencies in a South African savanna. *Journal of Applied Ecology* 54, 3: 955–962.

Castella J-C & Verburg PH 2007. Combination of process-oriented and pattern-oriented models of land use change in a mountain area of Vietnam. *Ecological Modelling* 202, 3–4: 410–420.

Chan KMA, Shaw MR, Cameron DR, Underwood EC & Daily GC 2006. Conservation Planning for Ecosystem Services. *PLoS Biology* 4, 11: e379.

Chapin FS, Matson PA & Vitousek PM 2011. *Principles of terrestrial ecosystem ecology*. Springer.

Chowdhury RR & Turner BL 2019. The parallel trajectories and increasing integration of landscape ecology and land system science. *Journal of Land Use Science* 14, 2: 135-154.

Christ S 2017. Spatial visualization of uncertainty. Master's thesis. Stellenbosch: Stellenbosch University. [online]. Available from: http://hdl.handle.net/10019.1/100949 [Accessed 24 April 2017].

Clawson M & Stewart CL 1965. *Land use information: A critical survey of U.S. statistics including possibilities for greater uniformity*. Baltimore, MD: The John Hopkins Press for Resources for the Future.

Cleugh HA, Leuning R, Mu Q & Running SW 2007. Regional evaporation estimates from flux tower and MODIS satellite data. *Remote Sensing of Environment* 106, 3: 285–304.

Cleveland RB, Cleveland WS, McRae JE & Terpenning I 1990. STL: A seasonal-trend decomposition procedure based on loess. *Journal of Official Statistics* 6, 1: 3–73.

Cleveland WS 1979. Robust locally weighted regression and smoothing scatterplots. *Journal of the American Statistical Association* 74, 368: 829–836.

Clulow AD, Everson CS & Gush MB 2011. *The long-term impact of Acacia Mearnsii trees on evaporation, stream flow, and ground water resources*. Pretoria: Water Research Commission.

Comber A, Balzter H, Cole B, Fisher P, Johnson S & Ogutu B 2016. Methods to quantify regional differences in land cover change. *Remote Sensing* 8, 3: 176.

Comber A, Brunsdon C, Charlton M & Harris P 2017. Geographically weighted correspondence matrices for local error reporting and change analyses: Mapping the spatial distribution of errors and change. *Remote Sensing Letters* 8, 3: 234–243.

Comber A, Fisher P, Brunsdon C & Khmag A 2012. Spatial analysis of remote sensing image classification accuracy. *Remote Sensing of Environment* 127: 237–246.

Comber AJ 2013. Geographically weighted methods for estimating local surfaces of overall, user and producer accuracies. *Remote Sensing Letters* 4, 4: 373-380.

Congalton RG & Green K 2009. *Assessing the Accuracy of Remotely Sensed Data: Principles and Practices*. 2nd ed. Boca Raton, FL: CRC Press.

Congalton RG 2001. Accuracy assessment and validation of remotely sensed and other spatial information. *International Journal of Wildland Fire* 10, 4: 321.

Coppin P, Jonckheere I, Nackaerts K, Muys B & Lambin E 2004. Digital change detection methods in ecosystem monitoring: A review. *International Journal of Remote Sensing* 25, 9: 1565–1596.

Costanza R, D'Arge R, De Groot R, Farber S, Grasso M, Hannon B, Limburg K, Naeem S, O'Neill RV, Paruelo J, Raskin RG, Sutton P & Van den Belt M 1997. The value of the world's ecosystem services and natural capital. *Nature* 387: 253–260.

Cowling RM, Egoh B, Knight AT, O'Farrell PJ, Reyers B, Rouget M, Roux DJ, Welz A & Wilhelm-Rechman A 2008. An operational model for mainstreaming ecosystem services for implementation. *Proceedings of the National Academy of Sciences of the United States of America* 105, 28: 9483–9488.

Crist EP & Cicone RC 1984. A Physically-Based Transformation of Thematic Mapper Data---The TM Tasseled Cap. *IEEE Transactions on Geoscience and Remote Sensing* GE-22, 3: 256–263.

Crossman ND, Bryan BA, de Groot RS, Lin Y-P & Minang PA 2013a. Land science contributions to ecosystem services. *Current Opinion in Environmental Sustainability* 5, 5: 509–514.

Crossman ND, Burkhard B, Nedkov S, Willemen L, Petz K, Palomo I, Drakou EG, Martín-Lopez B, McPhearson T, Boyanova K, Alkemade R, Egoh B, Dunbar MB & Maes J 2013b. A blueprint for mapping and modelling ecosystem services. *Ecosystem Services* 4: 4–14.

Cunha JEBL, Nóbrega RLB, Rufino IAA, Erasmi S, Galvão C de O & Valente F 2018. Surface albedo as a proxy for land cover change in seasonal dry forests: evidence from the Brazilian Caatinga biome. *Remote Sensing of Environment* 20 June 2019, 111250. [online]. Available from: https://doi.org/10.1016/j.rse.2019.111250 [Accessed 31 July 2019].

Daily G 1997. *Nature's Services: Societal Dependence on Natural Ecosystems*. Washington DC: Island Press.

Dark SJ & Bram D 2007. The modifiable areal unit problem (MAUP) in physical geography. *Progress in Physical Geography* 31, 5: 471–479.

Davin EL & de Noblet-Ducoudré N, 2010. Climatic Impact of Global-Scale Deforestation: Radiative versus non-radiative processes. *Journal of Climate* 23, 1: 97–112.

De Beurs KM & Henebry GM 2010. Spatio-temporal statistical methods for modelling land surface phenology. In Hudson IL & Keatly MR (eds) *Phenological Research*, 177–208. Springer Science+Business Media.

De Jong R, De Bruin S,De Wit A, Schaepman ME & Dent DL 2011. Analysis of monotonic greening and browning trends from global NDVI time series. *Remote Sensing of Environment* 115, 2: 692–702.

De Klerk JN 2004. *Bush Encroachment in Namibia: Report on Phase 1 of the Bush Encroachment Research, Monitoring, and Management Project*. Windhoek: Ministry of Environment and Tourism, Directorate of Environmental Affairs.

De Neergaard A, Saarnak C, Hill T, Khanyile M, Berzosa AM & Birch-Thomsen T 2005. Australian wattle species in the Drakensberg region of South Africa: An invasive alien or a natural resource? *Agricultural Systems* 85, 3: 216–233.

De Oliveira Faria T, Rodrigues TR, Curado LFA, Gaio DC & Nogueira J de S 2018. Surface albedo in different land use and cover types in Amazon forest region. *Ambiente Agua - An Interdisciplinary Journal of Applied Science* 13, 2: e2120.

De Villiers C, Driver A, Clark B, Euston-Brown D, Day E, Job N, Helme N, Holmes P, Brownlie S & Rebelo A 2005. Ecosystem guidelines for environmental assessment in the Western Cape. In *Fynbos Forum*, Conservation Unit, Kirstenbosch. Cape Town: Botanical Society of South Africa.

Debats SR, Luo D, Estes LD, Fuchs TJ & Caylor KK 2016. A generalized computer vision approach to mapping crop fields in heterogeneous agricultural landscapes. *Remote Sensing of Environment* 179: 210–221.

Definiens 2003. Definiens eCognition User Guide, Version 4.0. [online]. Available from: http://www.definiens-imaging.com [Accessed 5 May 2017].

DeFries RS, Foley JA & Asner GP 2004. Land use choice : Balancing human needs and ecosystem function. *Frontiers in Ecology and the Environment* 2, 5: 249–257.

Deininger K, Selod H & Burns A 2011. *The Land Governance Assessment Framework*. The World Bank. [online]. Available from: http://elibrary.worldbank.org/doi/book/10.1596/978-0-8213-8758-0 [Accessed 26 June 2019].

Densham PJ 1991. Spatial decision support systems. In Maguire DJ, Goodchild MF & Rhind DW (eds) *Geographical Information Systems: Principles and Applications*, 403–412. Harlow, UK: *Addison Wesley Longman.*

Díaz S, Fargione J, Chapin FS, Tilman D & Arcenas A 2006. Biodiversity Loss Threatens Human Well-Being. *PLoS Biology* 4, 8: e277.

Dietterich TG 2009. Machine learning in ecosystem informatics and sustainability. In *Proceedings of the Twenty-First International Joint Conference on Artificial Intelligence*, 8–13. [online]. Available from: https://www.ijcai.org/Proceedings/09/Papers/013.pdf [Accessed 12 April 2017].

Doan HTX & Foody GM 2007. Increasing soft classification accuracy through the use of an ensemble of classifiers. *International Journal of Remote Sensing* 28, 20: 4609–4623.

Doré T, Makowski D, Malézieux E, Munier-Jolain N, Tchamitchian M & Tittonell P 2011. Facing up to the paradigm of ecological intensification in agronomy: Revisiting methods, concepts and knowledge. *European Journal of Agronomy* 34, 4: 197–210.

Doughty CE, Loarie SR & Field CB 2012. Theoretical impact of changing albedo on precipitation at the southernmost boundary of the ITCZ in South America. *Earth Interactions* 16, 8: 1–14.

Driver A, Sink KJ, Nel JN, Holness S, Van Niekerk L, Daniels F, Jonas Z, Majiedt PA, Harris L & Maze K 2012. *National Biodiversity Assessment 2011: An assessment of South Africa's biodiversity and ecosystems: Synthesis Report*. [online]. Available from: http://catalog.ipbes.net/system/assessment/195/references/files/570/original/NBA_2011_Synthesis_Report_%28low_resolution%29.pdf?1364385861 [Accessed 4 May 2017].

Duarte GT, Santos PM, Cornelissen TG, Ribeiro MC & Paglia AP 2018. The effects of landscape patterns on ecosystem services: Meta-analyses of landscape services. *Landscape Ecology* 33, 8: 1247–1257.

Duveiller G, Forzieri G, Robertson E, Li W, Georgievski G, Lawrence P, Wiltshire A, Ciais P, Pongratz J, Sitch S, Arneth A & Cescatti A 2018. Biophysics and vegetation cover change: A process-based evaluation framework for confronting land surface models with satellite observations. *Earth System Science Data* 10, 3: 1265–1279.

Duveiller G, Hooker J & Cescatti A 2018. The mark of vegetation change on Earth's surface energy balance. *Nature Communications* 9, 1: 679.

DWA 2013. *National Water Resource Strategy (NWRS-2): Managing water for an equitable and sustainable future*. Second. Pretoria: Department Water Affairs. [online]. Available from: http://www.dwa.gov.za/documents/Other/Strategic Plan/NWRS2-Final-email-version.pdf [Accessed 26 April 2017].

DWAF 2004. *Berg Water Management Area: Internal Strategic Perspective.* Prepared by Ninham Shand (Pty) Ltd in association with Jakoet and Associates, Umvoto Africa and Tlou and Matji, on behalf of the Directorate: National Water Resource Planning. DWAF Report No P WMA19/000/00/0304. [online]. Available from: http://www.dwaf.gov.za/Documents/Other/WMA/19/BergISPJan04full.pdf [Accessed 2 July 2019].

Dye PJ, Jarmain C, Le Maitre D, Everson CS, Gush M & Clulow A 2008. *Modelling vegetation water use for general application in different categories of vegetation*.

Eastman JR 2016. IDRISI Terrset Manual. Worcester, MA: Clark Labs, Clark University. [online]. Available from https://clarklabs.org/wp-content/uploads/2016/10/Terrset-Manual.pdf [Accessed 2 July 2019].

Eastman JR, Van Fossen ME & Solorzano LA 2005. Transition potential modeling for land cover change. In Maguire D Batty M & Goodchild M (eds) *GIS, spatial analysis and modeling*, 357–386. Redlands, CA: ESRI Press.

Eddy IMS, Gergel SE, Coops NC, Henebry GM, Levine J, Zerriffi H & Shibkov E 2017. Integrating remote sensing and local ecological knowledge to monitor rangeland dynamics. *Ecological Indicators* 82: 106–116.

Editors 2011. The American Heritage dictionary of the English language [online]. Available from: https://www.dictionary.com/browse/ecosystem [Accessed 20 June 2019].

Egoh B, Drakou EG, Maes J & Willemen L 2012. *Indicators for mapping ecosystem services : A review*. European Commission, Joint Research Centre (JRC).

Egoh B, Reyers B, Rouget M, Richardson DM, Le Maitre DC & Van Jaarsveld AS 2008. Mapping ecosystem services for planning and management. *Agriculture, Ecosystems & Environment* 127, 1–2: 135–140.

Egoh BN, Reyers B, Rouget M & Richardson DM 2011. Identifying priority areas for ecosystem service management in South African grasslands. *Journal of Environmental Management* 92, 6: 1642–1650.

Ehrlich PR & Ehrlich A. 1981. *Extinction: The Causes and Consequences of the Disappearance of Species*. New York, NY: Random House.

Eigenbrod F, Armsworth PR, Anderson BJ, Heinemeyer A, Gillings S, Roy DB, Thomas CD & Gaston KJ 2010. The impact of proxy-based methods on mapping the distribution of ecosystem services. *Journal of Applied Ecology* 47, 2: 377–385.

Eklundh L & Olsson L 2003. Vegetation index trends for the African Sahel 1982-1999. *Geophysical Research Letters* 30, 8.

Enaruvbe GO & Pontius RG 2015. Influence of classification errors on Intensity Analysis of land changes in southern Nigeria. *International Journal of Remote Sensing* 36, 1: 244–261.

Englund O, Berndes G & Cederberg C 2017. How to analyse ecosystem services in landscapes:A systematic review. *Ecological Indicators* 73: 492–504.

ESRI 2016. ArcGIS Desktop: Release 10.4. Redlands, CA: Environmental Systems Research Institute. [online]. Availabe from: https://www.esri.com/en-us/arcgis/products/arcgis-desktop/overview [Accessed 2 July 2019].

Estes L, Chen P, Debats S, Evans T, Ferreira S, Kuemmerle T, Ragazzo G, Sheffield J, Wolf A, Wood E & Caylor K 2018. A large-area, spatially continuous assessment of land cover map error and its impact on downstream analyses. *Global Change Biology* 24, 1: 322–337.

Estes LD, Searchinger T, Spiegel M, Tian D, Sichinga S, Mwale M, Kehoe L, Kuemmerle T, Berven A, Chaney N, Sheffield J, Wood EF & Caylor KK 2016. Reconciling agriculture, carbon and biodiversity in a savannah transformation frontier. *Philosophical Transactions of the Royal Society B: Biological Sciences* 371, 1703: 20150316.

Fensholt R, Horion S, Tagesson T, Ehammer A, Ivits E & Rasmussen K 2015. Global-scale mapping of changes in ecosystem functioning from Earth observation-based trends in total and recurrent vegetation. *Global Ecology and Biogeography* 24, 9: 1003–1017.

Fensholt R, Langanke T, Rasmussen K, Reenberg A, Prince SD, Tucker C, Scholes RJ, Le QB, Bondeau A, Eastman R, Epstein H, Gaughan AE, Hellden U, Mbow C, Olsson L, Paruelo J, Schweitzer C, Seaquist J & Wessels K 2012. Greenness in semi-arid areas across the globe 1981-2007: An earth observing satellite based analysis of trends and drivers. *Remote Sensing of Environment* 121: 144–158.

Feranec J, Jaffrain G, Soukup T & Hazeu G 2010. Determining changes and flows in European landscapes 1990-2000 using CORINE land cover data. *Applied Geography* 30, 1: 19–35.

Fisher P, Arnot C, Wadsworth R & Wellens J 2006. Detecting change in vague interpretations of landscapes. *Ecological Informatics* 1, 2: 163–178.

Foody GM 2002. Status of land cover classification accuracy assessment. *Remote Sensing of Environment* 80, 1: 185–201.

Foody GM 2005. Local characterization of thematic classification accuracy through spatially constrained confusion matrices. *International Journal of Remote Sensing* 26, 6: 1217–1228.

Foody GM 2008. Harshness in image classification accuracy assessment. *International Journal of Remote Sensing* 29, 11: 3137–3158.

Foody GM, See L, Fritz S, Van der Velde M, Perger C, Schill C & Boyd DS 2013. Assessing the accuracy of volunteered geographic information arising from multiple contributors to an internet based collaborative project. *Transactions in GIS* 17, 6: 847–860.

Forkel M & Wutzler T 2015. Greenbrown - land surface phenology and trend analysis. A package for the R software. [online]. Available from: http://greenbrown.r-forge.r-project.org/ [Accessed 3 October 2018].

Forkel M, Carvalhais N, Verbesselt J, Mahecha MD, Neigh CSR & Reichstein M 2013. Trend change detection in NDVI time series: Effects of inter-annual variability and methodology. *Remote Sensing* 5, 5: 2113–2144.

Friedl MA & Brodley CE 1997. Decision tree classification of land cover from remotely sensed data. *Remote Sensing of Environment* 61, 3: 399–409.

Friedl MA, Gray JM, Melaas EK, Richardson AD, Hufkens K, Keenan TF, Bailey A & O'Keefe J 2014. A tale of two springs: Using recent climate anomalies to characterize the sensitivity of temperate forest phenology to climate change. *Environmental Research Letters* 9, 5: 054006.

Friedl MA, Sulla-Menashe D, Tan B, Schneider A, Ramankutty N, Sibley A & Huang X 2010. MODIS Collection 5 global land cover: Algorithm refinements and characterization of new datasets. *Remote Sensing of Environment* 114, 1: 168–182.

Fuller RM, Smith GM & Devereux BJ 2003. The characterisation and measurement of land cover change through remote sensing: Problems in operational applications? *International Journal of Applied Earth Observation and Geoinformation* 4, 3: 243–253.

Gaertner M, Nottebrock H, Fourie H, Privett SDJ & Richardson DM 2012. Plant invasions, restoration, and economics: Perspectives from South African fynbos. *Perspectives in Plant Ecology, Evolution and Systematics* 14, 5: 341–353.

Gang C, Wang Z, Chen Y, Yang Y, Li J, Cheng J, Qi J & Odeh I 2016. Drought-induced dynamics of carbon and water use efficiency of global grasslands from 2000 to 2011. *Ecological Indicators* 67: 788–797.

Ganguly S, Friedl MA, Tan B, Zhang X & Verma M 2010. Land surface phenology from MODIS: Characterization of the Collection 5 global land cover dynamics product. *Remote Sensing of Environment* 114, 8: 1805–1816.

Gao BC 1996. NDWI: A normalized difference water index for remote sensing of vegetation liquid water from space. *Remote Sensing of Environment* 58: 257–266.

Georgescu M, Lobell DB & Field CB 2011. Direct climate effects of perennial bioenergy crops in the United States. *Proceedings of the National Academy of Sciences of the United States of America* 108, 11: 4307–4312.

GeoTerraImage 2015. *2013 - 2014 South African National Land cover Dataset*. GeoTerraImage. [online]. Available from: http://www.geoterraimage.com [Accessed 2 July 2019].

GeoTerraImage 2016. *1990 South African National Land cover Dataset*. GeoTerraImage. [online]. Available from: http://www.geoterraimage.com [Accessed 2 July 2019].

Gibson L, Münch Z, Palmer A & Mantel S 2018. Future land cover change scenarios in South African grasslands: Implications of altered biophysical drivers on land management. *Heliyon* 4, 7: e00693.

Gollini I, Lu B, Charlton M, Brunsdon C & Harris P 2015. GWmodel: an R Package for Exploring Spatial Heterogeneity using Geographically Weighted Models. *Journal of Statistical Software* 63, 17: 1–50.

Gómez C, White JC & Wulder MA 2016. Optical remotely sensed time series data for land cover classification: A review. *ISPRS Journal of Photogrammetry and Remote Sensing* 116: 55–72.

Goodchild MF & Densham PJ 1990. *Research initiative six, spatial decision support systems: Scientific report for*

the specialist meeting. Santa Barbara: Technical Report 90-5, National Center for Geographic Information and Analysis.

Gorelick N, Hancher M, Dixon M, Ilyushchenko S, Thau D & Moore R 2017. Google Earth Engine: Planetary-scale geospatial analysis for everyone. *Remote Sensing of Environment* 202: 18–27.

Gouws AJ & Shackleton CM 2019. Abundance and correlates of the Acacia dealbata invasion in the northern Eastern Cape, South Africa. *Forest Ecology and Management* 432: 455–466.

Graw V, Ghazaryan G, Dall K, Delgado Gómez A, Abdel-Hamid A, Jordaan A, Piroska R, Post J, Szarzynski J, Walz Y, Dubovyk O 2017. Drought Dynamics and Vegetation Productivity in Different Land Management Systems of Eastern Cape, South Africa–A Remote Sensing Perspective. *Sustainability* 9, 10: 1728.

Grêt-Regamey A, Brunner SH, Altwegg J & Bebi P 2013. Facing uncertainty in ecosystem services-based resource management. *Journal of Environmental Management* 127, August: S145–S154

Grêt-Regamey A, Weibel B, Bagstad KJ, Ferrari M, Geneletti D, Klug H, Schirpke U & Tappeiner U 2014. On the effects of scale for ecosystem services mapping. *PLoS ONE* 9, 12: 1–26.

Guay KC, Beck PSA, Berner LT, Goetz SJ, Baccini A & Buermann W 2014. Vegetation productivity patterns at high northern latitudes: A multi-sensor satellite data assessment. *Global Change Biology* 20, 10: 3147–3158.

Gwate O, Mantel SK, Finca A, Gibson LA, Münch Z & Palmer AR 2016. Exploring the invasion of rangelands by Acacia mearnsii (black wattle): Biophysical characteristics and management implications. *African Journal of Range and Forage Science* 33, 4: 265–273.

Gwate O, Mantel SK, Gibson LA, Münch Z & Palmer AR 2018. Exploring dynamics of evapotranspiration in selected land cover classes in a sub-humid grassland: A case study in quaternary catchment S50E, South Africa. *Journal of Arid Environments* 157, February: 66–76.

Haboudane D 2004. Hyperspectral vegetation indices and novel algorithms for predicting green LAI of crop canopies: Modeling and validation in the context of precision agriculture. *Remote Sensing of Environment* 90, 3: 337–352.

Haines-Young R, Potschin M & Kienast F 2012. Indicators of ecosystem service potential at European scales: Mapping marginal changes and trade-offs. *Ecological Indicators* 21: 39–53.

Haining R 1993. *Spatial data analysis in the social and environmental sciences*. Cambridge University Press.

Halmy MWA, Gessler PE, Hicke JA & Salem BB 2015. Land use/land cover change detection and prediction in the north-western coastal desert of Egypt using Markov-CA. *Applied Geography* 63: 101–112.

Hansen MC & Loveland TR 2012. A review of large area monitoring of land cover change using Landsat data. *Remote Sensing of Environment* 122: 66–74.

Hansen MC, Roy DP, Lindquist E, Adusei B, Justice CO & Altstatt A 2008. A method for integrating MODIS and Landsat data for systematic monitoring of forest cover and change in the Congo Basin. *Remote Sensing of Environment* 112, 5: 2495–2513.

Hartshorne R 1939. The nature of geography: A critical survey of current thought in the light of the past. *Annals of the Association of American Geographers* 29, 3: 173.

Hauck J, Görg C, Varjopuro R, Ratamäki O, Maes J, Wittmer H & Jax K 2013. "Maps have an air of authority": Potential benefits and challenges of ecosystem service maps at different levels of decision making. *Ecosystem Services* 4: 25–32.

Henderson-Sellers A & Wilson MF 1983. Surface albedo data for climatic modeling. *Reviews of Geophysics* 21, 8: 1743.

Hobbs RJ 2016. Degraded or just different? Perceptions and value judgements in restoration decisions. *Restoration Ecology* 24, 2: 153–158.

Holden CE & Woodcock CE 2016. An analysis of Landsat 7 and Landsat 8 underflight data and the implications for time series investigations. *Remote Sensing of Environment* 185: 16–36.

Holobâcă I-H, Ivan K & Alexe M 2019. Extracting built-up areas from Sentinel-1 imagery using land cover classification and texture analysis. *International Journal of Remote Sensing* 40, 20: 8054–8069.

Homer C, Dewitz J, Yang L, Jin S, Danielson P, Xian G, Coulston J, Herold N, Wickham J & Megown K 2015. Completion of the 2011 national land cover database for the conterminous United States: Representing a decade of land cover change information. *Photogrammetric Engineering and Remote Sensing* 81, 5: 345–354.

Hong NS 1998. *The relationship between well-structured and ill-structured problem solving in multimedia simulation*. The Pensylvania State University.

Huang C & Asner GP 2009. Applications of remote sensing to alien invasive plant studies. *Sensors* 9, 6: 4869–4889.

Huete A, Didan K, Miura T, Rodriguez EP, Gao X & Ferreira LG 2002. Overview of the radiometric and biophysical performance of the MODIS vegetation indices. *Remote Sensing of Environment* 83, 1-2: 195–213.

Huffman GJ, Adler RF, Bolvin DT & Nelkin EJ 2010. The TRMM Multi-satellite Precipitation Analysis (TMPA). In Hossain F & Gebremichael M (eds) *Satellite Rainfall Applications for Surface Hydrology*, 3–22. New York, NY: Springer.

Huffman GJ, Bolvin DT, Nelkin EJ, Wolff DB, Adler RF, Gu G, Hong Y, Bowman KP & Stocker EF 2007. The TRMM Multisatellite Precipitation Analysis (TMPA): Quasi-Global, Multiyear, Combined-Sensor Precipitation Estimates at Fine Scales. *Journal of Hydrometeorology* 8, 1: 38–55.

Hughes RF, Archer SR, Asner GP, Wessman CA, McMurtry C, Nelson J & Ansley RJ 2006. Changes in aboveground primary production and carbon and nitrogen pools accompanying woody plant encroachment in a temperate savanna. *Global Change Biology* 12, 9: 1733–1747.

Hussain M, Chen D, Cheng A, Wei H & Stanley D 2013. Change detection from remotely sensed images: From pixel-based to object-based approaches. *ISPRS Journal of Photogrammetry and Remote Sensing* 80: 91–106.

Jansen LJM & Di Gregorio A 2002. Parametric land cover and land use classifications as tools for environmental change detection. *Agriculture, Ecosystems & Environment* 91, 1-3: 89–100.

Jewitt D, Goodman PS, Erasmus BFN, O'Connor T & Witkowski E 2015. Systematic land cover change in KwaZulu-Natal , South Africa : Implications for biodiversity. *South African Journal of Science* 111, 9: 1–9.

Jiang Z, Huete AR, Didan K & Miura T 2008. Development of a two-band enhanced vegetation index without a blue band. *Remote Sensing of Environment* 112, 10: 3833–3845.

Johnson GW, Snapp R, Villa F & Bagstad K 2012. Modelling ecosystem services flows under uncertainty with stochastic SPAN. In Seppelt et al. (eds) International Environmental Modelling and Software Society (iEMSs) 2012 International Congress on Environmental Modelling and Software. Managing Resources of a Limited Planet: Pathways and Visions under Uncertainty, Sixth Biennial Meeting, Leipzig, Germany.

Jones JP & Hanham RQ 1995. Contingency, realism, and the expansion method. *Geographical Analysis* 27, 3: 185–207.

Justice CO, Townshend JRG, Vermote EF, Masuoka E, Wolfe RE, Saleous N, Roy DP & Morisette JT 2002. An overview of MODIS Land data processing and product status. *Remote Sensing of Environment* 83, 1-2: 3–15.

Justice CO, Vermote EF, Townshend JRG, DeFries RS, Roy DP, Hall DK, Salomonson V V, Privette JL, Riggs G, Strahler AH, Lucht W, Myneni RB, Knyazikhin Y, Running SW, Nemani RR, Wan Z, Huete AR, van Leeuwen W, Wolfe RE, Giglio L, Muller JP, Lewis P & Barnsley M 1998. The Moderate Resolution Imaging

Spectroradiometer (MODIS): Land remote sensing for global change research. *Geoscience and Remote Sensing, IEEE Transactions on* 36, 4: 1228–1249.

Kahinda JM, Lillie ESB, Taigbenu AE, Taute M & Boroto RJ 2008. Developing suitability maps for rainwater harvesting in South Africa. *Physics and Chemistry of the Earth, Parts A/B/C* 33, 8: 788–799.

Kakembo V 2001. Trends in vegetation degradation in relation to land tenure, rainfall, and population changes in Peddie District, Eastern Cape, South Africa. *Environmental Management* 28, 1: 39–46.

Kamusoko C, Aniya M, Adi B & Manjoro M 2009. Rural sustainability under threat in Zimbabwe – Simulation of future land use/cover changes in the Bindura district based on the Markov-cellular automata model. *Applied Geography* 29, 3: 435–447.

Kandziora M, Burkhard B & Müller F 2013. Mapping provisioning ecosystem services at the local scale using data of varying spatial and temporal resolution. *Ecosystem Services* 4: 47–59.

Kauth RJ & Thomas GS 1976. *The tasseled cap-A graphic description of the spectral-temporal development of agricultural crops as seen by Landsat*. Proceedings of the Symposium on Machine Processing of Remotely Sensed Data. West Lafayette, IN: Purdue University.

Keesstra S, Nunes J, Novara A, Finger D, Avelar D, Kalantari Z & Cerdà A 2018. The superior effect of nature based solutions in land management for enhancing ecosystem services. *Science of The Total Environment* 610–611: 997–1009.

Kennedy RE, Andrefouet S, Cohen WB, Gomez C, Griffiths P, Hais M, Healey SP, Helmer EH, Hostert P, Lyons MB, Meigs GW, Pflugmacher D, Phinn SR, Powell SL, Scarth P, Sen S, Schroeder TA, Schneider A, Sonnenschein R, Vogelmann JE, Wulder MA & Zhu Z 2014. Bringing an ecological view of change to landsat-based remote sensing. *Frontiers in Ecology and the Environment* 12, 6: 339–346.

Kennedy RE, Cohen WB & Schroeder TA 2007. Trajectory-based change detection for automated characterization of forest disturbance dynamics. *Remote Sensing of Environment* 110, 3: 370–386.

Khatami R, Mountrakis G & Stehman S V. 2016. A meta-analysis of remote sensing research on supervised pixel-based land cover image classification processes: General guidelines for practitioners and future research. *Remote Sensing of Environment* 177: 89–100.

Khatami R, Mountrakis G & Stehman SV. 2017. Mapping per-pixel predicted accuracy of classified remote sensing images. *Remote Sensing of Environment* 191: 156–167.

Kinkeldey C 2014. Incorporating uncertainty information into exploratory land cover change analysis : A geovisual analytics approach. Doctoral dissertation. Hamburg, Germany: HafenCity Universität.

Kiruki HM, Van der Zanden EH, Malek Ž & Verburg PH 2017. Land cover change and woodland degradation in a charcoal producing semi-arid area in Kenya. *Land Degradation and Development* 28, 2: 472–481.

Kitchener KS & King PM 1981. Reflective judgment: Concepts of justification and their relationship to age and education. *Journal of Applied Developmental Psychology* 2, 2: 89–116.

Kolb M, Mas J-F & Galicia L 2013. Evaluating drivers of land use change and transition potential models in a complex landscape in Southern Mexico. *International Journal of Geographical Information Science* 27, 9: 1804–1827.

Koohafkan P, Lantieri D & Nachtergaele F 2003. *Land Degradation Assessment in Drylands (LADA): Guidelines for a methodological approach*. Rome: Land and water development division, Food and Agriculture Organization (FAO).

Kotzé I, Beukes H, Van der Berg E & Newby T 2010. *National invasive alien plant survey*. Report number: gw/a/2010/21. Stellenbosch, South Africa: ARC-Institute for Soil, Climate and Water.

Kuenzer C, Dech S & Wagner W 2015. *Remote Sensing Time Series*. [online]. Available from: http://link.springer.com/10.1007/978-3-319-15967-6 [Accessed 12 April 2017].

Kuenzer C, Ottinger M, Wegmann M, Guo H, Wang C, Zhang J, Dech S & Wikelski M 2014. Earth observation satellite sensors for biodiversity monitoring: Potentials and bottlenecks. *International Journal of Remote Sensing* 35, 18: 6599–6647.

Laliberte AS, Fredrickson EL & Rango A 2007. Combining decision trees with hierarchical object-oriented image analysis for mapping arid rangelands. *Photogrammetric Engineering and Remote Sensing* 73: 197–207.

Lambin EF, Geist HJ & Lepers E 2003. Dynamics of land use and land cover change in tropical regions. *Annual Review of Environment and Resources* 28, 1: 205–241.

Lang S 2008. Object-based image analysis for remote sensing applications: Modeling reality – dealing with complexity. In Blaschke T, Lang S & Hay GJ (eds) *Object-Based Image Analysis. Lecture Notes in Geoinformation and Cartography*, 3–27. Berlin, Heidelberg: Springer.

Lasaponara R & Lanorte A 2012. Satellite time series analysis. *International Journal of Remote Sensing* 33, 15: 4649–4652.

Lautenbach S, Mupepele A, Dormann CF, Lee H, Schmidt S, Scholte SS, Seppelt R, van Teeffelen AJ, Verhagen W & Volk M 2015. Blind spots in ecosystem services research and implementation. *BioRxiv*, p.033498. [online]. Available from: https://doi.org/10.1101/033498 [Accessed 5 May 2017].

Lavorel S, Bayer A, Bondeau A, Lautenbach S, Ruiz-Frau A, Schulp N, Seppelt R, Verburg PH, Van Teeffelen AJA, Vannier C, Arneth A, Cramer W & Marba N 2017. Pathways to bridge the biophysical realism gap in ecosystem services mapping approaches. *Ecological Indicators* 74: 241–260.

Lavorel S, Grigulis K, Lamarque P, Colace M-P, Garden D, Girel J, Pellet G & Douzet R 2011. Using plant functional traits to understand the landscape distribution of multiple ecosystem services. *Journal of Ecology* 99, 1: 135–147.

Le Maitre DC, Forsyth GG, Dzikiti S & Gush MB 2016. Estimates of the impacts of invasive alien plants on water flows in South Africa. *Water SA* 42, 4: 659–672.

Le Maitre DC, Gush MB & Dzikiti S 2015. Impacts of invading alien plant species on water flows at stand and catchment scales. *AoB PLANTS* 7, 1: 1-21.

Le Maitre DC, O'Farrell PJ & Reyers B 2007. Ecosystems services in South Africa: A research theme that can engage environmental, economic and social scientists in the development of sustainability science? *South African Journal of Science* 103, 9-10: 367–376.

Lei T, Pang Z, Wang X, Li L, Fu J, Kan G, Zhang X, Ding L, Li J, Huang S & Shao C 2016. Drought and carbon cycling of grassland ecosystems under global change: A Review. *Water* 8, 10: 460.

Li J & Roy DP 2017. A global analysis of Sentinel-2A, Sentinel-2B and Landsat-8 data revisit intervals and implications for terrestrial monitoring. *Remote Sensing* 9, 9: 902.

Li M, Zang S, Zhang B, Li S & Wu C 2014. A review of remote sensing image classification techniques: The role of spatio-contextual information. *European Journal of Remote Sensing* 47, 1: 389–411.

Li X, Myint SW, Zhang Y, Galletti C, Zhang X & Turner BL 2014. Object-based land cover classification for metropolitan Phoenix, Arizona, using aerial photography. *International Journal of Applied Earth Observation and Geoinformation* 33, 1: 321–330.

Li Z, Xu D & Guo X 2014. Remote sensing of ecosystem health: opportunities, challenges, and future perspectives. *Sensors (Basel, Switzerland)* 14, 11: 21117–21139.

Liang S 2001. Narrowband to broadband conversions of land surface albedo I Algorithms. *Remote Sensing of Environment* 76, 2000: 213–238.

Liang S, Shuey CJ, Russ AL, Fang H, Chen M, Walthall CL, Daughtry CST & Hunt R 2003. Narrowband to broadband conversions of land surface albedo: II. Validation. *Remote Sensing of Environment* 84, 1: 25–41.

Liebetrau AM 1983. Measures of Association; Quantitative Applications in the Social Sciences Series, Volume 32. Newbury Park, CA, USA: Sage Publications.

Linke J, McDermid GJ, Pape AD, McLane AJ, Laskin DN, Hall-Beyer M & Franklin SE 2009. The influence of patch-delineation mismatches on multi-temporal landscape pattern analysis. *Landscape Ecology* 24, 2: 157–170.

Liu D & Cai S 2012. A spatial-temporal modeling approach to reconstructing land cover change trajectories from multi-temporal satellite imagery. *Annals of the Association of American Geographers* 102, 6: 1329–1347.

Liu D & Xia F 2011. Assessing object-based classification: advantages and limitations. *Remote Sensing Letters* 1: 187-194.

Loarie SR, Lobell DB, Asner GP & Field CB 2011. Land cover and surface water change drive large albedo increases in South America. *Earth Interactions* 15, 7: 1–16.

Long H & Qu Y 2018. Land use transitions and land management: A mutual feedback perspective. *Land Use Policy* 74: 111–120.

Lorenzo P, Rodríguez J, González L & Rodríguez-Echeverría S 2016. Changes in microhabitat, but not allelopathy, affect plant establishment after Acacia dealbata invasion. *Journal of Plant Ecology* 10, 4: 610–617.

Loveland TR, Reed BC, Brown JF, Ohlen DO, Zhu Z, Yang L & Merchant JW 2000. Development of a global land cover characteristics database and IGBP DISCover from 1 km AVHRR data. *International Journal of Remote Sensing* 21, 6-7: 1303–1330.

Lovett GM, Jones CG, Turner MG & Weathers KC 2005. Ecosystem function in heterogeneous landscapes. In *Ecosystem Function in Heterogeneous Landscapes*, 1–4. New York, NY: Springer New York.

Lowry JH, Douglas Ramsey R, Stoner LL, Kirby J & Schulz K 2008. An ecological framework for evaluating map errors using fuzzy sets. *Photogrammetric Engineering & Remote Sensing* 74, 12: 1509–1519.

Lu D, Mausel P, Brondízio E & Moran E 2004. Change detection techniques. *International Journal of Remote Sensing* 25, 12: 2365–2401.

Lück W & Diemer N 2008. Landcover class definition report. Prepared for Chief Directorate of Surveys and Mapping. Pretoria: CSIR Satellite Applications Centre.

Lück W, Mhangara P, Kleyn L & Remas H 2010. Landcover Field Guide. Prepared for Chief Directorate of Surveys and Mapping. Pretoria: CSIR Satellite Applications Centre.

Lutz DA & Howarth RB 2014. Valuing albedo as an ecosystem service: Implications for forest management. *Climatic Change* 124, 1–2: 53–63.

MacFadyen S, Hui C, Verburg PH & Van Teeffelen AJA 2016. Quantifying spatio-temporal drivers of environmental heterogeneity in Kruger National Park, South Africa. *Landscape Ecology* 31, 9: 2013–2029.

MacLean MG & Congalton RG 2012. Map accuracy assessment issues when using an object-oriented approach. In *Proceedings of the American Society for Photogrammetry and Remote Sensing*, 1–5. Sacramento, California: American Society for Photogrammetry and Remote Sensing (ASPRS).

Macleod RD & Congalton RG 1998. A Quantitative Comparison of Change Detection Algorithms for Monitoring Eelgrass from Remotely Sensed Data. *Photogrammetric Engineering & Remote Sensing* 64, 3: 207–216.

Maes J, Egoh B, Willemen L, Liquete C, Vihervaara P, Schägner JP, Grizzetti B, Drakou EG, La Notte A, Zulian G, Bouraoui FF, Luisa Paracchini M, Braat L & Bidoglio G 2012. Mapping ecosystem services for policy support and decision making in the European Union. *Ecosystem Services* 1, 1: 31–39.

Maherry A, Tredoux G, Clarke S & Engelbrecht P 2010. *State of Nitrate Pollution in Groundwater in South Africa*. [online]. Available from: http://researchspace.csir.co.za/dspace/bitstream/10204/4288/1/Maherry_2010_P.pdf [Accessed 5 May 2017].

Malek Ž, Scolobig A & Schröter D 2014. Understanding land cover changes in the Italian Alps and Romanian Carpathians combining remote sensing and stakeholder interviews. *Land* 3: 52–73.

Malingreau J-P 1986. Global vegetation dynamics: Satellite observations over Asia. *International Journal of Remote Sensing* 7, 9: 1121–1146.

Mann HB 1945. Nonparametric tests against trend. *Econometrica* 13: 245–259.

Marceau DJ 1999. The scale issue in the social and natural sciences. *Canadian Journal of Remote Sensing* 25, 4: 347–356.

Martínez-Harms MJ & Balvanera P 2012. Methods for mapping ecosystem service supply: A review. *International Journal of Biodiversity Science, Ecosystem Services & Management* 8, 1-2: 17–25.

Mas J-F 1999. Monitoring land cover changes: A comparison of change detection techniques. *International Journal of Remote Sensing* 20, 1: 139–152.

Mas J-F, Kolb M, Paegelow M, Camacho Olmedo MT & Houet T 2014. Inductive pattern-based land use/cover change models: A comparison of four software packages. *Environmental Modelling & Software* 51, 51: 94–111.

Mas J-F, Soares Filho B, Pontius RG, Farfán Gutiérrez M & Rodrigues H 2013. A suite of tools for ROC Analysis of spatial models. *ISPRS International Journal of Geo-Information* 2, 3: 869–887.

Matthews HD, Weaver AJ, Meissner KJ, Gillett NP & Eby M 2004. Natural and anthropogenic climate change: incorporating historical land cover change, vegetation dynamics and the global carbon cycle. *Climate Dynamics* 22, 5: 461–479.

McGwire KC & Fisher P 2001. Spatially variable thematic accuracy: Beyond the confusion matrix. In *Spatial Uncertainty in Ecology*, 308–329. New York, NY: Springer.

MEA 2005. *Millennium ecosystem assessment. Ecosystems and Human Well-Being: Biodiversity Synthesis*. Washington, DC: World Resources Institute.

Megahed Y, Cabral P, Silva J & Caetano M 2015. Land cover mapping analysis and urban growth modelling using remote sensing techniques in Greater Cairo Region—Egypt. *ISPRS International Journal of Geo-Information* 4, 3: 1750–1769.

Meijninger WML & Jarmain C 2014. Satellite-based annual evaporation estimates of invasive alien plant species and native vegetation in South Africa. *Water SA* 40, 1: 95–107.

Meskell L 2011. *The nature of heritage: The new South Africa*. John Wiley & Sons.

Midekisa A, Holl F, Savory DJ, Andrade-Pacheco R, Gething PW, Bennett A & Sturrock HJW 2017. Mapping land cover change over continental Africa using Landsat and Google Earth Engine cloud computing Schumann GJ-P (ed). *PLOS ONE* 12, 9: e0184926.

Miller JA & Hanham RQ 2011. Spatial nonstationarity and the scale of species–environment relationships in the Mojave Desert, California, USA. *International Journal of Geographical Information Science* 25, 3: 423–438.

Milne A 1959. The centric systematic area-sample treated as a random sample. *Biometrics* 15, 2: 270–297.

Monteith JL 1965. Evaporation and environment. *Symposia of Society for Experimental Biology* 19, 205–234.

Moser G, Serpico SB & Benediktsson JA 2013. Land cover mapping by Markov Modeling of spatial–contextual information in very-high-resolution remote sensing images. *Proceedings of the IEEE* 101, 3: 631–651.

Mu Q, Heinsch FA, Zhao M & Running SW 2007. Development of a global evapotranspiration algorithm based on MODIS and global meteorology data. *Remote Sensing of Environment* 111, 4: 519–536.

Mu Q, Zhao M & Running SW 2011. Improvements to a MODIS global terrestrial evapotranspiration algorithm. *Remote Sensing of Environment* 115, 8: 1781–1800.

Mucina L & Rutherford MC 2006. *The Vegetation Map of South Africa, Lesotho and Swaziland*. Pretoria: South African National Botanical Institute. [online]. Available from: http://www.sanbi.org/products/publications/stelitzia.htm [Accessed 5 May 2017].

Mudau N 2010. SPOT building count supporting informed decisions. *Position IT* 10: 51–52.

Münch Z, Okoye PI, Gibson L, Mantel S & Palmer A 2017. Characterizing degradation gradients through land cover change analysis in rural Eastern Cape, South Africa. *Geosciences* 7, 1: 7.

Munyati C & Ratshibvumo T 2011. Characterising vegetation cover in relation to land use in the Inkomati catchment, South Africa, using Landsat imagery. *Area* 43, 2: 189–201.

Nackley LL, West AG, Skowno AL & Bond WJ 2017. The nebulous ecology of native invasions. *Trends in Ecology and Evolution* 32, 11: 814–824.

Nagendra H, Munroe DK & Southworth J 2004. From pattern to process: Landscape fragmentation and the analysis of land use/land cover change. *Agriculture, Ecosystems and Environment* 101, 2-3: 111–115.

Nahlik AM, Kentula ME, Fennessy MS & Landers DH 2012. Where is the consensus? A proposed foundation for moving ecosystem service concepts into practice. *Ecological Economics* 77: 27–35.

NDMC 2007. *National Disaster Management Centre Inagural Annual Report 2006/2007*. Pretoria, South Africa: Department of Local and Provincial Government.

Nemec KT & Raudsepp-Hearne C 2013. The use of geographic information systems to map and assess ecosystem services. *Biodiversity and Conservation* 22, 1: 1–15.

Ngorima A & Shackleton CM 2019. Livelihood benefits and costs from an invasive alien tree (Acacia dealbata) to rural communities in the Eastern Cape, South Africa. *Journal of Environmental Management* 229: 158–165.

Nikolakopoulos KG 2008. Comparison of nine fusion techniques for very high resolution data. *Photogrammetric Engineering and Remote Sensing* 74: 647–659.

O'Connor TG, Puttick JR & Hoffman MT 2014. Bush encroachment in southern Africa: Changes and causes. *African Journal of Range and Forage Science* 31, 2: 67–88.

Oelofse M, Birch-Thomsen T, Magid J, De Neergaard A, Van Deventer R, Bruun S & Hill T 2016. The impact of black wattle encroachment of indigenous grasslands on soil carbon, Eastern Cape, South Africa. *Biological Invasions* 18, 2: 445–456.

Okoye PI 2016. Grassland rehabilitation after alien invasive tree eradication: Landscape degradation and sustainability in rural Eastern Cape. Master's thesis. Stellenbosch: Stellenbosch University.

Oksanen J, Blanchet FG, Friendly M, Kindt R, Legendre P, McGlinn D, Minchin PR, O'Hara RB, Simpson GL, Solymos P, Stevens MHH, Szoecs E & Wagner H 2018. Vegan: Community ecology package.

Olofsson P, Foody GM, Herold M, Stehman S V., Woodcock CE & Wulder MA 2014. Good practices for estimating area and assessing accuracy of land change. *Remote Sensing of Environment* 148: 42–57.

Olofsson P, Foody GM, Stehman SV. & Woodcock CE 2013. Making better use of accuracy data in land change studies: Estimating accuracy and area and quantifying uncertainty using stratified estimation. *Remote Sensing of Environment* 129: 122–131.

Openshaw S & Taylor P 1979. A million or so correlation coefficients: Three experiments on the modifiable areal unit problem. In *Statistical Applications in the Spatial Sciences*, 127–144. London, UK: Pion.

Ortiz-Burgos S 2016. Shannon-Weaver Diversity Index. In Kennish MJ (ed) *Encyclopedia of Earth Sciences*

Series, 572–573. Dordrecht, Netherlands: Springer.

Overmars KP, De Groot WT & Huigen MGA 2007. Comparing inductive and deductive modeling of land use decisions: Principles, a model and an illustration from the Philippines. *Human Ecology* 35, 4: 439–452.

Ozdogan M & Woodcock CE 2006. Resolution dependent errors in remote sensing of cultivated areas. *Remote Sensing of Environment* 103, 2: 203–217.

Paegelow M & Camacho MO 2008. Advances in geomatic simulations for environmental dynamics. In Paegelow M & Camacho Olmedo MT (eds) *Modelling Environmental Dynamics. Advances in Geomatic Simulations*, 3–54. Berlin, Heidelberg: Springer.

Paegelow M, Camacho Olmedo MT, Mas JF, Houet T & Pontius RG 2013. Land change modelling: Moving beyond projections. *International Journal of Geographical Information Science* 27, 9: 1691–1695.

Pal M & Mather PM 2003. An assessment of the effectiveness of decision tree methods for land cover classification. *Remote Sensing of Environment* 86, 4: 554–565.

Pal M & Mather PM 2005. Support vector machines for classification in remote sensing. *International Journal of Remote Sensing* 26, 5: 1007–1011.

Palmer AR, Finca A, Mantel SK, Gwate O, Münch Z & Gibson LA 2017. Determining fPAR and leaf area index of several land cover classes in the Pot River and Tsitsa River catchments of the Eastern Cape, South Africa. *African Journal of Range and Forage Science* 34, 1: 33–37.

Pasquarella VJ, Holden CE, Kaufman L & Woodcock CE 2016. From imagery to ecology: Leveraging time series of all available Landsat observations to map and monitor ecosystem state and dynamics. *Remote Sensing in Ecology and Conservation* 2, 3: 152–170.

Pebesma E, Bivand R, Rowlingson B, Gomez-Rubio V, Hijmans R, Sumner M, MacQueen D, Lemon J, O'Brien J & O'Rourke J 2018. Package "sp" title classes and methods for spatial data.

Perera AH, Sturtevant BR & Buse LJ 2015. Simulation modeling of forest landscape disturbances: Where do we go from here? In Perera AH Sturtevant BR & Buse LJ (eds) *Simulation Modeling of Forest Landscape Disturbances*, 287–311. Springer International Publishing Switzerland.

Pérez-Hoyos A, García-Haro FJ & San-Miguel-Ayanz J 2012. Conventional and fuzzy comparisons of large scale land cover products: Application to CORINE, GLC2000, MODIS and GlobCover in Europe. *ISPRS Journal of Photogrammetry and Remote Sensing* 74: 185–201.

Pérez-Vega A, Mas J-F & Ligmann-Zielinska A 2012. Comparing two approaches to land use/cover change modeling and their implications for the assessment of biodiversity loss in a deciduous tropical forest. *Environmental Modelling & Software* 29, 1: 11–23.

Petit CC, Baguette M, Dumont JP, Lambin EF & Petit S 2002. Impact of data integration technique on historical land use / landcover change : Comparing historical maps with remote sensing data in the Belgian Ardennes. *Landscape Ecology* 17, 2: 117–132.

Pinzon JE & Tucker CJ 2014. A non-stationary 1981–2012 AVHRR NDVI3g time series. *Remote Sensing* 6, 8: 6929–6960.

Pontius RG 2002. Statistical methods to partition effects of quantity and location during comparison of categorical maps at multiple resolutions. *Photogrammetric Engineering and Remote Sensing* 68, 10: 1041–1050.

Pontius RG 2019. Component intensities to relate difference by category with difference overall. *International Journal of Applied Earth Observation and Geoinformation* 77: 94–99.

Pontius RG & Chen H 2006. GEOMOD Modeling: Land use & cover change modeling. Tutorial notes. Worcester, MA: Clark University, Clark Labs, 1–44.

Pontius RG & Cheuk ML 2006. A generalized cross-tabulation matrix to compare soft-classified maps at multiple

resolutions. *International Journal of Geographical Information Science* 20, 1: 1–30.

Pontius RG, Cornell JD & Hall CA. 2001. Modeling the spatial pattern of land use change with GEOMOD2: application and validation for Costa Rica. *Agriculture, Ecosystems & Environment* 85, 1-3: 191–203.

Pontius RG, Gao Y, Giner N, Kohyama T, Osaki M & Hirose K 2013. Design and interpretation of intensity analysis illustrated by land change in central Kalimantan, Indonesia. *Land* 2, 3: 351–369.

Pontius RG, Huffaker D & Denman K 2004. Useful techniques of validation for spatially explicit land change models. *Ecological Modelling* 179, 4: 445–461.

Pontius RG & Li X 2010. Land transition estimates from erroneous maps. *Journal of Land Use Science* 5, 1: 31–44.

Pontius RG & Lippitt CD 2006. Can error explain map differences over time? *Cartography and Geographic Information Science* 33, 2: 159–171.

Pontius RG & Malizia NR 2004. Effect of category aggregation on map comparison. In Egenhofer MJ, Freksa C & Miller HJ (eds) *Geographic Information Science*, Proceedings of Third International Conference 251–268. Adelphi, MD. Berlin Heidelberg, Germany: Springer.

Pontius RG & Millones M 2011. Death to Kappa: Birth of quantity disagreement and allocation disagreement for accuracy assessment. *International Journal of Remote Sensing* 32, 15: 4407–4429.

Pontius RG & Santacruz A 2014. Quantity, exchange, and shift components of difference in a square contingency table. *International Journal of Remote Sensing* 35, 21: 7543–7554.

Pontius RG & Santacruz A 2015. Package 'diffeR': Metrics of difference for comparing pairs of maps: 23. [online]. Available from: https://cran.r-project.org/web/packages/diffeR/diffeR.pdf [Accessed 12 April 2017].

Pontius RG & Schneider LC 2001. Land-cover change model validation by an ROC method for the Ipswich watershed, Massachusetts, USA. *Agriculture, Ecosystems & Environment* 85, 1-3: 239-248.

Pontius RG, Shusas E & McEachern M 2004. Detecting important categorical land changes while accounting for persistence. *Agriculture, Ecosystems and Environment* 101, 2-3: 251–268.

Puertas OL, Brenning A & Meza FJ 2013. Balancing misclassification errors of land cover classification maps using support vector machines and Landsat imagery in the Maipo river basin (Central Chile, 1975-2010). *Remote Sensing of Environment* 137: 112–123.

Quan B, Ren H, Pontius RG & Liu P 2018. Quantifying spatio-temporal patterns concerning land change in Changsha, China. *Landscape and Ecological Engineering* 14, 2: 257–267.

R Core Team 2017. R: A language and environment for statistical computing. [online]. Available from: https://www.r-project.org/ [Accessed 8 October 2018].

Radoux J & Defourny P 2007. A quantitative assessment of boundaries in automated forest stand delineation using very high resolution imagery. *Remote Sensing of Environment* 110: 468–475.

Ramoelo A, Cho M, Mathieu R & Skidmore AK 2015. Potential of Sentinel-2 spectral configuration to assess rangeland quality. *Journal of Applied Remote Sensing* 9, 1: 094096.

Ramoelo A, Majozi N, Mathieu R, Jovanovic N, Nickless A & Dzikiti S 2014. Validation of global evapotranspiration product (MOD16) using flux tower data in the African Savanna, South Africa. *Remote Sensing* 6, 8: 7406–7423.

Reyers B, O'Farrell PJ, Cowling RM, Egoh BN, Le Maitre DC & Vlok JHJ 2009. Ecosystem services, land cover change, and stakeholders: Finding a sustainable foothold for a semiarid biodiversity hotspot. *Ecology and Society* 14, 1: 1-23.

Reyers B, Rouget M, Jonas Z, Cowling RM, Driver A, Maze K & Desmet P 2007. Developing products for

conservation decision-making: lessons from a spatial biodiversity assessment for South Africa. *Diversity and Distributions* 13, 5: 608–619.

Richter R & Schlapfer D 2013. *Atmospheric/Topographic Correction for Airborne Imagery: ATCOR-4 User Guide*. Wessling, Germany: German Aerospace Center (DLR).

Rindfuss RR, Walsh SJ, Turner BL, Fox J & Mishra V 2004. Developing a science of land change: Challenges and methodological issues. *Proceedings of the National Academy of Sciences of the United States of America* 101, 39: 13976–13981.

Robinson GM & Carson DA 2013. Applying landscape science to natural resource management. *Ecology and Society* 18, 1: art32.

Röder A, Udelhoven T, Hill J, Del Barrio G & Tsiourlis G 2008. Trend analysis of Landsat-TM and -ETM+ imagery to monitor grazing impact in a rangeland ecosystem in Northern Greece. *Remote Sensing of Environment* 112, 6: 2863–2875.

Rodríguez-Echeverría S, Afonso C, Correia M, Lorenzo P & Roiloa SR 2013. The effect of soil legacy on competition and invasion by Acacia dealbata Link. *Plant Ecology* 214, 9: 1139–1146.

Rotenberg E & Yakir D 2010. Contribution of semi-arid forests to the climate system. *Science* 327, 5964: 451–455.

Roy DP, Wulder MA, Loveland TR, Woodcock CE, Allen RG, Anderson MC, Helder D, Irons JR, Johnson DM, Kennedy R, Scambos TA, Schaaf CB, Schott JR, Sheng Y, Vermote EF, Belward AS, Bindschadler R, Cohen WB, Gao F, Hipple JD, Hostert P, Huntington J, Justice CO, Kilic A, Kovalskyy V, Lee ZP, Lymburner L, Masek JG, McCorkel J, Shuai Y, Trezza R, Vogelmann J, Wynne RH & Zhu Z 2014. Landsat-8: Science and product vision for terrestrial global change research. *Remote Sensing of Environment* 145: 154–172.

Runfola DSM & Pontius RG 2013. Measuring the temporal instability of land change using the flow matrix. *International Journal of Geographical Information Science* 27, 9: 1696–1716.

Running S & Mu Q 2015. MOD17A3H MODIS/Terra Gross Primary Productivity Yearly L4 Global 500m SIN Grid. NASA LP DAAC.

Saaty TL 1978. Modeling unstructured decision problems: The theory of analytical hierarchies. *Mathematics and Computers in Simulation* 20, 3: 147–158.

Samberg LH, Gerber JS, Ramankutty N, Herrero M & West PC 2016. Subnational distribution of average farm size and smallholder contributions to global food production. *Environmental Research Letters* 11: 124010.

Savage M, Everson C, Odhiambo G, Mengistu M & Jarmain C 2004. *Theory and practice of evaporation measurement, with special focus on surface layer scintillometry as an operational tool for the estimation of spatially of spatially averaged evaporation*. *Water Research Commission Report No 1335/1/04*

Schaaf CB, Gao F, Strahler AH, Lucht W, Li X, Tsang T, Strugnell NC, Zhang X, Jin Y, Muller J-P, Lewis P, Barnsley M, Hobson P, Disney M, Roberts G, Dunderdale M, Doll C, d'Entremont RP, Hu B, Liang S, Privette JL & Roy D 2002. First operational BRDF, albedo nadir reflectance products from MODIS. *Remote Sensing of Environment* 83, 1-2: 135–148.

Schoeman F, Newby TS, Thomson MW & Van den Berg EC 2013. South African National Land cover Change Map. *South African Journal of Geomatics* 2, 2: 94–105.

Scholes RJ & Archer SR 1997. Tree-grass interactions in savannas. *Annual Review of Ecology and Systematics* 28, 1: 517–544.

Schulze RE 2007. Rainfall: Background. In Schulze RE (ed) *South African Atlas of Climatology and Agrohydrology, WRC Report 1489/1/06*. Pretoria, South Africa: Water Research Commission.

Scorer C, Mantel SK & Palmer AR 2019. Do abandoned farmlands promote spread of invasive alien plants?

Change detection analysis of black wattle in montane grasslands of the Eastern Cape. *South African Geographical Journal* 101, 1: 36–50.

Sen PK 1968. Estimates of regression coefficient based on Kendall's Tau. *Journal of American Statistical Association* 63, 324: 1379–1389.

Seppelt R, Dormann CF, Eppink FV., Lautenbach S & Schmidt S 2011. A quantitative review of ecosystem service studies: Approaches, shortcomings and the road ahead. *Journal of Applied Ecology* 48, 3: 630–636.

Shackleton CM, McGarry D, Fourie S, Gambiza J, Shackleton SE & Fabricius C 2007. Assessing the effects of invasive alien species on rural livelihoods: Case examples and a framework from South Africa. *Human Ecology* 35, 1: 113–127.

Shackleton CM, Ruwanza S, Sinasson Sanni GK, Bennett S, De Lacy P, Modipa R, Mtati N, Sachikonye M & Thondhlana G 2016. Unpacking Pandora's Box: Understanding and categorising ecosystem disservices for environmental management and human wellbeing. *Ecosystems* 19, 4: 587–600.

Sholto-Douglas C, Shackleton CM, Ruwanza S & Dold T 2017. The effects of expansive shrubs on plant species richness and soils in semi-arid communal lands, South Africa. *Land Degradation and Development* 28, 7: 2191–2206.

Siegel AF 1982. Robust regression using repeated medians. *Biometrika* 69, 1: 242–244.

Singh A 1989. Review article: Digital change detection techniques using remotely sensed data. *International Journal of Remote Sensing* 10, 6: 989–1003.

Skidmore AK, Bijker W, Schmidt K & Kumar L 1997. Use of remote sensing and gis for sustainable land management. *ITC Journal* 3, 4: 302–315.

Skowno AL 2018. Woody plant encroachment in arid and mesic South African savanna-grasslands: same picture, different story? Doctoral dissertation. Grahamstown: Rhodes University. [online]. Available from: http://opus.sanbi.org/bitstream/20.500.12143/5786/1/Skowno%20PhD%20Final%2012March2018.pdf [Accessed 12 June 2019].

Skowno AL, Thompson MW, Hiestermann J, Ripley B, West AG & Bond WJ 2017. Woodland expansion in South African grassy biomes based on satellite observations (1990-2013): General patterns and potential drivers. *Global Change Biology* 23, 6: 2358–2369.

Small C 2005. A global analysis of urban reflectance. International Journal of Remote Sensing 26, 4: 661–681.

Steele BM, Winne J & Redmond RL 1998. Estimation and mapping of misclassification probabilities for thematic land cover maps. *Remote Sensing of Environment* 66, 2: 192–202.

Steffen W, Jager J, Carson DJ & Bradshaw C (eds) 2003. *Challenges of a Changing Earth. Series: Global Change: The IGBP Series*. Heidelberg, Germany: Springer.

Stehman S V. 2009. Model-assisted estimation as a unifying framework for estimating the area of land cover and land cover change from remote sensing. *Remote Sensing of Environment* 113, 11: 2455–2462.

Stehman SV 2014. Estimating area and map accuracy for stratified random sampling when the strata are different from the map classes. *International Journal of Remote Sensing* 35, 13: 4923–4939.

Stehman SV & Wickham JD 2006. Assessing accuracy of net change derived from land cover maps. *Photogrammetric Engineering and Remote Sensing* 72, 2: 175–185.

Stehman SV, Sohl TL & Loveland TR 2003. Statistical sampling to characterize recent United States land cover change. *Remote Sensing of Environment* 86, 4: 517–529.

Stott A & Haines-Young R 1998. Linking land cover, intensity of use and botanical diversity in an accounting framework in the UK. In Uno K & Bartelmus P (eds) *Environmental Accounting in Theory and Practice*, 245–260. Dordrecht: Springer Netherlands.

Strahler AH, Boschetti L, Foody GM, Friedl MA., Hansen C, Herold M, Mayaux P, Morisette JT, Stehman SV & Woodcock CE 2006. *Global land cover validation: Recommendations for evaluation and accuracy assessment of global land cover maps.* Luxembourg: European Communities 51.4.

Sulkava M, Luyssaert S, Rautio P, Janssens IA & Hollmén J 2007. Modeling the effects of varying data quality on trend detection in environmental monitoring. *Ecological Informatics* 2, 2: 167–176.

Swann ALS, Fung IY & Chiang JCH 2012. Mid-latitude afforestation shifts general circulation and tropical precipitation. *Proceedings of the National Academy of Sciences of the United States of America* 109, 3: 712–716.

Sweeney S, Ruseva T, Estes L & Evans T 2015. Mapping cropland in smallholder-dominated savannas: integrating remote sensing techniques and probabilistic modeling. *Remote Sensing* 7, 11: 15295–15317.

Szantoi Z, Brink A, Buchanan G, Bastin L, Lupi A, Simonetti D, Mayaux P, Peedell S & Davy J 2016. A simple remote sensing based information system for monitoring sites of conservation importance. In Nagendra H & Rocchini D (eds) *Remote Sensing in Ecology and Conservation* 2, 1: 16–24.

Teixeira Z, Marques JC & Pontius RG 2016. Evidence for deviations from uniform changes in a Portuguese watershed illustrated by CORINE maps: An intensity analysis approach. *Ecological Indicators* 66, June: 282–290.

Tewkesbury AP, Comber AJ, Tate NJ, Lamb A & Fisher PF 2015. A critical synthesis of remotely sensed optical image change detection techniques. *Remote Sensing of Environment* 160: 1–14.

Theil H 1950. A rank invariant method for linear and polynomial regression analysis. *Koninklijke Nederlandse Akademie van Wetenschappen Proceedings. Series A.* 53, Part I: 386–392, 521–525, 1397–1412.

Thomas A 2015. Modelling of spatially distributed surface runoff and infiltration in the Olifants River catchment/water management area using GIS. *International Journal of Advanced Remote Sensing and GIS* 4, 1: 828–862.

Tobler W 1970. A computer movie simulating urban growth in the Detroit region. *Economic Geography* 46, Supplement: 234–240.

Trenberth KE, Fasullo JT, Kiehl J, Trenberth KE, Fasullo JT & Kiehl J 2009. Earth's global energy budget. *Bulletin of American Meteorological Society* 90, 3: 311–324.

Troy A & Wilson MA 2006. Mapping ecosystem services: Practical challenges and opportunities in linking GIS and value transfer. *Ecological Economics* 60, 2: 435–449.

Tseng M-H, Chen S-J, Hwang G-H & Shen M-Y 2007. A genetic algorithm rule-based approach for land cover classification. *ISPRS Journal of Photogrammetry and Remote Sensing* 63: 202–212.

Tsutsumida N & Comber AJ 2015. Measures of spatio-temporal accuracy for time series land cover data. *International Journal of Applied Earth Observation and Geoinformation* 41: 46–55.

Tucker CJ, Justice CO & Prince SD 1986. Monitoring the grasslands of the Sahel 1984-1985. *International Journal of Remote Sensing* 7, 11: 1571–1581.

Tucker CJ, Pinzon JE, Brown ME, Slayback DA, Pak EW, Mahoney R, Vermote EF & El Saleous N 2005. An extended AVHRR 8-km NDVI dataset compatible with MODIS and SPOT vegetation NDVI data. *International Journal of Remote Sensing* 26, 20: 4485–98.

Turner BL 2009. Land change (systems) science. In Castree N, Demeritt D, Liverman D & Rhoads B (eds) *A Companion to Environmental Geography (Blackwell Companions to Geography)*, John Wiley & Sons.

Turner BL 2017. Land change science. In *International Encyclopedia of Geography: People, the Earth, Environment and Technology*, 1–6. Oxford, UK: John Wiley & Sons.

Turner BL, Lambin EF & Reenberg A 2007. The emergence of land change science for global environmental

change and sustainability. *Proceedings of the National Academy of Sciences* 104, 52: 20666–20671.

Turner MG & Gardner RH 1991. *Quantitative methods in landscape ecology*. New York: Springer.

Turner MG & Gardner RH 2015. *Landscape Ecology in Theory and Practice*. New York: Springer.

Turner BL & Robbins P 2008. Land change science and political ecology: Similarities, differences, and implications for sustainability science. *Annual Review of Environment and Resources* 33, 1: 295–316.

Turpie JK, Marais C & Blignaut JN 2008. The working for water programme: evolution of a payments for ecosystem services mechanism that addresses both poverty and ecosystem service delivery in South Africa. *Ecological Economics* 65: 788–798.

USGS 2004. Shuttle Radar Topography Mission, 1 Arc Second scene SRTM, Filled Finished 2.0, Global Land Cover Facility, University of Maryland, College Park, Maryland, February 2000.

Van den Berg E, Kotzé I & Beukes H 2013. Detection, quantification and monitoring of Prosopis in the Northern Cape Province of South Africa using remote sensing and GIS. *South African Journal of Geomatics* 2, 2: 68–81.

Van den Berg EC, Plarre C, Van den Berg HM & Thompson MW 2008. *The South African National Land Cover 2000, Report GW/A/2008/86*. Pretoria, South Africa: Agricultural Research Council-Institute for Soil, Climate and Water.

Van Niekerk A 2013. *Stellenbosch University Digital Elevation Model (SUDEM)*. Working Paper 2013 Edition Version 13.24. Stellenbosch, South Africa: Centre for Geographical Analysis, Stellenbosch University.

Van Wilgen BW & Richardson DM 2014. Challenges and trade-offs in the management of invasive alien trees. *Biological Invasions* 16, 3: 721–734.

Van Wilgen BW & Wannenburgh A 2016. Co-facilitating invasive species control, water conservation and poverty relief: Achievements and challenges in South Africa's Working for Water programme. *Current Opinion in Environmental Sustainability* 19: 7–17.

Van Wilgen BW, Forsyth GG, Le Maitre DC, Wannenburgh A, Kotzé JDF, Van den Berg E & Henderson L 2012. An assessment of the effectiveness of a large, national-scale invasive alien plant control strategy in South Africa. *Biological Conservation* 148, 1: 28–38.

Van Wilgen BW, Reyers B, Le Maitre DC, Richardson DM & Schonegevel L 2008. A biome-scale assessment of the impact of invasive alien plants on ecosystem services in South Africa. *Journal of Environmental Management* 89, 4: 336–349.

Veldkamp A & Lambin EF 2001. Predicting land use change. *Agriculture, Ecosystems and Environment* 85, 1-3: 1-6.

Verbesselt J, Herold M, Hyndman R, Zeileis A & Culvenor D 2011. A robust approach for phenological change detection within satellite image time series. *2011 6th International Workshop on the Analysis of Multi-Temporal Remote Sensing Images, Multi-Temp 2011, Proceedings, 2011* July: 41–44.

Verbesselt J, Hyndman R, Newnham G & Culvenor D 2010a. Detecting trend and seasonal changes in satellite image time series. *Remote Sensing of Environment* 114, 1: 106–115.

Verbesselt J, Hyndman R, Zeileis A & Culvenor D 2010b. Phenological change detection while accounting for abrupt and gradual trends in satellite image time series. *Remote Sensing of Environment* 114, 12: 2970–2980.

Verburg PH, Crossman N, Ellis EC, Heinimann A, Hostert P, Mertz O, Nagendra H, Sikor T, Erb KH, Golubiewski N, Grau R, Grove M, Konaté S, Meyfroidt P, Parker DC, Chowdhury RR, Shibata H, Thomson A & Zhen L 2015. Land system science and sustainable development of the earth system: A global land project perspective. *Anthropocene* 12: 29–41.

Verburg PH, de Koning GHJ, Kok K, Veldkamp A & Bouma J 1999. A spatial explicit allocation procedure for

modelling the pattern of land use change based upon actual land use. *Ecological Modelling* 116, 1: 45–61.

Verburg PH, Kok K, Pontius RGJ & Veldkamp A 2006. Modeling land use and land cover change. In Lambin ER & Geist H (eds) *Land use and land cover change: local processes and global impacts*, 117–136. Berlin Heidelberg: Springer.

Verburg PH, Neumann K & Nol L 2011. Challenges in using land use and land cover data for global change studies. *Global Change Biology* 17, 2: 974–989.

Verburg PH, Soepboer W, Veldkamp A, Limpiada R, Espaldon V & Mastura SSA 2002. Modeling the spatial dynamics of regional land use: The CLUE-S model. *Environmental Management* 30, 3: 391–405.

Vitousek PM, Mooney HA, Lubchenco J & Melillo JM 1997. Human domination of Earth's ecosystems. *Science* 277, 5325: 494–499.

Vogelmann JE, Gallant AL, Shi H & Zhu Z 2016. Perspectives on monitoring gradual change across the continuity of Landsat sensors using time series data. *Remote Sensing of Environment* 185: 258–270.

Vogelmann JE, Xian G, Homer C & Tolk B 2012. Monitoring gradual ecosystem change using Landsat time series analyses: Case studies in selected forest and rangeland ecosystems. *Remote Sensing of Environment* 122: 92–105.

Wang M, Fei X, Zhang Y, Chen Z, Wang X, Tsou JY, Liu D & Lu X 2018. Assessing texture features to classify coastal wetland vegetation from high spatial resolution imagery using completed local binary patterns (CLBP). *Remote Sensing* 10, 5: 778.

Wang Z, Liu C & Huete A 2002. From AVHRR-NDVI to MODIS-EVI: Advances in vegetation index research. *Acta Ecologica Sinica* 23: 979–987.

Wang Z, Schaaf CB, Sun Q, Kim J, Erb AM, Gao F, Román MO, Yang Y, Petroy S, Taylor JR, Masek JG, Morisette JT, Zhang X & Papuga SA 2017. Monitoring land surface albedo and vegetation dynamics using high spatial and temporal resolution synthetic time series from Landsat and the MODIS BRDF/NBAR/albedo product. *International Journal of Applied Earth Observation and Geoinformation* 59: 104–117.

Wang Z, Schaaf CB, Sun Q, Shuai Y & Román MO 2018. Capturing rapid land surface dynamics with Collection V006 MODIS BRDF/NBAR/Albedo (MCD43) products. *Remote Sensing of Environment* 207: 50–64.

Wehmann A & Liu D 2015. A spatial–temporal contextual Markovian kernel method for multi-temporal land cover mapping. *ISPRS Journal of Photogrammetry and Remote Sensing* 107: 77–89.

Wessels KJ, Van den Bergh F & Scholes RJ 2012. Limits to detectability of land degradation by trend analysis of vegetation index data. *Remote Sensing of Environment* 125: 10–22.

Willemen L, Hein L, Van Mensvoort MEF & Verburg PH 2010. Space for people, plants, and livestock? Quantifying interactions among multiple landscape functions in a Dutch rural region. *Ecological Indicators* 10, 1: 62–73.

Wotshela L 2009. Land redistribution politics in the Eastern Cape midlands: The case of the Lukhanji municipality, 1995 – 2006. *Kronos* 35, 1: 142–174.

WRC 2013. *Vulnerability, Adaptation to and Coping with Drought: The Case of Commercial and Subsistence Rainfed Farming in the Eastern Cape. Deliverable 1: Description and Demarcation of Study Area. WRC Project K4/2280*. [online]. Available from: http://dimtecrisk.ufs.ac.za/wrc_ec/study_area/WRC_2280_study_area.htm [Accessed 5 May 2017].

Wulder MA & Masek JG 2012. Preface to Landsat Legacy special issue: Continuing the Landsat Legacy. *Remote Sensing of Environment* 122: 1.

Wulder MA, Coops NC, Roy DP, White JC & Hermosilla T 2018. Land cover 2.0. *International Journal of Remote Sensing* 39, 12: 4254–4284.

Wulder MA, White JC, Loveland TR, Woodcock CE, Belward AS, Cohen WB, Fosnight EA, Shaw J, Masek JG & Roy DP 2016. The global Landsat archive: Status, consolidation, and direction. *Remote Sensing of Environment* 185: 271–283.

Yapi TS, O'Farrell PJ, Dziba LE & Esler KJ 2018. Alien tree invasion into a South African montane grassland ecosystem: impact of Acacia species on rangeland condition and livestock carrying capacity. *International Journal of Biodiversity Science, Ecosystem Services & Management* 14, 1: 105–116.

Zeileis A, Kleiber C, Krämer W & Hornik K 2003. Testing and dating of structural changes in practice. *Computational Statistical Data Analysis* 44: 109–123.

Zhai J, Liu R, Liu J, Huang L & Qin Y 2015. Human-induced landcover changes drive a diminution of land surface albedo in the Loess Plateau (China). *Remote Sensing* 7, 3: 2926–2941.

Zhang HK & Roy DP 2017. Using the 500 m MODIS land cover product to derive a consistent continental scale 30 m Landsat land cover classification. *Remote Sensing of Environment* 197: 15–34.

Zhang J & Goodchild MF 2002. *Uncertainty in Geographical Information*. London, UK: Taylor & Francis.

Zhang L, Dawes WRR & Walker GRR 2001. Response of mean annual ET to vegetation changes at catchment scale. *Water Resources Research* 37, 3: 701–708.

Zhang X, Wang J, Gao F, Liu Y, Schaaf C, Friedl M, Yu Y, Jayavelu S, Gray J, Liu L, Yan D & Henebry GM 2017. Exploration of scaling effects on coarse resolution land surface phenology. *Remote Sensing of Environment* 190: 318–330.

Zhao M, Heinsch FA, Nemani RR & Running SW 2005. Improvements of the MODIS terrestrial gross and net primary production global dataset. *Remote Sensing of Environment* 95, 2: 164–176.

Zhou P, Huang J, Pontius RG & Hong H 2014. Land classification and change intensity analysis in a coastal watershed of Southeast China. *Sensors (Switzerland)* 14, 7: 11640–11658.

Zhu Z, Fu Y, Woodcock CE, Olofsson P, Vogelmann JE, Holden C, Wang M, Dai S & Yu Y 2016. Including land cover change in analysis of greenness trends using all available Landsat 5, 7, and 8 images: A case study from Guangzhou, China (2000–2014). *Remote Sensing of Environment* 185: 243–257.

APPENDICES

APPENDIX A. SUPPLEMENTARY MATERIAL FOR CHAPTER 3

Table A-1 Accuracy assessment of the ENLC 2000 (T1) per catchment based on sample points. Rows represent map categories; columns show reference categories

T35B ENLC 2000											
Class	UG	FITBs	BRS	Wb	Wl	CLs	FP	UrBu	Total	Map Area ha	%
UG	1172	105	39	1	25	37	67	0	1446	29912	76
FITBs	39	202	0	0	0	12	2	0	255	3306	8
BRS	0	0	0	0	0	0	0	0	0	3	0
Wb	0	0	0	15	0	1	0	0	16	33	0
Wl	26	0	0	1	129	51	22	0	229	1220	3
CLs	19	18	0	0	17	421	15	0	490	2417	6
FP	11	6	0	0	2	1	501	0	521	2566	7
UrBu	1	6	0	0	0	11	0	0	18	91	0
Total	1268	337	39	17	173	534	607	0	2975	39547	100
T12A ENLC 2000											
Class	UG	FITBs	BRS	Wb	Wl	CLs	FP	UrBu	Total	Map Area ha	%
UG	1088	61	5	2	4	25	0	27	1212	20,948	75
FITBs	23	563	2	0	0	6	0	0	594	2733	10
BRS	0	0	0	0	0	0	0	0	0	3	0
Wb	1	0	0	3	0	0	0	0	4	1	0
Wl	13	0	0	0	2	0	0	0	15	14	0
CLs	15	3	0	0	0	230	0	13	261	2403	9
FP	1	128	0	0	0	0	0	0	129	397	1
UrBu	35	3	0	0	0	12	0	185	235	1365	5
Total	1176	758	7	5	6	273	0	225	2450	27,866	100
S50E ENLC 2000											
Class	UG	FITBs	BRS	Wb	Wl	CLs	FP	UrBu	Total	Map Area ha	%
UG	1284	103	15	10	48	128	4	33	1625	27,510	62
FITBs	28	595	0	6	0	8	29	0	666	4328	10
BRS	1	0	0	0	0	0	0	0	1	13	0
Wb	0	0	0	430	1	2	0	0	433	1368	3
Wl	2	0	0	0	24	11	0	0	37	193	0
CLs	45	12	0	1	0	837	0	8	903	7269	16
FP	1	119	0	0	0	0	624	1	745	2027	5
UrBu	32	3	0	0	1	32	1	233	302	2050	5
Total	1393	832	15	447	74	1018	658	275	4712	44,759	100

Table A-2 Accuracy assessment of DLC 2014 (T2) per catchment based on sample points. Rows represent map categories; columns show reference categories

T35B DLC 2014											
Class	UG	FITBs	BRS	Wb	Wl	CLs	FP	UrBu	Total	Map Area ha	%
UG	1255	158	6	2	95	15	12	1	1544	31607	80
FITBs	28	167	0	0	1	0	0	0	196	1599	4
BRS	2	0	13	0	0	1	0	0	16	65	0
Wb	0	2	0	39	6	0	0	0	47	17	0
Wl	15	6	0	17	63	0	2	0	103	463	1
CLs	17	8	0	1	17	400	0	2	445	2444	6
FP	14	0	0	0	0	0	186	0	200	3274	8
UrBu	2	0	0	0	0	0	0	6	8	77	0
Total	1333	341	19	59	182	416	200	9	2559	39547	100
T12A DLC 2014											
Class	UG	FITBs	BRS	Wb	Wl	CLs	FP	UrBu	Total	Map Area ha	%
UG	766	68	2	2	2	10	0	21	871	19,007	68
FITBs	20	290	0	0	0	1	0	0	311	3450	12
BRS	0	0	4	0	0	0	0	1	5	43	0
Wb	4	0	0	9	0	0	0	0	13	1	0
Wl	8	0	0	0	53	0	0	0	61	17	0
CLs	54	8	6	0	0	192	0	17	277	2537	9
FP	0	0	0	0	0	0	11	0	11	95	0
UrBu	28	2	0	0	0	5	0	178	213	2716	10
Total	880	368	12	11	55	208	11	217	1762	27,866	100
S50E DLC 2014											
Class	UG	FITBs	BRS	Wb	Wl	CLs	FP	UrBu	Total	Map Area ha	%
UG	1261	137	0	12	73	39	0	20	1542	25,354	57
FITBs	27	1018	0	1	0	8	37	0	1091	4812	11
BRS	3	1	7	0	0	0	0	0	11	85	0
Wb	0	0	0	125	0	0	0	0	125	1301	3
Wl	3	0	0	0	5	0	0	0	8	57	0
CLs	20	16	0	3	18	985	0	6	1048	8107	18
FP	1	2	0	0	0	0	344	3	350	806	2
UrBu	9	4	0	0	2	0	0	209	224	4237	10
Total	1324	1178	7	141	98	1032	381	238	4399	44,759	100

Table A-3 Theoretical accuracy of land cover change analysis

	Datasets		
Catchments	ENLC 2000 (T1)	DLC 2014 (T2)	% Land cover change
T35B	81	83	67
T12A	87	88	76
S50E	83	87	72
Overall	84	85	71

APPENDIX B. SUPPLEMENTARY MATERIAL FOR CHAPTER 4

Figure B-1 Spatial distribution of overall difference, quantity, exchange and shift difference computed at 3 km bandwidth

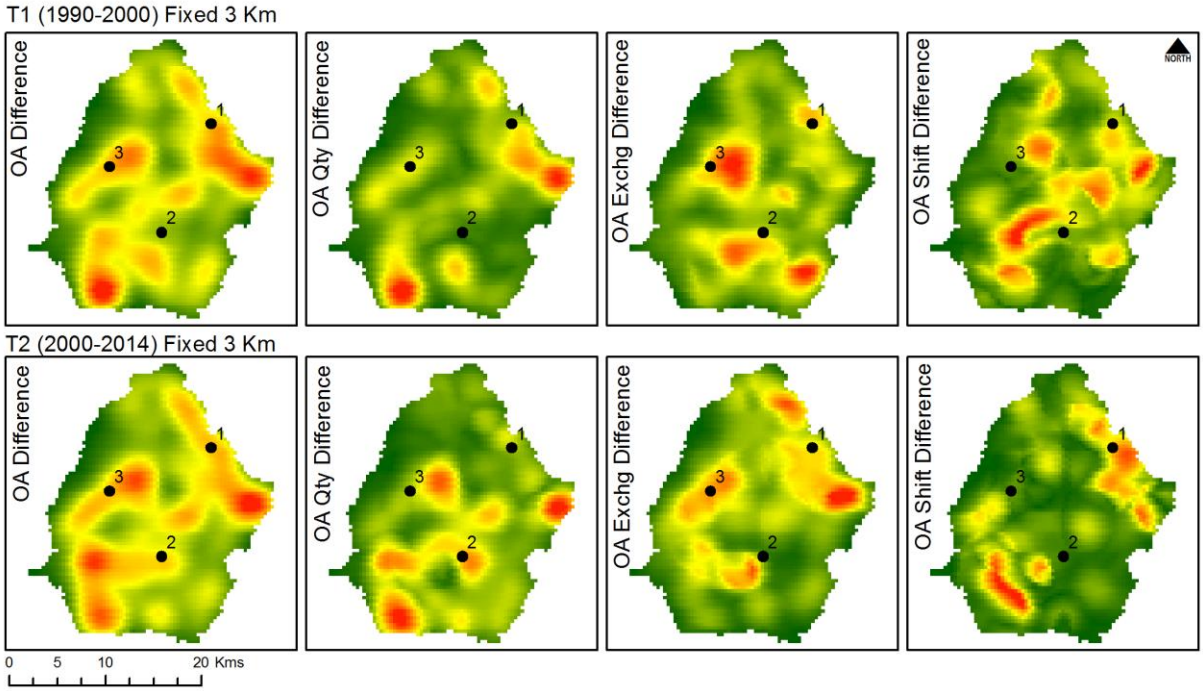

Figure B-1 Spatial distribution of overall difference, quantity, exchange and shift difference computed at 3 km bandwidth

APPENDIX C. SUPPLEMENTARY MATERIAL FOR CHAPTER 5

Table C-1 MLP Sub-models for S50E with associated explanatory variables and performance indicators

Sub-model	Explanatory variables	*Transition* / Persistence Class	Minimum cells *transition* / persist	Class skill measure (ratio)	Sub-model Accuracy (%)	Sub-model skill	RMS Train	RMS Test
If: FITBs intensification	*Elev* *Slope* *D_FP* *D_FITBs* *D_rd* *D_res*	*UG to FITBs* *CLS to FITBs* *FP to FITBs* Persistence : UG Persistence : CLS Persistence : FP	*1 846* 7 918	*0.442* *0.800* *0.759* 0.464 0.679 0.660	69.4	0.632	0.269	0.273
Ia : Agricultural intensification	*Elev* *Slope* *Asp* *D_res* *EV*	***UG to CLS*** *FITBs to CLS* *Wb to CLS* *Wl to CLS* *UrBu to CLS* Persistence : UG Persistence : FITBs Persistence : Wb Persistence : Wl Persistence : UrBu	*32* 508	***0.869*** *-0.111* *-0.111* *0.352* *-0.032* 0.673 0.722 1.000 0.236 0.524	50.3	0.448	0.245	0.253
Iu: Urban intensification	*Elev* *D_FITBs* *D_rd* *D_res*	*UG to UrBu* *FITBs to UrBu* *CLS to UrBu* Persistence : UG Persistence : FITBs Persistence : CLS	*1 875* 30 778	*-0.105* ***0.840*** *0.478* 0.419 0.605 0.462	54.3	0.452	0.320	0.320
R: Afforestation	*Elev* *Asp* *D_FP* *D_FITBs*	*UG to FP* *FITBs to FP* Persistence : UG Persistence : FITBs	*342* 30 778	*0.540* *0.487* 0.462 -0.169	49.4	0.325	0.379	0.386
D: Deforestation	*Elev* *Asp* *D_riv* *D_rd*	*FP to UG* *FP to BRS* Persistence : FP	*137* 7 918	*0.127* ***0.843*** 0.519	66.5	0.498	0.380	0.397
A: Abandonment	*Elev* *Slope* *Asp*	*CLS to UG* *UrBu to UG* Persistence : CLS Persistence : UrBu	*503* 20 948	*0.193* *0.506* 0.099 -0.139	37.5	0.166	0.415	0.421
Dn: Natural dynamic	*Elev* *Slope* *Asp* *D_riv*	*UG to Wb* *UG to Wl* *Wb to UG* *Wl to UG* Persistence : UG Persistence : Wb Persistence : Wl	*32* 162	*0.325* *0.198* *-0.167* *-0.167* 0.570 0.922 0.271	39.1	0.290	0.313	0.320
De: Degradation	*Elev* *Slope* *Asp* *D_riv* *D_res* *EV*	*UG to BRS* Persistence : UG	*409* 252 574	*0.431* 0.359	69.8	0.395	0.400	0.446
Re: Reclamation	*Elev* *Slope* *D_riv* *D_res* *EV* *D_FITBs*	*FITBs to UG* Persistence : FITBs	*13 843* 30 778	*0.087* 0.414	62.5	0.249	0.472	0.475

Table C-2 MLP Sub-models for T35B with associated explanatory variables and performance indicators

Sub-model	Explanatory variables	*Transition*/ Persistence Class	Minimum cells *transition* / persist	Class skill measure (ratio)	Sub-model Accuracy (%)	Sub-model skill	RMS Train	RMS Test
If: FITBs intensification	*Elev* *Slope* *D_FP* *D_rd* *D_riv* *EV*	*UG to FITBs* *CLS to FITBs*	*222*	*0.675* *0.423*	67.9	0.572	0.320	0.327
		Persistence : UG Persistence : CLS	19 736	0.207 0.539				
Ia : Agricultural intensification	*Elev* *Slope* *D_rd* *D_riv* *EV*	*UG to CLS* *FITBs to CLS* *FP to CLS* *WI to CLS* *UrBu to CLS*	*122*	*0.346* *0.967* *0.945* *0.663* *0.436*	65.0	0.611	0.214	0.220
		Persistence : UG Persistence : FITBs Persistence : FP Persistence : WI Persistence : UrBu	309	0.436 0.665 0.444 0.648 0.521				
Iu: Urban intensification	*Elev* *Slope* *D_FP* *D_rd* *D_riv*	*UG to UrBu* *FITBs to UrBu*	*187*	*0.903* *0.900*	82.8	0.771	0.331	0.327
		Persistence : UG Persistence : FITBs	7 586	0.536 0.739				
R: Afforestation	*Elev* *D_FP* *D_rd* *EV*	*UG to FP* *FITBs to FP* *WI to FP* *CLS to FP*	*569*	*0.926* *0.910* *0.968* *1.000*	89.3	0.878	0.166	0.173
		Persistence : UG Persistence : FITBs Persistence: WI Persistence: CLS	1 996	0.710 0.925 0.777 0.812				
D: Deforestation	*Elev* *Asp* *EV*	*FP to UG* *FP to WI*	*437*	*0.341* *0.787*	53.0	0.295	0.430	0.434
		Persistence : FP	23 904	-0.254				
A: Abandonment	*Elev* *D_FP* *EV*	*CLS to UG* *UrBu to UG* *CLS to WI*	*387*	*0.27* *0.5833* *0.528*	42.7	0.284	0.345	0.345
		Persistence : CLS Persistence : UrBu	309	-0.250 0.270				
Dn: Natural dynamic	*Elev* *Slope* *Asp*	*FITBs to WI* *UG to WI* *Wb to UG* *WI to UG*	*155*	*0.514* *-0.143* *0.460* *-0.143*	36.5	0.274	0.305	0.311
		Persistence : UG Persistence : Wb Persistence: FITBs Persistence : WI	65	0.336 0.536 0.633 -0.143				
De: Degradation	*Asp* *EV* *D_FP* *D_FITBs*	*UG to BRS*	*605*	*0.351*	71.2	0.423	0.447	0.447
		Persistence : UG	306 061	0.498				
Re: Reclamation	*Elev* *Slope* *D_rd* *D_FP* *EV*	*FITBs to UG*	*26 674*	*0.017*	54.7	0.094	0.493	0.496
		Persistence : FITBs	7 586	0.170				

APPENDIX D.SUPPLEMENTARY MATERIAL FOR CHAPTER 6

Table D-1 Correlation coefficients per land cover class and transition. Correlations for S50E are presented above the diagonal in italics, and correlations for T35B are presented below the diagonal. *p < 0.05

	UG **T35B: n=1516 *S50E: n=1249***				**FB** **T35B: n=45 *S50E: n=136***				**CL** **T35B: n=92 *S50E: n=323***				**FP** **T35B: n=123 *S50E: n=42***				**UB** **T35B: n=3 *S50E: n=103***			
	1	2	3	4	1	2	3	4	1	2	3	4	1	2	3	4	1	2	3	4
1.PSA	-	*-0.24*	*-0.08*	*0.09*	-	*-0.10*	*-0.02*	*0.14*	-	*-0.37*	*-0.30*	*-0.20*	-	*-0.18*	*-0.06*	*0.03*	-	*-0.30*	*-0.52**	*-0.35*
2.NPP	-0.01	-	*0.00*	*-0.04*	0.02	-	*-0.33*	*-0.07*	-0.12	-	*-0.09*	*-0.13*	0.30	-	*0.70**	*0.55**	-0.42	-	*-0.06*	*-0.10*
3.NDVI	-0.20	0.33	-	*0.86**	-0.09	0.41	-	*0.90**	-0.58*	0.26	-	*0.88**	-0.62*	0.18	-	*0.92**	-0.45	0.27	-	*0.86**
4.ET	0.11	0.19	0.84*	-	0.13	0.27	0.83*	-	-0.34	0.15	0.87*	-	-0.39	0.13	0.90*	-	-0.17	0.14	0.79*	-
	If T35B: n=54 *S50E: n=101*				A T35B: n=28 *S50E: n=39*				De T35B: n=3 *S50E: n=3*				Re T35B: n=108 *S50E: n=70*				Dn T35B: n=60 *S50E: n=15*			
	1	2	3	4	1	2	3	4	1	2	3	4	1	2	3	4	1	2	3	4
1.PSA	-	*-0.40*	*-0.07*	*0.11*	-	*-0.23*	*-0.19*	*-0.15*	-	*-0.13*	*-0.45*	*-0.35*	-	*-0.32*	*-0.17*	*-0.01*	-	*-0.01*	*-0.37*	*-0.34*
2.NPP	0.04	-	*0.17*	*0.10*	0.14	-	*-0.18*	*-0.13*	-0.28	-	*0.14*	*-0.05*	0.14	-	*-0.08*	*-0.07*	0.66*	-	*-0.07*	*-0.19*
3.NDVI	-0.03	0.41	-	*0.88**	-0.37	0.24	-	*0.91**	-0.36	0.32	-	*0.81**	-0.22	0.34	-	*0.90**	-0.38	-0.32	-	*0.82**
4.ET	0.29	0.31	0.84*	-	-0.25	0.17	0.88*	-	-0.21	0.13	0.84*	-	-0.05	0.21	0.83*	-	-0.20	-0.19	0.89*	-
	Ia T35B: n=41 *S50E: n=117*				Iu T35B: n=2 *S50E: n=120*				R T35B: n=60 *S50E: n=6*				D T35B: n=23 *S50E: n=35*							
	1	2	3	4	1	2	3	4	1	2	3	4	1	2	3	4				
1.PSA	-	*-0.32*	*-0.45*	*-0.29*	-	*-0.28*	*-0.40*	*-0.22*	-	*-0.56**	*0.11*	*-0.01*	-	*-0.75**	*-0.81**	*-0.67**				
2.NPP	-0.14	-	*-0.08*	*-0.15*	-0.38	-	*-0.07*	*-0.11*	0.63*	-	*-0.20*	*-0.04*	0.70*	-	*0.86**	*0.75**				
3.NDVI	-0.54*	0.22	-	*0.87**	-0.63*	0.19	-	*0.87**	-0.61*	-0.38	-	*0.90**	-0.63*	-0.55*	-	*0.93**				
4.ET	-0.29	0.11	0.87*	-	-0.29	0.05	0.81*	-	-0.29	-0.29	0.86*	-	-0.31	-0.42	0.87*	-				

UG-grasslands, FB-shrublands, CL-croplands, FP-forest/plantation, UB-urban,
If-woody encroachment, A-abandonment, De-degradation Re- reclamation, Dn-natural dynamics,
Ia-increased cultivation, Iu-increased urban, R-afforestation, D-deforestation

Table D-2 Total and significant change in PSA per catchment T35B, reported in percentage and PSA change (highlighted in light grey).

Study area		Total area				Significant change				Negative sig. change				Positive sig. change			
		%		PSA change		%		PSA change		%		PSA change		%		PSA change	
	LC	MOD	*LS*	MOD	*LS*	MOD	*LS*	MOD	*LS*	MOD	*LS*	MOD	*LS*	MOD	*LS*	MOD	*LS*
T35B				-0.001	*0.003*	11.1	*11.3*	-0.013	*0.004*	7.9	*4.3*	-0.026	*-0.039*	3.2	*7.0*	0.019	*0.031*
T35B Persistent	UG	70.4	*69.3*	0.000	*0.005*	4.0	*5.3*	0.000	*0.017*	2.1	*0.7*	-0.017	*-0.023*	1.9	*4.6*	0.018	*0.023*
	FB	2.1	*1.7*	-0.001	*0.001*		*0.1*		*0.012*		*0.0*		*-0.029*		*0.1*		*0.030*
	CL	4.3	*4.5*	0.003	*0.009*	0.5	*0.9*	-0.001	*0.029*	0.2	*0.2*	-0.029	*-0.038*	0.3	*0.7*	0.023	*0.045*
	FP	5.7	*5.4*	-0.015	*-0.012*	2.5	*2.2*	-0.031	*-0.038*	2.5	*2.1*	-0.031	*-0.039*		*0.1*		*0.020*
	UB	0.1	*0.1*	-0.005	*0.011*	0.0	*0.0*	-0.024	*0.030*	0.0	*0.0*	-0.024	*-0.020*		*0.0*		*0.039*
	P	82.7	*81.0*	-0.001	*0.004*	7.4	*8.4*	-0.011	*0.007*	5.0	*2.8*	-0.025	*-0.039*	2.4	*5.6*	0.018	*0.030*
T35B Transition	If	2.5	*2.3*	-0.002	*-0.003*	0.2	*0.1*	-0.006	*-0.003*	0.1	*0.1*	-0.022	*-0.030*	0.1	*0.1*	0.018	*0.029*
	A	1.3	*1.3*	0.002	*0.009*	0.1	*0.2*	-0.008	*0.022*	0.0	*0.0*	-0.028	*-0.033*	0.0	*0.2*	0.012	*0.031*
	De	0.1	*0.1*	-0.003	*0.005*		*0.0*		*0.022*		*0.0*		*-0.022*		*0.0*		*0.031*
	Re	5.0	*6.0*	0.000	*0.004*	0.3	*0.4*	-0.009	*0.023*	0.2	*0.1*	-0.022	*-0.025*	0.1	*0.4*	0.023	*0.031*
	Ia	1.9	*1.7*	0.005	*0.012*	0.0	*0.4*	0.023	*0.033*		*0.1*		*-0.031*	0.3	*0.3*	0.023	*0.045*
	Iu	0.1	*0.1*	-0.004	*0.012*		*0.0*		*0.029*		*0.0*		*-0.030*		*0.0*		*0.038*
	R	2.8	*2.8*	-0.014	*-0.013*	1.0	*1.0*	-0.029	*-0.034*	1.0	*0.9*	-0.029	*-0.038*		*0.1*		*0.020*
	D	1.1	*0.9*	-0.019	*-0.008*	0.6	*0.2*	-0.031	*-0.021*	0.6	*0.2*	-0.031	*-0.032*		*0.0*		*0.022*
	Dn	2.8	*2.4*	-0.005	*0.003*	0.8	*0.3*	-0.021	*0.008*	0.7	*0.1*	-0.027	*-0.034*	0.1	*0.3*	0.024	*0.025*
	T	17.6	*17.8*	-0.004	*0.001*	3.4	*2.8*	-0.017	*-0.002*	2.7	*1.4*	-0.027	*-0.040*	0.7	*1.4*	0.023	*0.036*

UG-grasslands, FB-shrublands, CL-croplands, FP-forest/plantation, UB-urban,
If-woody encroachment, A-abandonment, De-degradation Re- reclamation
Ia-increased cultivation, Iu-increased urban, R-afforestation, D-deforestation
Dn-natural dynamics

Table D-3. Total and significant change in PSA per catchment S50E, reported in percentage and PSA change (highlighted in light grey)

Study area		Total catchment				Significant change				Negative sig. change				Positive sig. change			
		%		PSA change		%		PSA change		%		PSA change		%		PSA change	
		MOD	*LS*	MOD	*LS*	MOD	*LS*	MOD	*LS*	MOD	*LS*	MOD	*LS*	MOD	*LS*	MOD	*LS*
S50E				0.004	*0.004*	8.5	*16.1*	0.016	*0.017*	1.9	*4.1*	-0.018	*-0.026*	6.6	*12.0*	0.026	*0.032*
S50E Persistent	UG	50.8	*50.2*	0.004	*0.004*	3.1	*6.3*	0.017	*0.016*	0.6	*1.0*	-0.012	*-0.023*	2.5	*5.3*	0.024	*0.023*
	FB	6.4	*6.6*	-0.002	*-0.006*	0.7	*1.5*	-0.023	*-0.018*	0.5	*1.3*	-0.032	*-0.026*	0.1	*0.2*	0.013	*0.027*
	CL	15.3	*15.6*	0.005	*0.008*	1.3	*2.4*	0.018	*0.028*	0.2	*0.3*	-0.012	*-0.028*	1.1	*2.2*	0.024	*0.034*
	FP	2.0	*1.8*	-0.004	*-0.006*	0.3	*0.6*	-0.013	*-0.019*	0.3	*0.5*	-0.017	*-0.034*	0.0	*0.1*	0.018	*0.044*
	UB	4.9	*4.7*	0.007	*0.008*	0.3	*0.7*	0.015	*0.023*	0.0	*0.1*	-0.016	*-0.022*	0.2	*0.6*	0.020	*0.027*
	P	87.7	*85.5*	0.004	*0.004*	5.4	*10.9*	0.013	*0.013*	1.3	*2.9*	-0.023	*-0.027*	4.1	*8.0*	0.025	*0.027*
S50E Transition	If	4.8	*5.3*	0.005	*0.006*	0.9	*1.3*	0.012	*0.016*	0.4	*0.6*	-0.023	*-0.028*	0.5	*0.8*	0.038	*0.050*
	A	1.8	*1.8*	0.005	*0.006*	0.0	*0.3*	0.002	*0.021*		*0.1*		*-0.026*	0.0	*0.2*	0.002	*0.031*
	De	0.1	*0.1*	-0.003	*0.000*		*0.0*		*0.009*		*0.0*		*-0.031*		*0.0*		*0.037*
	Re	3.3	*3.5*	0.003	*0.003*	0.2	*0.5*	0.012	*0.008*	0.0	*0.2*	-0.003	*-0.024*	0.1	*0.3*	0.017	*0.034*
	Ia	5.5	*4.8*	0.005	*0.010*	0.2	*0.9*	0.009	*0.029*	0.1	*0.1*	-0.017	*-0.029*	0.1	*0.8*	0.027	*0.033*
	Iu	5.7	*5.9*	0.006	*0.005*	0.4	*0.8*	0.021	*0.015*	0.0	*0.2*	-0.008	*-0.027*	0.4	*0.7*	0.024	*0.026*
	R	0.3	*0.2*	0.004	*0.001*		*0.0*		*0.002*		*0.0*		*-0.026*		*0.0*		*0.036*
	D	1.7	*1.5*	0.032	*0.056*	0.8	*0.9*	0.038	*0.068*		*0.0*		*-0.026*	0.8	*0.9*	0.038	*0.070*
	Dn	0.7	*0.6*	-0.001	*-0.001*		*0.1*		*0.002*		*0.0*		*-0.035*	0.0	*0.0*		*0.027*
	T	24.0	*23.8*	0.007	*0.009*	3.0	*5.0*	0.023	*0.029*	0.5	*1.1*	-0.020	*-0.027*	2.5	*3.9*	0.032	*0.045*

UG-grasslands, FB-shrublands, CL-croplands, FP-forest/plantation, UB-urban,
If-woody encroachment, A-abandonment, De-degradation Re- reclamation
Ia-increased cultivation, Iu-increased urban, R-afforestation, D-deforestation
Dn-natural dynam